ISBN: 978-3-95450-253-0 ISSN: 2673-5571 doi:10.18429/JACoW-HB2023-MOA1I1

BEAM PERFORMANCE WITH THE LHC INJECTORS UPGRADE

G. Rumolo*, S. Albright, R. Alemany, M. E. Angoletta, C. Antuono, T. Argyropoulos, F. Asvesta, M. Barnes, H. Bartosik, P. Baudrenghien, G. Bellodi, N. Biancacci, C. Bracco, N. Bruchon, E. Carlier, J. Coupard, H. Damerau, G.P. Di Giovanni, E. de la Fuente Garcia, A. Findlay, M. Fraser, A. Funken, R. Garoby, S. Gilardoni, B. Goddard, G. Hagmann, K. Hanke, A. Huschauer, G. Iadarola, V. Kain, I. Karpov, J.-B. Lallement, A. Lasheen, T. Levens, K. Li, A. Lombardi, E. Maclean, D. Manglunki, I. Mases Sole, M. Meddahi, L. Mether, B. Mikulec, E. Montesinos, Y. Papaphilippou, G. Papotti, K. Paraschou, C. Pasquino, F. Pedrosa, T. Prebibaj, S. Prodon, D. Quartullo, F. Roncarolo, B. Salvant, M. Schenk, R. Scrivens, E. Shaposhnikova, L. Sito, P. Skowronski, A. Spierer, R. Steerenberg, M. Sullivan, F. Velotti, R. Veness, C. Vollinger, R. Wegner, C. Zannini
CERN, Geneva, Switzerland

Abstract

The LHC Injectors Upgrade (LIU) project was put in place between 2010 and 2021 to increase the intensity and brightness in the LHC injectors to match the challenging requirements of the High-Luminosity LHC (HL-LHC) project, while ensuring reliable operation of the injectors complex up to the end of the HL-LHC era (ca. 2040). During the 2019–2020 CERN accelerators shutdown, extensive hardware modifications were implemented in the entire LHC proton and ion injection chains, involving the new Linac4, the Proton Synchrotron Booster (PSB), the Proton Synchrotron (PS), the Super Proton Synchrotron (SPS) and the ion PS injectors, i.e. the Linac3 and the Low Energy Ion Ring (LEIR). Since 2021, beams have been recommissioned throughout the injectors chain and the beam parameters are being gradually ramped up to meet the LIU specifications using new beam dynamics solutions adapted to the upgraded injectors. This paper focuses on the proton beams and describes the current state of the art.

A COMPACT RECAP OF THE LIU PROJECT

The main goal of the LIU project was to enable the LHC injectors to reliably produce beams for LHC with intensity and brightness matching the HL-LHC specifications for both protons and lead (Pb) ions [1]. The project had to identify simultaneously, and prioritise, the means to reach the required beam parameters and the interventions that would ensure high availability and reliable operation of the injector complex up to the end of the HL-LHC era (ca. 2040), in close collaboration with the accelerator consolidation (CONS) project [2]. All this translated into the implementation of a series of major upgrades in all accelerators of the LHC injectors chain, which are detailed in [3, 4]. The principal items are listed separately in the next section.

Table 1 summarises the main target parameters at SPS extraction for both protons and Pb ions, as well as the values achieved until 2018, i.e., before the full implementation of the LIU upgrades. For protons, the single bunch parameters will have to be roughly doubled in both intensity and brightness. The filling pattern assumes four trains of 72 bunches spaced by 25 ns per SPS-to-LHC injection (200 ns between trains). For Pb ions, the single bunch parameters were already demonstrated thanks to a dedicated LIU crash program in 2015–16 as well as subsequent LEIR improvements in 2017-18 and 2021–22 which provided margin on the extracted intensity and excellent operational stability and reproducibility [5–7]. The LIU upgrades are only expected to permit doubling the total number of bunches in the LHC thanks to a novel production scheme in the SPS, the so-called momentum slip stacking. Slip stacked beams were successfully injected into the LHC in October 2022 for a short test ion run [8] and the full performance is expected in fall 2023, when 7 trains with 8 bunches spaced by 50 ns (100 ns between trains) will be provided for each SPS-to-LHC injection. The remaining part of this paper will solely focus on proton beams.

Table 1: Beam parameters at LHC injection for protons and Pb ions, HL-LHC target and achieved in Run 2.

	N (10^{11} p/b)	$\epsilon_{x,y}$ (μm)	Bunches
HL-LHC	2.3	2.1	2760
Pre-LIU	1.15	2.5	2760
	N (10^8 ions/b)		
HL-LHC	2.0	1.5	1248
Pre-LIU	2.0	1.5	648

The LIU project lifecycle spanned from 2010 to 2021 and its baseline items were gradually refined thanks to extensive beam studies that took place in Run 1 (2009–2013) and Run 2 (2014–2018). A first subset of upgrade items, mainly in the form of prototypes, were already installed during the Long Shutdown 1 (LS1: March 2013–June 2014 for the injectors) or, when possible, during the Year-End Technical Stops (YETS), to allow tests with beam and/or to advance installations to alleviate the workload during Long Shutdown 2 (LS2: 2019 to 2020). In fact, the great majority of

* Giovanni.Rumolo@cern.ch

ISBN: 978-3-95450-253-0 ISSN: 2673-5571 doi:10.18429/JACoW-HB2023-MOA1I2

FRIB FROM COMMISSIONING TO OPERATION*

P. N. Ostroumov†, K. Fukushima, A. Gonzalez, K. Hwang, T. Kanemura,
T. Maruta, A. Plastun, J. Wei, T. Zhang, Q. Zhao
Facility for Rare Isotopes Beams, Michigan State University, East Lansing, MI, USA

Abstract

The Facility for Rare Isotope Beams (FRIB) was fully commissioned in early 2022, and the operation for physics experiments started shortly thereafter. Various ion beam species have been accelerated up to 240 MeV/u and delivered to the target. During the first year of user operations, the FRIB provided 4252 beam hours with 91% availability for nuclear science. In addition, FRIB delivered about 1000 hours of various ion beam species at beam energies up to 40 MeV/u for single-event experiments. Typically, the experiments with a specific species rare isotope beam last a week or two. Each experiment requires a different primary beam species with specific energies. The primary beam power has been gradually increased from 1 kW to 10 kW over the past 1.5 years. The Accelerator Physics (AP) group develops high-level physics applications to minimize machine set-up time. Focuses include identifying beam halo sources, controlling emittances of multiple-charge-state beams, and studying the beam loss mechanisms to prepare for the ultimate 400 kW operation. This paper discusses the experience and challenges of operating a high-power CW heavy ion accelerator.

INTRODUCTION

The FRIB is a major DOE nuclear physics research facility that will provide access to 80% of all isotopes predicted to exist in nature. FRIB construction started in 2013 and finished in 2022, on cost and ahead of schedule. The beam commissioning began in 2017, first with the Front End and continued until January 2022, when the fragment separator was commissioned with a 210 MeV/u ^{36}Ar beam. During operations, installation of accelerator equipment has been taking place interrupted with short, 1-2 weeks commissioning periods. Results of each stage have been reported in multiple conference proceedings and journal papers [1-5]. The FRIB facility is based on a high energy heavy-ion CW superconducting driver linac, capable of accelerating uranium ions to 200 MeV/u and higher energies for lighter ions with 400 kW power on-target [1]. The layout of the linac is shown in Fig. 1. In this paper, we report results of the final commissioning stage, the first year of operation, and ongoing developments to support experiments with various ion beam species and the beam power ramp-up from 1 kW to 10 kW. We also discuss R&D initiatives to reach the ultimate beam power of 400 kW. To date, the primary ion beams of ^{36}Ar, ^{40}Ar, ^{48}Ca, ^{64}Zn, ^{70}Zn, ^{82}Se, ^{86}Kr, ^{124}Xe, and ^{198}Pt up to 240 MeV/u have been delivered to the target and used to produce more than 200 unstable isotopes for 12 nuclear physics experiments.

* This material is based upon work supported by the U.S. Department of Energy, Office of Science, Office of Nuclear Physics and used resources of the FRIB, which is a DOE Office of Science User Facility, operated by Michigan State University, under Award Number DE-SC0000661.
† Ostroumov@frib.msu.edu

FRONT END

The linac Front End (FE) includes two Electron Cyclotron Resonance (ECR) ion sources, a Low Energy Beam Transport (LEBT) section that selects desired ion species, a Radiofrequency Quadrupole (RFQ), and a Medium Energy Beam Transport (MEBT) section. Proper tuning of the FE is critical to provide low-emittance and low-halo beams at the entrance of the SC linac. The main strategies for the beam tuning in the FE have been discussed in previous publications (see [3] and references therein).

Initial ion beams are produced by a room temperature Electron Cyclotron Resonance (ECR) ion source, ARTEMIS, for the linac commissioning and initial operation [6]. At the beginning of this year, a new superconducting High Power ECR (HP-ECR) was commissioned [7]. The new HP-ECR significantly increased the flexibility of the FRIB to prepare and provide various ion species for experiments. In addition, the new HP-ECR and following beam transport produce a higher quality beam. To reduce the beam halo at the entrance to the SC linac, we started using two round collimators in the LEBT positioned for proper collimation in the phase space. These collimators remove 5-10% of the total beam intensity and result in a more compact beam phase-space. The beam profile measurements in the MEBT shown in Fig. 2 illustrate the effectiveness of the collimation.

Machine Learning Application in Front End

The unknown distribution of mechanical misalignments in the FE results in simulated beam trajectory predictions being insufficiently accurate for on-axis RFQ injection tuning. A “black-box” local optimization using the Nelder-Mead method and data from BPMs and post-RFQ Faraday Cup (FC) measurements, has been utilized until recently for beam centering and current maximization. However, local optimum solutions obtained were often not satisfactory. Therefore, we developed a Machine Learning (ML) tool based on Bayesian optimization to more efficiently explore the global decision domain utilizing all the collected data during the optimization procedure. We tailored the improved optimization algorithm to minimize corrector magnet ramping time and magnet polarity crossings which is the major time-consuming factor. We suppressed polarity changes by favoring the decision candidates with the same polarity at the present magnet set values in the acquisition function used for the decision candidate search. The polarity favouring is carefully structured so as not to limit the capability of searching for the optimum tune. The objective

ISBN: 978-3-95450-253-0 ISSN: 2673-5571 doi:10.18429/JACoW-HB2023-MOA1I3

INTENSE BEAM ISSUES IN CSNS ACCELERATOR BEAM COMMISSIONING

L. Huang[1], M. Huang[1], S. Xu[1], H. Liu[1], L. Rao[1], X. Lu[1],
Y. Li[1], J. Chen[1], Y. An[1], Z. Li[1], J. Peng[1], X. Luo[1], S. Wang[†,1]
Institute of High Energy Physics, Chinese Academy of Sciences, Beijing, China
[1]also at Spallation Neutron Source Science Center, Dongguan, China

Abstract

The China Spallation Neutron Source (CSNS) consists of an 80 MeV H- Linac, an 1.6 GeV Rapid Cycling Synchrotron (RCS), beam transport lines, a target station, and three spectrometers. The CSNS design beam power is 100 kW, with the capability of upgrading to 500 kW. In August 2018, the CSNS was officially opened to domestic and international users. By February 2020, the beam power had reached 100 kW. With the implementation of improvements such as the addition of harmonic cavities, the beam power was further increased to 140 kW in Oct. 2022. During the beam commissioning, the most significant factor limiting the beam power was the beam loss caused by space charge effects and collective instabilities. The unexpected collective effects, the coherent oscillation of the bunches, were observed when the beam power exceeded 50 kW. By implementing the various mitigations, the beam loss caused by space charge effects and collective instabilities were effectively controlled. This paper is focused on these intense beam issues observed during the beam commissioning and the methods utilized to mitigate them. Additionally, the study on the collective effects in the upgrade project (CSNS-II) is also introduced.

INTRODUCTION

The China Spallation Neutron Source (CSNS) [1, 2] comprises of an 80 MeV H- Linac, a 1.6 GeV Rapid Cycling Synchrotron (RCS), beam transport lines, a target station, and three spectrometers. The RCS accumulates 80 MeV beam through a multi-turn charge-exchange scheme and accelerates the beam to 1.6 GeV with repetition rate of 25 Hz. The RCS provides beam power of 100 kW with intensity of 1.56×10^{13}. In the upgrade of CSNS (CSNS-II), the beam power will be upgraded to 500 kW with an injection energy of 300 MeV. Due to the high beam intensity and high repetition rate, the beam loss must be controlled to a much lower level.

The RCS is a four-fold structure. Each super-period consists of two straight sections and an arc section. There are four 11-meter uninterrupted straight sections, and this benefits for accommodation of injection, extraction, RF cavity and transverse collimation system. Figure 1 displays the Twiss parameters in one super-period, and the main parameters of CSNS and CSNS-II are respectively listed in Table 1. The lattice is based on triplet cells with circumference of 227.92 meters, including 24 dipole magnets and 48 quadrupole magnets, all excited by a 25 Hz DC-biased sinusoidal current pattern [3]. The 48 quadrupoles are powered by 5 families power supply. The nominal tune is set as (4.86, 4.78) with natural chromaticity of (-4, -9). Although the chromaticity correction is not mandatory for the RCS running below transition energy, the DC sextupole is applied for a better control over the chromaticity. The focusing and defocusing sextupole magnets, eight magnets in each family are powered by one power supply, are accommodated in the arc where the horizontal dispersion is about 2 meters, and the chromaticity is corrected to reduce the tune spread, specially at low beam energy stage. Due to that the DC field of sextupole magnet is not ramped with the beam energy, the chromaticity will decrease with the energy increasing. The transverse acceptance of the RCS is designed as 540 π·mm·mrad.

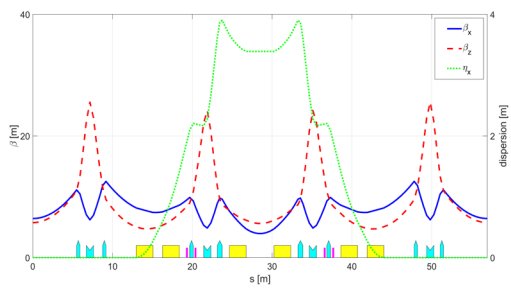

Figure 1: The Twiss parameters of RCS.

Table 1: Main RCS Parameters

Parameter	Unit	CSNS	CSNS-II
Circumference	m	227.92	227.92
Energy (Inj./Ext.)	GeV	0.08/1.6	0.3/1.6
Repetition rate	Hz	25	25
Bunch number		2	2
Beam intensity	10^{13}	1.56	7.8
Nominal tune (H/V)		4.86/4.78	4.86/4.78
Chromaticity (H/V)		-4/-9	-4/-9
SC tune shift		0.27	0.17
RF Voltage	kV	165	170

The RF acceleration system consists of eight ferrite loaded cavities [4]. The designed frequency and voltage pattern are shown in Fig. 2. In order to ensure the maximum efficiency in the process of beam capture,

wangs@ihep.ac.cn

ISBN: 978-3-95450-253-0 ISSN: 2673-5571 doi:10.18429/JACoW-HB2023-MOA3I1

BEAM DYNAMICS CHALLENGES IN THE DESIGN OF THE ELECTRON-ION COLLIDER*

Y. Luo†, M. Blaskiewicz, A. Blednykh, D. Marx, C. Montag, V. Ptitsyn, V. Ranjbar, S. Verdú-Andrés, E. Wang, F. Willeke, Brookhaven National Laboratory, Upton, NY, USA
S. Nagaitsev, Thomas Jefferson National Accelerator Facility, Newport News, VA, USA

Abstract

The Electron-Ion Collider (EIC), which will be constructed at Brookhaven National Laboratory, will collide polarized high-energy electron beams with hadron beams, achieving luminosities up to $1 \times 10^{34}\text{cm}^{-2}\text{s}^{-1}$ in the center-of-mass energy range of 20-140 GeV. To achieve such high luminosity, we adopt high bunch intensities for both beams, small and flat transverse beam sizes at the interaction point, a large crossing angle of 25 mrad, and a novel strong hadron cooling in the Hadron Storage Ring to counteract intra-beam scattering (IBS) at the collision energies. In this article, we will review the beam dynamics challenges in the design of the EIC, particularly the beam-beam interaction, impedance budget and instabilities, polarization maintenance, and dynamic aperture. We will also briefly mention some technical challenges associated with beam dynamics in the design of EIC, such as strong hadron cooling, noises of crab cavities and power supply current ripples.

INTRODUCTION

The Electron-Ion Collider (EIC) will be built at Brookhaven National Laboratory (BNL) in a full partnership between BNL and the Thomas Jefferson National Accelerator Facility (JLab). The EIC will uniquely address three profound questions about nucleons—neutrons and protons, and how they assemble to form the nuclei of atoms: 1) How does the mass of the nucleon arise? 2) How does the spin of the nucleon arise? 3) What are the emergent properties of dense systems of gluons? [1]

The storage ring-based design of the EIC meets or even exceeds the requirements referenced in the 2015 Long Range Plan for U.S. Nuclear Physics [2]: 1) Center-of-mass energy range from 20 to 100 GeV, upgradable to 140 GeV; 2) Ion beams from deuterons to the heaviest stable nuclei, 3) High luminosity, up to $1 \times 10^{34}\text{cm}^{-2}\text{s}^{-1}$ for electron-proton collisions; 4) Highly spin-polarized electron, proton, and light-ion beams, 5) An interaction region and integrated detector capable of nearly 100% kinematic coverage, with the capability of incorporating a second such interaction region as needed.

Figure 1 presents the schematic diagram of the EIC layout. The hadron storage ring (HSR) comprises arcs of the two superconducting Relativistic Heavy Ion Collider (RHIC) storage rings. An electron storage ring (ESR) will be installed in the existing RHIC tunnel, where it will provide beam collisions with the HSR hadron beam in up to two interaction regions (IRs). High polarized electron bunches will be provided to the ESR by a rapid-cycling synchrotron (RCS) in the same tunnel [3].

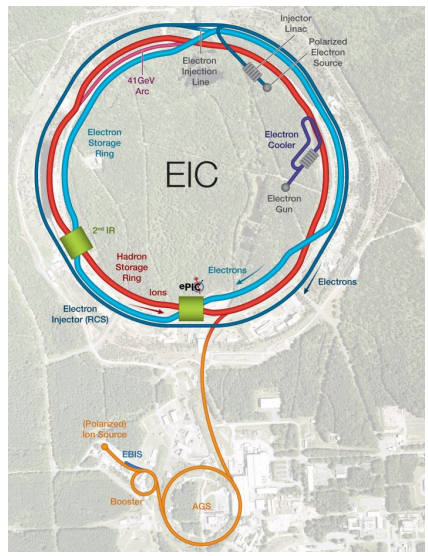

Figure 1: Schematic diagram of the EIC.

HIGHLIGHTS OF EIC DESIGN

The maximum luminosity in the EIC is limited by a range of factors. The primary factors are attainable beam-beam parameters (ξ_h, ξ_e), maximum beam divergences (σ_h', σ_e') at the interaction point (IP) defined by the interaction region magnet apertures and detector forward acceptance requirements, and maximum beam currents [1,4]. The luminosity can be written as

$$L = f_b \frac{\pi \gamma_h \gamma_e}{r_{0,h} r_{0,e}} (\xi_h \sigma_h')(\xi_e \sigma_e') \frac{(1+K)^2}{K} H \qquad (1)$$

where f_b is the bunch repetition rate, $\gamma_{h,e}$ are the relativistic factors of the respective beams, and $r_{0,h,e}$ are the classical radii of the electron and the hadron. $K = \sigma_y^*/\sigma_x^*$ is the aspect beam size ratio at the IP, where the beam sizes of electron and hadron beams are assumed fully matched. The factor H describes the luminosity modification due to the hourglass effect and crossing angle. For maximum luminosity one needs high beam-beam parameters, flat beams at the IP and as many bunches as allowed by average beam current limits or bunch spacing related limits.

For the EIC design, collision parameters of unequal species for each beam are chosen as if they would collide

* Work supported by the U.S. Department of Energy, Office of Science under contracts DE-SC0012704 and DE-AC05-06OR23177.
† yluo@bnl.gov

ISBN: 978-3-95450-253-0 ISSN: 2673-5571 doi:10.18429/JACoW-HB2023-MOA3I3

HIGH-POWER TARGETRY AND THE IMPACT INITIATIVE AT PAUL SCHERRER INSTITUTE

D. Kiselev†, Paul Scherrer Institut, 5232 Villigen PSI, Switzerland

Abstract

The main challenges to operate a high power target include heat dissipation and radiation damage. The latter refers to the damage of the material. Since the breakdown of the material depends on the operation temperature and other conditions, like the material treatment before irradiation, it is difficult to predict.

To reduce failures, target operation parameters and beam properties have to be monitored carefully. After the failure of the neutron spallation target (SINQ) in 2016, several improvements at the HIPA (High intensity Proton Accelerator) beam line at Paul Scherrer Institute (PSI), as well as the target installation, were implemented.

MW beams are not a prerequisite for the need of high power targets. This is the case at one of the two new target stations within the IMPACT initiative at PSI. One target station will produce radionuclides for research in cancer therapy, while the other will improve the surface muon rate by a factor of 100 for experiments in particle and material physics.

In this report, strategies for successful operation of high-power targets are shown. Furthermore, the IMPACT initiative at PSI, with focus on the two planned target stations, will be presented.

MOTIVATION AND CHALLENGES

Most experimental target stations are overbooked, i.e., the demand for beam time based on proposals submitted far exceeds the beam time available. In addition, measurements are repeated, aiming for better statistics, which means that the time for data taking would increase significantly without an increase of particle fluxes. The worldwide experimental quest for new physics beyond the standard model, which aims to lower the upper cross-section limit of forbidden reactions, is a good example thereof. Nowadays, state-of-the-art detectors and electronics are capable to process high data rate efficiently, with small dead time, and data analyses on high-performance computers can cope with the large amount of data collected.

The demand for higher particle fluxes leads to the development of more powerful accelerators, planned from the beginning or later as an upgrade. Figure 1 illustrates this trend. Many accelerators worldwide announced a major upgrade or provide increased power with respect to its initial design value. SNS was originally targeted to 1.4 MW, however, recently reached 1.7 MW, a world record [1]. Further, SNS envisaged a challenging power upgrade towards 2.8 MW in the PPU project (Proton Power Upgrade) [2]. While J-PARC and CSNS are in the process of gradually

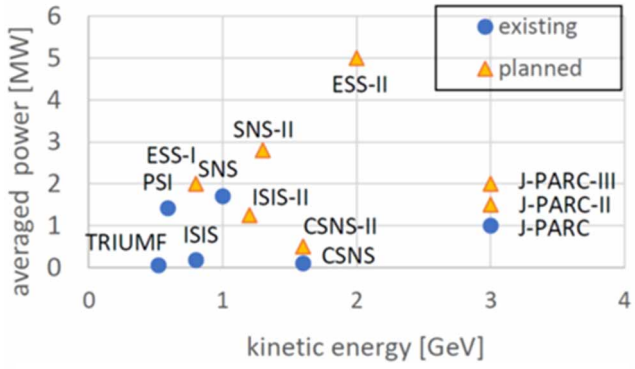

Figure 1 Accelerators with high-power targets.

ramping up their power, ISIS, too, has major plans for a upgrade. According to the ISIS-II roadmap, it might be a new stand-alone facility or a facility upgrade which reuses as much existing ISIS infrastructure as possible [3].

High-power accelerators require high-power targets (HPT) for efficient use of the power. The operation of such HPTs is a challenge. As these targets are operating at the limit of feasibility, the beam properties have to be carefully monitored to avoid target failure due to deviation from the nominal beam power distribution. Such a situation could likely lead to overheating and damage of the target. If a critical deviation is detected, a fast interlock system (machine protection system = MPS) has to quickly stop the beam to avoid damage. At HIPA [4, 5], PSI, the time between detection of a beam state outside predefined boundaries and switching off the beam takes less than 10 ms [6]. Reliable beam diagnostics is also needed, as well as enough additional monitors to ensure redundancy, such that monitors, which fail completely or show wrong signals, are detected at an early stage. HPTs also often require a wider distribution of the beam power on the target to reduce the power deposition per surface area. The simplest method is to enlarge the Gaussian beam profile, which is the default beam shape provided by most accelerators, using two quadrupoles. However, the Gaussian is not optimal due to its power concentration in the centre. A rectangular profile is ideal, however, it requires space for a couple of higher-order magnets like sextupoles, octupoles or a combination of them to form the Gaussian beam to a rectangular profile. An alternative is wobbling or painting a beam of small or medium size. For this, two magnets are needed to bend the beam in horizontal and vertical directions, respectively. Often, Lissajous figures are used to fill a profile as homogenously as possible. In Fig. 2 an example is shown. Depending on the size of the beam and the target

† Daniela.Kiselev@psi.ch

ISBN: 978-3-95450-253-0 ISSN: 2673-5571 doi:10.18429/JACoW-HB2023-MOA4I1

DESIGN OF A FIXED-FIELD ACCELERATING RING FOR HIGH POWER APPLICATIONS*

S. Machida†, STFC Rutherford Appleton Laboratory, Didcot, UK

Abstract

A fixed field accelerating ring has an advantage to achieve high beam power over conventional ring accelerators. It would be also a sustainable option as a future proton driver. First we will look back to the historical background of high power accelerator developments. We will then discuss how we achieve the high power beam and critical design issues.

INTRODUCTION

Making the CW beams is the most effective way to increase the average beam current and thus the beam power. That is a cyclotron's way of operation where all the hardware is running in a DC mode. Injection, acceleration and extraction can be done simultaneously. Once some of the hardware has to be pulsed, an accelerator cycle is dictated by that timing. Injection, acceleration and extraction no longer take place simultaneously. Usually acceleration is the major part in a cycle. The average beam current is reduced to a fraction of the whole cycle, namely the injection duration, which is relatively small. It is hard to recover the same average current by increasing the peak current during injection.

When people realised that RF frequency modulation is needed to go beyond the non-relativistic regime, from an isochronous cyclotron to a synchrocyclotron or a synchrotron, reduction of the average beam current was a big issue. Nevertheless, a history tells that a synchrotron becomes the major type of ring accelerators because it is easier to increase the beam energy than any other type of accelerators. A synchrotron can compensate the reduction of the average beam current to some extent by its higher energy. Note that the beam power is a product of the average beam current and the beam energy. It is interesting to compare the beam power of the PSI cyclotron which is a CW accelerator gives around 2 MW with 590 MeV while SNS and J-PARC RCS which are a pulsed ring accelerator give 1 to 1.4 MW with 1 GeV (SNS) and 3 GeV (J-PARC RCS).

There was another method to recover a reduction of the average beam current proposed in the early stage of synchrotron developments. That is the invention and development of a Fixed Field Alternating Gradient Accelerator (FFA) at Midwestern Universities Research Association (MURA) [1]. They accepted that an accelerator had to operate in a pulsed mode when the beam energy goes into the relativistic regime. They found, however, there is a way to reduce the size of a ring accelerator compared with an isochronous cyclotron or a synchrocyclotron without using the magnet ramping. The primary benefit of this scheme is that the whole operation cycle can be very high such as 1 kHz as long as enough RF power is provided and RF frequency is modulated fast, that is much easier than the magnet ramping. Fast acceleration increases the fraction of injection and thus the higher average beam current.

A proposal at MURA using the FFA concept did not go further mainly because it was so novel. More than 20 years later, however, an FFA drew an attention as a proton driver of a spallation neutron source. The optimum energy of spallation neutron production is around 1 to 3 GeV, that is above the energy range of a cyclotron, but not high compared with other synchrotrons especially for energy frontier particle physics research. On the other hand, the beam power must be higher than any accelerator previously built. As a spallation neutron source, the beam has to be pulsed. Considering all above, an FFA seemed to be the right choice. The proposal is called ASPUN that was studied at Argonne National Laboratory in the early 1980s' [2]. Unfortunately the project ended with a paper study only.

About 10 years later, another project to use an FFA as a proton driver for a spallation neutron source started. That was a part of European Spallation Source (ESS) project in the early 1990s' [3]. At that time, two different configurations were studied: one is a full energy linac plus an accumulator ring to make a short pulse. The other is a relatively low energy linac plus an FFA accelerator (Fig. 1). Eventually we know a long pulse spallation source with a full energy linac only was built as ESS in Lund.

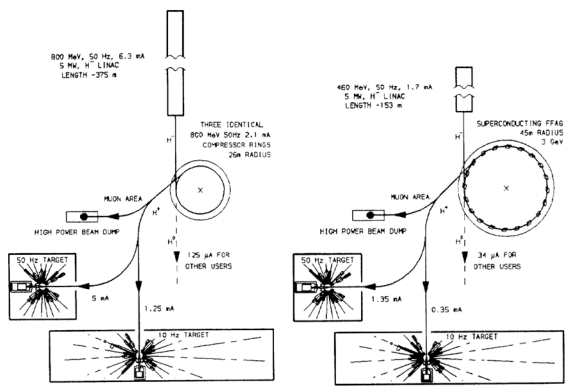

Figure 1: Two proposed schemes as ESS. (left) A full energy linac plus an accumulator ring, (right) medium energy linac plus an FFA [from Ref. [3]].

In the early 2000s', Mori and his teams built a proton FFA with a high repetition rate of 1 kHz [4]. The primary goal was to show that technology was mature enough to build a proton FFA. Computational power of the 3D magnet modelling and a magnetic alloy based RF cavity are some examples which was not available in the MURA days. On the other hand, the direction of the development since

* Work by FFA task members of ISIS-II feasibility study.
† email address shinji.machida@stfc.ac.uk

ISBN: 978-3-95450-253-0 ISSN: 2673-5571 doi:10.18429/JACoW-HB2023-TUA1I2

NEW UNDERSTANDING OF LONGITUDINAL BEAM INSTABILITIES AND COMPARISON WITH MEASUREMENTS

I. Karpov*, CERN, Geneva 23, Switzerland

Abstract

Beam instabilities driven by broad- and narrowband impedance sources have been treated separately so far. In this contribution, we present the generalised beam stability analysis based on the concept of van Kampen modes. In the presence of broadband impedance, the loss of Landau damping (LLD) in the longitudinal plane can occur above a certain single-bunch intensity. For significantly higher intensities, the broad-band impedance can drive violent radial or azimuthal mode-coupling instabilities. We have shown that the synchrotron frequency spread due to RF field non-linearity, counter-intuitively, reduces the single-bunch instability threshold. We have also demonstrated that a multi-bunch instability driven by a narrow-band impedance source can be significantly affected by LLD when adding broad-band impedance. These findings are supported by macroparticle simulations and beam observations in the Super Proton Synchrotron and the Large Hadron Collider at CERN.

INTRODUCTION

Interaction of particle beams with the accelerator environment (described in terms of beam-coupling impedance) can lead to beam quality degradation and particle losses. Accelerator performance can be limited by single- or multi-bunch instabilities in the longitudinal plane considered here. Their mechanisms were studied with different approaches [1–24]. Another consequence of beam-impedance interaction could be undamped bunch oscillations observed in different accelerators (Tevatron [25], RHIC [26], SPS [27], and LHC [28]). Usually, they are attributed to the loss of Landau damping (LLD) [1, 2, 4, 6, 7, 29–35], but an alternative theory also exists (soliton solutions of nonlinear equations [26]).

Synchrotron particle oscillations can be described as van Kampen modes [36, 37], which were introduced to accelerator physics in [7]. They represent incoherent synchrotron oscillations as well as undamped or even unstable coherent modes emerged above a certain intensity threshold. The first set of equations to evaluate the stability of bunched beams was proposed in [1]. In general, it has to be solved numerically for a specific stationary longitudinal particle distribution function $\mathscr{F}$ and impedance Z. Under certain assumptions, however, the Lebedev equation [1] allows us to derive the analytical expression for thresholds of coupled-bunch instability (CBI) [10, 38], LLD [35], and generalised multi-bunch instability [39, 40].

A method of solving the linearized Vlasov equation numerically was proposed in [13]. It requires the special ansatz of the perturbed distribution function to convert the Sacherer equation [3] into an eigenvalue problem. This method was originally used for the analysis of single-bunch instabilities in the presence of the potential-well distortion (PWD) revealing a new mechanism of radial mode-coupling instability [13]. Later it was applied to LLD studies [33, 34].

This contribution summarises recent works on LLD [35], single-bunch instabilities in the CERN Super Proton Synchrotron (SPS) [41], and the impact of LLD on multi-bunch beam stability [39, 40].

LOSS OF LANDAU DAMPING

Landau damping of an infinitesimally small perturbation can be understood as the phase mixing of van Kampen modes [7, 33]. Interacting with accelerator impedance, their frequencies are modified as bunch intensity changes. Above a certain threshold, a mode leaves the band of incoherent synchrotron frequencies becoming an undamped coherent mode. This intensity corresponds to the LLD threshold, which is discussed in the following subsection.

Threshold of Loss of Landau Damping

We considered a bunch of particles in a stationary single-RF bucket and dominating inductive impedance above transition energy $\eta \mathrm{Im}Z/k > 0$ (or space charge below transition). The LLD threshold for the dipole mode ($m = 1$) corresponds to a bunch intensity when the coherent frequency, Ω, equals the maximum incoherent frequency of the bunch. According to [35] the LLD threshold in terms of the number of particles in the bunch, N_p, is given by

$$N_{\mathrm{LLD}} = \frac{V_0}{qh\omega_0}\left[\sum_{k=-\infty}^{\infty} G_{kk}(\Omega)\frac{Z_k(\Omega)}{k}\right]^{-1}, \qquad (1)$$

where V_0 is the RF voltage amplitude, q the electrical charge of the particles, h the harmonic number, $f_0 = \omega_0/2\pi$ the revolution frequency, G_{kk} the elements of the beam transfer matrix [42], and $Z_k(\Omega) = Z(k\omega_0 + \Omega)$ the impedance at frequency $k\omega_0 + \Omega$ with $k = \pm 1, \pm 2, ...$

We analysed the binomial family of the stationary distribution function,

$$\mathscr{F}(\mathscr{E}) \propto (1 - \mathscr{E}/\mathscr{E}_{\max})^{\mu}, \qquad (2)$$

with μ defining the bunch shape and $\mathscr{E}$ being the energy of the synchrotron oscillations. The elements G_{kk} at the LLD threshold can be computed analytically by deploying a short bunch approximation (half bunch length in radians $\phi_{\max} \ll \pi$):

$$G_{kk} \approx -i\frac{16\mu(\mu+1)}{\pi\phi_{\max}^4}\left[1 - {}_1F_2\left(\frac{1}{2}; 2, \mu; -y^2\right)\right]. \qquad (3)$$

* ivan.karpov@cern.ch

ISBN: 978-3-95450-253-0 ISSN: 2673-5571 doi:10.18429/JACoW-HB2023-TUA1C1

MAJOR LONGITUDINAL IMPEDANCE SOURCES IN THE J-PARC MAIN RING

Aine Kobayashi* for the MR impedance working group, KEK, Tokai, Ibaraki, Japan

Abstract

Beam intensity upgrade at the Japan Proton Accelerator Research Complex main ring is ongoing. Beam instability is controlled by feedback systems in longitudinal and transverse directions. However, in recent years, microbunch structures have been observed during debunching, inducing electron cloud, and transverse beam instability, which is a topic of concern. Thus, the cause of this problem must be identified and countermeasures must be taken accordingly. A summary of model and measurement comparisons are reported for the major impedances RF-cavities, FX-kickers, and FX-septum magnets.

INTRODUCTION

The Japan Proton Accelerator Research Complex (J-PARC) is a high-intensity proton beam accelerator facility. It consists of 400 MeV linac [1], 3 GeV rapid cycling synchrotron [2], and 30 GeV main ring (MR) synchrotron [3]. The MR supplies beams to the neutrino and hadron experimental facilities with fast (FX) and slow (SX) extractions and increases the beam power, aiming for operation at 1.3 MW in FX operation and ≧100 kW in SX operation [4].

The amount of beam loss tolerated in MR is determined by the residual dose and the limited beam intensity so it does not exceed that value. We are preparing to increase the beam intensity by adding an acceleration cavity and upgrading hardware, such as extraction equipment. However, these upgrades can lead to beam instability and preventive measures must be put in place.

Currently, longitudinal beam instability in the debunching beam has become a problem in SX operation. Microbunch structures with beam instabilty were generated at the beginning of the debunching operation. Possibly, these structures were closely related to the generation of electron clouds, transverse beam instability, and beam loss. Therefore, we are working on investigating and considering countermeasures for these concerns. This could be a problem in future FX operation candidates with time structures with low peak currents. Attempts were made to address these problem through beam manipulation, such as RF gymnastics [5], but this is not a sufficient solution. The cause of the beam instability must be investigated and countermeasures must be taken. Currently, we aim for the reduced longitudinal impedance Z_L/n to be $< 0.5\ \Omega$ in MR [6]. This value considers the Keil-Schnell criterion [7] at SX (100 kW) and the values of measured devices.

To understand the impedance of the device, measurements [8] have been made using the stretched wire method [9] and simulations have been performed using the CST wakefield solver [10].

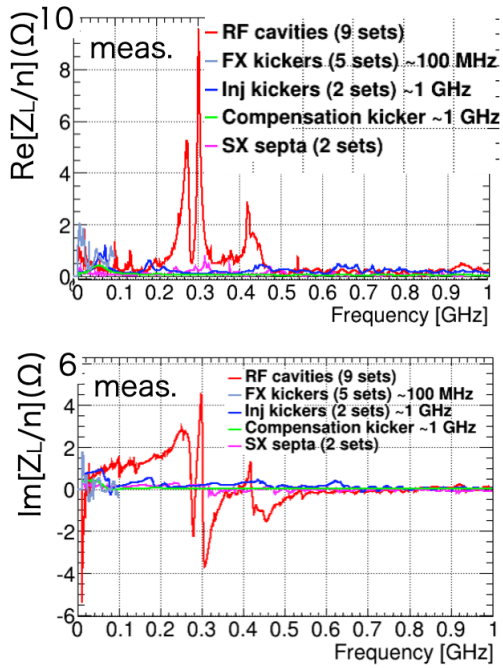

Figure 1: The major longitudinal impedance around MR.

RF CAVITIES

The MR synchrotron had seven fundamental accelerating cavities and two second-harmonic cavities to reduce space-charge effects. In the high-repetition operation started in FY2022, beam operation was started with eight accelerating cavities (fundamental) and two second harmonic cavities. To further increase the beam repetition rate, we planned to increase the number of accelerating cavities (fundamental) to 11 [4]. The accelerating cavities used in MR were made of metallic magnetic materials to achieve a high accelerating field gradient. Structurally, the cavities with four or five accelerating gaps are installed in the accelerator ring, but one gap is short-circuited in the five-gap cavity, and all cavities are basically used as four-gap cavities for beam operation. Figure 1 shows the longitudinal impedance around the ring estimated from the measurement results. From these measurements, the accelerating cavity impedance can be considereda significant contributor to the longitudinal impedance of the ring.

Simulation Model

We investigated the origin of the major resonances distributed in the 300 MHz-range shown in Fig. 1 through measurements [8] and simulations [11]. Fig. 2 shows a simula-

* aine.kobayashi@kek.jp

ISBN: 978-3-95450-253-0 ISSN: 2673-5571 doi:10.18429/JACoW-HB2023-TUC1I1

MULTI-BEAM OPERATION OF LANSCE ACCELERATOR FACILITY

Y. K. Batygin, Los Alamos National Laboratory, Los Alamos, NM, USA

Abstract

The Los Alamos Neutron Science Center (LANSCE) accelerator facility has been in operation for 50 years performing important scientific support for national security. The unique feature of the LANSCE accelerator facility is multi-beam operation, delivering beams to five experimental areas. The near-term plans are to replace obsolete and almost end-of-life systems of the LANSCE linear accelerator with a modern 100-MeV Front End with significant improvement in beam quality. This paper summarizes experimental results obtained during the operation of the LANSCE accelerator facility and considers plans to expand the performance of the accelerator for near- and long-term operations.

LANSCE ACCELERATOR FACILITY

The 800 MeV LANSCE accelerator (formerly known as the Los Alamos Meson Physics Facility, LAMPF) started routine operation in 1972 with an average proton beam current of 1 mA delivering 800 kW of average beam power for meson physics research and provided high-power proton beam for a quarter century [1]. Within 50 years of operation, the accelerator facility was continuously upgraded and modified to support the Laboratory's national security mission and provide needs in fundamental nuclear physics.

The layout of the existing LANSCE accelerator facility is shown schematically in Fig. 1. The accelerator is equipped with two independent injectors for H^+ and H^- beams. Each injector has a Cockcroft-Walton type generator and an ion source to produce either positively charged protons (H^+) or negatively charged hydrogen ions (H^-) with a final energy of 750 keV. Two independent beamlines deliver H^+ and H^- beams, merging at the entrance of a 201.25 MHz Drift Tube Linac (DTL). The DTL performs acceleration up to the energy of 100 MeV. After the DTL, the Transition Region beamline directs the 100 MeV proton beam to the Isotope Production Facility (IPF), while H^- beam is accelerated up to the final energy of 800 MeV in an 805 MHz Coupled Cavity Linac (CCL). The H^- beams, created with different time structures imparted by a low-energy chopper are distributed in the Switch Yard to four experimental areas: Lujan Neutron Science Center equipped with the Proton Storage Ring (PSR), Weapons Neutron Research (WNR) Facility, Proton Radiography Facility (pRad), and Ultra-Cold Neutron Facility (UCN). The accelerator operates at 120 Hz repetition rate with 625 μs pulse length. Parameters of all beams are presented in Table 1.

batygin@lanl.gov

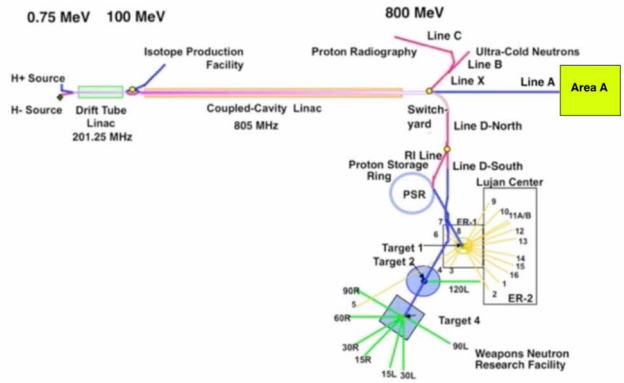

Figure 1: Overview of the LANSCE accelerator and user facility complex.

Table 1: Beam Parameters of LANSCE Accelerator

Area	Rep. Rate (Hz)	Curent/ Bunch (mA)	Average Current (μA)	Average Power (kW)
Lujan	20	10	100	80
IPF	100	4	250	25
WNR	100	25	4.5	3.6
pRad	1	10	<1	<1
UCN	20	10	10	8

BEAM TIME STRUCTURE

A unique feature of the LANSCE accelerator facility is the acceleration of four H^- beams (differing in time structure) and one H^+ beam. This is achieved by a combination of chopper and RF bunchers. Figure 2 illustrates the time structure of LANSCE beams. Figure 3 shows the time pattern of beam cycles. The H^- chopper, which creates various time structures of H^- beams, is located downstream of the H^- Cockcroft-Walton column. It consists of two traveling-wave helix electrodes, which apply a vertical kick to the beam. The chopper is normally energized so that no beam gets through. An electrical pulse of various lengths between 36 - 290 ns travels along the chopper allowing the un-chopped part of the beam pulse to pass through. The minimum width of the chopper pulse is determined by the chopper's rise time, which is about 10 ns. Following the chopper, the leading and trailing edges of the beam are bent vertically.

The Lujan Center receives 20 Hz x 625 μs pulses of H^- beam with 10 mA/bunch peak current, corresponding to an average current of 100 μA and an average beam power of 80 kW (see Fig. 3a). This beam is chopped within a time

ISBN: 978-3-95450-253-0 ISSN: 2673-5571 doi:10.18429/JACoW-HB2023-TUC1C1

EFFECT OF THREE-DIMENSIONAL QUADRUPOLE MAGNET MODEL ON BEAM DYNAMICS IN THE FODO LINE AT THE SPALLATION NEUTRON SOURCE BEAM TEST FACILITY*

T. E. Thompson†, A. Aleksandrov, T. Gorlov, K. Ruisard, A. Shishlo
ORNL, Oak Ridge, Tennessee, USA

Abstract

The research program at the Spallation Neutron Source (SNS) Beam Test Facility (BTF) focuses on improving accelerator model accuracy. This study explores the effect of two different models of permanent magnet quadrupoles, which comprise a 9.5-cell FODO line in the BTF. The more realistic model includes all higher-order terms, while the simple, in use model, is a perfect quadrupole. Particular attention is paid to high-amplitude particles to understand how the choice of quadrupole model will affect beam halo distributions. In this paper, we compare particle tracking through a FODO line that contains only linear terms - a perfect quadrupole model - to a full 3D model.

INTRODUCTION

The Beam Test Facility (BTF) at the Spallation Neutron Source (SNS) is a functional duplicate of the Front End of the SNS accelerator. Current research at the BTF is focused on beam distribution, including full 6D measurements, and halo growth during beam transport. Of particular interest is how halo grows within a FODO line and accurately simulating this growth.

The FODO line at the Beam Test Facility consists of 19 permanent magnet quadrupoles [1]. Current simulations at Oak Ridge National Laboratory (ORNL) model the FODO line as perfect quadrupoles. However, in the aperture region of FODO lines it is known that the magnetic field becomes complex and differs from a perfect quadrupole. Understanding how much of an effect this difference causes is important for creating accurate simulations of halo distributions.

Recently, we developed an analytic model of the full magnetic field of the quadrupoles in the FODO line. The magnets being oriented in a Halbach Array made this possible as the field for each permanent magnet can be calculated and then combined with the fields of the other magnets. This analytic model along with the model for a perfect quadrupole can be used to create simulated quadrupoles for comparison. The quadrupole fields are similar (Fig. 1) but their field strengths increase differently in the transverse plane. This paper examines how the differences between these magnetic fields affect particle transport in the BTF FODO line.

* This material is based upon work supported by the U.S. Department of Energy, Office of Science, Office of High Energy Physics. This work has been autherd by UT-Battelle, LLC under Contract No. DE-AC05-00OR22725 with the U.S. Department of Energy. This research used resources at the Spallation Neutron Source, a DOE Office of Science User Facility operated by the Oak Ridge National Laboratory.
† thompsonte@ornl.gov

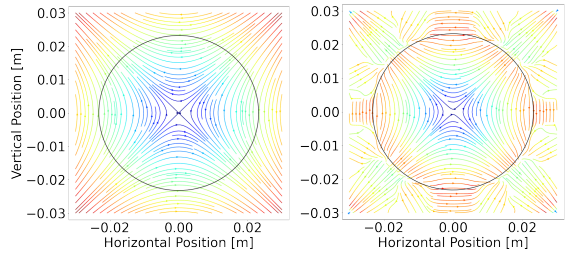

Figure 1: Magnetic field models of a perfect quadrupole (left) and full analytic solution quadrupole (right). The black circle in each shows the beam pipe aperture.

VIRTUAL FODO LINE

The strengths of the magnet models were scaled to create a realistic simulation of the BTF FODO lines. They were scaled to match the design integrated field strengths in the 1.817 T BTF magnets (Fig. 2)[1].

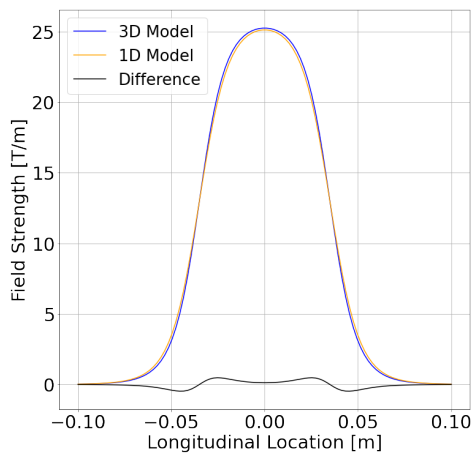

Figure 2: Longitudinal field profile of analytic models.

After scaling to match the strengths of the BTF magnets, two virtual FODO lines were created. Each line having the 19 quadrupoles in the same focusing order as the BTF with the same quadrupole length, spacing, and aperture as the design BTF FODO line[2].

TRACKING

The Runge-Kutta (RK4) method was used within PyORBIT[3] to track the particles through the virtual FODO lines using each particle's position and momentum. The particles were initially arranged in a circle in the normalized phase space then transformed using the matched Twiss parameters

ISBN: 978-3-95450-253-0 ISSN: 2673-5571 doi:10.18429/JACoW-HB2023-TUC1C2

THE IMPACT OF HIGH-DIMENSIONAL PHASE SPACE CORRELATIONS ON THE BEAM DYNAMICS IN A LINEAR ACCELERATOR*

A. Hoover†, K. Ruisard, A. Aleksandrov, A. Zhukov, S. Cousineau, A. Shishlo
Oak Ridge National Laboratory, Oak Ridge, TN, USA

Abstract

Hadron beams develop intensity-dependent transverse-longitudinal correlations within radio-frequency quadrupole (RFQ) accelerating structures. These correlations are only visible in six-dimensional phase space and are destroyed by reconstructions from low-dimensional projections. In this work, we estimate the effect of artificial decorrelation on the beam dynamics in the Spallation Neutron Source (SNS) linac and Beam Test Facility (BTF). We show that the evolution of a realistic initial distribution and its decorrelated twin converge during the early acceleration stages; thus, low-dimensional projections are probably sufficient for detailed predictions in high-power linacs.

INTRODUCTION

Predicting halo formation in linear hadron accelerators is complicated by incomplete knowledge of the beam's initial distribution in six-dimensional phase space [1–3]. Denoting the positions by x, y, z and momenta by p_x, p_y, p_z, the distribution function $f(x,p_x,y,p_y,z,p_z)$ is typically reconstructed from the set of orthogonal two-dimensional projections $\{f(x,p_x),f(y,p_y),f(z,p_z)\}$:

$$f(x,p_x,y,p_y,z,p_z) = f(x,p_x)f(y,p_y)f(z,p_z). \quad (1)$$

Alternatively, if only the covariance matrix is known, it is common to assume an analytic, ellipsoidally symmetric distribution function. It is unclear whether such approximations are sufficient to predict the detailed beam evolution at the halo level in high-power linear accelerators.

The research program at the Spallation Neutron Source (SNS) Beam Test Facility (BTF) aims to predict halo formation over a short distance. The BTF contains a replica of the SNS linac front-end, including a negative hydrogen ion source, electrostatic low-energy beam transport (LEBT), and 402.5 MHz radio-frequency quadrupole (RFQ). The medium-energy beam transport (MEBT) is similar to the SNS but has no rebunching cavities and is followed by a 9.5-cell FODO transport line, where halo is expected to form. A suite of high-dimensional and high-dynamic-range phase space diagnostics are located at both ends of the MEBT [4].

Previous work at the BTF has focused on reconstructing and visualizing the phase space distribution at the MEBT entrance [5–9]. These studies have unveiled high-dimensional, intensity-dependent correlations between phase space coordinates. One way to investigate the origin of these features is to simulate the upstream beam evolution. The distribution in the LEBT cannot be measured in the BTF, but we have access to older measurements of $\{f(x,p_x),f(y,p_y)\}$ from a similar ion source [6]. By propagating samples from this uncorrelated, unbunched LEBT distribution through the RFQ and MEBT, we obtain a "model" distribution that can be compared to direct measurements.

We have evidence that the model distribution is realistic — the RFQ and MEBT simulations capture the essential beam dynamics. It follows that we can use the model distribution to estimate the impact of artificial *decorrelation* (see Eq. (1)) on the beam evolution. In this paper, we summarize our comparisons of the model and measured distributions. We then estimate the influence of the relevant high-dimensional features on the beam evolution in the BTF and as well as in the SNS linac. We conclude that reconstructions from two-dimensional measurements, as in Eq. (1), are probably sufficient for detailed predictions in high-power linacs.

PARMTEQ VS. REALITY

We use transverse slits, a dipole-slit energy spectrometer, and a bunch shape monitor (BSM) to reconstruct the phase space distribution in the MEBT, 1.3 meters past the RFQ. Six-dimensional measurements still have quite low resolution ($\approx 10^6$ points) and dynamic range ($\approx 10^2$) since their first demonstration (although these numbers are expected to improve in the near future [10]). Four- and five-dimensional measurements are high-resolution alternatives that capture most correlations of interest. We refer the reader to Refs. [6, 7, 9] for details. Reference [6] also contains a detailed description of the PARMTEQ [11] model and LEBT distribution used in our RFQ simulations.

Figure 1 compares the low-dimensional projections of the model distribution to a five-dimensional measurement. Note that the RFQ model predicts a 42 mA beam current, higher than the 25 mA measured current. Although the predictions are incorrect by a large margin, normalizing both data sets to unit covariance brings the predicted projections fairly close to the measured projections. From now on, we let x, p_x, y, p_y, z, p_z represent these normalized coordinates.

A striking conclusion drawn from the BTF measurements is that various higher dimensional projections of the six-

* This manuscript has been authored by UT- Battelle, LLC under Contract No. DE-AC05-00OR22725 with the U.S. DOE. The US government retains and the publisher, by accepting the article for publication, acknowledges that the US government retains a nonexclusive, paid-up, irrevocable, worldwide license to publish or reproduce the published form of this manuscript, or allow others to do so, for US government purposes. DOE will provide public access to these results of federally sponsored research in accordance with the DOE Public Access Plan (http://energy.gov/downloads/doe-public-access-plan).
† hooveram@ornl.gov

ISBN: 978-3-95450-253-0 ISSN: 2673-5571 doi:10.18429/JACoW-HB2023-TUA2I1

Xsuite: AN INTEGRATED BEAM PHYSICS SIMULATION FRAMEWORK

G. Iadarola*, R. De Maria, S. Łopaciuk, A. Abramov, X. Buffat, D. Demetriadou,
L. Deniau, P. Hermes, P. Kicsiny, P. Kruyt, A. Latina, L. Mether, K. Paraschou,
G. Sterbini, F. F. Van Der Veken, CERN, Geneva, Switzerland
P. Belanger, TRIUMF, Vancouver, Canada
P. Niedermayer, GSI, Darmstadt, Germany
D. Di Croce, T. Pieloni, L. Van Riesen-Haupt, M. Seidel, EPFL, Lausanne, Switzerland

Abstract

Xsuite is a newly developed modular simulation package combining in a single flexible and modern framework the capabilities of different tools developed at CERN in the past decades, notably Sixtrack, Sixtracklib, COMBI and PyHEADTAIL. The suite consists of a set of Python modules (Xobjects, Xpart, Xtrack, Xcoll, Xfields, Xdeps) that can be flexibly combined together and with other accelerator-specific and general-purpose python tools to study complex simulation scenarios. The code allows for symplectic modeling of the particle dynamics, combined with the effect of synchrotron radiation, impedances, feedbacks, space charge, electron cloud, beam-beam, beamstrahlung, and electron lenses. For collimation studies, beam-matter interaction is simulated using the K2 scattering model or interfacing Xsuite with the BDSIM/Geant4 library. Tools are available to compute the accelerator optics functions from the tracking model and to generate particle distributions matched to the optics. Different computing platforms are supported, including conventional CPUs, as well as GPUs from different vendors.

INTRODUCTION

CERN has a long tradition in the development of software tools for beam physics in circular accelerators. In particular, over the years it has provided the following tools to the user community:

- MAD-X, which has become a standard to describe accelerator lattices, to perform optics calculation, design, and tracking simulations [1];
- SixTrack, a fast tracking program used mainly for long single-particle tracking simulations [2];
- SixTracklib, a C/C++ library for single-particle tracking compatible with Graphics Processing Units (GPUs) accelerators [3];
- COMBI, a simulation code for the simulation of beam-beam effects using strong-strong modelling [4];
- PyHEADTAIL, a Python toolkit for the simulation of collective effects (impedance, feedbacks, space charge, and e-cloud) [5].

These tools were developed over several years, mostly by independent teams. Although they provide very advanced features in their respective domains, with the exception of PyHEADTAIL and SixTracklib [6–8], their design does not allow effectively combining them for integrated simulations involving complex heterogeneous effects.

Several of these simulations are very well suited for computation acceleration based on GPUs. However, it would be cumbersome to retrofit such a capability in the existing codes.

Furthermore, some of the tools provide their own user interface, consisting in some cases in input/output text files, in some others in an ad-hoc scripting language like in the case of MAD-X. In contrast to this approach, the present de-facto standard in scientific computing is to provide software tools in the form of Python packages that can be easily used in notebooks or integrated within more complex Python codes. This allows leveraging an ever-growing arsenal of general-purpose Python libraries (e.g. for statistics, linear algebra frequency analysis, optimization, data visualization), which is boosted by substantial investments from general industry, especially for applications related to data science and artificial intelligence.

Based on these considerations, in 2021 the Xsuite project [9] has been launched to bring the know-how built in developing and exploiting the aforementioned codes into a modern Python toolkit for accelerator simulations, which is designed for seamless integration among the different components and for compatibility with different computing platforms, including multicore CPUs and GPUs from different vendors.

Xsuite has by now reached a mature stage of development and has already been adopted as "production tool" for several types of simulations across a quite large user community.

In this contribution, we will first describe the overall code structure and development strategy and then illustrate the main features and applications of Xsuite.

STRUCTURE, RESOURCES, AND DEVELOPMENT STRATEGY

Xsuite is composed of six modules:

- **Xtrack**: provides a single-particle tracking engine, featuring thick and thin maps for a variety of accelerator components, together with tools to load and save beam line models, track particles ensembles, characterize the beamline optics;
- **Xpart**: provides functions for the generation of particle distributions matched to the beamline optics;

* giovanni.iadarola@cern.ch

ISBN: 978-3-95450-253-0 ISSN: 2673-5571 doi:10.18429/JACoW-HB2023-TUA2I2

COMMUNITY MODELING TOOLS FOR HIGH-BRIGHTNESS BEAM PHYSICS

C. Mitchell * †, A. Huebl, J. Qiang, R. Lehe, M. Garten, R. Sandberg, J-L. Vay
Lawrence Berkeley National Laboratory, Berkeley, CA, USA

Abstract

Pushing accelerator technology toward operation with higher intensity hadron beams is critical to meet the needs of future colliders, spallation neutron sources, and neutrino sources. To understand the dynamics of such beams requires a community effort with a comprehensive approach to modeling, from the source to the end of the beam lifetime. One needs efficient numerical models with high spatial resolution and particle statistics, insensitivity to numerical noise, and the ability to resolve low-density halo and particle loss. To meet these challenges, LBNL and collaborators have seeded an open ecosystem of codes, the Beam pLasma & Accelerator Simulation Toolkit (BLAST), that can be combined with each other and with machine learning frameworks to enable integrated start-to-end simulation of accelerator beamlines for accelerator design. Examples of BLAST tools include the PIC codes WarpX and ImpactX. These codes feature GPU acceleration and mesh-refinement, and have openPMD standardized data I/O and a Python interface. We describe these tools and the advantages that open community standards provide to inform the modeling and operation of future high-brightness accelerators.

INTRODUCTION

The modeling of charged-particle beams plays a critical role in accelerator design and operation. The needs of high-intensity and high-brightness hadron facilities pose a special challenge to accelerator beam dynamics modeling, due in part to the broad range of physics effects at interplay. For example, high spatial resolution and good particle statistics are required to model and predict low-density beam halo formation [1–3], to understand intensity-dependent beam loss mechanisms [4], to understand space charge induced emittance growth [5], and to model and mitigate collective instabilities [6–8]. For storage rings and colliders, the modeling of self-consistent collective effects in beams for large turn numbers must address the challenges of simulation artifacts (noise) and long computation times.

* This work was supported by the Director, Office of Science of the U.S. Department of Energy under Contracts No. DE-AC02-05CH11231 and DE-AC02-07CH11359. This material is based upon work supported by the CAMPA collaboration, a project of the U.S. Department of Energy, Office of Science, Office of Advanced Scientific Computing Research and Office of High Energy Physics, Scientific Discovery through Advanced Computing (SciDAC) program. This research used resources of the National Energy Research Scientific Computing Center, a DOE Office of Science User Facility supported by the Office of Science of the U.S. Department of Energy under Contract No. DE-AC02-05CH11231 using NERSC award HEP-ERCAP0023719.
† ChadMitchell@lbl.gov

To address these challenges effectively, a community approach is required. In addition to sharing expertise regarding physics and algorithm development, collaborative code development based on shared standards and common code interfaces can enhance existing workflows. For example, in start-to-end modeling of complex multi-stage accelerator facilities, one typically must chain multiple simulation codes, involving different numerical models, input and output formats, and user expertise. In addition, one needs reliable methods to benchmark, exchange data, and compare results from multiple simulation codes.

To model intense beams with improved fidelity over the entire beam lifetime with reasonable computing times, to enable large ensembles of simulation runs for optimization and for training of machine learning (ML) models, and to prepare for future Exascale computing systems, software must be developed and/or modernized to take advantage of state-of-the-art computer hardware, including GPUs. Examples of collaborative multi-institute code development efforts include the Collaboration for Advanced Modeling of Particle Accelerators (CAMPA) [9], the Exascale Computing project [10, 11], and HEP SciDAC-5 [12].

GOALS OF A COMMUNITY ECOSYSTEM

One primary community goal is to understand and exploit the physics of high intensity beams for improved accelerator design, using full-physics 6-D computer simulations of entire accelerator systems that incorporate all components (including any conventional and advanced concepts sections) and all pertinent physical effects and that execute quickly and reliably (“end-to-end virtual accelerators", EVAs) [13]. Furthermore, these EVAs should be able to leverage modern computing infrastructure such as HPC clusters and GPU computing and fully integrate AI/ML tools to maximize efficiency for practical applications.

One approach to this goal is through an ecosystem of interoperable modeling tools with various levels of integration and fidelity. Figure 1 illustrates a proposed example of such an ecosystem [14]. Individual components are represented as boxes with dependencies building on top of each other. The fundamental building blocks are implementations of solvers/numerical schemes, efficient I/O, parallelization, and a performance portability layer (*Math & Computer Science libraries*). Depending on this functionality, domain-specific libraries for RF, beam, or plasma modeling can be implemented (*Accelerator & Beam Toolkits*) that then act as toolkits to be combined into concrete applications. Compatibility, development productivity, usage, and quality assurance

ISBN: 978-3-95450-253-0 ISSN: 2673-5571 doi:10.18429/JACoW-HB2023-TUA2C2

RECENT ADVANCES IN THE CERN PS IMPEDANCE MODEL AND INSTABILITY SIMULATIONS

S. Joly*,[1], M. Migliorati[1,2], University of Rome 'La Sapienza', Roma, Italy
G. Iadarola, N. Mounet, B. Salvant, C. Zannini, CERN, Geneva, Switzerland
[1]also at CERN, Geneva, Switzerland
[2]also at Istituto Nazionale di Fisica Nucleare, Roma, Italy

Abstract

Transverse instability growth rates in the CERN Proton Synchrotron (PS) are studied thanks to the recently updated impedance model of the machine. Using this model, macroparticle tracking simulations were performed with a new method well-suited for the slicing of short wakes, which achieves comparable performance to the originally implemented method while reducing the required number of slices by a factor of 5 to 10. Dedicated beam-based measurement campaigns were carried out to benchmark the impedance model. Until now, the model underestimated instability growth rates at injection energy. Thanks to a recent addition to the impedance model, namely the kicker magnets' connecting cables and their external circuits, the simulated instability growth rates are now comparable to the measured ones.

INTRODUCTION

A horizontal instability appeared in the PS at injection energy on operational LHC-type beams (of longitudinal emittance $_1$ = 2 eV.s) during the gradual beam parameters ramp-up to reach LIU (LHC Injectors Upgrade project) specifications [1]. Once the instability was mitigated by correcting chromaticity, exhaustive instability growth rates measurements were performed with the aim to continue the benchmark of the post-LIU PS impedance model with beam-based measurements [2]. It turned out that the current model was not able to reproduce the instability through PyHEADTAIL [3] simulations: its growth rates were underestimated. Nonetheless, it provided valuable insight on the origin of the discrepancy and pointed to a missing impedance source. In this contribution, the transverse impedance frequency range responsible for the instability is narrowed down thanks to the measured instability intra-bunch motion. Then, a candidate impedance contribution missing in the model for this frequency range is studied: the connecting cables and external circuits of the kicker magnets. An analytical model based on the transmission line theory is derived to model this impedance contribution. Before performing macroparticles tracking simulations to assess the impact of this new contribution, a novel method to compute the wake kick in macroparticles tracking codes is proposed to speed up simulations. Finally, simulations using the updated model are compared with beam-based measurements.

* sebastien.joly@cern.ch

MEASUREMENTS OF THE FLAT BOTTOM HORIZONTAL INSTABILITY

The instability characterization and the mitigation strategies to tackle it were presented in [4]. Following the instability mitigation efforts, numerous instability growth rate measurements were performed while deactivating the transverse feedback and using a single bunch. The horizontal chromaticity was set to positive ($Q'_x = 0.6$ when the instability was observed for the first time), zero and negative values during the measurements. Simulations failed at reproducing the beam-based measurements as they underestimated the instability growth rates by a factor 5 to 10. Subsequently, an investigation started aiming at understanding the origin of this discrepancy.

Horizontal Instability Characterisation

During the measurements campaign, instability growth rates were measured as well as the instability intra-bunch motion. In the PS, the bunch centroid and intra-bunch motion can be observed by means of a wide-band pick-up. This device allows acquiring the longitudinal and transverse motion within a specified time interval spanning between a single bunch length to a revolution period. Observing in parallel the longitudinal and transverse signals allows us to identify the number of nodes in the transverse pattern, as well as a potential asymmetry between the head and the tail. The longitudinal and transverse motions of a bunch at the beginning of the exponential increase of the beam centroid were measured with the wide-band pick-up over 50 acquisitions every 3 turns. Additionally, the instability power spectrum is computed by means of a Fourier Transform using the NEFFINT [5,6] algorithm. Both the intra-bunch motion and power spectrum are displayed in Fig. 1. Each acquisition spectrum is computed and their average plotted in white dashed lines in the plots. The instability intra-bunch motion is characterized by a mode-0-like envelope (no node) featuring an asymmetry between head and tail of the bunch. Its resulting power spectrum exhibits three main peaks around 0, 1 and 3 MHz.

The peaks observed in the power spectrum might correspond to resonant modes in the impedance spectrum. As the power spectrum is the frequency domain equivalent of the transverse oscillations, it allows to quantify the frequencies of interest when overlapped with the impedance spectrum. In the following we will investigate this possibility.

ISBN: 978-3-95450-253-0 ISSN: 2673-5571 doi:10.18429/JACoW-HB2023-TUC2I2

SNS LINAC BEAM DYNAMICS: WHAT WE UNDERSTAND, AND WHAT WE DON'T*

A.P. Shishlo†, SNS, Oak Ridge National Laboratory, Oak Ridge, TN, USA

Abstract

The Spallation Neutron Source (SNS) linac accelerates H^- ions to 1.05 GeV before injecting them into the ring. The beam power on the target is 1.7 MW. The linac includes three main parts: a front-end with an ion source, radiofrequency quadrupole (RFQ), and Medium Energy Beam Transport (MEBT) section; a room temperature linac with Drift Tube Linac (DTL) and Coupled Cavity Linac (CCL) sections; and a superconducting linac (SCL). The linac has been operating since 2005. This talk discusses the beam diagnostics and simulation models used in the linac tuning and beam loss reduction efforts over the past 18 years. Considerations about future beam physics experiments and simulation software improvements are outlined.

INTRODUCTION

The Spallation Neutron Source (SNS) accelerator includes a pulsed linac which accelerates negative hydrogen ions to 1.05 GeV, a storage ring that accumulates a proton beam for 1 ms, and beam transport lines that deliver ions to the ring and protons to a liquid mercury target [1]. These protons produce neutrons in spallation reactions. The Spallation Neutron Source is a user facility that provides a reliable and predictable high-density flux of neutrons to 19 instrument stations. The minimal 90% availability goal during the scheduled production time demands an efficient operation of the complex SNS facility. An important contribution to these efforts was acquiring an empirical and model-based knowledge of the beam dynamics in the linac.

During the early stage of SNS commissioning, there was a hope to set the operational parameters of the SNS linac to their design values using computer simulation models and the available diagnostic tools. It did not happen. The biggest problem was unexpected beam loss in the superconducting section of the linac [2]. Later, it was found that the source of beam loss in the SCL was the intra-beam stripping (IBSt) mechanism [3]. This problem was solved before it was explained. The beam loss was reduced empirically by reducing the transverse focusing by 40% [2]. Since then, empirical beam loss reduction in the linac and other parts of the machine has become routine practice at the SNS. Nevertheless, we have not given up the idea of a model-based description of the beam dynamics in the linac.

This paper describes practical observations and the progress of our beam dynamics understanding since the last comprehensive overview that was presented at the HB2010 conference 13 years ago [4].

After descriptions of the linac, simulation models, and available diagnostics, the discussion will follow the classification suggested in [4]. We will talk about our success or failures in predictions and control of beam trajectories, longitudinal motion, bunch sizes and beam loss.

SNS LINAC

Different components of the SNS linac are shown in Fig. 1. All these components have different types of accelerating RF cavities. MEBT cavities are 1 RF gap cavities, and they perform longitudinal re-bunching of the beam after RFQ and matching longitudinal Twiss of the bunches to inject them into the DTL. The DTL and CCL have RF cavities with many RF gaps. The quadrupoles in the DTL cavities are permanent magnets, so transverse matching is performed in the MEBT section. The SCL has 97 RF cavities, and this is the most flexible section of the linac in terms of the cavity amplitudes and phases. The SNS linac produces 1 ms beam pulses with 38 mA peak current at 60 Hz repetition rate. Each 1 ms pulse is chopped into approximately 1000 mini pulses to provide a time structure for the ring injection. The chopping is performed before the entrance of the RFQ.

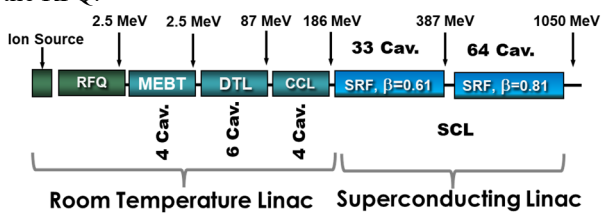

Figure 1: SNS linac.

LINAC SIMULATION CODES

Many linac simulation codes have been used at SNS during different stages of operation history, including PARMILA (the SNS was designed using this code), Trace3D, IMPACT3D, TRACK, XAL (or OpenXAL), and PyORBIT. Most of them were used in the early days of operations and power ramp-up. Lately, the most used code has been OpenXAL Online Model [5]. This code was developed initially at SNS and implements functionality similar to Trace3D, therefore it inherited all limitations of envelope simulation codes. For example, it cannot be used for beam loss calculations. The advantage of this type of code is its computational speed, which allows us to fit model parameters to real life data right in the control room. Combining this model with a graphical user interface (GUI) creates pow-

* This manuscript has been authored by UT-Battelle, LLC under Contract No. DE-AC05-00OR22725 with the U.S. Department of Energy. The United States Government retains and the publisher, by accepting the article for publication, acknowledges that the United States Government retains a non-exclusive, paid-up, irrevocable, worldwide license to publish or reproduce the published form of this manuscript, or allow others to do so, for United States Government purposes. The Department of Energy will provide public access to these results of federally sponsored research in accordance with the DOE Public Access Plan (http://energy.gov/downloads/doe-public-access-plan).
† shishlo@ornl.gov

ISBN: 978-3-95450-253-0 ISSN: 2673-5571 doi:10.18429/JACoW-HB2023-TUC2C1

BEAM PHYSICS SIMULATION STUDIES OF 70 MeV ISIS INJECTOR LINAC

S. Ahmadiannamin, A. Letchford, S. R. Lawrie, H. V. Cavanagh,
ISIS, STFC, Rutherford Appleton Laboratory, Oxfordshire, UK

Abstract

The ISIS neutron spallation source is a pioneering research infrastructure in the field of high-intensity accelerator physics, catering to scientific users. Comprising a 70 MeV injector linac and an 800 MeV Rapid cycling synchrotron with two beam targets, this facility has witnessed several upgrades in recent years, leading to enhanced transmission efficiency. Further optimization efforts are underway to ensure continuous improvement. This article focuses on beam physics simulation studies conducted on the current ISIS linac, aiming to gain a deeper understanding and analysis of various phenomena observed during routine operations and accelerator physics experimentation. By examining these phenomena, valuable insights can be obtained to inform the future development of high-efficiency injectors for ISIS-II.

INTRODUCTION

Over nearly 40 years, the ISIS spallation source, based at the Rutherford Appleton Laboratory, has consistently provided neutrons to scientists worldwide, establishing itself as a pivotal hub for research in the physical and life sciences in UK and Europe.

The accelerator comprises a 70 MeV H- injector, an 800 MeV synchrotron, and two target stations. The injector begins with an H- ion source, followed by a three-solenoid low-energy beam transport line (LEBT) and a 665 keV, four-rod Radio Frequency Quadrupole (RFQ) operating at 202.5 MHz. A Drift Tube Linac (DTL) consisting of four tanks accelerates the beam to 70 MeV [1, 2].

The layout of each section, including the ion source and RFQ, new Medium Energy Beam Transport (MEBT, to be installed), DTL, and High Energy Drift Space (HEDS), is depicted in Fig. 1.

In recent years, the ISIS machine has undergone several upgrades that have enhanced its reliability and broadened its utility for both users and accelerator physics experiments. [3, 4].

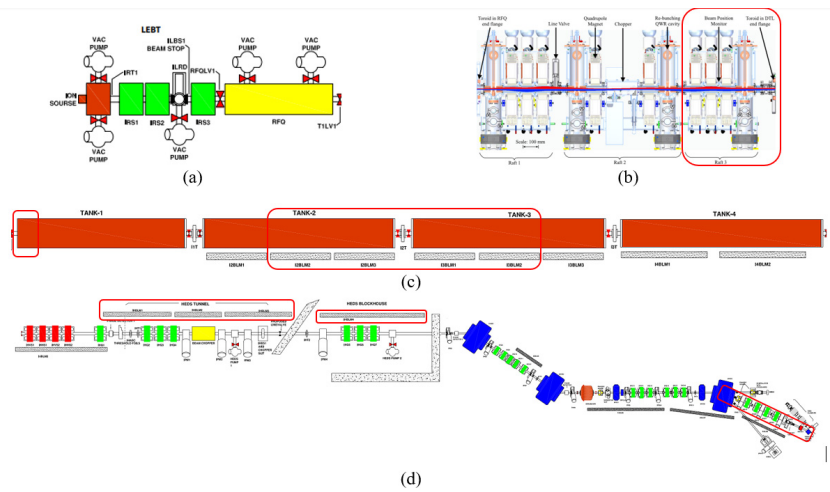

Figure 1: Schematic representation of pre-injector of ISIS (a) ion source, LEBT, RFQ; (b) MEBT design; (c) Drift Tube Linac Tanks, (d) High Energy Drift Section (HEDS) [5, 6].

The parameter settings in each section of the accelerator profoundly impact the transmission efficiency of other sections. It is crucial to view the MEBT, DTL, and HEDS sections as integrated units within the accelerator. This holistic approach enables us to gain a more comprehensive understanding of the events that occur during machine operation, particularly in the areas highlighted with red rectangles in Fig. 1, where non-negligible beam loss is routinely measured. In the subsequent sections the machine's current operational status will be outlined and compared to simulation results before and after implementing the proposed new MEBT. These simulations were conducted using the Parmila code for beam dynamic simulations [7].

SIMULATION AND MODELING

The linac comprises four amplifier chains, each consisting of three RF amplifiers, with one chain dedicated to each tank. These amplifier chains comprise a 3-kW solid-state amplifier, a 200-kW tetrode intermediate-power driver stage, and a 2 MW triode high-power output stage. Each of the output stages, delivering approximately 2 MW of power in 400 µs pulses. [8].

ISBN: 978-3-95450-253-0 ISSN: 2673-5571 doi:10.18429/JACoW-HB2023-TUC2C2

EVALUATING PyORBIT AS UNIFIED SIMULATION TOOL FOR BEAM-DYNAMICS MODELING OF THE ESS LINAC

C. Zlatanov, J. F. Esteban Müller, Y. Levinsen, N. Milas,
European Spallation Source ERIC, Lund, Sweden
A. Zhukov, A. P. Shishlo, ORNL, Oak Ridge, TN, USA

Abstract

The design of the ESS proton linac was supported by the simulation code TraceWin, a closed-source commercial software for accurate multiparticle simulations. Conversely, high-level physics applications used for beam commissioning and machine tuning rely on the Open XAL framework and its online model for fast envelope simulations. In this paper, we evaluate PyORBIT for both online modeling of the linac for machine commissioning and tuning as well as for more accurate offline simulations for beam-dynamics studies. We present the modifications done to the code to adapt it to this use case, namely porting the code to Python 3, adding an envelope tracker, and integrating with the EPICS control systems. Finally, we show the results of benchmarking PyORBIT against our current modeling tools.

INTRODUCTION

At ESS, we mainly rely on two codes for beam-dynamics simulations: the Open XAL [1] online model, an envelope code; and TraceWin [2], a powerful and feature-rich commercial code for both envelope and multiparticle simulations. This setup has worked fine, but we identified some weak points: we need to maintain two different lattice files, TraceWin is a closed-source code therefore we can't investigate implementation details or extend it, and Open XAL is written in Java while Python remains the favorite language among accelerator physicists.

PyORBIT [3] is an open-source Python code for multiparticle beam-dynamics simulations in linacs and synchrotrons that is very rich in features. It implements three different algorithms for space charge, a numerical integrator for tracking particles under arbitrary electromagnetic fields, routines for beam-coupling impedance and beam-matter interaction, as well as MPI integration for parallel computing.

Being an open-source project, we can extend PyORBIT and adapt it to our needs, for instance, by integrating it with our control system, or by adding an envelope tracker. For this reason, in this paper we are evaluating the code to use it for all beam-dynamics studies at ESS.

Furthermore, at ESS we are also involved in other projects that would require a synchrotron, for example ESSnuSB [4] and the muon collider [5]. In both cases, we are evaluating software tools for the design and simulation of synchrotrons and transfer lines, which PyORBIT can do.

PORTING CODE TO PYTHON 3

At the time when we started considering using PyORBIT at ESS, the latest version only supported Python 2.7 or older, which has been deprecated since 2020. For that reason, we focused the first efforts on porting the code to make it compatible with the latest releases of Python 3.

At the same time, we improved the build mechanism to produce a Python package that can be installed using the `pip` command, which should simplify installation and usage of the tool. In previous versions of PyORBIT, users had to build a custom Python interpreter that automatically loaded the PyORBIT libraries as built-in Python modules.

ESS LATTICE DEFINITION

PyORBIT supports several formats for describing the accelerator lattice, such as MAD-X [6], SAD [7], and a custom XML format.

At ESS, we are exploring the option to generate our lattice directly in Python. We defined a set of helper functions that simplify instantiating the sequences and elements in the lattice, as well as a function to pre-process the lattice to add the drift elements.

On Listing 1 we show a basic example of how we define a lattice in Python. In this example, we create a lattice with one section that contains one RF cavity with a single gap and a quadrupole magnet.

Listing 1: This is a snippet showing an example of a lattice defined in Python. In the snippet, we instantiate a Lattice object and add to it a sequence containing an RF cavity with one RF gap and a quadrupole magnet.

```
from typing import List
from orbit.lattice import AccLattice, AccNode
from orbit.py_linac.lattice import
    LinacAccLattice, Sequence
import lattice_builder as builder

# Instantiating a Lattice element
lattice = LinacAccLattice("ESS Lattice")
frequency = 352.21e6
maxDriftLength = 0.005

accSeqs: List[Sequence] = []

# Adding the DTL sequence
dtl_seq = builder.addSequence(
    lattice=lattice,
    accSeqs=accSeqs,
    name="DTL",
    length=33.1528945,
    bpmFrequency=7.0442e+08,
    start_position=0)

# Adding a cavity element
dtl_tank_1 = builder.addCavity(
    sequence=dtl_seq,
    name="DTL-010:EMR-Cav-001",
```

ISBN: 978-3-95450-253-0 ISSN: 2673-5571 doi:10.18429/JACoW-HB2023-TUA3I1

SPIRAL2 COMMISSIONING AND OPERATIONS

A. K. Orduz*, M. Di Giacomo, J-M. Lagniel, G. Normand
Grand Accélérateur National d'Ions Lourds (GANIL), Caen, France
D. Uriot, IRFU, CEA, Université Paris-Saclay, Gif-sur-Yvette, France

Abstract

The SPIRAL2 linac is now successfully commissioned; H^+, $^4He^{2+}$, D^+ and $^{18}O^{6+}$have been accelerated up to nominal parameters and $^{18}O^{7+}$ and $^{40}Ar^{14+}$ beams have been also accelerated up to 7 MeV/A. The main steps with 5 mA H^+, D^+ beams and with 0.6 mA $^{18}O^{6+}$ are described. The general results of the commissioning of the RF, cryogenic and diagnostics systems, as well as the preliminary results of the first experiments on NFS are presented. In addition of an improvement of the matching to the linac, the tuning procedures of the 3 Medium Energy Beam Transport (MEBT) rebunchers and 26 linac SC cavities were progressively improved to reach the nominal parameters in operation, starting from the classical "signature matching method". The different cavity tuning methods developed to take into account our particular situation (very low energy and large phase extension) are described. The tools developed for an efficient linac tuning in operation, e.g., beam energy and intensity changes are also discussed.

INTRODUCTION

The Grand Accélérateur National d'Ions (GANIL) accelerator complex in France has now two machines in operation, the cyclotrons and the SC linear accelerator SPIRAL2 [1]. Research with these beams covers mainly nuclear physics, nuclear astrophysics and astrochemistry, as well as interdisciplinary topics such as materials irradiation, nanostructuring and radiobiology. These beams are also used to irradiate electronic components and polymer membranes [2]. In contrast to the original GANIL facility comprising 5 cyclotrons in operation since 1983, the SPIRAL2 linear accelerator started delivering beams in 2021 [3].

This new accelerator has two injectors (Low Energy Beam Transport LEBT1 and LEBT2), one for heavy ions with a mass-to-charge ratio $A/Q \leq 3$ and another for H^+/ D^+ beams, with maximum intensities of 1 mA and 5 mA CW, respectively. This is followed by the LEBTc where the beam can be chopped with a frequency between 1 Hz to 100 Hz, and the intensity and emittance controlled by a set of 6 H and V slits [4, 5]. The MEBT includes three rebunchers for longitudinal beam tuning and one Single-Bunch-Selector (SBS) used for NFS experiments [6]. The SC linac is divided into a low β (0.07) and high β (0.12) section, the first one composed by 12 cryomodules, each containing 1 quarter wave resonator (QWR) designed by CEA and the second one composed by 7 cryomodules, each containing 2 QWR designed by CNRS [7, 8]. A global layout of SPIRAL2 is shown in Fig. 1. Finally, three High Energy Beam Transport (HEBT) lines drive the beam to the experimental rooms Neutron For Science (NFS) and Super Separator Spectrometer (S^3), or to the main beam dump (SAFARI) [9, 10]. The diagnostics along the linac are located in the "warm sections" between cryomodules, as shown in Fig. 1, which contain the quadrupole doublets, Beam Position Monitors (BPMs), Beam Extension Monitors (BEMs) and vacuum gauges and pumping systems [11].

Table 1 summarizes the variety of beams available in SPIRAL2. The 4th column includes the parameters of the new injector NEWGAIN which is in the construction phase and is described later in this paper.

Table 1: SPIRAL2 Beam Specifications

Parameter	H^+	D^+	$A/Q \leq 3$	$A/Q \leq 7$
A/Q	1	2	3	7
Max I (mA)	5	5	1	1
Max E (MeV/A)	33	20	14.5	7
Beam power (kW)	165	200	45	16

The linac commissioning was carried out between 2019 and 2021 at the same time as the transition to operation with first tests performed in NFS [12, 13]. H^+, D^+ and $^4He^{2+}$ beams were successfully tuned and sent through the LEBT, Radio frequency Quadrupole (RFQ), MEBT, SC linac and HEBT to SAFARI at their nominal energy of 33 MeV for H^+ and 40 MeV for D^+ and $^4He^{2+}$ with 100% transmission. Results obtained during power ramps up to 16 kW with a H^+ beam and to 10 kW with a D^+ beam showed that SPIRAL2 can operate at its full power of 165 and 200 kW, respectively [1, 14]. Losses were studied and controlled by monitoring the 27 Beam Loss Monitors (BLMs) located along the linac and HEBT as shown in Fig. 1. In addition, the beam losses were controlled by different measurements such as the transmission with ACCT and DCCT, the vacuum pressure variation with vacuum gauges, the beam position and ellipticity with BPM and the segmented ring current with the temperature of SAFARI thermocouples [15].

Since 2022, SPIRAL2 delivers beams for physics experiments, mainly to the NFS room and also to carry out the preliminary studies for the S^3 commissioning in 2024. The studies carried out were related to the heavy ions tuning and transport at low energy through the linac. This article focuses on the last commissioning results and the first year of operation of SPIRAL2. The first part presents the tuning process and the results of the first heavy ion acceleration. Finally, the second part describes the operation timetable in 2022, the development of applications to optimize the

* angie.orduz@ganil.fr

ISBN: 978-3-95450-253-0 ISSN: 2673-5571 doi:10.18429/JACoW-HB2023-TUA3I2

MEASUREMENTS OF MOMENTUM HALO DUE TO THE REDUCED RFQ VOLTAGE DURING THE LIPAc BEAM COMMISSIONING

K. Hirosawa*, A. De Franco, K. Masuda, A. Mizuno, S. Kwon,
K. Kondo, M. Sugimoto, K. Hasegawa, QST, Rokkasho, Japan
I. Moya, F. Scantamburlo, F. Benedetti[1], D. Gex, H. Dzitko, Y. Carin, F4E, Garching, Germany
I. Podadera[2], J. C. Morales Vega, IFMIF-DONES España, Granada, Spain
[1]also at CEA, France
[2]also at CIEMAT, Madrid, Spain

Abstract

The Linear IFMIF Prototype Accelerator, LIPAc, is being commissioned aiming at validating the RFQ up to 5 MeV beam acceleration. Eventually, the nominal beam of 5 MeV-125 mA in 1 ms length and 1 Hz rate pulsed mode was achieved in 2019. The beam operation has been resumed since July 2023 after long maintenance including recovery from unexpected problems in the RFQ RF system. This new phase aims at the commissioning of the full configuration except SRF linac, which is replaced by a temporary beam transport line. Focusing on the RFQ behaviour, it will be interesting to operate it at higher duty especially for longer pulses. Indeed, a beam simulation study suggested that the beam extracted from the RFQ includes considerable momentum halo when the vane voltage reduces by more than 5 percent, with a slight decrease of mean energy. It can be a potential source of quench like the mismatched beam in the cryomodule. This could be studied measuring the energy from the Time-of-Flight among multiple BPMs while monitoring beam loss around the dipole, where momentum halo should be lost. During the upcoming commissioning in the present Phase, we propose to study them by scanning the RFQ voltage.

INTRODUCTION

LIPAc The Linear IFMIF Prototype Accelerator) is the accelerator to validate low energy part up to 9 MeV where the space charge dominant region of the design of the International Fusion Material Irradiation Facility (IFMIF), which is the accelerator-based neutron source for the test facility of the materials for the fusion reactor. carried out in Rokkasho, Aomori, Japan, under the collaboration framework between EU and Japan [1]. The system, in the design, is aiming to accelerate the 125 mA deuteron beam with continuous wave (CW) [2]. We are now in the stage of intermediate of the full commissioning, called as Phase-B+ [3], which is positioned between the Phase-B, RFQ acceleration, and the Phase-C, superconducting RF linac [4] and the high-power beam dump [5].

We had a beam commissioning to validate the system RFQ acceleration with the low energy beam dump, 125 mA, 1 ms pulse is successfully accelerated in 2019 [6]. Most of the accelerator construction has been done by in kind contribution of EU facilities until 2021. Remaining component toward to full specification is the cryomodule linac, which can accelerate the beam from 5 MeV to 9 MeV. While preparation of superconducting linac to fix some issues found during construction, the beam operation was started in June of 2021 [7]. RFQ commissioning to be reached to CW had been also performed, but then the destructive sparks are happened in the transition part of a circulator, used to protect the tetrode system from the reflection power. During the following optional challenge to drive RFQ with 7 of 8 RF stations, vacuum leak from RF input couplers had been observed. As above two events became the decisive damage of our RFQ-RF system, we moved to a long maintenance term to recover the system over one year. The beam commissioning has been resumed from July of 2023 [8-10].

In this report, we share our progress of the beam commissioning, concentrating on the proceeding of the RFQ beam commissioning diagnosed by using beam position and phase monitors (BPMs) [11, 12] with the improved digitizer unit and beam loss monitors (BLoMs) [13, 14], which are ionization chambers and 3He detectors, positioned along newly constructed downstream transport up to the large beam dump.

LIPAc STATUS

Overview of the LIPAc Phase-B+

The Phase-B+ stage of our LIPAc has only RFQ cavity as the accelerating component. Downstream part consists of beam transport section with several beam diagnostics and the large beam dump as the new feature from this commissioning phase. Bridge section called MEBT Extension Line (MEL) between MEBT and HEBT instead of the cryomodule linac, is temporary inserted specifically in this commissioning phase.

The Stage-1 beam commissioning was performed with much low current beams of 10 mA H+, as the test, and 20 mA D+. For the ion source part, a 6 mm φ small extraction aperture was adopted. We could observe the 20 mA transmission up to the beam dump with chopped 100 μs beam in 1 Hz repetition rate. The purpose of this stage is checking the alignment of newly installed components and functionality of each diagnostic, to prepare coming high current and high duty beam operation and the beginning stage of Phase-C commissioning. We found some issues for diagnostics, espe-

* hirosawa.koki@qst.go.jp

ISBN: 978-3-95450-253-0 ISSN: 2673-5571 doi:10.18429/JACoW-HB2023-TUA3I3

ESS NORMAL CONDUCTING LINAC COMMISSIONING RESULTS

Y. Levinsen*, R. Miyamoto, N. Milas, D. Noll, M. Eshraqi
on behalf of the ESS Accelerator Collaboration, European Spallation Source ERIC, Sweden

Abstract

The European Spallation Source is designed to be the world's brightest neutron source once in operation, driven by a 5 MW proton linac. The linac consists of a normal conducting front end followed by a superconducting linac. The normal conducting part has been commissioned in several stages, with the latest stage involving all but one DTL tank now in 2023. During this commissioning period, we successfully transported a 50 µs pulse of the nominal 62.5 mA beam current. We will present an overview of the commissioning results, with a focus on what we achieved in this latest stage.

INTRODUCTION

The European Spallation Source (ESS) is a long pulse neutron source driven by a 5 MW proton linac [1]. The facility is currently under construction in Lund, Sweden. A rotating tungsten target is bombarded by a 2.86 ms long proton beam pulse at 2 GeV beam energy 14 times per second. The Start of User Programme (SOUP) is planned for 2026.

The protons are accelerated through a 600 m long linac, comprising of a normal conducting front-end (NCL) followed by a super-conducting linac (SCL) performing the bulk of the acceleration. The front-end RF is at 352.21 MHz, same as the first class of SC cavities (Spokes). After that we have two elliptical cavity families running at twice this bunching frequency.

The NCL has been installed and commissioned in several stages over the past years [2–6]. The latest and final stage of dedicated NCL commissioning was performed in the second quarter of 2023.

Main Goals of Commissioning Run

The primary goal of each commissioning stage is to have all necessary sub-systems integrated and commissioned, and show the ability to transport and accelerate the nominal beam. Except for the LEBT FC, the beam destinations used cannot receive the full proton pulse length (or more generally, the average charge deposition), but we are still able to prove transport of the nominal beam current which can give us confidence in the transverse beam optics. Transporting a 50 µs pulse is expected to be sufficient to prove that we can provide a stable RF for the full pulse. The ESS accelerator will nominally operate at 14 Hz, which is also important to test, in particular during reliability studies and for RF.

A "safe to be lost" beam mode called probe beam has been defined with a 6 mA, 1 Hz, 5 µs envelope. To verify ability to transport we then have other beam modes which vary one or several of the envelope parameters up to 62.5 mA, 14 Hz, 50 µs which were used during the commissioning run.

* yngve.levinsen@ess.eu

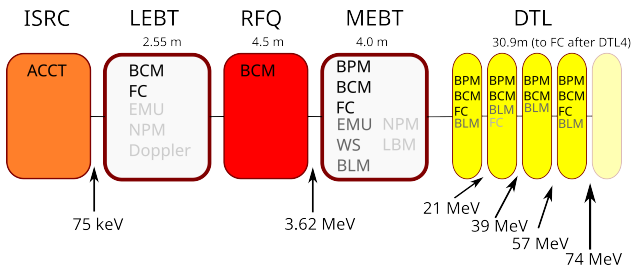

Figure 1: The ESS normal conducting linac during commissioning, with diagnostic systems for each section indicated. Dark grey indicates partial availability, while light grey indicates not ready. All RF in the NCL run at 352.21 MHz. The final energy out of the 5th DTL tank is 90 MeV.

The beam modes are an underlying concept for machine protection at ESS and the operator choice is enforced via an interlock implemented through the Beam Current Monitor (BCM) system. To prevent damage, some beam modes had special restrictions or were not allowed for certain beam destinations.

NORMAL CONDUCTING LINAC

The NCL comprises an ion source (ISRC), a low-energy beam transport (LEBT), a radio-frequency quadrupole (RFQ), a medium-energy beam transport (MEBT) and finally a drift-tube linac (DTL). During the final stage of NCL commissioning, 4 out of 5 DTL tanks were installed, while a temporary shielding wall (TSW) was installed in the location of the 5th tank. This wall ensured that work could continue uninterrupted in the rest of the tunnel, downstream of the NCL (and wall). The total linac length was around 42 m, and the layout is depicted in Fig. 1. The diagnostics used are discussed in more detail in Ref. [7].

ISRC and LEBT

The ion source is a plasma discharge ion source with a voltage gap of 75 kV. Three magnetic coils are available to

Table 1: ESS Linac High-level Schedule

Step	Start	Energy [MeV]
Commissioning to LEBT	2018-09	0.075
Commissioning to MEBT	2021-11	3.62
Commissioning to DTL1	2022-05	21
Commissioning to DTL4	2023-04	74
Commissioning to dump	2024	570
Commissioning to target	2025	570
Start of user operations	2026	800

ISBN: 978-3-95450-253-0 ISSN: 2673-5571 doi:10.18429/JACoW-HB2023-TUA3I4

SARAF MEBT COMMISSIONING

N. Pichoff†, J. Dumas, A. Chance, F. Gougnaud, F. Senée, D. Uriot
Commissariat à l'énergie atomique et aux énergies alternatives, Gif-Sur-Yvette, France
A. Kreisel, Y. Luner, A. Perry, E. Reinfeld, R. Weiss-Babai, L. Weissman
Soreq Nuclear Research Center, Yavne, Israel

Abstract

SNRC in Israel is in the process of constructing a neutron production accelerator facility called SARAF. The facility will utilize a linac to accelerate a 5 mA CW deuteron and proton beam up to 40 MeV. In the first phase of the project, SNRC completed construction and operation of a linac (referred to as SARAF Phase I) which included an ECR ion source, a Low-Energy Beam Transport (LEBT) line, and a 4-rod RFQ. The second phase of the project involves collaboration between SNRC and Irfu in France to manufacture the linac. The injector control system has been updated and the Medium Energy Beam Transport (MEBT) line has been installed and integrated into the infrastructure. Recent testing and commissioning of the injector and MEBT with 5 mA CW protons and 5 mA pulsed Deuterons, completed in 2022 and 2023, will be presented and discussed. A special attention will be paid to the experimental data processing with the Bayesian inference of the parameters of a digital twin.

INTRODUCTION

The SARAF-Linac [1] is presented. The 5 mA proton or deuteron beam is bunched with a 176 MHz four-rods RFQ (~4 m) and accelerated with a superconducting linac consisting in 27 HWR and 20 Solenoids in four cryomodules (~5 m each).

Between the RFQ and the superconducting linac, the 5 m Medium Energy Beam Transport (MEBT) section consists of 3 rebunchers and 8 quadrupoles, each equipped with a steerer for orbit correction. The MEBT serves various purposes, including matching the beam from the RFQ to the Linac, minimizing the residual gas sent to the Superconducting Linac (SCL), characterizing beam properties such as current, position, phase, energy, transverse and longitudinal profiles, and emittances and, if needed, shape the beam using three sets of slits and a fast chopper (which will be installed at a later date).

The MEBT was initially constructed and tested at CEA Saclay during the first half of 2020. A dedicated test stand was utilized to ensure proper alignment, vacuum, cooling, power supplies, and associated control systems. Subsequently, the MEBT was transported to Israel in August 2020 to be installed and integrated by SNRC teams in its final position downstream the RFQ. The MEBT commissioning was conducted in parallel with other activities. Interceptive diagnostics are placed in 2 Diagnostics Boxes called DB1 at the middle of the MEBT and DB2 at the end of the MEBT.

Figure 1 shows the MEBT layout enhancing beam diagnostics:

- two ACCTs (ACCT2 and ACCT3) for current monitoring, transmission, and machine protection,
- one Faraday Cup (FC) in DB2 to stop the beam and measure its current,
- four BPMs to measure beam average positions and phase,
- one Fast Faraday Cup (FFC) in DB1 to measure the bunch length,
- one Wire Scanner (WS) in DB1 to measure the beam transverse profiles,
- one SEM-Grid (SG) in DB2 to measure the beam transverse profiles.

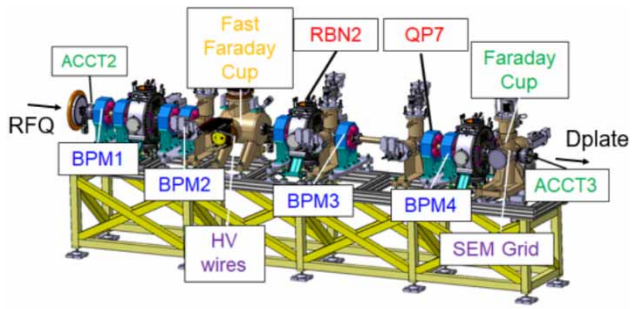

Figure 1: Layout of the MEBT, the 8 quadrupoles (QP) are in blue, the 3 rebunchers (RBN) are in light grey, and beam diagnostics are specifically shown.

For the MEBT commissioning, a D-plate previously employed during Phase I was connected downstream the MEBT. Figure 2 shows available beam diagnostics in the D-plate such as phase probes, FFC, MPCT (for current monitoring) and a set of slits and wires for transverse emittance measurements.

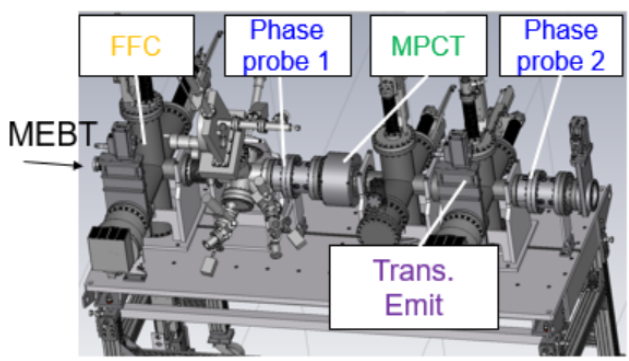

Figure 2: D-plate beam diagnostics [2].

ISBN: 978-3-95450-253-0 ISSN: 2673-5571 doi:10.18429/JACoW-HB2023-TUC3I1

ULTRA-LOW EMITTANCE BUNCHES FROM LASER COOLED ION TRAPS FOR INTENSE FOCAL POINTS

S. J. Brooks*, Brookhaven National Laboratory, Upton, NY, USA

Abstract

Laser-cooled ion traps are used to prepare groups of ions in very low temperature states, exhibiting such phenomena as Coulomb crystallization. This corresponds to very small normalized RMS emittances of 10^{-13}–10^{-12} m, compared to typical accelerator ion sources in the 10^{-7}–10^{-6} m range. Such bunches could potentially be focused a million times smaller, compensating for the lower number of ions per bunch. Such an ultra-low emittance source could enable high-specific-luminosity colliders where reduced beam current and apertures are needed to produce a given luminosity. Further advances needed to enable such colliders include linear, helical or ring cooling channel designs for increased bunch number or current throughput. Novel high density focal points using only a single bunch also appear possible, where the high density particles collide with themselves. At collider energies ~100 GeV, these approach the nuclear density and offer a way of studying larger quantities of neutron star matter and other custom nuclear matter in the lab.

LASER COOLED ION TRAPS

Laser cooling can be applied to ions in any type of trap, for example the Paul trap configuration shown in Fig. 1. This configuration has four AC/RF transverse electrodes powered to produce a quadrupole, with DC longitudinal end caps that are positive like the ions. The rapidly varying transverse electrostatic quadrupole produces an overall dynamic focussing effect on the ions transversely that is analogous to alternating gradient focussing in accelerators.

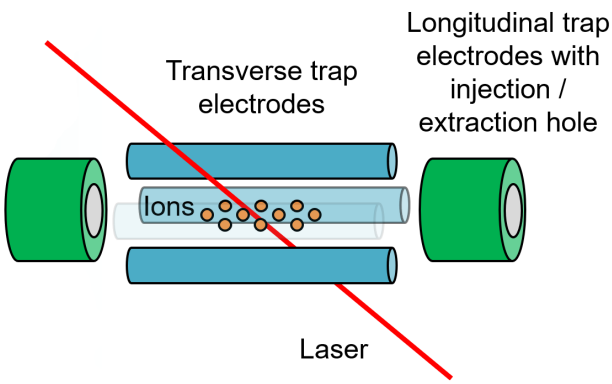

Figure 1: Paul ion trap geometry.

The mechanism of laser Doppler cooling relies on the absorption and subsequent emission of a photon by an allowed transition of the electrons orbiting the ion [1, 2]. One key feature is that the absorbed photons have momentum in the direction of the laser beam, whereas the emitted photons are in random directions, meaning a net force is exerted on the ion. The second required feature is that the transition cross-section has a linewidth that depends on frequency strongly enough that ion travelling towards the laser can be preferentially slowed. A force depending on velocity can act as a non-conservative damping term.

A frequently used example is the Ca^+ ion that has a transition around 397 nm with linewidth $\Gamma = 2\pi \times 23$ MHz. The photon itself has a frequency $f = c/397\,\text{nm} = 755$ THz. Comparing the linewidth to this and expressing as a fraction of the speed of light, we would expect the transition to be active over a velocity range of approximately $c(23\,\text{MHz}/755\,\text{THz}) = 9.1$ m/s.

Once the laser is carefully tuned to interact with ions nearly at rest, cooling can proceed. Because of the scattering from re-emission of photons, there is a well-known Doppler cooling limit temperature $T_D = \hbar\Gamma/2k_B = 0.552$ mK here.

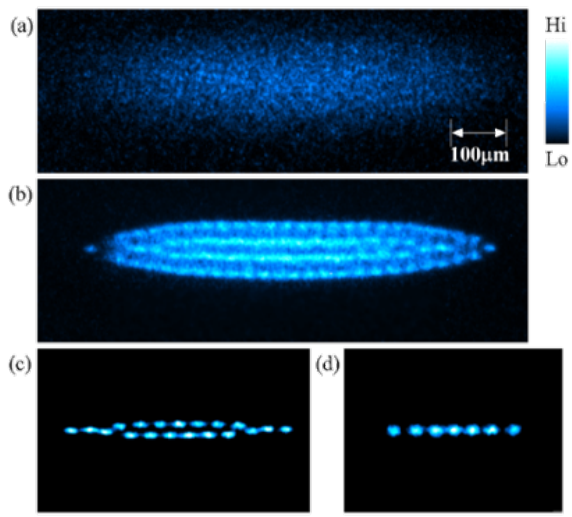

Figure 2: Fluorescence of a Coulomb crystal in the S-POD trap [3] at the University of Hiroshima.

The limiting temperature is so small that the ions can attain the solid 'Coulomb crystal' state where a lattice is held by the balance of repulsive space charge forces and the effective trapping potential. Figure 2 shows an experimental result where the Coulomb crystal structure is made visible by the ion fluorescence (emitted photons from the cooling process).

The hardware required to construct a Paul trap is comparatively simple, with Fig. 3 showing the IBEX trap [4] operated at Rutherford Appleton Laboratory (RAL).

* sbrooks@bnl.gov

ISBN: 978-3-95450-253-0 ISSN: 2673-5571 doi:10.18429/JACoW-HB2023-TUC3I2

SHAPING HIGH BRIGHTNESS AND FIXED TARGET BEAMS WITH THE CERN PSB CHARGE EXCHANGE INJECTION

C. Bracco*, S. Albright, F. Asvesta, G.P. Di Giovanni, F. Roncarolo, CERN, Geneva, Switzerland

Abstract

CERN adopted the charge exchange injection technique for the first time in the PS Booster after the Long Shutdown 2. This allowed to overcome space charge limitations, tailor high brightness beams for the LHC and deliver a high intensity flux of protons to fixed target experiments. Details about the concept, physics, hardware and diagnostic tools are presented while retracing the exciting steps of the successful commissioning period and the first years of operation with this system. A look to the future is taken by explaining the next stages to achieve the ambitious Luminosity targets foreseen for the HL-LHC era.

INTRODUCTION

One of the main upgrades implemented in the Large Hadron Collider (LHC) injectors during the Long Shutdown 2 (LS2) [1] was the replacement of a conventional multi-turn injection system with an H^- charge exchange in the PS Booster (PSB). This, combined with an increase of energy at injection, allowed to overcome previous limitations in the achievable beam brightness and intensity due to both the very nature of the old injection system and to space charge phenomena. The first year after LS2 was dedicated to recommissioning the PSB and reestablishing pre-LS2 operational conditions. The following years were instead devoted to beam production and optimisation studies to finally reach the targeted brightness and intensity for the High Luminosity LHC (HL-LHC) [2] and experimental area (ISOLDE [3], nTOF, North Area, East area, etc.) beams respectively. The full process was impressively smooth and the performance reached by the produced beam, time- and quality-wise, was beyond expectations. In the following, the main highlights of the first years of operation of the new charge exchange injection system are described. Ways to further increase the stored intensity to maximize the flux of particles towards fixed target experiments are being investigated and the first promising results are mentioned.

THE NEW CHARGE EXCHANGE SYSTEM

Originally, 50 MeV protons were injected from Linac2 into the PSB by using a conventional multi-turn injection system. Four slow horizontal bumpers where used to move the closed orbit towards the injection septum that was used to merge the injected with the circulating beam. The injection bump amplitude was reduced at each turn to paint the beam and fill the horizontal phase space. The presence of the septum implied high losses (up to 30-40%) from the circulating beam hitting the septum blade, a limited number of injection turns (10-20 turns) and thus of the achievable stored intensity plus a linear increase of the emittance at each turn translating in a limited brightness.

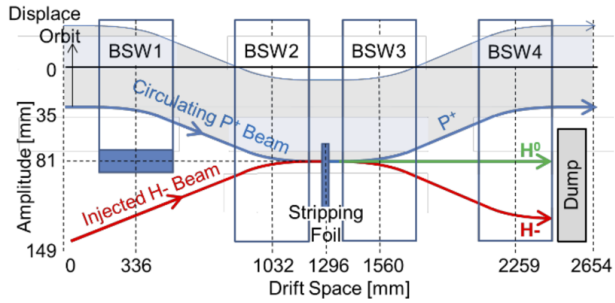

Figure 1: Schematic view of the new PSB H^- charge exchange injection system

All these constraints could be overcome by modifying the injection region of each of the four superposed PSB rings to host an H^- charge exchange system. This consists of four chicane dipoles (BSW1,2,3 and 4, Fig. 1) which move the closed orbit of the circulating beam by 46 mm towards the 160 MeV H^- beam coming from Linac4. A thin Carbon stripping foil, located in the middle of the chicane, is used to strip the two electrons from the H^- ions to convert them into protons which follow the PSB closed orbit. This allows to accumulate particles in the same phase space area and hence increase the charge density. Four horizontal kickers (KSW), installed in the ring lattice, are used to further move the closed orbit by 35 mm and for the transverse phase space painting. The painting, together with the higher injection energy with respect to pre-LS2 operation, mitigate space charge effects and allow to keep the emittance growth under control. Partially (H^0) and unstripped (H^-) ions are dismissed on a 70 mm thick Ti beam dump. A current monitor, installed in front of the dump, allows to measure the amount of H^0 an H^- particles and thus the stripping efficiency of the foil. Charge exchange injection is a multi-turn process that can be performed over hundreds of turns and is characterized by very low losses. In the PSB up to 150 turns injections can be performed and losses can be kept at the order of a percent. Moreover, the controlled decay of the painting bump permits to tailor the beam emittance and make it suitable to the requirements of the different PSB users [4].

The Chicane

The BSWs are rectangular pulsed magnets, independently powered, which apply a kick of 66 mrad to the beam. BSW1 acts as a septum to divide the high-field region for the circulating beam from the field-free region for the

* chiara.bracco@cern.ch

ISBN: 978-3-95450-253-0 ISSN: 2673-5571 doi:10.18429/JACoW-HB2023-TUC3I3

LASER STRIPPING OF H⁻ BEAM*

T. Gorlov†, A. Aleksandrov, S. Cousineau, Y. Liu, A. R. Oguz, N. Evans
Oak Ridge National Laboratory, Oak Ridge, TN, USA
P. K. Saha, Japan Atomic Energy Agency, J-PARC Center, Tokai-mura, Ibaraki, Japan

Abstract

Basic principles of laser assisted charge exchange injection for H^- ion and H^0 beams are presented. Theoretical aspects of electromagnetic interaction of laser with hydrogen atom and H^- ions are discussed. Laser excitation, photoionization and interaction of atoms and ions with a strong electro-magnetic fields are discussed and compared. Different techniques of LACE for stripping of high current stochastic beams are presented. The optimum parameters of LACE are estimated and compared for various ion beam energies. Experimental developments of laser stripping at the SNS are reviewed. Future plans of LACE at the SNS and J-PARC are discussed.

INTRODUCTION

In this paper we review basic principles and the current status of Laser Assisted Charge Exchange injection LACE at the Spallation Neutron Source SNS. Some other options of LACE with parameters different from SNS are also discussed. For example J-PARC project is developing LACE for H^- beam injection [1–3] and we will discuss challenges and options for it.

Development of LACE is motivated by issues with foil-based charge exchange injection at high-power. Foil heating imposes limitations on the power density before excessive heating leads to foil sublimation. Interaction of the beam with foil material represents a major source of loss, with the injection region of the SNS being the most activated area of the accelerator outside of the neutron production target. Additionally, interaction of beam with the foil causes mechanical deformation of foils that can lead to operational uncertainty, as curled, twisted, or otherwise compromised foils can change the effective thickness of foils modifying the stripping, or loss characteristics [4].

The concept of photo-detachment of neutral atoms or ions by lasers has been known for a long time but the cross-section of that process is too small that makes it practically inapplicable for high efficiency ionization or stripping of 99% of the beam. I. Yamane and V. Danilov proposed the concept of the effective three step laser assisted charge exchange injection LACE [5, 6] that involves realistic powerful lasers and strong magnetic fields for stripping of H^- beam without any foil: $H^- \rightarrow p^+ + 2e^-$. Later on, the idea has been demonstrated experimentally in proof-of-principles experiments at the SNS [7]. The experiment demonstrated high efficiency ~90% stripping of very short ~6 ns longitudinal H^- beam. The real accelerated beam of SNS has 402.5 MHz structure from RF system with multi-microseconds duration. Another experiment [8] demonstrated high efficiency ~90% stripping of few microsecond beam. In this way experiment demonstrated scalability of stripping from shorter to longer pulses. Another experiment at the SNS [9, 10] demonstrated four step LACE scheme that is supposed to be more effective than three step scheme [6] at some particular H^- beam energies.

All LACE experiments carried out at SNS have been performed for beam in the LINAC without real accumulation of the protons into the Ring. The experimental stand was located in the LINAC part of SNS and demonstrated pure stripping of single pass beam $H^- \rightarrow p^+ + 2e^-$ followed by the full beam loss of protons and unstripped H^0 downstream of the experiment. The real operational LACE must provide injection and accumulation of the proton beam into the Ring and this is much more challenging problem than simple demonstration of high efficiency electron detachment. Reference [11] demonstrated the scope of problems and constrains for development of the real LACE system for SNS. The problem becomes even more challenging assuming that SNS has been designed for foil based operation and LACE must be embedded into this existing design as an experimental addition without interference into the foil based operation of SNS.

LACE design and optimization strongly depends on beam parameters and must be considered and developed individually for different accelerator facilities. The beam energy is one of the most key parameters around which we can start designing LACE project. From general considerations of LACE theory we can say that more H^- beam energy will simplify the design in general. Anyway, every particular energy requires individual consideration and 100 MeV difference for the beam energy can dramatically change the whole design of LACE.

The future Proton Power Upgrade PPU project of SNS will update the beam energy from 1.0 GeV to 1.3 GeV [12]. The new energy makes a big difference for choice of LACE optimal scheme compared to 1.0 GeV scheme used in our previous experiments. We discussed different LACE options for 1.3 GeV energy in Ref. [13].

We begin this paper with basic theory of interaction of electromagnetic field and lasers with a single H^0 atom and

* This manuscript has been authored by UT-Battelle, LLC, under Contract No. DE-AC05-00OR22725 with the U.S. Department of Energy. The United States Government retains, and the publisher, by accepting the article for publication, acknowledges that the United States Government retains a non-exclusive, paid-up, irrevocable, world-wide license to publish or reproduce the published form of this manuscript, or allow others to do so, for United States Government purposes. The Department of Energy will provide public access to these results of federally sponsored research in accordance with the DOE Public Access Plan (http://energy.gov/downloads/doe-public-access-plan).
† tg4@ornl.gov

ISBN: 978-3-95450-253-0 ISSN: 2673-5571 doi:10.18429/JACoW-HB2023-TUA4I2

1-MW BEAM OPERATION AT J-PARC RCS WITH MINIMUM BEAM LOSS

P. K. Saha*, H. Harada, K. Okabe, H. Okita, Y. Shobuda, F. Tamura, K. Yamamoto, M. Yoshimoto
J-PARC Center, JAEA and KEK Joint Project, Ibaraki-ken, Japan
H. Hotchi, KEK, Ibaraki-ken, Japan

Abstract

We have achieved a routine operation of the 3-GeV RCS (Rapid Cycling Synchrotron) of J-PARC (Japan Proton Accelerator Research Complex) at a beam power close to the designed value of 1 MW. Based on the numerical simulations and experimental studies, the beam loss has been well minimized to a sufficiently low level and also controlled to occur only at lower beam energy localizing almost at the collimator section to realize a stable operation with less machine activation. We have optimized both longitudinal and transverse injection paintings and obtained as much as more than 60% beam loss mitigation. The beam intensity for operation to the muon and neutron production target at the MLF (Material and Life Science Experimental Facility) is now about 8.0×10^{13} ppp (proton per pulse) with respect to the required 8.33×10^{13} for 1-MW beam power. This corresponds to 960 kW equivalent beam power, which is just 4% less than 1 MW due to absence of one failure RF cavity out of 12 in total. The RF cavity is under repair and will be back in service at the beginning of April 2024 to realize the user operation with a full beam intensity.

INTRODUCTION

The 3-GeV RCS (Rapid Cycling Synchrotron) of J-PARC (Japan Proton Accelerator Research Complex) is a high intensity proton driver of 1-MW beam power for the pulsed muon and neutron productions at the MLF (Materials and Life Science Experimental Facility) as well as an injector to the MR (30-GeV Main Ring Synchrotron) [1]. The beam sharing ratio between MLF and the MR from the RCS is 88:12 or 97:3 depending on the fast or slow operation cycle of the MR. The injected beam energy is 400 MeV, which is accelerated to 3 GeV at a repetition rate of 25 Hz and simultaneously delivered to the MLF and MR.

Figure 1 shows a schematic view of the RCS. The H^- charge-exchange injection (CEI) system followed by the beam collimation section is placed at the first straight section. The beam extraction section is placed the 2nd straight section, while the RF cavities are placed at the 3rd straight section. The collimator limit is 4 kW, which means a maximum 3% of 133 kW injected beam power can be lost if the beam loss occurs at around the injection energy. In addition, the beam loss localization at the collimator section is also highly necessary for a regular accelerator maintenance works and to realize a stable operation.

Figure 2 shows RCS beam power history for beam operation to the MLF so far. We have demonstrated 1-MW operation at 25 Hz several times, where the latest longer one

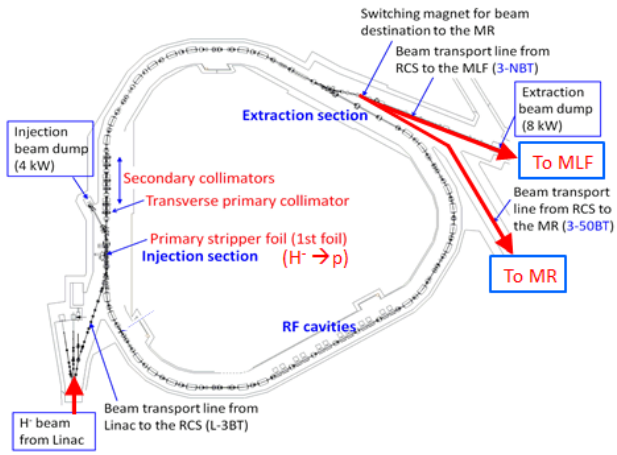

Figure 1: A schematic view of the 3-GeV RCS at J-PARC. The CEI system followed by the collimation system are placed at the first straight section. The extracted beam is simultaneously delivered to the MLF and MR.

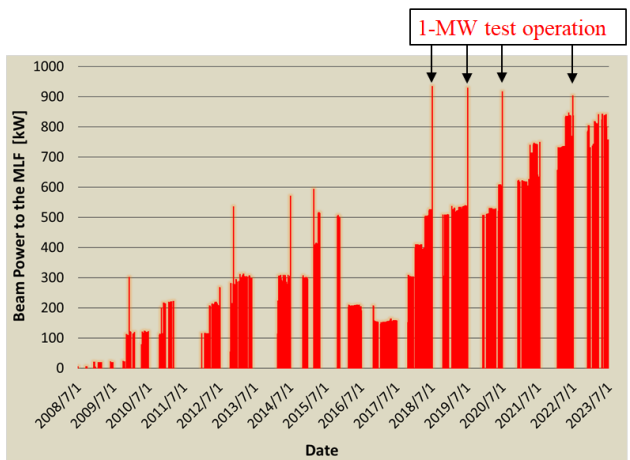

Figure 2: History of RCS beam power to the MLF. The beam power is reached almost to the designed value of 1 MW with 0.1 MW step per year recently according to the operation strategy of the neutron production target.

was done for about 1.5 days in 2020. At present the beam power for operation to the MLF is set to be nearly 850 KW at maximum. The number of particles per pulse (ppp) is about 8.0×10^{13}, which is equivalent to 960 kW beam power, but the net beam power becomes 950 kW at 88% duty factor to the MLF when the MR operates for the fast extraction mode. On the other hand, it gives 930 kW net beam power with 97% duty factor when MR operates for the slow extraction mode.

* saha.pranab@j-parc.jp

ISBN: 978-3-95450-253-0 ISSN: 2673-5571 doi:10.18429/JACoW-HB2023-TUA4C1

RECENT PROGRESS IN LOSS CONTROL FOR THE ISIS HIGH-INTENSITY RCS: GEODETIC MODELLING, TUNE CONTROL AND OPTIMISATION

H. Rafique*, E. K. Bansal, H. V. Cavanagh, C. M. Warsop
ISIS Neutron and Muon Source, RAL, Chilton, UK

Abstract

ISIS operates a high intensity 50 Hz rapid cycling synchrotron (RCS), accelerating up to 3×10^{13} protons from 70 to 800 MeV. Protons are delivered to one muon and two neutron targets over two target stations, totalling 0.2 MW of beam power, enabling around 1000 experiments for approximately 3500 users a year. Minimisation of beam loss and optimisation of its control are central to achieving the best facility performance with minimal machine activation. We summarise recent work aimed at improving loss control in the RCS. Using geodetic survey data we aim to develop lattice models with realistic magnet alignment errors. Building on recent measurement campaigns a new and improved system of tune control has been developed and verified using updated lattice models in cpymad. More rigorous and quantitative measures of beam loss are being developed in order to optimise loss control.

INTRODUCTION

The ISIS RCS is loss-limited: beam induced activation has to be controlled to allow hands on maintenance. The ISIS facility operates multiple user cycles a year, each necessitating periods of machine setup, with regular maintenance and upgrades performed in the short shutdowns between. Therefore, activation must be kept at levels such that hands-on maintenance may be performed shortly after the end of a user cycle.

The RCS, 163 m in circumference, accelerates up to 3×10^{13} protons from 70 to 800 MeV at 50 Hz, in a 10 ms machine cycle. The RCS consists of 10 super-periods (SPs), each containing a combined function main dipole, a main quadrupole doublet, trim quadrupole doublet, and main quadrupole singlet, as illustrated in Fig. 1.

This paper describes historical loss control in the RCS, relevant issues identified after a long shutdown in 2021, solutions and long-term plans for performance optimisation learned from this experience.

A Brief History of ISIS Operations

Reduction of beam loss is a perpetual goal in a loss-limited machine such as the RCS. ISIS has operated since 1995 with <12 % beam loss, <7 % in the early 2000s and <3 % by 2019 [1]. RCS beam loss and intensity since 2016 is summarised in Fig. 2.

Linac tank 4 was replaced during a long shutdown in 2021, due to ongoing issues and difficulty in maintenance due to age [2]. Alongside this, multiple upgrade and maintenance projects took place including significant upgrades to the second harmonic RF systems. The target, reflector and moderator assembly for target station 1 were also replaced, and is still in commissioning for high intensity operations. Since the 2021 long shutdown, operational issues have been identified and resolved, whilst others remain the focus of investigation.

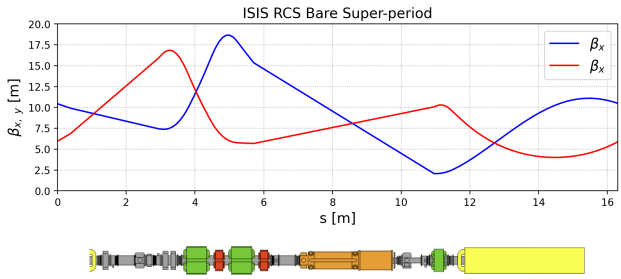

Figure 1: Top: Beta functions for design ISIS RCS superperiod. Bottom: Diagram of ISIS superperiod general layout. Quadrupole doublet (green), trim quadrupoles (red), RF cavity (orange), defocussing quadrupole singlet (green), combined function dipole (yellow).

R&D Aims

ISIS accelerator physics R&D aims [3] include the development of more robust lattice models for operational understanding, and a focus on a more measurement-based setup.

In order to identify issues, a campaign of regular beam-based lattice measurements was instigated, including; investigations of the closed orbit, tune control, and optimisation of beam loss data. The aim of this work is to optimise the use of existing diagnostics and data, and to build on existing tools to better identify and further protect from issues. Such optimisation should result in reduced activation, by extension enhanced machine and personnel protection, as well as maximised equipment lifetime.

ORBIT CONTROL

In the user cycles after the 2021 shutdown, operational issues were identified and rectified, some of which fall under human error, such as incorrect cabling and aperture restrictions. Once more easily rectifiable issues were corrected, underlying issues were identified such as larger than expected losses were observed in SPs 8 and 9, shown in Fig. 3.

* haroon.rafique@stfc.ac.uk

ISBN: 978-3-95450-253-0 ISSN: 2673-5571 doi:10.18429/JACoW-HB2023-TUA4C2

APPLICATION OF PROGRAMMABLE TRIM QUADRUPOLES IN BEAM COMMISSIONING OF CSNS/RCS

Y. Li*,[1,2,3], Y. H. Liu[1,2], Y. S. Yuan[1,2], S. Y. Xu[1,2], Y. W. An[1,2], C. D. Deng[1,2], X. Qi[1,2], S. Wang[1,2,3]
[1]Institute of High Energy Physics, Chinese Academy of Sciences, Beijing, China
[2]Spallation Neutron Source Science Center, Dongguan, China
[3]University of Chinese Academy of Sciences, Beijing, China

Abstract

The China Spallation Neutron Source (CSNS) achieved its design beam power of 100 kW in 2020 and is currently stably operating at 140 kW with a tolerable beam loss level after a series of suppression methods. In the process of increasing beam power, 16 programmable trim quadrupoles were installed in the Rapid Cycling Synchrotron (RCS) of CSNS to enable rapid variation of tunes, effective adjustment of twiss parameters, and restoration of lattice superperiodicity through the machine cycle. This paper will provide a detailed introduction to the design of the trim quadrupoles and various applications in beam commissioning. The beam experiments show that the trim quadrupoles play a crucial role in increasing beam power after exceeding 100 kW.

INTRODUCTION

CSNS is a high-power pulsed spallation neutron source, which consists of an accelerator, a target station and several spectrometers [1]. The accelerator chain includes a negative hydrogen (H^-) linac and a rapid cycling synchrotron (RCS). The H^- beams at 80 MeV are injected from the linac into the RCS via a multi-turn charge-exchange process, accelerated to 1.6 GeV within 20000 turns in the RCS, and extracted to shoot the tungsten target with a repetition frequency of 25 Hz to produce neutrons. The design output beam power is 100 kW in CSNS-I and 500 kW in CSNS-II. The beam commissioning of CSNS/RCS started in May 2017 and the first neutron beam was successfully obtained on August, 2017. In February 2018, the output beam power reached 10 kW. Since then, a step-by-step beam commissioning process has been performed to further increase the beam current and beam power. In February 2020, the design goal of 100 kW beam power has been successfully achieved with a tolerable beam loss level [2]. In September 2022, the beam power has been raised to 140 kW and further enhanced to more than 150 kW in this year.

It was found that the lattice of CSNS/RCS requires more precise tuning as the beam power increases. To address issues such as rapid adjustment of the tunes and twiss parameter correction through the machine cycle, similar high-intensity synchrotron like ISIS and J-PARC have installed pulsed trim quadrupoles (QTs) [3, 4]. During the summer maintenance period in 2021, 16 programmable QTs are installed in the CSNS/RCS for beam parameters correction. The subsequent beam experiments have demonstrated that the QTs played a significant role with enhanced beam power. The article is organized as follows: the first part introduces the design scheme of the QTs. The second part focuses on three different applications of the QTs during beam commissioning in CSNS/RCS. Finally, there is a summary and discussion.

DESIGN OF TRIM QUADRUPOLES

The CSNS/RCS is a four-fold symmetric structure and adopts a triplet cell as the fundamental unit of the lattice model. The layout of the magnets in one super-period is shown in Fig. 1. The 48 main quadrupole magnets in the whole ring are powered by 5 sets of power supplies. By comparing the correction effects of the β-beat and tunes with different numbers and positions of QTs, it was finally determined to install 4 QTs in one super-period, as shown in green in the Fig. 1. The QTs are placed at one end of the main quadrupole magnet QDs, as shown in Fig. 2. Each QT has a 136 mm bore radius and shares a ceramic vacuum tube with the neighboring main quadrupole. The core length of each QT is set to as short as 150 mm due to the limited installation space. Unlike the main quadrupole magnets, all QTs are designed to be independently powered, allowing a fine tuning of the β-functions and bare tunes at 21 time points in one 20 ms ramping time. The maximum current change rate of the QTs is 300 A/ms, ensuring fast operating the tunes even in the high-energy region.

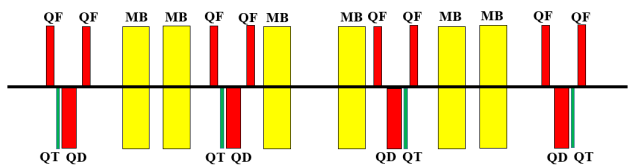

Figure 1: Layout of QTs in one super-period.

APPLICATIONS

Tunes Optimization

The harmonic injection method for the main quadrupole power supplies was used in CSNS/RCS, causing a relatively smooth variation of the tunes throughout the entire cycle and limited tuning capability with main quads in short time, especially for rapidly variation. However, the installation of QTs enables fast variation of tunes for a specific energy range or tuning in the entire cycle. Here are two examples.

* liyong@ihep.ac.cn

ISBN: 978-3-95450-253-0 ISSN: 2673-5571 doi:10.18429/JACoW-HB2023-TUC4I1

A KICKER IMPEDANCE REDUCTION SCHEME WITH DIODE STACK AND RESISTOR AT THE RCS IN J-PARC

Y. Shobuda, H. Harada, P.K. Saha, T. Takayanagi, F. Tamura, T. Togashi, Y. Watanabe, K. Yamamoto, M. Yamamoto, JAEA, Tokaimura, Ibaraki, Japan

Abstract

At the 3-GeV Rapid Cycling Synchrotron (RCS) within the Japan Proton Accelerator Research Complex (J-PARC), kicker impedance causes beam instability. A 1 MW-beam with a large emittance can be delivered to the Material and Life Science Experimental Facility (MLF) by suppressing beam instabilities without the need for a transverse feedback system simply by turning off the sextuple magnets. However, we require other high-intensity and high-quality beams with smaller emittances for the Main Ring (MR). To address this, we proposed a scheme for suppressing the kicker impedance using a diode stack and resistors, which effectively reduces beam instability. Importantly, these devices have a negligible effect on the extracted beam from the RCS.

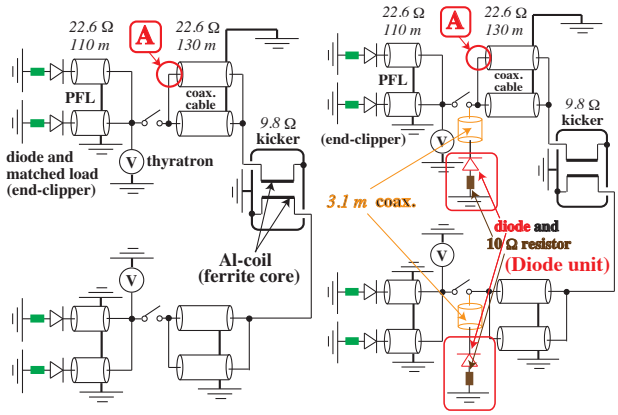

Figure 1: Kicker without (left) and with diode units (right).

INTRODUCTION

The RCS in J-PARC [1] has accelerated two bunches, each containing 4.15×10^{13} particles, from 400 MeV to 3 GeV in 20 ms. This acceleration, with a repetition rate of 25 Hz, has made 1 MW-beam operation possible [2].

The RCS provides proton beams downstream to both the MLF and the MR [3]. The standard unnormalized transverse painting emittance, the unnormalized value of the entire painting area, for the MLF, is relatively large (e.g., 200π mm.mrad), which can easily stabilize a high-intensity beam (even a 1 MW-beam). However, the emittance must be less than 50π mm.mrad for the MR, because the beams extracted from the RCS are delivered to the MR through the beam extraction line with a small mechanical aperture, exciting a large residual dose.

Since the RCS was designed such that all impedance sources are below the impedance budget, except the kicker impedance, the beam instability [4] excited by the extraction kicker magnet has been the main issue that limits the generation of the high-intensity beam [5].

However, theoretical, simulation, and experimental measurements have clarified the mechanism of space-charge effects, including indirect space-charge effects, to suppress beam instability in a space-charge-dominated machine (like the RCS) [6–8]. Hence, if the machine parameters, including tunes, chromaticities,... are appropriately chosen, the 1 MW-beam is realized without any transverse feedback system for a larger emittance beam by making use of the indirect space charge effects.

On the other hand, small emittance broadens the transverse tune spreads due to space-charge effects, restricting the variable tune-tracking pattern during the acceleration period. Furthermore, suppression of beam instability is more difficult with a smaller transverse emittance than with a larger emittance, because the suppression effect due to the indirect space charge force is relatively mitigated for the smaller transverse emittance beam [7, 8].

In the end, lowering the kicker impedance [4] is required for the generation of high-intensity and high-quality small emittance beams by the RCS.

As shown in Fig. 1, the kicker at the RCS is a transmission line-type embedding two ferrite cores [9]. The kicker has four terminals, two of which are connected to the power supply through 130 m-long coaxial cables [10], and the other two are terminated in a short circuit [9]. The shorted ends are beneficial for beam extraction, owing to the doubled excitation currents. However, the drawback is that these terminal conditions enhance the kicker impedance [11, 12].

The standard method of suppressing the kicker impedance involves inserting matched resistors at the end of the kicker terminals [13]. However, the scheme makes void the merit of the doubled excitation currents with the shorted ends.

To overcome this difficulty, we suggested inserting diodes with matched resistors (diode unit) at the end of the kicker terminals in front of the thyratron switch, as shown in the right panel of Fig. 1 [14, 15]. This scheme guarantees doubled excitation currents with the shorted ends by preventing the forward current created by the Pulse Forming Line (PFL) from flowing into the matched resistor. Meanwhile, the high-frequency beam-induced current can pass through the diodes and is absorbed into the matched resistors suppressing the kicker impedance. This is because diodes act as a capacitor as well as a rectifier for beam-induced currents when a reverse voltage is applied, creating the insulated depletion layer between the anode and cathode sides, in turn reducing the impedance for high-frequency components.

ISBN: 978-3-95450-253-0 ISSN: 2673-5571 doi:10.18429/JACoW-HB2023-TUC4I2

DEVELOPMENT OF AN IMPEDANCE MODEL FOR THE ISIS SYNCHROTRON AND PREDICTIONS FOR THE HEAD-TAIL INSTABILITY

D. W. Posthuma de Boer*,[1], B. A. Orton, C. M. Warsop, R. E. Williamson
ISIS Neutron and Muon Source, Harwell, UK
[1]also at John Adams Institute, Oxford, UK

Abstract

ISIS is the pulsed, spallation neutron and muon source at the Rutherford Appleton Laboratory in the UK. The rapid cycling synchrotron which drives the facility accelerates 3×10^{13} protons-per-pulse from 70 to 800 MeV at 50 Hz, and delivers a mean beam power of 0.2 MW to two target stations. Beam-loss mechanisms must be understood to optimise performance and minimise equipment activation and to develop mitigation methods for future operations and new accelerators.

Substantial beam-losses are driven by a vertical head-tail instability which has also limited beam intensity. Beam-based impedance measurements suggest the instability is driven by a low frequency narrowband impedance but its physical origin remains unknown. More generally, research into the nature of the instability is hindered without a detailed transverse impedance model.

This paper presents a survey of low frequency vertical impedance estimates for ISIS equipment, using analytical methods, CST simulations and lab-based coil measurements. The final impedance estimate is then used as an input to a new linearised Vlasov solver, and predicted growth rates compared with previously obtained experimental results.

INTRODUCTION

The ISIS Neutron and Muon Source has been successfully operating for close to 40 years. Key parameters of the rapid cycling synchrotron (RCS) which drives the facility are listed in Table 1. Its dual harmonic RF system captures and accelerates up to 3×10^{13} protons with a repetition rate of 50 Hz, producing a mean beam power of 0.2 MW. Following extraction, accelerated protons are directed to one of two targets stations (TS1 and TS2), with beam to TS1 also intercepting an intermediate target for muon production.

ISIS has reported a vertical head-tail instability for more than three decades [1, 2]. In contrast with the observed mode 1 instability, indicated by the single node in the difference signal of Fig. 1, it was found that the sinusoidal mode approximation [3] predicted modes 2 or 3 to be most unstable. Measurements confirmed that the growth rate grew as vertical tune approached an integer ($Q_y \sim 3.83 \rightarrow 4$), supporting a theory that the instability was driven by resistive wall [2]. However, with a thick resistive wall model, simplified instability theories [4] predicted growth times on the order of ms, whilst the instability grew with characteristic times on the order of 100 µs.

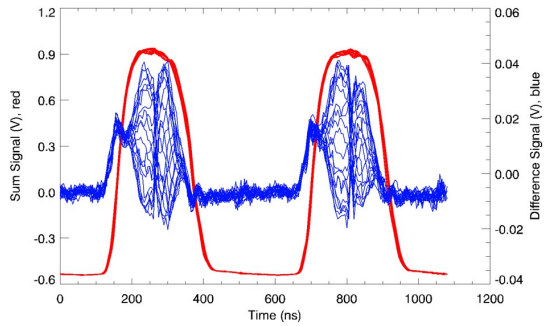

Figure 1: Position monitor sum (red) and difference (blue) signals, taken close to 2 ms into the synchrotron acceleration cycle during routine operations [10].

These apparent contradictions between theory and observation motivated an extensive measurement campaign [5–11] an alternative formulation of transverse bunched-beam instabilities [12], and the development of an experimental damping system [13]. Measurements of real effective transverse impedance with a coasting beam, have hinted at the existence of a 85 kHz narrowband impedance, which was subsequently corroborated by measurements of head-tail growth rate versus vertical tune; see Fig. 2 [8].

Table 1: Key ISIS Synchrotron Parameters

Property	Value
Kinetic Energy Range	70 - 800 MeV
Number of Bunches (M)	2
Circumference	163.3 m
No. of Superperiods	10
Gamma Transition	5.034
Nominal Tunes (Q_x, Q_y)	4.31, 3.83 (variable)
Peak Incoherent Tune Shift	Exceeding ~ -0.5 [8]
Chromaticity (ξ_x, ξ_y)	-1.4, -1.4
No. of RF Cavities (h = 2,4)	6, 4
Injection Scheme	H^- charge-exchange
Extraction Scheme	Single-turn, vertical

This paper will develop an improved low frequency resistive wall impedance model with modern analytical and numerical methods to specific equipment within the ISIS synchrotron. This will then be compared with the thick resistive wall model that has been applied until now. Res-

* david.posthuma-de-boer@stfc.ac.uk

ISBN: 978-3-95450-253-0 ISSN: 2673-5571 doi:10.18429/JACoW-HB2023-TUC4C1

BEAM COUPLING IMPEDANCE OF THE MAIN EXTRACTION KICKERS IN THE CERN PS

M. Neroni[1,2,*], M. J. Barnes[1], A. Lasheen[1], A. Mostacci[2], B. Popovic[3], C. Vollinger[1]
[1]CERN, Geneva, Switzerland
[2]La Sapienza University, Rome, Italy
[3]Argonne National Laboratory, Illinois, United States

Abstract

In view of the High Luminosity (HL) upgrade of the LHC, the beam intensity must be doubled in the injector chain. To perform reliable beam dynamics simulations, the beam coupling impedance in the injectors, such as the Proton Synchrotron (PS), must be followed closely by including all contributing elements into the impedance model. The existing kicker magnets of the PS had been optimized for large kick strength and short rise/fall times, but not necessarily to minimise beam coupling impedance. Hence, unwanted beam induced voltage can build up in their electrical circuits, with an impact on the beam. The beam coupling impedances of the two main kicker magnets used for the fast extraction from PS, the KFA71 and KFA79, are extensively characterized in this study. In particular, electromagnetic simulation results for the longitudinal and transverse coupling impedance are shown. The critical impedance contributions are identified, and their effect on beam stability is discussed. Moreover, the impact of the cable terminations on the electromagnetic field pattern and possible mitigation techniques are presented, providing a complete impedance evaluation of the entire kicker installation.

INTRODUCTION

The KFA71 and KFA79 (Kicker Full Aperture) are the fast kickers, together with the septum magnet SMH16 (Septum Magnetic Horizontal) and a set of bumper magnets, involved in the extraction from PS towards SPS (Super Proton Synchrotron) and experimental areas. The extraction kicker system consists of twelve magnet modules which, due to space constraints, were split into two different devices: nine modules are located in a vacuum tank in section 71 (KFA71) and three in section 79 (KFA79) of the PS accelerator. These magnets were first installed in the 1970s [1], and they are nowadays part of the PS multi-turn extraction process, introduced in 2006 to split the beam transversely prior to extraction [2]. In the context of the multi-turn extraction, a measurement campaign of the beam coupling impedance of the PS kickers involved in the process was launched [3]. The impedance of two new kickers, KFA13 and KFA21, which consists of modules similar to those of the PS fast extraction kickers, were measured at that time.

Thereafter, in the framework of the PS machine impedance model and in view of the LHC Injectors Upgrade (LIU), the kickers were identified as the main source of broadband impedance, responsible for the longitudinal loss of Landau damping in the PS [4]. Due to mechanical modifications of the components over the years and due to the high computing resources required to analyse such complex geometries, the beam coupling impedance of the KFA71 and KFA79 was calculated in different iterations with the aim of keeping the PS impedance model updated [5, 6]. The two kicker magnets have been designed for the same functionality, therefore the complete characterization of the beam coupling impedance of the three modules magnet (KFA79) can be used as guiding case also for the nine modules magnet (KFA71). Longitudinal beam coupling impedance calculation results for the KFA79 were presented together with a mitigation solution to reduce the critical impedance contributions [7]. This completed the picture of the longitudinal beam coupling impedance of the KFA79 together with the transverse impedance results, and the study carried out on the nine modules kicker, the KFA71.

The objective of the present work was to present an up-to-date beam coupling impedance model of the PS extraction kickers KFA71 and KFA79, based on the longitudinal and transverse electromagnetic (EM) simulations results. In addition, the influence of the High-Voltage (HV) cables termination on the beam coupling impedance is here introduced and discussed for the KFA79.

ELECTROMAGNETIC CALCULATIONS

The kickers KFA71 and KFA79 are composed respectively by nine and three modules. Each module is a 15 Ω delay line consisting of an assembly of nine C-shaped ferrite cells, separated by aluminum alloy laminations (Fig. 1). Both kicker magnets have a similar layout, with the high voltage connectors of each module facing alternately towards the inside or outside of the PS ring. While the modules of the two kickers do not have exactly the same geometry, their assembly is comparable, with analogous impedance behaviour expected.

The EM calculations have been carried out by using the Wakefield solver in CST Studio Suite [8]. Both three dimensional (3D) geometries have been built in CST starting from previous models and by making use of the most recent drawings and CAD projects (Fig. 2). The three modules kicker, KFA79, is 0.89 m long, and it is assembled inside an octagonal vacuum tank, whereas the nine module magnet, KFA71, is 2.45 m long and it is contained in a round tank.

The dispersive behaviour of the ferrite material 8C11 [9] has been included by importing measured values of the mag-

* michela.neroni@cern.ch

ISBN: 978-3-95450-253-0 ISSN: 2673-5571 doi:10.18429/JACoW-HB2023-TUC4C2

MITIGATING COLLIMATION IMPEDANCE AND IMPROVING HALO CLEANING WITH NEW OPTICS AND SETTINGS STRATEGY OF THE HL-LHC BETATRON COLLIMATION SYSTEM*

B. Lindström, R. Bruce, X. Buffat, R. De Maria, L. Giacomel, P. Hermes, D. Mirarchi, N. Mounet, T. Persson, S. Redaelli, R. Tomás, F. F. Van der Veken, A. Wegscheider
CERN, Geneva, Switzerland

Abstract

With High Luminosity Large Hadron Collider (HL-LHC) beam intensities, there are concerns that the beam losses in the dispersion suppressors around the betatron cleaning insertion might exceed the quench limits. Furthermore, to maximize the beam lifetime it is important to reduce the impedance as much as possible. The collimators constitute one of the main sources of impedance in HL-LHC, given the need to operate with small collimator gaps. To improve this, a new optics was developed which increases the beta function in the collimation area, as well as the single pass dispersion from the primary collimators to the downstream shower absorbers. Other possible improvements from orbit bumps, to further enhance the locally generated dispersion, and from asymmetric collimator settings were also studied. The new solutions were partially tested with 6.8 TeV beams at the LHC in a dedicated machine experiment in 2022. In this paper, the new performance is reviewed and prospects for future operational deployment are discussed.

INTRODUCTION

Efficient management of beam losses is crucial for the effective functioning of the Large Hadron Collider (LHC) and to prevent the superconducting magnets from quenching [1, 2]. In order to achieve this, the LHC lattice includes two specialized cleaning insertion regions (IRs), namely the momentum cleaning in IR3 and the betatron cleaning in IR7. The deployment of a well-defined multi-stage transverse hierarchy of collimators in these IRs is intended to disperse and absorb the energy carried by the beam halo, thus avoiding any impact on the superconducting magnets [3–5]. However, there is inevitably some leakage of particles from the collimators. Of concern are leaked particles with large momentum offsets since they are lost in the dispersion suppressor (DS) downstream of the IR, where the first dispersion peaks occur.

The primary objective of the High Luminosity LHC (HL-LHC) project [6] is to double the bunch population from 1.15×10^{11} to 2.3×10^{11} protons. For the same loss assumptions, this will produce higher DS losses that may trigger quenches in the superconducting dipole magnets situated in that region [2]. To address this issue, the collimation upgrade baseline planned to substitute one of the main dipole magnets with two shorter 11T dipoles to create space in the DS for the installation of a new collimator, TCLD [7]. The implementation of these changes has been descoped due to delays in the production of the 11 T dipoles [8].

The latest beam-based assessment of collimation performance and quench limit of the most exposed DS magnets indicate that the present performance is compatible with the HL-LHC proton beam parameters [9]. Nevertheless, to minimize any uncertainty, alternative strategies to mitigate the losses in the IR7 DS are studied. New optics were developed for this purpose similar to those proposed in Ref. [10]. These optics increase the beta function at the primary collimators, as well as the single-pass dispersion from the primary to the secondary collimators and absorbers. Both of these changes reduce the fraction of particles leaking into the DS. Other mitigation methods using orbit bumps and special collimator setups were explored in Ref. [11].

Another concern for the HL-LHC is that the increased bunch brightness might trigger beam instabilities [12], in particular given recent results on the crab cavity impedance [13]. To maximize beam lifetime it is important to reduce the impedance as much as possible, and one of the main sources of impedance is the collimators [14]. With the increased beta functions of the new optics, the physical gaps of the collimators are increased. This reduces their impedance contribution, while ensuring the same collimation hierarchy.

A dedicated beam experiment in the LHC in 2022 aimed to test the new optics and the alternative mitigation methods. The initial results are summarized in this paper, and the prospects for future operational deployment are discussed.

OPTICS DESIGN AND COLLIMATION SETUP

The IR7 optics were rematched such that the beta functions in the primary and secondary collimators were maximized and the single pass dispersion from the primary collimators to the absorbers was increased. Matching of $(\beta_x, \beta_y, \alpha_x, \alpha_y, \mu_x, \mu_y, D_x, D_{px})$ at the start and end of IR7 was done to ensure that the optics change only had a local effect. The resulting optics are shown in Fig. 1.

Collimator Cuts

When protons impact one of the primary collimators, a certain fraction of them scatter out. These protons generally receive transverse kicks, as well as a loss of momentum. Downstream secondary and absorber collimators are designed to dispose of the largest fraction of this halo in the multi-turn beam dynamics [15], such that most of their energy can be dispersed in the warm section of IR7. A

* Work supported by the High Luminosity LHC project

ISBN: 978-3-95450-253-0 ISSN: 2673-5571 doi:10.18429/JACoW-HB2023-WEA1I2

ANALYTICAL AND NUMERICAL STUDIES ON KICKED BEAMS IN THE CONTEXT OF HALF-INTEGER STUDIES*

G. Franchetti[1,2], GSI Helmholtzzentrum für Schwerionenforschung, Darmstadt, Germany
F. Asvesta, H. Bartosik, T. Prebibaj[1], CERN, Geneva, Switzerland
[1] also at Goethe Universität, Frankfurt am Main, Germany
[2] also at Helmholtz Forschungsakademie Hessen für FAIR (HFHF), Frankfurt am Main, Germany

Abstract

In the context of half-integer studies an investigation of the kicked beam dynamics has revealed surprising characteristics. The coupling of space charge with chromaticity in addition to usual damping/non-damping dynamics, exhibits new properties typical of a linear coupling. This article gives the status of these studies which were carried out with analytical and numerical approaches as well as preliminary results of experimental investigations in the CERN PS Booster.

LANDSCAPE

The delivery of high-intensity beams is constrained by several effects, among which the effect of machine error resonances is of significant impact [1]. Operational scenarios at injection should prevent the space charge tune-spread from overlapping with any machine resonance and, as the lower-order resonances are the strongest, they should be avoided or corrected.

Gradient errors affect single particle dynamics in such a way that they alter optical functions and generate beta-beating [2]. They also create an instability stop-band, where the particle's motion is subject to an exponential amplitude growth. This view considers the unperturbed lattice joint with the distribution of linear errors as "another linear lattice", which can be treated with the usual optics tools for stable dynamics [3], and also with ad-hoc optics for unstable single-particle dynamics [4].

For a high-intensity beam, dynamics are more complex. Frank Sacherer has shown that for a KV coasting beam, the resonance location is shifted with respect to the one of the single particle resonance [5]. This effect is "coherent" as dynamics are completely determined by global quantities and not by a single particle. On the other hand, this result is fully valid for a perturbative gradient error and for a KV distribution. The beam response is not localized for non-perturbative errors and non-KV beam distributions, and a typical spread of the beam response results from the resonance dynamics. The disentangling of the effect created by a half-integer resonance is of interest to several laboratories such as GSI [6–8], CERN [9, 10], RAL [11], and FNAL [12, 13].

Recently, an experimental campaign has been carried out at the CERN PSB on the effect of half-integer resonances on an intense coasting beam [14, 15]. Several scenarios have been investigated, from the effect for fixed accelerator parameters to the investigation of a dynamical crossing of the half-integer resonance. The associated simulation effort to explain and interpret the experimental findings has revealed an anomalous pattern, which brought the attention to the dynamics of an intense coasting beam performing coherent oscillation during the resonance crossing, and on the effect of space charge on coherent/decoherent dynamics. Studies on the instability of coasting beams are presented in Refs. [16, 17], and a discussion on its relation to the half-integer resonance is presented in Ref. [18]. Studies of decoherence in bunched beams have also been carried out in Refs. [19, 20].

We focus here on the dynamics of a kicked coasting beam when subject to pure direct space charge fields, i.e. we neglect the effect of impedance and other collective effects.

EFFECT OF THE CHROMATICITY

A displaced coasting beam in the phase space, when subject only to chromatic effects, can be analyzed from the single particle dynamics point of view. Each beam particle performs a specific harmonic oscillation, which has a main frequency plus a shift proportional to the particle momentum offset. The small focusing shift does not affect the optics, as we carry out this investigation off the half-integer resonance (and off-momentum beta-beating is neglected). The resulting effect on the center of mass is that the amplitude of oscillation is modulated by the function $\Lambda(\tau s)$, where

$$\tau = \left(\frac{Q_{x0} \xi_x \sigma_p}{R} \right). \tag{1}$$

Here, Q_{x0} is the tune, ξ_x is the normalized chromaticity, R the accelerator radius, and σ_p the rms momentum spread. The function $\Lambda(u)$ is given by

$$\Lambda(u) = \int \cos(u\lambda) g(\lambda) d\lambda \tag{2}$$

and the function $g(\lambda)$ is the normalized distribution of the momentum offsets satisfying the properties

$$g(-x) = g(x), \qquad \int g(x)dx = 1,$$
$$\int x g(x)dx = 0, \qquad \int x^2 g(x)dx = 1.$$

For a uniform distribution of $(\delta p/p)$ we have

$$\Lambda(u) = \frac{\sin\left(\sqrt{3}u\right)}{\sqrt{3}u}, \tag{3}$$

* Work partially supported by the European Union's Horizon 2020 Research and Innovation programme under Grant Agreement No. 101004730 (iFAST).

ISBN: 978-3-95450-253-0 ISSN: 2673-5571 doi:10.18429/JACoW-HB2023-WEA1C1

BUNCH-BY-BUNCH TUNE SHIFT STUDIES FOR LHC-TYPE BEAMS IN THE CERN SPS

I. Mases Solé*,[1], H. Bartosik, K. Paraschou, M. Schenk, C. Zannini
CERN, Geneva, Switzerland
[1]also at Goethe University Frankfurt am Main, Germany

Abstract

After the implementation of major upgrades as part of the LHC Injector Upgrade Project (LIU), the Super Proton Synchrotron (SPS) delivers high intensity bunch trains with 25 ns bunch spacing to the Large Hadron Collider (LHC). These beams are exposed to several collective effects in the SPS, such as beam coupling impedance, space charge and electron cloud, leading to relatively large bunch-by-bunch coherent and incoherent tune shifts. Tune correction to the nominal values at injection is crucial to ensure beam stability and good beam transmission. Measurements of the bunch-by-bunch coherent tune shifts have been performed under different beam conditions. In this paper, we present the measurements of the bunch-by-bunch tune shift as function of bunch intensity for trains of 72 bunches. The experimental data are compared to multi-particle tracking simulations (including other beam variants such as 8b4e beam and hybrid beams) using the SPS impedance model.

INTRODUCTION

In preparation of the high luminosity upgrade of the LHC (HL-LHC) [1], the LHC injectors including the SPS have been upgraded in the context of the LIU project [2] to allow the production of high intensity and high brightness beams. Because of the high intensity of the bunches, there is a pronounced bunch-by-bunch coherent and incoherent tune shift in the SPS caused by the transverse beam coupling impedance. Moreover, at injection energy, the proton beam is sensitive to instabilities induced mainly by the impedance contribution from the resistive wall. In order to stabilize the beam, it is thus necessary to measure the horizontal and vertical bunch-by-bunch tunes at injection and correct the average coherent tunes such that they are close to the central tunes programmed for the bunch-by-bunch transverse damper. The nominal values of the horizontal and vertical tunes, in the SPS Q20 optics [3], are $Q_x = 20.13$ and $Q_y = 20.18$.

The bunch-by-bunch transverse tune shift depends strongly on the beam configuration. The most important parameters are the intensity per bunch, and the total intensity of the beam through the number of bunches and the number of batches (i.e. bunch trains from the injector), as illustrated schematically in Fig. 1. The spacing between both individual bunches and trains of bunches is also important, as wakefields decay, which in turn affects the tune shift. Since the majority of SPS vacuum pipes are flat chambers (i. e. no circular symmetry), the horizontal and vertical impedances are not the same, resulting in different bunch-by-bunch tune shifts in the transverse planes. In the vertical plane, the broadband impedance sources in the SPS, i. e. mostly the kicker magnets, result in a relatively large tune shift already for single bunches (denoted in the image as ΔQ_{SB}) in the machine [4]. Due to the resistive wall impedance and other narrow-band impedances in the machine, the wakefield builds up along the train, resulting in an increasing bunch-by-bunch tune shift (denoted as ΔQ_{BbB}) for the trailing bunches. Moreover, if the wakefield does not fully decay within one turn of the machine, an additional tune shift from these long range wakefields (denoted as ΔQ_{MBMT} in Fig. 1) is experienced even by the first bunches of the train. In the horizontal plane, $\Delta Q_{\mathrm{SB}} \sim 0$ and $\Delta Q_{\mathrm{BbB}} \sim 0$, so the multi-turn tune shift ΔQ_{MBMT} is the responsible for the positive tune shift of all bunches, as seen in Fig. 1 bottom.

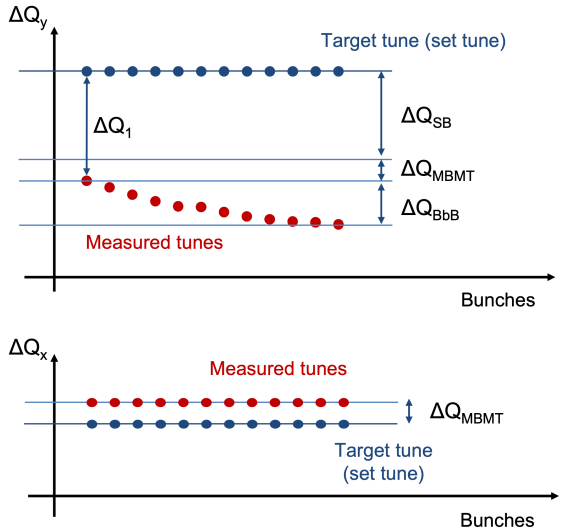

Figure 1: Schematic view of vertical (top) and horizontal (bottom) tune shift along the bunch train (explanation in the text).

Measuring bunch-by-bunch tune shifts at intensities higher than 2.0×10^{11} p/b is not transparent to the machine operation, as it leads to beam degradation, due to the excitation of transverse oscillations required for the measurement. The aim of the bunch-by-bunch tune shift studies is thus to build a model for predicting the transverse tune shifts experienced by each train injected in the SPS as a function of the beam configuration: filling scheme, number of trains, number of bunches and intensity per bunch. The predictive model should allow to compute the tune corrections needed for LHC-type beams without performing measurements dur-

* ingrid.mases.sole@cern.ch

ISBN: 978-3-95450-253-0 ISSN: 2673-5571 doi:10.18429/JACoW-HB2023-WEC1I1

RADIATION HARDENED BEAM INSTRUMENTATIONS FOR MULTI-MEGA-WATT BEAM FACILITIES

K. Yonehara*, Fermilab, Batavia, IL, USA

Abstract

Beam instrumentation is a critical component for the successful operation of particle accelerators, integrating beam diagnostics and beam control systems into beam optics. However, the performance of beam instrumentation is often constrained by factors such as prompt radiation dose, integrated radiation dose, operational (ambient) temperature and humidity, available space, and the strength of embedded electromagnetic fields at the monitoring point. These constraints can limit the dynamic range of operational beam parameters, including the maximum achievable beam power. To address this, a seamless R&D effort should be dedicated to developing radiation-hardened beam instrumentation for future multi-Mega-Watt beam facilities. In this paper, we describe a radiation-hardened beam instrumentation system based on the operational experience gained from the NuMI beam line.

INTRODUCTION

Modern beam facilities employ advanced accelerator technology to generate intense beams for exploration across a wide range of accelerator applications, such as a collider, accelerator neutrino beam, intense muon source, spallation neutron source, accelerator-driven subcritical nuclear reactor, Radioactive-Isotope (RI) beam, etc. Table 1 shows the beam parameter of a selected beam facilities [1, 2].

Each facility faces the challenge of developing radiation-hardened beam instrumentation which is operated in severe environments. Some examples are provided in Ref. [1]. In this paper, we specially address the challenge of radiation-hardened beam instrumentation, drawing on our experience with the operation of NuMI targetry system, especially in the context of a future accelerator neutrino facility.

Beam instrumentation plays an essential role in ensuring the successful operation of particle accelerators. Its primary function is to characterize the beam phase space by measuring various parameters related to an ensemble of charged particles. These parameters include:

- Spatial distribution: this determines the spatial characteristics of the charged particle ensemble, including the centroid position, orientation, and profile of the beam ensemble.
- Intensity measurement: this involves quantifying the amount of beam ensemble in a certain time period.
- Time structure measurement: this includes assessing the time differential beam intensity and the bunch structure of the charged particle ensemble.

The beam instrumentation often incorporates a feedback loop to maintain stable beam operation. The concept of a feedback loop system differs between circular and linear accelerators.

In a circular accelerator, where the beam circulates for many revolutions, the beam parameters of the same beam ensemble can be adjusted via a feedback loop system. On the other hand, in a linear accelerator, the beam parameters cannot be corrected for the same beam ensemble because the beam passes through the accelerator only once. Therefore, a feedback loop system is applied to correct the beam parameters for the next incoming beam ensemble.

Additionally, the beam instrumentation serves as an anomaly detector. If the observed parameter exceeds some threshold, the feedback loop triggers a special signal to the beam control system. In the worst case, the beam control system aborts the beam to protect the accelerator or maintain beam quality.

In the case of NuMI targetry system operation, special beam instrumentation is used to monitor and control the proton beam in the transport line reaching the target. We demonstrate the beam control system and the beam abort signal in the NuMI targetry system in the beam control and beam permit systems section.

Especially, the thermocouple beam position sensor positioned in front of the target is an extremely reliable detector, even when intercepting the intense proton beam. We present the performance of the thermocouple beam position sensor in the thermocouple beam position monitor section.

The neutrino target is usually bare, or minimize the use of supporting structure materials for the target. Materials surrounding the target that do not contribute pion production, could absorb pions originally created at the target. Consequently, there is no in-situ target health monitor for the neutrino target. In the NuMI targetry system, four layers of ionization chamber grid downstream of the target and horns are used to monitor the condition of the targetry system. We present the performance of the ionization chambers in the following section. The first ionization chamber, referred to as the hadron monitor, was inspected after the beam operations, revealing various types of the radiation damage. We present those damages in the hadron monitor section.

BEAM INSTRUMENTATION IN NuMI

Figure 1 depicts the layout of the NuMI target and horn system (referred to as "targetry system"), including the four layers of ionization chamber grids. Every 1.2 s, a 120 GeV proton beam is transported from the Main Injector to the NuMI target system. The beam spill length is 9.6 ms. The highest beam intensity is 5.6×10^{13} protons on target (POT) per spill demonstrated in Spring 2022. The proton beam

* yonehara@fnal.gov

ISBN: 978-3-95450-253-0 ISSN: 2673-5571 doi:10.18429/JACoW-HB2023-WEC1C1

IMPROVEMENT DESIGN OF A BEAM CURRENT MONITOR BASED ON A PASSIVE CAVITY UNDER HEAVY HEAT LOAD AND RADIATION

P. A. Duperrex†, J. Sun, J. E. Bachmann, M. Rohrer
Paul Scherrer Institut, 5232 Villigen PSI, Switzerland

Abstract

The High Intensity Proton Accelerator (HIPA) at PSI delivers a continuous proton beam of up to 2.4 mA with a maximum energy of 590 MeV to two meson production targets, M and E, and then to the SINQ spallation target. The scattered particles from the beam's interaction with Target E affect the performance of a resonator-based current beam monitor. To minimize these issues, a graphite monitor was designed to replace the older aluminum one.

Based on years of operating experience with this graphite cavity, improvements to the design have been considered, including refining beam position pickups, implementing online calibration methods, and addressing manipulation and maintenance issues. Detailed aspects of the monitor's performance and its improved design are presented.

INTRODUCTION

The HIPA can generate up to 1.4 MW continuous proton beam [1]. After the main cyclotron extraction, the beam is transported through a 60 m long beam line with two graphite target stations, TM and TE for Muon and Pion production. The TM has a thickness of 5 mm and absorbs ~1% of the beam. The TE is 40 mm (alternatively 60 mm) thick and absorbs ~8% (~12%) of protons. Then the remaining beam is directed to the SINQ spallation source for neutron production. Collimators or local shielding are responsible for further beam losses leading to additional ~20% (~30%) beam losses while the remaining ~72% (~58%) of protons are transmitted to the SINQ target through a 55 m beam line [2].

A proton beam current monitor, called MHC5, is located 8 meters downstream of target E in the high-energy beam line of HIPA. It is a coaxial cavity tuned to the second harmonic (101.26 MHz) of the proton beam pulse frequency. MHC5 is a key element for beam operation, as any deviation from the expected transmission from target E could damage the SINQ target.

A main concern for MHC5 is the energy deposition from the scattered particle shower due to the target E. This causes large temperature variations in the resonator, leading to resonance frequency and calibration drifts during beam operation [3].

To address this issue, an aluminum cavity with active cooling was first implemented. However, the resonance frequency shift was still too large. A later study showed that the cavity thermal gradient due to active cooling was inducing an even larger shift [4]. Therefore, materials with lower thermal expansion coefficients and higher radiation emissivity (since the resonator is in the beam line vacuum) were considered for a new MHC5 design.

† pierre-andre.duperrex@psi.ch

PASSIVE CAVITY MADE OF GRAPHITE

Advantages

Graphite has several advantages over aluminum for the MHC5 cavity. Its lower thermal expansion coefficient reduces thermal deformation, leading to smaller frequency drift. Its higher radiation emissivity improves cooling and reduces temperature excursions. Without active cooling, thermal gradient issues are minimized. Additionally, its lower electrical conductivity reduces the cavity's Q factor, making the resonator less sensitive to frequency drift.

Figure 1 shows the graphite cavity under laboratory test, with eight graphite screws used for fine tuning. The monitor was installed on the beam line in early 2015.

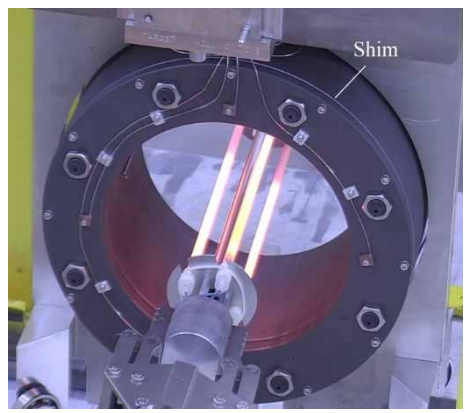

Figure 1: The graphite MHC5 being tested after maintenance in 2017, quartz tube in the center of the monitor to test the thermal load effects on the resonator the beam.

Further simulation studies show that thermal expansion always causes negative frequency drift, with a higher temperature leading to a lower resonance frequency. One possible way to counteract this effect is to use a second material with a much larger expansion coefficient to increase the capacitor gap, thereby increasing the resonance frequency. This self-compensating method was implemented by inserting a thin aluminum shim at the capacitor gap position, as shown in Fig. 1.

Performances

Figure 2 shows historical data of the MHC5 and a NPCT Bergoz [5] current monitor (MHC6B) during a service day of HIPA, with a beam intensity of up to 1800 µA. As the Bergoz monitor performs an absolute measurement of the beam current, it can be used to calibrate the MHC5. This calibration procedure cannot be considered "online" because the Bergoz electronics must be compensated at each calibration, which requires interrupting the beam for several seconds. The MHC5 shows good linearity with the Bergoz monitor before the beam is stopped, because the

ISBN: 978-3-95450-253-0 ISSN: 2673-5571 doi:10.18429/JACoW-HB2023-WEC1C2

CHALLENGES OF TARGET AND IRRADIATION DIAGNOSTICS OF THE IFMIF-DONES FACILITY

C. Torregrosa-Martin*, J. Maestre, I. Alvarez, A. Roldan, J. Valenzuela
Universidad de Granada, Granada, Spain
A. Ibarra, S. Becerril, I. Podadera, Consorcio IFMIF-DONES España, Granada, España
F.S. Nitti, ENEA, Brasimone, Italy
S. Fiore, CERN, Geneva, Switzerland
J. Castellanos, Universidad de Castilla la Mancha, Ciudad Real, Spain
C. De la Morena, D. Regidor, F. Mota, D. Jimenez-Rey, C. Oliver, CIEMAT, Madrid, Spain
F. Arbeiter, B. Brenneis, Y. Qiu, KIT, Karlsruhe, Germany
T. Tadic, Ruder Boskovic Institute, Zagreb, Croatia
L. Buligins, Institute of Physics, University of Latvia, Latvia
N. Chauvin, CEA, Saclay, France, U. Wiacek, IFJ PAN, Krakow, Poland
P. Matia-Hernando, J. Martínez, T. Siegel, ASE Optics Europe, Barcelona, Spain

Abstract

IFMIF-DONES will be a first-class scientific infrastructure consisting of an accelerator-driven neutron source delivering around 10^{17} n/s with a broad peak at 14 MeV. Such neutron flux will be created by impinging a continuous wave 125 mA, 40 MeV, 5 MW deuteron beam onto a liquid Li jet target, circulating at 15 m/s. Material specimens subjected to neutron irradiation will be placed a few millimeters downstream. Some of the most challenging technological aspects of the facility are the Diagnostics to monitor the Li jet, beam parameters on target, and characterization of the neutron irradiation field, with transversal implications in the scientific exploitation, machine protection and safety. Multiple solutions are foreseen, considering among others, Li jet thickness measurement methods based on laser measurement and millimeter-wave radar techniques, Li electromagnetic flowmeters, beam footprint measurements based on residual gas excitation, online neutron detectors such as SPNDs and micro-fission chambers, as well as offline neutron fluence measurements by activation foils or spheres. This contribution provides an overview of these aspects and the associated R&D activities.

INTRODUCTION

The International Fusion Materials Irradiation Facility-DEMO Oriented Neutron Source (IFMIF-DONES) is a scientific infrastructure whose objective is to provide an intense neutron source (in the order of 10^{17} n/s) for the qualification of materials to be used in future fusion power reactors [1].

IFMIF-DONES will be an accelerator-driven neutron source, where a 40 MeV deuteron beam produced by a superconducting LINAC is directed towards a liquid lithium target to produce neutrons by stripping nuclear reactions [1]. The deuteron accelerator consists in a 100 m length 40 MeV LINAC operating in continuous wave (CW) with a nominal average intensity of 125 mA and an output power of 5 MW [2]. The Target will consist of a 25 mm thick liquid Li curtain, circulating at 15 m/s inside the Target Vacuum Chamber (TVC), which is directly connected to the accelerator vacuum chamber. For providing such curtain, a closed loop of liquid Li with a flow of 100 l/s is required. The Target accomplishes a double function; (i) it produces the required neutron field for samples irradiation and (ii) it evacuates the 5 MW power deposited by the incident beam via heat exchangers and secondary cooling loops [3, 4].

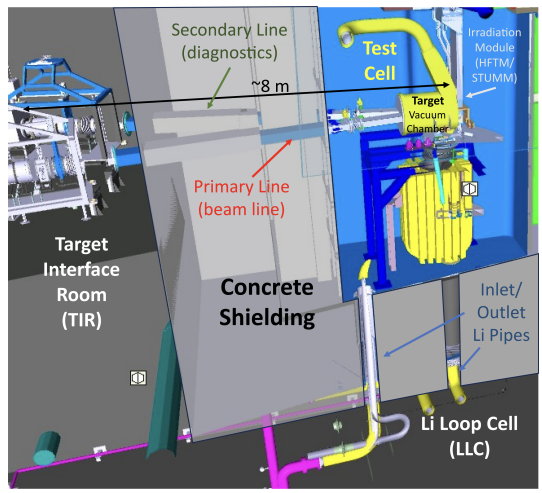

Figure 1: Image showing the arrangement of the Target and Irradiation Modules inside the Test Cell, the Target Interface Room (TIR) upstream, and the Li Loop Cell (underneath).

Figure 1 shows the arrangement of the IFMIF-DONES Target (yellow), and the Irradiation Module, which is placed a few millimeters downstream the Target. The first two types of exchangeable Irradiation Modules foreseen are; (i) the so-called High Flux Test Module (HFTM) and (ii) the Start-Up Monitoring Module (STUMM). The STUMM will be

* cltorregrosa@ugr.es

ISBN: 978-3-95450-253-0 ISSN: 2673-5571 doi:10.18429/JACoW-HB2023-WEA2I1

COMPENSATION OF THIRD-ORDER RESONANCES IN THE HIGH-INTENSITY REGIME

C. E. Gonzalez-Ortiz*, P. N. Ostroumov[1], Michigan State University, East Lansing, MI, USA
R. Ainsworth, Fermilab, Batavia, IL, USA
[1] also at FRIB, East Lansing, MI, USA

Abstract

As the Fermilab Accelerator Complex enters the high-intensity era, the Recycler Ring (RR) needs to mitigate the detrimental effect of third-order resonance crossing. Third-order resonance lines can be compensated to first order by cancelling out the global Resonance Driving Terms (RDTs) using the response matrix method. This compensation scheme has been proven to work at low intensities, i.e., in the single-particle regime. In order to evaluate the effectiveness of this compensation scheme at higher intensities, this study looks at dynamic and static tune scans, with and without resonance compensation, and different space charge tune shifts.

INTRODUCTION

The Recycler Ring is a permanent-magnet storage ring located in the Fermilab Accelerator Complex. This machine stores bunched protons at a fixed energy of 8 GeV. It shares the same tunnel with the Main Injector (MI), both with a circumference of around 3.3 km (2.06 miles). For high-intensity operation, i.e., for beam delivery to the Neutrinos at Main Injector (NuMI) experiment, the RR slip-stacks protons coming from Booster and, ultimately doubles the intensity for the stored beam. Protons are then injected into MI, where they are accelerated to an energy of 120 GeV and sent to NuMI [1–3]. Table 1 summarizes the properties of typical beam in the RR that gets sent to NuMI.

The Proton Improvement Plan II (PIP-II) is the first step in establishing the Fermilab Accelerator Complex as a multi-MW proton facility [4]. The near-future objective is to deliver a 1.2 MW proton beam to the Deep Underground Neutrino Experiment (DUNE) through the Long-Baseline Neutrino Facility (LBNF). In order to meet this goal, several upgrades are being planned in the accelerator complex, including a new 800 MeV superconducting linear accelerator. With minimal upgrades to the Main Injector and Recycler Ring, but with a substantial overhaul of the Booster Ring, this will allow for a 50 % increase in particles per pulse intensity. Table 1 also specifies some upgrades that will happen for the PIP-II era. Some examples include an increase of the particle per bunch intensity, a shortening of the Main Injector acceleration ramp and an increase in the Booster ramping rate.

As the Recycler Ring starts to deal with higher intensities, it is important to mitigate the harmful effects of space charge. Specifically, this work focuses on the excitation of third-order betatron resonances due to the incoherent space charge detuning of particles in the beam. Particles in the core of the beam will experience a larger space charge force leading to detuning in their betatron frequencies. Given the incoherent nature of this process, this leads to the beam having a larger tune spread in the tune diagram. Figure 1 shows the tune footprint for particles with transverse amplitudes up to 3σ, assuming a Gaussian bunched beam. This detuning was calculated using PySCRDT [5, 6], but can also be estimated assuming a uniform bunched beam [7, 8]. Particles will also experience an additional tune shift due to uncorrected chromaticity and slip stacking operation [3].

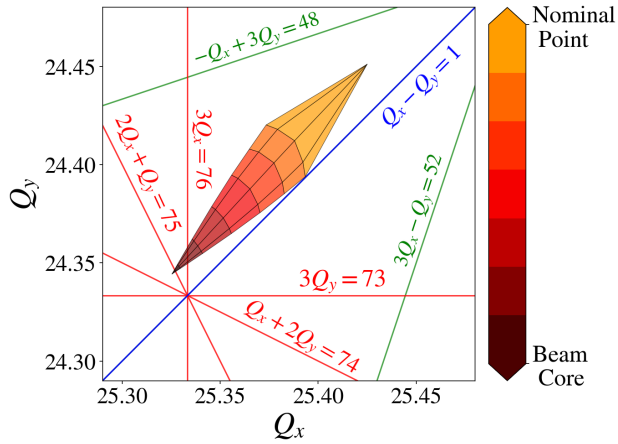

Figure 1: Space charge tune footprint calculated using PySCRDT [5] for 1×10^{11} particles per bunch in a PIP-II Recycler Ring.

Figure 1 shows how for typical operation to NuMI under future PIP-II specifications, there is a space charge tune shift of around 0.1 in both planes. At nominal tunes, it is clear that for high-intensity operation the particles in the core of the beam will start to operate on top of third-order resonances. These third-order resonances include two normal sextupole lines ($3Q_x = 76$ and $Q_x + 2Q_y = 74$) and two skew sextupole lines ($3Q_y = 73$ and $2Q_x + Q_y = 75$). It is also worth pointing out that the coupling line $Q_x - Q_y = 1$ is already being corrected for with skew quadrupoles. The following work, complemented with previous work in Refs. [9, 10], explores how cancelling out the global resonance driving terms (RDTs) of these resonance lines can mitigate their harmful effect in the low and high-intensity regime. Furthermore, this work outlines the challenges to overcome for complete implementation of the mitigation scheme for high-intensity operation at the Fermilab Recycler Ring.

* gonza839@msu.edu

ISBN: 978-3-95450-253-0 ISSN: 2673-5571 doi:10.18429/JACoW-HB2023-WEA2I2

SPACE CHARGE INDUCED RESONANCES AND SUPPRESSION IN J-PARC MR

T. Yasui*
J-PARC center, KEK&JAEA, Tokai, Naka, Ibaraki, Japan

Abstract

In the main ring synchrotron (MR) of Japan Proton Accelerator Research Complex (J-PARC), we identified that the space charge induced resonance $8\nu_y = 171$ is the main source of beam losses in the neutrino operation, except for random resonances. We found that this resonance can be suppressed by beam optics modification while maintaining the tune. We confirmed the superiority of the newly-developed optics via analytical calculations of resonance potentials, beam loss simulations, Poincaré maps, beam loss measurements, and frequency map analyses.

INTRODUCTION

The main ring synchrotron (MR) [1] of Japan Proton Accelerator Research Complex (J-PARC) is the synchrotron providing high power proton beams to the neutrino and hadron experiments. Eight-bunch beams are injected with a kinetic energy of 3 GeV, and they are accelerated to 30 GeV. In 2021, we operated with an intensity of 2.66×10^{14} protons per pulse (ppp), corresponding to 3.3×10^{13} protons per bunch (ppb), and a cycle time of 2.48 s in the neutrino fast extraction (FX) operation. For further intensity increase, we launched a plan to upgrade the beam power to 1.3 MW in the FX operation [2]. In JFY2022, we made a long-term shutdown for hardware upgrade to realize faster cycling. As a result, the cycle time became 1.36 s. Although the beam intensity was temporarily reduced due to the capability of the RF system, the beam power was recorded at 766 kW [3]. To realize 1.3 MW operation, we are going to increase the beam intensity to 3.3×10^{14} ppp and further reduce the cycle time.

To increase the beam intensity, we need not only to upgrade the RF system but also to control the beam loss. Tracking simulations show that the beam loss occurs even when we assume perfect magnetic fields and alignments because of space-charge-induced resonances. In fact, the beam loss can be found before and during very early stages of acceleration, showing strong space charge effects. The longitudinal beam size becomes stable after approximately 5 ms from beam injection and the space charge effect becomes stable. In this paper, we focus on the period when the longitudinal beam size is stable.

Figure 1 shows the tune spread after the longitudinal beam size has stabilized. It was obtained by the space charge tracking simulation code SCTR [5, 6], which employs the particle-in-cell algorithm. The working point was optimized at $(\nu_x, \nu_y) = (21.35, 21.43)$ [7, 8]. In fact, Fig. 1 shows that most of the particles can avoid the differential resonance

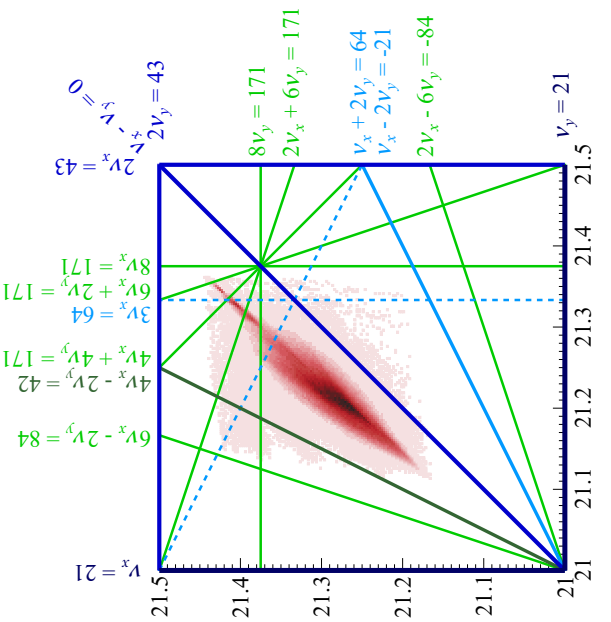

Figure 1: Tune spread (approximately 30 ms from beam injection) and major resonances (lines) in FX operation [4]. The tune spread was obtained by the tracking simulation assuming a beam intensity of 3.2×10^{13} ppb.

$\nu_x - \nu_y = 0$ (or the space-charge-induced 4th-order structure resonance $2\nu_x - 2\nu_y = 0$), the half-integer resonance $2\nu_y = 43$, and the space-charge-induced 6th-order structure resonance $4\nu_x - 2\nu_y = 42$. The beam is crossing the dashed skyblue lines and some of light green lines. The dashed skyblue lines represent the resonances $3\nu_x = 64$ and $\nu_x + 2\nu_y = 64$, which are nonstructure resonances driven by sextupole magnetic fields. They are compensated using four trim coils of sextupole magnets [2]. The light green lines denotes space-charge-induced 8th-order structure resonances. Since the superperiodicity of the MR is only three, it is difficult to completely avoid high-order structure resonances.

IDENTIFICATION OF BEAM LOSS SOURCE

To suppress space charge effects, second harmonic RF cavities are used in the MR. The top panel of Fig. 2 shows the longitudinal phase-space distribution of the beam after stabilization, the middle panel shows its projection to the z coordinate, and the bottom panel shows the distribution of the lost particles. Most of the lost particles are found at locations of high line densities. It shows that the beam loss is caused by space charge effects. It also shows the importance of peak suppression by the second harmonic RF cavities.

* takaaki.yasui@kek.jp

ISBN: 978-3-95450-253-0 ISSN: 2673-5571 doi:10.18429/JACoW-HB2023-WEA2C1

TUNE OPTIMIZATION FOR ALLEVIATING SPACE CHARGE EFFECTS AND SUPPRESSING BEAM INSTABILITY IN THE RCS OF CSNS

Shouyan Xu[1,†], Mingyang Huang[1], Liangsheng Huang[1], Yong Li[1], Sheng Wang[1]
Institute of High Energy Physics, Chinese Academy of Sciences (CAS), Beijing, China
[1]also at Spallation Neutron Source Science Centre, Dongguan, China

Abstract

The design Betatron tune of the Rapid Cycling Synchrotron (RCS) of China Spallation Neutron Source (CSNS) is (4.86, 4.80), which allows for incoherent tune shifts to avoid serious systematic Betatron resonances. When the operational bare tune was set at the design value, serious beam instability in the horizontal plane and beam loss induced by half-integer resonance in the vertical plane under space charge detuning were observed. The tunes over the whole acceleration process were optimized based on space charge effects and beam instability. The optimized tune pattern was able to well control the beam loss induced by space charge and beam instability. The beam power of CSNS achieved the design value of 100 kW with small uncontrolled beam loss.

INTRODUCTION

The China Spallation Neutron Source (CSNS) is designed to accelerate proton beam pulses to 1.6 GeV kinetic energy, striking a solid metal target to produce spallation neutrons. CSNS has two major accelerator systems, a linear accelerator (80 MeV Linac) and a 1.6 GeV rapid cycling synchrotron (RCS). The RCS accumulates and accelerates the proton beam to 1.6 GeV. The 1.6 GeV proton beam is extracted to the target at a repetition rate of 25 Hz. The RCS is designed to extract a beam power of 100 kW, corresponding to 1.56×10^{13} protons per pulse in two bunches. The lattice of the RCS is a four-fold structure based on triplet cells. The entire ring comprises 16 triplet cells, with a circumference of 227.92 m. In each super-period, an 11 m long drift space is available between two triplet cells, providing uninterrupted space for accommodating the injection, extraction, acceleration, and transverse collimation system, as shown in Fig. 1. Table 1 provides the primary parameters of the RCS [1, 2].

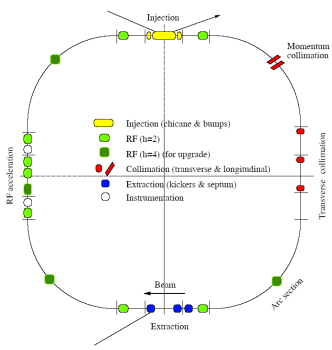

Figure 1: The schematic layout of the RCS of CSNS.

† xusy@ihep.ac.cn

The designed tune of the RCS is (4.86, 4.80), which allows for incoherent tune shifts to avoid serious systematic Betatron resonances. Figure 2 illustrates the resonance map around the design tune, where the red lines signify the structure resonances up to the 4th order. However, serious beam instability in the horizontal plane with the design tune was observed in the beam commissioning.

Table 1: The Primary Parameters of the RCS of CSNS

Parameters	Value
Output Beam Power (kW)	100
Injection Energy (MeV)	80
Extraction Energy (GeV)	1.6
Pulse repetition rate (Hz)	25
Ramping Pattern	Sinusoidal
Acceleration Time (ms)	20
Circumference (m)	227.92
Number of Dipoles	24
Number of Quadrupoles	48
Lattice Structure	Triplet
Nominal Betatron Tunes (H/V)	4.86/4.80
Mode of Chromaticity Sextupoles	DC
Natural Chromaticity (H/V)	-4.0/-8.2
Ring Acceptance (πmm-mrad)	540
Number of Bunches	2
Number of Particles per Pulse	1.56×10^{13}
Space-Chare Tune Shift	-0.28

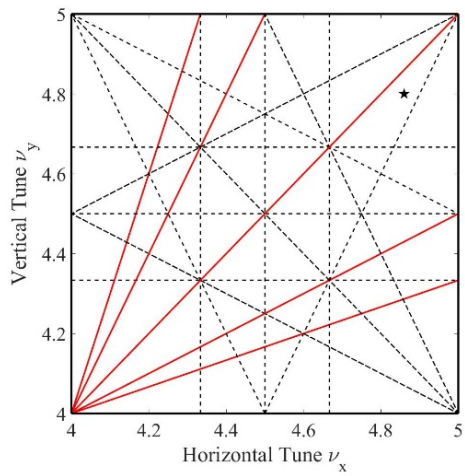

Figure 2: The design tune location in the resonance map, in which the red lines represent the structure resonances up to 4th order.

ISBN: 978-3-95450-253-0 ISSN: 2673-5571 doi:10.18429/JACoW-HB2023-WEA2C2

MEASUREMENT OF TRANSVERSE STATISTICAL DEPENDENCE FOR NON-GAUSSIAN BEAM DISTRIBUTIONS VIA RESONANCES IN THE CERN PSB

E. Lamb*,[1], F. Asvesta, H. Bartosik, G. Sterbini, CERN, Geneva, Switzerland
[1]also at EPFL, Lausanne, Switzerland

Abstract

Non-Gaussian heavy-tail transverse beam profiles can be used to reconstruct the 4D beam distribution in phase space under two different conditions, that is independent or dependent distribution functions across the x-y-plane. The two conditions lead to different implications for the physics of the beam. In the case of dependent distributions, this results in profile changes in one plane through a loss process on the other. This work explores how different resonances, either 1D or 2D can lead to tail population with statistical dependence. Original measurements performed in the Proton Synchrotron Booster at the CERN accelerator complex demonstrate this effect and are hereby presented and discussed.

INTRODUCTION

We often observe heavy-tail non-Gaussian beam profiles in the CERN accelerator complex at the LHC [1] and in the injectors [2]. For luminosity studies in the LHC, but also for scenarios involving loss mechanisms, it is interesting to reconstruct the most realistic particle distribution corresponding to the profile observed.

We define a normalised phase space, for a linear machine, via a transformation:

$$\begin{bmatrix} 1/\sqrt{\beta}_x & 0 \\ \alpha_x/\sqrt{\beta}_x & \sqrt{\beta}_x \end{bmatrix} \begin{bmatrix} x_1 & p_{x_1} \\ x_2 & p_{x_2} \\ \dots & \dots \end{bmatrix}^T \tag{1}$$

yielding a rotationally symmetric x-p_x phase space, where α_x, β_x are the machine optics functions. The equivalent is true in the y plane. We define the normalised profile in one of the transverse planes (x, y) as an integration of a 4D (x, p_x, y, p_y) distribution function in the other three planes, e. g. for the horizontal plane:

$$f_{1D}(x) = \iiint f_{4D}(x, p_x, y, p_y)\, \mathrm{d}p_x\, \mathrm{d}y\, \mathrm{d}p_y. \tag{2}$$

To reconstruct the probability density function $f_{4D}(x, p_x, y, p_y)$ of the matched distribution there is a constraint that in the normalised x-p_x and y-p_y phase space, the beam is rotationally symmetric. To reconstruct the 2D distribution functions $f_{2D}(x, p_x)$ and $f_{2D}(y, p_y)$, we can use a form of the inverse Abel transform [3, 4], of which the 'inverse' transform is given by:

$$f_{2D}(r) = -\frac{1}{\pi} \int_r^\infty \frac{\mathrm{d}f_{1D}(x)}{\mathrm{d}x} \frac{\mathrm{d}x}{\sqrt{x^2 - r^2}}, \tag{3}$$

where $r^2 = x^2 + p_x^2$, which transforms the 1D profile projection to a 2D distribution under this constraint. To find the 4D phase space distribution, there are not enough constraints, thus there are infinite distributions with the same 1D projection (for the non-Gaussian case). We show two examples, one forming f_{4D} assuming independent distributions in x and y, and the other using a constraint that the beam is rotationally symmetric also in the normalised x-y-plane.

Choosing independent, or factorisable distributions, we generate the 4D particle distribution function (PDF)

$$f_{4D}(x, p_x, y, p_y) = f_{2D}(x, p_x) \times f_{2D}(y, p_y). \tag{4}$$

This results in a 'cross'-shaped beam in the x-y-space for heavy tailed profiles, as can be seen in Fig. 1 (top), using the example of a q-Gaussian [5] with q-parameter 1.4.

Alternatively, to reconstruct f_{4D} assuming rotational symmetry in the x-y-plane, we use a series of inverse Abel transforms, exploiting the property that they can find higher dimensional distributions as long as they are axisymmetric. Then, the full distribution is populated via a Box-Müller type random 4D generator [6, 7]. Figure 1 (bottom) shows the rotationally symmetric distribution, which gives the same 1D projection, or 'profile' as the other method.

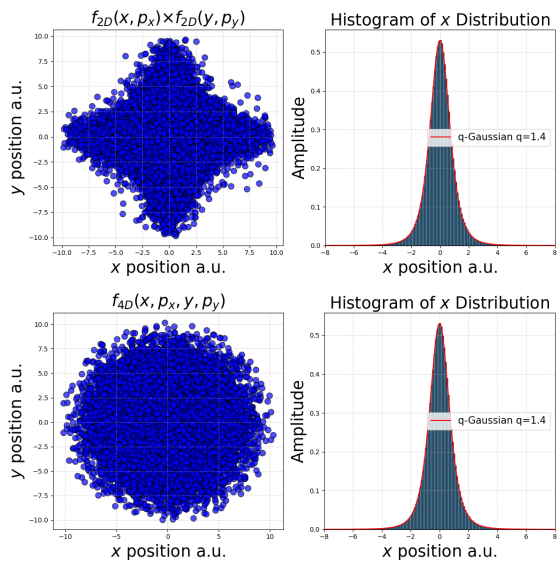

Figure 1: A heavy tailed beam generated in normalised phase space with two methods, giving the same projection on the x (and y) plane and matched distributions in a linear and uncoupled lattice: factorisable distributions (top) and assuming rotational symmetry in the x-y-plane (bottom).

* elamb@cern.ch

ISBN: 978-3-95450-253-0 ISSN: 2673-5571 doi:10.18429/JACoW-HB2023-WEC2C1

EVALUATION OF POWER DEPOSITION IN HL-LHC WITH CRYSTAL-ASSISTED HEAVY ION COLLIMATION*

V. Rodin†, R. Bruce, R. Cai, M. D'Andrea, L. S. Esposito, A. Lechner,

J.-B. Potoine, S. Redaelli, P. Schoofs, CERN, Geneva, Switzerland

Abstract

The LHC heavy-ion program, utilizing $^{208}Pb^{82+}$ beams with an energy of up to 7 ZTeV, will profit from significantly higher beam intensities in future runs. During periods of short beam lifetime, a potential performance limitation may arise from secondary ions produced through electromagnetic dissociation and hadronic fragmentation in the collimators of the betatron cleaning insertion. These off-rigidity fragments risk quenching superconducting magnets when they are lost in the dispersion suppressor. To address this concern, an alternative collimation scheme will be introduced for forthcoming heavy ion runs, employing bent channeling crystals as primary collimators. In this contribution, we detail a thorough study of power deposition levels in superconducting magnets through multi-turn halo dynamics and FLUKA shower simulations for the crystal-based collimation system. The study focuses on the downstream dispersion suppressor regions of the betatron cleaning insertion, where the quench risk is the highest. Based on this work, we quantify the expected quench margin in future runs with $^{208}Pb^{82+}$ beams, providing crucial insights for the successful execution of the upgraded heavy-ion program at the HL-LHC.

INTRODUCTION

In 2023, the LHC heavy-ion program will profit for the first time from High Luminosity LHC (HL-LHC) beam intensities [1]. Numerous improvements were carried out within the LIU [2] and HL-LHC projects [3], which allow for beam intensities above 2×10^{11} $^{208}Pb^{82+}$ ions. Moreover, the $^{208}Pb^{82+}$ energy will be increased from the previous operational value of 6.37 ZTeV in 2018 to 6.8 ZTeV in 2023, with a total stored beam energy expected to reach about 20 MJ. In a superconducting machine like the LHC, even a small fraction of such stored energy is enough to cause quenches of superconducting magnets [3–5]. To counter the adverse effects of beam halo losses, multi-stage betatron and momentum collimation systems are installed in the LHC [6]. In conjunction with the Beam Loss Monitor (BLM) system [7], which continuously monitors beam losses and can trigger beam aborts, this setup protects from beam-induced quenches and, in the worst case, against potential damage to the accelerator equipment.

The collimation of heavy-ion beams poses a greater challenge compared to regular LHC proton operation, due to the occurrence of nuclear fragmentation and electromagnetic dissociation (EMD) when particles interact with the collimator material. These processes enhance particle leakage to cold magnets and hence the likelihood of beam-induced quenches. In order to improve the collimation efficiency for ions, crystal-assisted halo collimation [8, 9] has been implemented for $^{208}Pb^{82+}$ operation as part of the HL-LHC baseline [3]. The system will be used for the first time with high beam intensities in the 2023 heavy-ion run [10, 11]. Bent crystals can be used to guide halo particles onto a secondary collimator, limiting nuclear and electromagnetic fragmentation in the primary beam-intercepting device thanks to the channeling process. Fragments produced in the secondary collimator are much less likely to reach cold magnets, which increases the maximum allowed beam power loss without quenching.

Given the first operational use of crystal collimation in 2023, it is essential to assess the expected quench margin for the 2023 machine configuration (6.8 ZTeV) by predicting the power deposition in superconducting dispersion suppressor (DS) magnets next to the betatron cleaning insertion. A beam-induced quench in case of a significant beam lifetime drop would impose a machine downtime of eight or more hours, during which the affected superconducting magnets need to be brought back to their operational temperature. Quenches can be prevented by triggering a BLM abort when a certain loss threshold is exceeded. However, if thresholds are set too conservatively, this can lead to premature beam dumps, which would affect the machine availability. An accurate understanding of the expected power deposition in cold magnets is therefore crucial for setting BLM abort thresholds and for optimizing the performance. This paper presents the results of FLUKA [12–14] simulations that quantify the amount of power deposited in magnet coils for Run 3 operational conditions. It also provides an overview of crystal-assisted heavy ion collimation in the LHC, together with a brief introduction to the channeling process.

CRYSTAL-ASSISTED COLLIMATION

The multi-stage collimation system of the LHC was designed and put in place before launching operation in 2008 [3]. It contains two main sub-systems located in different insertion regions (IRs), the betatron cleaning system in IR7 and the off-momentum cleaning system in IR3. Currently, the collimation system comprises a total of more than 100 collimators for both beams. The betatron halo cleaning in IR7 is done with a three-stage collimator hierarchy for protons, with the addition of bent silicon crystals for ions, which substitute the standard primary collimators in

* Research supported by the HL-LHC project.
† volodymyr.rodin@cern.ch

ISBN: 978-3-95450-253-0 ISSN: 2673-5571 doi:10.18429/JACoW-HB2023-WEA3I1

SYNCHRONOUS PHASE AND TRANSIT TIME FACTOR

J-M. Lagniel†, GANIL, Caen, France

Abstract

Synchronous phases (φ_s) and transit time factors (T) are the key parameters for linac designs and operations. While the couple (φ_s, T) is still our way of thinking the longitudinal beam dynamics, it is important to have in mind that the original "Panofsky definition" of these parameters is no longer valid in the case of high accelerating gradients leading to high particle velocity changes. In this case, a new (φ_s, T) definition allowing to keep both acceleration and longitudinal focusing properties is proposed. Examples are given in the SPIRAL2 linac case.

INTRODUCTION

Synchronous phases (φ_s) and transit time factors (T) are by far THE main parameters for linac designs and operations. The choice of the synchronous phase evolution is a compromise between linac efficiency (higher acceleration then lower linac length and cost at higher φ_s) and linac longitudinal acceptance (reduced acceptances then higher risk of beam losses at higher φ_s). The choice of the transit time factors linked to the accelerating cell or cavity geometries is also a compromise between linac efficiency (higher acceleration then lower linac length and cost at higher T), technical risk (higher peak fields at higher T) and construction / operation complexity (more β-families for a linac design with higher T).

The couple (φ_s, T) has been defined by Panofsky in the framework of Drift Tube Linac cells [1] : φ_s is "the rf phase by which the synchronous particle crosses the electrical center of the gap relative to the time at which the electric field reaches its crest value", and T is a coefficient such that the on-axis energy gain is

$$\Delta W = q\, E_0 L\ \mathrm{T}\, cos(\varphi_s) \qquad (1)$$

with q the particle charge and $E_0 L$ the on-axis gap voltage

$$E_0 L = \int E_z(z, r=0)\, dz \qquad (2)$$

T is then the coefficient introduced to compute the energy gain taking into account the phase evolution during the gap traversal.

Using the smooth approximation, the Panofsky equation (1) also allows to write the equations of motion of the phase oscillations ($\delta\varphi$) around the synchronous particle.

$$\frac{d^2\delta\varphi}{dz^2} + {\sigma_{0l}}^2\ \frac{\cos(\varphi s + \delta\varphi) - \cos(\varphi_s)}{-\sin(\varphi_s)} = 0 \qquad (3a)$$

$$\frac{d^2\delta\varphi}{dz^2} + {\sigma_{0l}}^2\ \delta\varphi = 0 \qquad (3b)$$

$$\sigma_{0l} = \sqrt{\frac{-2\pi q\, E_0\, T \sin(\varphi_s)}{m_0 c^2 \lambda\, \beta_s^3 \gamma_s^3}} \qquad (3c)$$

† lagniel@ganil.fr

The nonlinear equation of motion (3a) allows to compute the large amplitude oscillations and the longitudinal acceptance defined by the so called separatrix. Its linear form (3b) shows that longitudinal focusing force for the small amplitude oscillations is function of the zero-current longitudinal phase advance σ_{0l} (3c).

To make it short, one can say that T $cos(\varphi_s)$ reflects the gap/cavity accelerating property through (1), and that T $sin(\varphi_s)$ reflects the gap/cavity longitudinal focusing property through (3c).

ENERGY GAIN AND CAVITY TUNING IN THE CASE OF HIGH ACCELERATING GRADIENT CAVITIES

As pointed out in Ref. [1], the Panofsky equation (1) is valid only if the fractional changes in velocity are small, a condition which is far to be fulfilled in linacs using superconducting cavities at low beta as in the SPIRAL2 case. Fig. 1 gives the example of a SPIRAL2 low beta QW cavity operated at 40% of its nominal field (2.6 MV/m) for deuterons at RFQ output energy (732 keV/u).

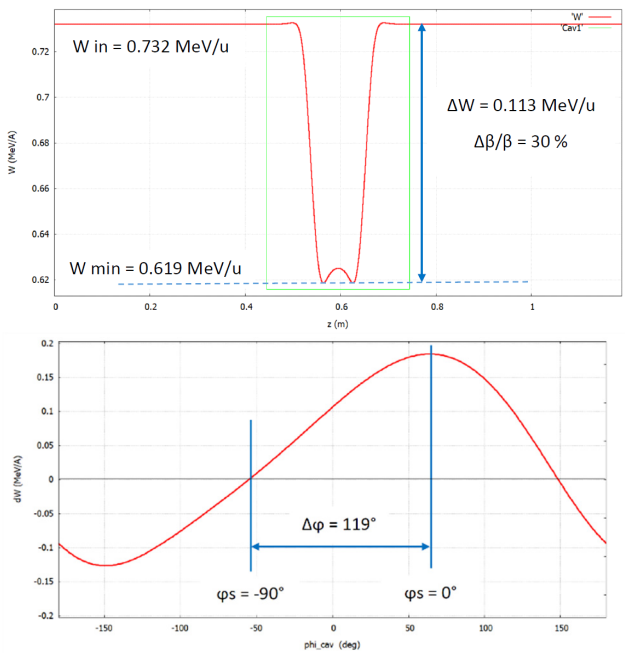

Figure 1: SPIRAL2 low beta cavity at 40% nominal field with deuterons at RFQ output energy. Top: energy evolution along a cavity tuned in buncher mode (φ_s = -90°). Bottom: energy gain for a 2π cavity phase scan.

Figure 1 shows that the fractional change in velocity is very large in this case (even in buncher mode) and that the energy gain has no longer a sinusoidal evolution function of the cavity phase. At the opposite of what is noted in [2], a phase angle defined with respect to the maximum energy gain in a given resonator can be far to be equal to the synchronous phase (-119° cavity phase shift to switch φ_s from

ISBN: 978-3-95450-253-0 ISSN: 2673-5571 doi:10.18429/JACoW-HB2023-WEA3C1

THE TRACKING CODE RF-Track AND ITS APPLICATION

A. Latina*, CERN, Geneva, Switzerland

Abstract

RF-Track is a CERN-developed particle tracking code that can simulate the generation, acceleration, and tracking of beams of any species through an entire accelerator, both in realistic field maps and conventional elements. RF-Track includes a large set of single-particle and collective effects: space-charge, beam-beam, beam loading in standing and travelling wave structures, short- and long-range wakefield effects, synchrotron radiation emission, multiple Coulomb scattering in materials, and particle lifetime. These effects make it the ideal tool for the simulation of high-intensity machines. RF-Track has been used for the simulation of electron linacs for medical applications, inverse-Compton-scattering sources, positron sources, protons in Linac4, and the cooling channel of a future muon collider. An overview of the code is presented, along with some significant results.

INTRODUCTION

RF-Track [1] is a tracking code developed at CERN currently used for the simulation, design, and optimisation of several diverse accelerators: electron-driven medical facilities, the positron sources of CLIC and FCC-ee, low-energy proton and ion linacs, electron coolers, and other exotic setups like the muon cooling channel of a future muon collider. The code was initially created as a tool to perform tracking simulations of a medical linac for hadron therapy featuring backwards travelling-wave structures [2]; then, it evolved into a multi-purpose accelerator toolbox capable of handling a large number of challenging simulation scenarios [3]. RF-Track can simulate beams of particles with arbitrary energy, mass, and charge, even mixed, and transport them through conventional matrix-based elements as well as through special elements and field maps. It implements two different particle tracking methods: tracking *in time* and tracking *in space*. The first is preferred in space-charge-dominated regimes, where the relative positions of the particles in space matter. The second is preferred when collective, intra-bunch effects are unimportant. Consistent and intuitive methods are available for seamlessly transitioning from one model to another.

Equipped with a friendly user interface based on the Octave or Python scientific languages, RF-Track is the ideal tool for performing complex numerical experiments in accelerator physics.

Integration Methods for the Equations of Motion

RF-Track offers several methods for integrating the equations of motion, depending on the tracking environment and beamline element. When tracking in space, it provides conventional thick-matrix-based elements such as quadrupoles, sector bends and drifts. In field maps, RF-Track numerically integrates the particle trajectories elements using numerical methods such as leap-frog, Runge-Kutta, Bulirsch-Stoer, and other higher-level routines for adaptive step-size control [4], up to the 12th order. When tracking in time, the equations of motion are always solved through numerical integration using the above-mentioned methods, with time being the independent variable.

BEAM LINE ELEMENTS

Two distinct environments have been created for space and time tracking: Lattice and Volume. Lattice represents a conventional sequence of beamline elements and is suitable for space tracking. Volume is a more general environment where elements can overlap, have arbitrary orientation in space, and particles can move in any direction. Elements' misalignment can be simulated in both environments.

In the following sections, elements unique to RF-Track: field maps and several special elements, are described.

Field Maps

RF-Track has the capability to import 1D, 2D, and 3D field maps of static and oscillating RF fields, standing or travelling in both the forward and backward directions. Field maps can be linearly or cubically interpolated.

1D Field Maps In the case of 1D maps, RF-Track accepts the longitudinal on-axis electric field and performs an off-axis field expansion, assuming cylindrical symmetry. Both the electric and the magnetic components of the field are computed. This expansion fulfils Maxwell's equations and is based on the method presented in [5], similar to what is done in ASTRA [6].

2D Field Maps In the case of 2D maps, the user provides the longitudinal and radial components of the electric and magnetic fields, and cylindrical symmetry is automatically applied.

3D Field Maps In the case of 3D maps, RF-Track guarantees a divergence-free interpolation of the field at any point, automatically correcting inaccuracies resulting from conventional interpolation or field measurement errors that would violate Maxwell's equations [7]. Additionally, in the case of symmetric fields, RF-Track accepts partial views of the field and automatically applies appropriate electric-wall and magnetic-wall symmetries for efficient memory usage. Figure 1 shows an example of tracking through the field map of an alpha magnet.

Special Elements

Electron Cooler Electron coolers are used in storage rings to reduce the phase space volume of heavy particles

* andrea.latina@cern.ch

ISBN: 978-3-95450-253-0 ISSN: 2673-5571 doi:10.18429/JACoW-HB2023-WEA3C2

BENCHMARKING OF PATH AND RF-Track IN THE SIMULATION OF LINAC4

G. Bellodi*, J.-B. Lallement, A. Latina, A. M. Lombardi, CERN, Geneva, Switzerland

Abstract

A benchmarking campaign has been initiated to compare PATH and RF-Track in modelling high-intensity, low-energy hadron beams. The development of extra functionalities in RF-Track was required to handle an unbunched beam from the source and to ease the user interface. The Linac4 RFQ and downstream accelerating structures were adopted as test case scenarios. This paper will give an overview of the results obtained so far and plans for future code development.

INTRODUCTION

RF-Track [1] is a tracking code developed at CERN for the optimization of low-energy ion linacs in the presence of space-charge effects. The code was initially created as a tool to perform tracking simulations of a medical linac for hadron therapy [2]; it then evolved to a multi-purpose accelerator toolbox capable of handling a large number of simulation scenarios [3]. RF-Track can simulate beams of particles with arbitrary energy, mass, and charge and transport them through conventional matrix-based elements as well as through field maps. It implements two different particle tracking methods: tracking in time and tracking in space. The first is preferred in space-charge-dominated regimes, where the relative positions of the particles in space matter.

The subject of this paper is the application of the RF-Track simulation capabilities to the case of low-energy, high-intensity hadron beams, such as the case of Linac4. For this purpose, a benchmarking campaign has recently started to compare RF-Track with the PATH [4] official simulation results, which were the reference for the design and commissioning of Linac4, showing extremely favourable comparisons with measurements . The use of RF-Track is motivated by the desire to extend the code's functionality to bridge the gap between electrons and ions while providing the Linac4 simulations with a modern code easily accessible through languages such as Octave and Python. As a first exercise, the RFQ and the Linac4 accelerating structures were adopted as test case scenarios, with the idea that the simulation should then be extended to cover from the source extraction at 45 keV to the final beam dump energy at 160 MeV.

MODELLING HIGH-INTENSITY LINACS

In a high-intensity linac the pulse length is typically much longer than the RF period . Nevertheless, after an initial transient, the beam dynamics on the scale of one RF period fully represents the behaviour of the whole pulse. The choice, in PATH, is to follow a section of the beam for as long as the RF period . The flow of particles from one RF bucket to the adjacent one is correctly compensated for by longitudinal folding. In a high-intensity regime, RF-Track calculates the space-charge forces and integrates the equations of motion *in time*. If the beam is transported *in time*, folding is not possible. For this reason, we transported through the linac five full RF periods, assuming that the central one represents the steady state. This constitutes a significant difference between the simulation assumptions made by the two codes. PATH and RF-Track implement two very different space-charge calculation algorithms. In PATH, space-charge effects are calculated using the SCHEFF algorithm [5], which uses a 2D-rings-of-charge approximation, implicitly assuming cylindrical symmetry. The space around the beam ellipsoid is mapped in the laboratory frame with a radial and longitudinal mesh with user-defined step sizes. The electric self-field is then calculated in both components in the beam frame at each mesh vertex, assuming a uniform charge distribution on the mesh rings. The electric field at the coordinates of a particle P within the mesh is interpolated by the field values at the four adjacent mesh vertices. The force acting on the particle is finally transformed back to the laboratory frame.

In RF-Track, the space-charge kick is computed by solving the 3D Maxwell's equations for the electric-scalar and magnetic-vector potentials via a cloud-in-cell method based on integrated Green's functions. The kick on each particle is then computed as the Lorentz force due to the fields obtained from the electromagnetic potentials. No particular beam symmetry is here assumed.

As mentioned above, RF-Track tracks the 3D spatial distribution as it evolves *in time*. In PATH, the integration of the equations of motion is performed *in space*, and the spatial 3D distribution of the bunch is reconstructed at each space-charge kick.

RFQ

The Linac4 352.2 MHz RFQ was assumed as the first test case for benchmarking the two codes. The RFQ was described by a field map built out of FEM electrostatic simulations performed with COMSOL Multiphysics© [6], with the physical vane geometry taken into account to define the apertures. The stepsize of the field map was 0.2 mm. The file was directly imported in both PATH and RF-Track, and an initial beam distribution of 500 k macro-particles was used. Figures 1, 2, and 3 show the excellent agreement reached when tracking without space charge. The difference in overall transmission through the RFQ between the two codes is less than 0.5%, and the output beam distributions overlap very nicely in all three transverse and longitudinal phase spaces.

* giulia.bellodi@cern.ch

ISBN: 978-3-95450-253-0 ISSN: 2673-5571 doi:10.18429/JACoW-HB2023-WEA3C3

DIFFERENTIAL ALGEBRA FOR ACCELERATOR OPTIMIZATION WITH TRUNCATED GREEN'S FUNCTION

Chong Shik Park*, Korea University, Sejong, South Korea

Abstract

Accelerator optimization is a critical problem in the design of high-performance particle accelerators. The truncated Green's function space charge algorithm is a powerful tool for simulating the effects of space charge in accelerators. However, the truncated Green's function algorithm can be computationally expensive, especially for large accelerators. In this work, we present a new approach to accelerator optimization using differential algebra with the truncated Green's function space charge algorithm. Our approach uses differential algebra to symbolically represent the equations of the truncated Green's function algorithm. This allows us to perform efficient symbolic analysis of the equations, which can be used to identify and optimize the accelerator parameters. We demonstrate the effectiveness of our approach by applying it to the optimization of a linear accelerator. We show that our approach can significantly reduce the computational cost of the truncated Green's function algorithm, while still achieving high accuracy.

INTRODUCTION

Computation of space charge fields in accelerator simulations presents significant challenges. While many accelerator modeling codes incorporate self-consistent space charge solvers to track multiple particles, solving electromagnetic or electrostatic space charge fields self-consistently and analytically is inherently intricate. Consequently, numerous solvers resort to Particle-in-Cell (PIC) methods with open boundary conditions.

During accelerator optimization simulations, gradient-free algorithms are frequently used due to the limited availability of derivative information regarding beam properties in relation to accelerator parameters. To address this constraint, techniques like Differential Algebra (DA) and Truncated Power Series Algebra (TPSA) come into play to bridge this gap.

DA and TPSA have demonstrated their effectiveness in calculating nonlinear maps for lattice elements and are widely embraced in many codes. These techniques hold particular promise in the realm of differentiable space charge simulations, where computational efficiency is paramount for beam dynamics simulations. Proposals for automatic differentiation of space charge simulations using TPSA have emerged, further augmenting their versatility.

DA techniques have become instrumental in solving complex problems in accelerator physics. There have been research contributions where DA methods have significantly enhanced space charge calculations, paving the way for innovative solutions in accelerator science. H. Zhang *et al* applied DA techniques to the Fast Multipole Method (FMM) for space charge calculations. Their research offers valuable insights into the effective use of DA in space charge effect computations [1]. B. Erdelyi *et al* employed the Duffy transformation method to address the Poisson equation with Green's functions. This transformative technique effectively splits integrals into smaller domains, eliminating the singularities associated with Green's functions [2]. Recently, J. Qiang focused on using TPSA techniques to derive local derivatives of beam properties concerning accelerator design parameters. This study investigates the behavior of coasting beams within a rectangular conducting pipe [3].

Collectively, these research contributions demonstrate the widespread adoption of DA techniques to enhance space charge calculations. The combination of DA and related algebraic techniques showcases the versatile and robust nature of these methods, ultimately shaping the future of accelerator science and simulation.

In this work, we have devised a differentiable self-consistent space charge model, harnessing the power of Green's function solvers and implementing the Vico-Greengard-Ferrando algorithms [4]. This approach furnishes several benefits, including enhanced computational efficiency for beam dynamics simulations and the capability to effectively manage differentiable space charge effects [5].

TRUNCATED SPACE CHARGE SOLVER

For a given charge distribution, ρ, the Poisson equation with an open boundary condition can be expressed as:

$$\vec{\nabla}^2\phi = -\frac{\rho}{\epsilon_0},$$

The general solution of the Poisson equation utilizing Green's function is expressed as follows:

$$\begin{aligned}\phi(\vec{r}) &= \frac{1}{\epsilon_0}\int G(\vec{r},\vec{r}')\,\rho(\vec{r}')\,d^3\vec{r}' \\ &= \frac{1}{4\pi\epsilon_0}\int \frac{1}{|\vec{r}-\vec{r}'|}\,\rho(\vec{r}')\,d^3\vec{r}'.\end{aligned}$$

The inclusion of boundary conditions adds a layer of complexity to the problem. In the context of accelerator simulations, open boundary conditions are often the preferred choice, particularly when the pipe radius in an accelerator significantly exceeds the transverse size of the beam bunch.

While the Green's function method provides valuable insights and computational techniques, it also presents challenges: 1) long-range integration: addressing issues

* kuphy@korea.ac.kr

ISBN: 978-3-95450-253-0 ISSN: 2673-5571 doi:10.18429/JACoW-HB2023-WEC3I1

SELF-CONSISTENT INJECTION PAINTING FOR SPACE CHARGE MITIGATION *

N. J. Evans†, A. Hoover, T. Gorlov, V. Morozov, Oak Ridge National Lab, Oak Ridge, TN, USA

Abstract

The {2,2}-Danilov distribution, or simply the *Danilov* distribution, has a uniform charge distribution, elliptical projections, and can be created by uniformly filling one transverse mode of a coupled ring. In addition to proposing the distribution as an example of beam distribution with linear space charge that satisfies the Vlasov equation, Danilov showed how such a distribution could be constructed using a sufficiently flexible charge exchange injection system, such as at the Spallation Neutron Source (SNS). In this paper we will outline some of the proposed applications of this distribution, provide an update on our attempts to paint one in the SNS ring using a scheme we refer to as 'eigenpainting', and discuss some open questions pertaining to the study of this distribution.

INTRODUCTION

The Danilov distribution, defined in Ref. [1], or simply the *Danilov* distribution offers an opportunity to create a beam with several properties of interest for high brightness beams. Because of the linear nature of the space charge, a Danilov distribution can be matched to a lattice and the resulting system is linear, similar to the K-V distribution [2]. Danilov realized that the correlations present in the distribution imply that it can be built-up successively over many turns by the process of phase space painting [1]. This makes the distribution scalable to more intense beams, not limited by the source, such as another similar distribution described by Liuten [3].

Controlling the speed at which a given footprint is filled allows control of the space charge, offering an interesting opportunity to study a distribution with a relatively tractable description over an easily tunable range of space charge. At SNS we are attempting to paint such a distribution in the accumulator ring to study the properties of these beams. To differentiate from existing painting where both modes of a (typically uncoupled) lattice are filled with amplitudes increasing together, correlated painting, or one amplitude increasing while the other decreases, uncorrelated painting, we refer to painting into a single mode as *eigenpainting*. Note that in the case of uncorrelated painting, the resulting distribution would be a K-V if it could be maintained in the presence of space charge during the painting process.

The benefits of a Danilov distribution fall into several categories due to: linear space charge, low 4D emittance, and non-zero angular momentum. The last two of these are a directly related to the fact that a uniform distribution of charge occupying one of two counter-rotating coupled modes is a Danilov distribution.

Because a properly matched Danilov distribution is a uniformly filled coupled mode with small emittance in the second mode, many of the arguments about possible applications in Refs. [4,5] hold. Notably for space charge mitigation, Burov suggests the use of circular modes for low-energy machines to preserve brightness and reduce tune shift since the larger of the two mode emittances determines to the real space distribution, allowing the other to be made arbitrarily small. For this purpose eigenpainting alone is beneficial without the further constraint of uniform charge density.

However, because the incoherent space-charge tune footprint vanishes for uniform charge distribution, while the tune shift remains, one can imagine a scenario where the tune footprint is compact enough, and the shift large enough that the beam hops over a resonance and resides on the other side of the line without operationally significant loss. There will still be a tail, that still crosses the resonance, but it should be much sparser than that of a Gaussian beam of similar dimensions, as only those particles near the edge of the distribution will experience non-linear forces. Whether this tail is sparse enough to allow this scheme to work is a question we plan on investigating in future simulations and experiments.

Additionally, Cheon et al. have done work investigating whether rotating beams could help reduce the effect of space charge driven resonances [6]. They considered resonances in linacs, which would require either pre-painting beam in a purpose-built low energy ring, or another method of preparation.

The rest of this manuscript will give a brief outline of the setup and techniques used for eigenpainting experiments at SNS and present recent results.

EXPERIMENTS AT THE SNS

The SNS consists of a 1.0 GeV H^- linac, which is currently being upgraded to 1.3 GeV, a 248 m accumulation ring equipped with first and second harmonic bunching RF cavities. Figure 1 shows the end of the linac, the ring, and Ring-Target Beam Transport (RTBT) line with relevant features identified.

Injection from the linac to the ring takes place via charge exchange injection facilitated by a thin nano-crystalline diamond foil. Phase space painting is achieved with a set of

* This manuscript has been authored by UT-Battelle, LLC, under Contract No. DE-AC05-00OR22725 with the U.S. Department of Energy. The United States Government retains, and the publisher, by accepting the article for publication, acknowledges that the United States Government retains a non-exclusive, paid-up, irrevocable, world-wide license to publish or reproduce the published form of this manuscript, or allow others to do so, for United States Government purposes. The Department of Energy will provide public access to these results of federally sponsored research in accordance with the DOE Public Access Plan (http://energy.gov/downloads/doe-public-access-plan).
† nhe@ornl.gov

ISBN: 978-3-95450-253-0 ISSN: 2673-5571 doi:10.18429/JACoW-HB2023-WEC3I2

MITIGATION OF SPACE CHARGE EFFECTS IN RHIC AND ITS INJECTORS

V. Schoefer*, C. Gardner, K. Hock, H. Huang, C. Liu, K. Zeno
Brookhaven National Laboratory, Upton, NY, USA

Abstract

The RHIC collider physics programs, in particular its polarized proton and low energy heavy ion components, present unique challenges for maintaining collider performance in the presence of space charge effects. Polarized beam performance is especially sensitive to emittance increases, since they decrease both the luminosity and polarization. Operation of the collider with gold beams at sub-injection energies (down to 3.85 GeV/n Au) with space charge tune shifts up to 0.1 required special care to optimize both the ion lifetime and its interaction with the electron-beam cooler. We describe the operational experience in these modes and some of the mitigation efforts.

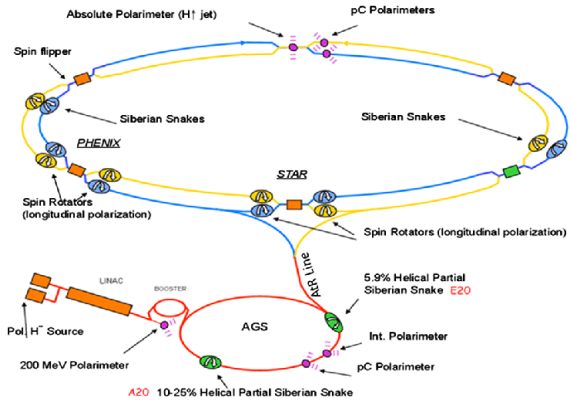

Figure 1: RHIC complex.

INTRODUCTION

The Relativistic Heavy Ion Collider and its injectors (Fig. 1) provide collisions of a wide range of nuclei for two main physics programs. The heavy ion program is aimed at studying the properties of the quark-gluon plasma. In particular, during operation from 2019-2021, the collider was operated with gold beam in a range of beam energies from 3.85 to 9.8 GeV/n, well below the design collision energy of 100 GeV/n (in fact at or below the nominal injection energy of 9.8 GeV/n). The goal of this measurement campaign (called Beam Energy Scan II or BES-II) was to explore center-of-masss collision energies in the range of the QCD critical point [1–3]. The second physics program consists of polarized proton collisions at beam energies of 100 and 255 GeV, which explores the origin and composition of the spin of the proton constituents [4]. While neither the heavy ion nor the polarized proton program are "intensity frontier" accelerator programs, their particular needs nevertheless require special care to mitigate the effects of space charge on collider performance.

For polarized beams, the figure of merit for collider operation with polarized beams is either LP^2 (for transverse polarization) or LP^4 (for longitudinal polarization) where L is the luminosity and P is the polarization. Since the main depolarizing mechanisms in RHIC and its injectors are intrinsic resonances, the effects of which increase with increasing emittance, any increase in the emittance degrades the figure of merit rapidly, since it decreases both the luminosity and the polarization [5, 6].

For heavy ion beams like gold, reaching the requisite per bunch intensities requires multiple longitudinal bunch merges in both the Booster and AGS. Limitation on the RF cavity frequency ranges require that these merges happen at relatively low energies, resulting in large space charge tune shifts and ensuing beam loss (e.g., [1, 7]).

RHIC low-energy heavy ion operation is a special case. At the nominal RHIC collision energy of 100 GeV/n, space charge effects are generally neglible. Operation for BES-II, however, posed a particular challenge because at the lowest energies, collisions took place with space charge tune shifts of up to 0.1. Low-energy operation also involved ion beam interaction with the electron beam of the Low-Energy RHIC electron Cooler (LEReC), further constraining the optimum configuration [1, 8–10].

In the following we review selected cases and mitigating measures where space charge effects have created bottlenecks to machine performance for both polarized proton and heavy ion operation.

POLARIZED PROTONS

The primary sources of depolarization in the RHIC injector chain are intrinsic resonances. The strengths of these resonance depend on the betatron amplitudes of the particles and are stronger for larger amplitudes. Depolarization due to these resonance results in a transverse polarization profile, where cross sections of the beam distribution with larger betatron amplitudes have lower polarization. Transverse emittance increases result therefore in decreases of both the luminosity and the polarization [5, 11]. The effects of intrinsic resonances are measured using a thin carbon target inserted at different transverse locations in the beam (Fig. 2).

Figure 3 shows typical measured deterioration of the polarization and transverse emittances with intensity at AGS extraction energy, which are well approximated by linear fits (show in the plots). One can use those measured linear dependences to make predictions of the relative change in

* schoefer@bnl.gov

ISBN: 978-3-95450-253-0 ISSN: 2673-5571 doi:10.18429/JACoW-HB2023-WEC3C1

BEYOND 1-MW SCENARIO IN J-PARC RAPID-CYCLING SYNCHROTRON

K. Yamamoto†, K. Moriya, H. Okita, I. Yamada, M. Chimura, P. K. Saha, Y. Shobuda, F. Tamura, M. Yamamoto and T. Morishita, J-PARC Center, Japan Atomic Energy Agency, Tokai-mura, Japan
H. Hotchi, J-PARC Center, High Energy Accelerator Research Organization, Tokai-mura, Japan

Abstract

The 3-GeV rapid-cycling synchrotron (RCS) at the Japan Proton Accelerator Research Complex (J-PARC) was designed to provide 1-MW proton beams to the following facilities. We have improved the accelerator system and successfully accelerated a 1-MW beam with a small beam loss. Currently, the beam power of RCS is limited due to the lack of an anode current in the radiofrequency (RF) cavity system rather than the beam loss. Recently, we developed a new acceleration cavity that can accelerate a beam with less anode current. This new cavity enables us to reduce the requirement for an anode power supply and accelerate more than a 1-MW beam. We have started to consider how to achieve more than a 1-MW beam acceleration. So far, up to a 1.5-MW beam can be accelerated after replacing the RF cavity. We have also continued studies to achieve more than a 2-MW beam in the J-PARC RCS.

INTRODUCTION

The 3-GeV rapid-cycling synchrotron (RCS) at the Japan Proton Accelerator Research Complex (J-PARC) was constructed and operated to provide high-intensity proton beams to the Material and Life science experimental Facility (MLF) and Main Ring (MR) [1]. We have been continuing the beam study and improvement it to accelerate a 1-MW beam and achieved more than an 800 kW beam operation for MLF users [2]. We also achieved a 1-MW beam operation in a few days with a small beam loss condition [1].

Currently, the beam power of RCS is limited due to the lack of an anode current in the radiofrequency (RF) cavity system rather than the beam loss. Recently, we developed a new acceleration cavity that can accelerate a beam with less anode current. This new cavity enables us to reduce the requirement for the anode power supply and accelerate more than a 1-MW beam. We have started to consider how to achieve beyond a 1-MW beam acceleration. This study summarizes the scenario for achieving more than 1-MW power.

DEMONSTRATION RESULTS BEYOND A 1-MW BEAM POWER

We studied the potential of the RCS beyond a 1-MW power [3]. Figure 1 shows the results of the injection and partial acceleration of various beam currents. Currently, the capacity of the anode power supply of the RF system limits the maximum number of particles that can be accelerated. The RF bucket is distorted due to the wake voltage caused by the high beam current of more than 1-MW, and all beams are lost at the middle stage of acceleration. Therefore, we accelerated the beam to only 0.8 GeV energy, and all beams are extracted at this timing in this study. Figure 1 shows that no significant loss occurs even after the 1.5-MW equivalent beam current injection and partial acceleration. The study results demonstrate the potential of the RCS beyond 1-MW power.

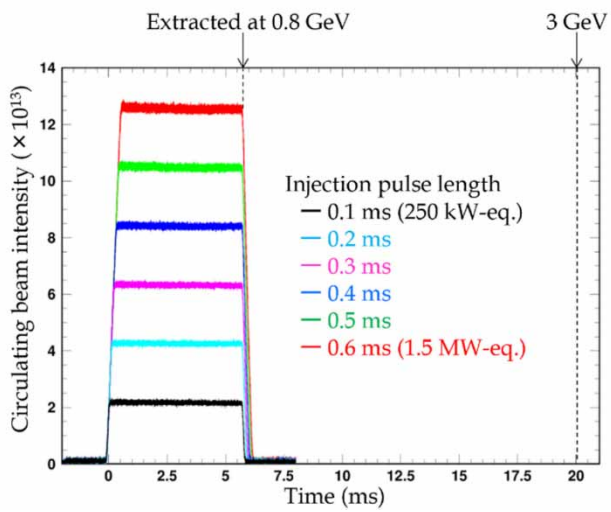

Figure 1: Experimental results; circulating beam intensities from injection to extraction [3].

IMPROVEMENT OF THE RF SYSTEM

We must reinforce the RF system to accelerate more than a 1-MW beam. Therefore, the J-PARC ring RF group developed a new cavity structure that can accelerate more than a 1-MW beam [4]. The conventional RF cavity is driven using a push–pull operation mode, where two vacuum tubes feed the RF power upstream and downstream of the acceleration gap. This configuration has the advantage of suppressing a higher harmonic distortion without the beam acceleration and shortening the cavity length.

However, in a high-intensity beam acceleration case, the multi-harmonic RF driving causes a severe imbalance of the anode voltage, leading to a deficiency in the anode current. Therefore, a new cavity (single-ended cavity) was developed so that only the downstream of the gap was excited [5]. This configuration reduced the input current in

† kazami@post.j-parc.jp

ISBN: 978-3-95450-253-0 ISSN: 2673-5571 doi:10.18429/JACoW-HB2023-WEC3C2

HIGH ENERGY COOLING

V. A. Lebedev†, Fermilab, Batavia, Illinois, USA

Abstract

The paper reviews methods of particle cooling and their application to future high energy hadron colliders. There are two major types of cooling: the electron cooling and stochastic cooling. The latter can be additionally subdivided on the microwave stochastic cooling (SC), the optical stochastic cooling (OSC) and the coherent electron cooling (CEC). OSC and CEC are essentially extensions of microwave SC, operating in 1-10 GHz frequency range, to the optical frequencies corresponding to 30-300 THz range. The OSC uses undulators as a pickup and a kicker, and an optical amplifier for signal amplification, while the CEC uses an electron beam for all these functions.

INTRODUCTION

In this paper we consider methods of particle cooling applicable for high energy heavy particles (protons or ions) in the high energy colliders. Further in all equations we assume protons – the most challenging case. To transit to ions, one needs to replace in the below equations, as appropriate, the proton classical radius r_p by $Z^2 r_p / A$, where Z and A are the charge and mass numbers of ion. Presently, there are two major methods of cooling: the electron cooling [1] and the stochastic cooling [2]. Up to recently, the stochastic cooling has been only operating at the microwave frequencies. A transition to much higher optical frequencies should enable much faster cooling of dense colliding bunches. The stochastic cooling at extremely high (optical) frequencies can be additionally subdivided into the optical stochastic cooling (OSC) [3] and the coherent electron cooling (CEC) [4]. OSC and CEC are essentially extensions of microwave stochastic cooling operating in the 1-10 GHz frequency range to the optical frequencies corresponding to the 30-300 THz range. At these frequencies one cannot use usual electro-magnetic pickups and kickers. Instead, the OSC uses undulators for both the pickup and the kicker, and an optical amplifier for signal amplification; while the CEC uses an electron beam for all these functions.

The electron and stochastic cooling are based on completely different principles. The electron cooling is dissipative in its principle of operation and therefore the Liouville theorem is not applicable. That enables direct reduction of the beam phase space. The stochastic cooling is a Hamiltonian process which formally does not violate the Liouville theorem and cooling happens due to the phase space reconfiguration so that phase space volumes containing particles are moved to the beam center while the rest mostly moves out. That makes stochastic colling rates strongly dependent on the beam particle density. As one will see below each method has its own domain where it achieves a superior efficiency. The electron cooling is preferred at a small energy, and its efficiency weakly depends on the particle density in the cooled beam; while the stochastic cooling is preferred at a high energy, but its efficiency reduces fast with increase of particle density.

† valebedev@jinr.ru

HIGH ENERGY ELECTRON COOLING

The highest energy electron cooling achieved to the present time is 4.3 MeV [5, 6]. It was used in Tevatron Run II for cooling 8 GeV antiprotons. The electron beam was accelerated in an electrostatic accelerator. The maximum beam current was 500 mA. The typical beam current used for antiproton storage was about 100 – 200 mA. That supported beam cooling time of about 20 min.

A transition to high energy colliders like Electron-Ion Collider [7] requires the electron beam energy above tens of MeV. That is impossible to achieve with electrostatic acceleration. Consequently, two radically different approaches to the beam acceleration were suggested. The first one suggests using the energy recovery superconducting linac [8], while the second approach uses an induction linac with electron beam injection into a ring where the electron beam circulates for many thousands turns [9]. That allows one to reduce the electron beam power to acceptable level. Reference [10] considers another modification of ring-based cooler where the cooling electron beam is cooled by its synchrotron radiation. That drops the frequency of reinjections and results in an additional reduction of linac power.

Before we consider these schemes, we need to write down equations for the cooling rates of relativistic beams. The corresponding derivations were carried out in Ref. [8]. They assume the Gaussian distributions for both the electron and proton beams and non-magnetized cooling. In all practical cases the longitudinal velocity spread is much smaller than the transverse one. Then the corresponding longitudinal and transverse emittance cooling rates for $\Theta_\parallel / (\gamma\Theta_\perp) \le 2$ can be approximated, with accuracy better than few percent, as following:

$$\lambda_\parallel \equiv \frac{1}{\theta_{\parallel p}^{\,2}} \frac{d}{dt} \theta_{\parallel p}^{\,2} \approx \frac{4\sqrt{2\pi} n_e r_e r_p L_c}{\gamma^4 \beta^4 \left(\Theta_\perp + 1.083\Theta_\parallel / \gamma\right)^{3/2} \sqrt{\Theta_\perp \Theta_\parallel}} L_{cs} f_0, \quad (1)$$

$$\lambda_\perp \equiv \frac{1}{\theta_{\perp p}^{\,2}} \frac{d}{dt} \theta_{\perp p}^{\,2} \approx \frac{\pi\sqrt{2\pi} n_e r_e r_p L_c}{\gamma^5 \beta^4 \Theta_\perp^{\,2} \left(\Theta_\perp + \sqrt{2}\Theta_\parallel / \gamma\right)} L_{cs} f_0 \ .$$

Here $\Theta_\parallel = \sqrt{\theta_{\parallel e}^{\,2} + \theta_{\parallel p}^{\,2}}$, $\Theta_\perp = \sqrt{\theta_{\perp e}^{\,2} + \theta_{\perp p}^{\,2}}$ are the effective longitudinal and transverse rms momentum spreads, $\theta_{\parallel p,e} \equiv \sqrt{\overline{\Delta p_{p,e}^{\,2}}} / p_{p,e}$ and $\theta_{\perp p,e} \equiv \sqrt{\overline{\Delta p_{\perp p,e}^{\,2}}} / p_e$ are the relative longitudinal and transverse rms momentum spreads in the proton/electron beam, γ and β are the relativistic factors, $n_e = \gamma n_e'$ is the electron beam density in the lab frame, r_e is the classical electron radius, L_c is the Coulomb logarithm, L_{cs} is the cooling section length, and f_0 is the revolution frequency for protons. These equations imply that the proton

ISBN: 978-3-95450-253-0 ISSN: 2673-5571 doi:10.18429/JACoW-HB2023-WEC3C3

SIMULATIONS AND MEASUREMENTS OF BETATRON AND OFF-MOMENTUM CLEANING PERFORMANCE IN THE ENERGY RAMP AT THE LHC

N. Triantafyllou*, R. Bruce, M. D'Andrea, K. Dewhurst, B. Lindstrom, D. Mirarchi, S. Redaelli, F. F. Van der Veken, CERN, Geneva, Switzerland

Abstract

The Large Hadron Collider (LHC) is equipped with a multi-stage collimation system that protects the machine against unavoidable beam losses at large betatron and energy offsets at all stages of operation. Dedicated beam validations and an understanding in simulations of the collimation performance are crucial for the energy ramp from 450 GeV to 6.8 TeV because complex changes of optics and orbit take place in this phase. Indeed, the betatron functions are reduced in all experiments for an efficient setup of the collisions at top energy. In this paper, simulations of the betatron and off-momentum cleaning during the energy ramp are presented. A particular focus is given to the off-momentum losses at the start of the ramp. The simulation results are benchmarked against experimental data, demonstrating the accuracy of newly developed simulation tools.

INTRODUCTION

The Large Hadron Collider (LHC) features a multi-stage collimation system designed to protect the superconducting magnets from quenching and sensitive aperture restrictions from damage from particle losses [1, 2]. It consists of more than 100 collimators, all consisting of two movable jaws with the beam passing in the centre, ordered into well-defined families. In the dedicated collimation insertions (IRs) – IR3 dedicated to momentum cleaning and IR7 to betatron cleaning – primary collimators (TCPs) are the closest to the beam and intercept the primary beam halo; secondary collimators (TCSGs) intercept the secondary particles scattered out of the TCPs, and the absorbers (TCLA) dispose of products from the showers produced by the interactions of halo particles with upstream collimator materials. In the experimental regions, tertiary collimators (TCTs) provide local protection around the Interaction Points (IPs) and minimize the physics background from beam-halo losses. In addition, the dump-protection collimators (TCSPs, TCDQs) in IR6 provide protection in case of asynchronous damp failures. The collimation system for beam 1 (B1) and beam 2 (B2) share the same setup. The majority of the collimators are installed IR3 (9/beam) and IR7 (19), and clean particles with high momentum and betatron offsets, respectively. In IR3, the dispersion is significantly higher than in IR7, and TCPs are only present in the horizontal plane. In contrast, in IR7, TCPs are installed in horizontal, vertical, and skew planes.

The system is setup through dedicated beam-based alignment procedures to ensure that the collimators are set precisely around the local orbit [3]. The cleaning performance is then qualified during the beam commissioning, before allowing high intensity in the machine, in order to validate that sensitive components are protected. The beam commissioning of the LHC typically takes place yearly, after extended periods of downtime during which there are no beams in the accelerator or significant modifications to the hardware. The validation of the cleaning performance is achieved by exciting low-intensity beams to induce artificial losses around the machine and assessing the resulting loss distribution at beam loss monitors (BLMs) [4, 5] throughout the ring. The resulting distribution of losses around the ring is referred to as loss map [6]. More detail on the procedure of the collimation qualification through loss maps can be found in Ref. [7–9]. In this paper, two types of loss maps will be discussed: betatron loss maps and off-momentum loss maps. Betatron loss maps are done by blowing up the beam using the transverse damper (ADT) in both the horizontal and vertical planes [10]. If the system is correctly setup, this causes primary losses in IR7. Off-momentum loss maps, on the other hand, are generated by shifting the RF frequency by a few hundred Hz, leading to primary losses in IR3.

There is always some particle leakage from the collimators into the machine aperture. To quantify the collimation performance, the local cleaning inefficiency is defined as [6, 11]: $\eta = N_{\mathrm{loc}}/(N_{\mathrm{tot}}\Delta s)$, where N_{loc} the local losses over a distance Δs and N_{tot} the total number of losses in the collimation system. The inefficiency is most critical in the dispersion suppression regions (DS) downstream of the IR7, since it is where the largest losses in cold magnets occur [6].

Qualification loss maps are conducted at several stages of the LHC cycle, typically following significant changes of energy, optics, reference orbit, or collimator settings. This paper provides a review of the LHC collimation system's performance at injection and during the energy ramp in the 2023 commissioning. This investigation is considered crucial due to the complex evolution in optics and closed orbit that occurs during this part of the cycle [12]. The measurements are compared against simulations conducted using the newly developed tools, Xsuite [13–15] and its tracking engine Xtrack [16]. These simulations mark the first of their kind during the LHC ramp and also the first off momentum loss maps using dynamic RF sweep in Xtrack.

MACHINE CONFIGURATION

The studies presented in this paper were conducted for the 2023 machine configuration, taking as input the validation loss maps [17]. The standard LHC cycle starts with injection

* natalia.triantafyllou@cern.ch

ISBN: 978-3-95450-253-0 ISSN: 2673-5571 doi:10.18429/JACoW-HB2023-WEA4I1

DEVELOPMENT OF NON-DESTRUCTIVE BEAM ENVELOPE MEASUREMENTS USING BPMs FOR LOW-BETA HEAVY ION BEAMS IN SRF CAVITIES

T. Nishi*, T. Adachi, O. Kamigaito, N. Sakamoto, T. Watanabe, K. Yamada
RIKEN Nishina Center, Wako, Saitama, Japan

Abstract

Accurate measurement and control of the beam envelope are crucial issues, particularly in high-power accelerator facilities. However, the use of destructive monitors is limited to low-intensity beams. Furthermore, in the case of beam transport between superconducting cavities, these destructive monitors should be avoided to prevent the generation of dust particles and outgassing. In the Superconducting RIKEN LINAC, or SRILAC, we utilize eight non-destructive Beam Energy Position Monitors (BEPMs)to measure beam positions and energies. Currently we are developing a method to estimate the beam envelope by combining the quadrupole moments from BEPMs, which consist of four cosine-shape electrodes, with transfer matricesWhile this method has been applied to electron and proton beams, it has not been practically demonstrated for heavy ion beams in $\beta \simeq 0.1$ regions. By combining BEPM simulations, we are making progress toward the reproduction of experimental results, overcoming specific issues associated with low β. This development will present the possibility of a new method for beam envelope measurement in LEBT and MEBT, especially for hadron beam facilities.

INTRODUCTION: SRILAC AND BEPMS

The Superconducting RIKEN LINAC, or SRILAC [1], started operation in 2020, and it has been providing a stable supply of heavy ion beam with intensity of a few pμA and beam energy of about 6 MeV/u [1, 2]. In the future, the intensity is planned to increase up to 10 pμA. SRILAC will be also used for medical isotope production as well as an injector for the RI beam factory, where higher beam intensities are required. Precise measurement and control of the beam dynamics are essential to achieve stable operation in high-intensity conditions. However, to suppress dust production and outgassing there are no destructive monitors between Superconducting RF (SRF) cavities. The only option to optimize the beam envelope inside the cavities was to minimize the vacuum levels between cavities. To estimate the beam dynamics in these sections, we performed Q-scan measurement downstream, changing the magnetic field of quadrupole magnets several times and measuring the beam profile for each magnetic field to reconstruct the phase ellipse [3]. Based on the obtained phase ellipse downstream of SRF cavities, we can estimate the beam envelope with transfer matrices [4] from the cavity sections to downstream sections. A disadvantage of the Q-scan method is that we cannot perform the measurement frequently during beam supply to the users because it takes at least 30 minutes and we need to temporary change the magnetic fields. Another restriction of the method is to decrease the beam intensity down to $\simeq$ 100 enA to avoid melting the wire and generating dust. Therefore, we started to develop an improved beam envelope measurement method using non-destructive monitors Beam Energy Position Monitors (BEPMs) [5].

Figure 1 shows the layout of SRILAC and beamline with eight BEPMs in between SRF cavities. There are two types of BEPMs: type-A (numbers 1 to 6) with a longitudinal length of 50 mm and type-B (numbers 7 and 8) with a longitudinal length of 60 mm. These detectors were originally introduced to measure beam position and energy and have contributed significantly to the stable beam operation of SRILAC. The beam energy is calculated by measuring the time of flight from the time difference between signals in pairs of each section. Figure 2 shows the CAD model of type-A BEPMs on CST simulation. These BEPMs have cosine-like shape electrodes. This shape realizes the ideal response of the quadrupole moment while maintaining good linear position sensitivity [5, 6].

PRINCIPLE TO MEASURE BEAM ENVELOPES USING BPMS

Methods for estimating beam emittance from BPM have been studied in past decades [4,7–10]. In order to understand the principle of the method, we initiate the expansion of the induced voltage of electrodes $V_{L,R,U,D}$ using transverse beam multipole moments such as the dipole ($D_{x,y}$ / $\langle x \rangle$, $\langle y \rangle$), quadrupole (M_2 / $\langle x^2 \rangle - \langle y^2 \rangle$), and higher order moment ($M_{ix,y}$, $i = 3, 4, \cdots$) [9, 10] as

$$\begin{aligned} V_R &= I_{\mathrm{beam}}(c_0 + c_1 D_x + c_2 M_2 + c_3 M_{3,x} + \cdots) \\ V_L &= I_{\mathrm{beam}}(c_0 - c_1 D_x + c_2 M_2 - c_3 M_{3,x} + \cdots) \\ V_U &= I_{\mathrm{beam}}(c_0 + c_1 D_y - c_2 M_2 + c_3 M_{3,y} + \cdots) \\ V_D &= I_{\mathrm{beam}}(c_0 - c_1 D_y - c_2 M_2 - c_3 M_{3,y} + \cdots), \end{aligned} \quad (1)$$

where I_{beam} denotes beam intensity and c_i denotes coefficient of each multipole term. By neglecting the higher order terms from this equation, $D_{x,y}$ and M_2 can be obtained as

* takahiro.nishi@riken.jp

ISBN: 978-3-95450-253-0 ISSN: 2673-5571 doi:10.18429/JACoW-HB2023-WEA4I2

LINAC4 SOURCE AND LOW ENERGY EXPERIENCE AND CHALLENGES

E. Sargsyan†, G. Bellodi, F. Di Lorenzo, J. Etxebarria, J.-B. Lallement, A. Lombardi, M. O'Neil,
CERN, Geneva, Switzerland

Abstract

At the end of Long Shutdown 2 (LS2), in 2020 Linac4 became the new injector of CERN's proton accelerator complex. The previous version of the Linac4 H^- ion source (IS03), produced an operational pulsed peak beam current of 35 mA, resulting in 27 mA after the Radio-Frequency Quadrupole (RFQ). This limited transmission was mainly due to the extracted beam emittance exceeding the acceptance of the RFQ.

A new geometry of the Linac4 source extraction electrodes has been developed with the aim of decreasing the extracted beam emittance and increasing the transmission through the RFQ. The new source (IS04) has been studied and thoroughly tested at the Linac4 source test stand. At the start of the 2023 run, the IS04 was installed as operational source in the Linac4 tunnel and is being successfully used for operation with 27 mA peak current after the RFQ. During high-intensity tests, the source, the linac, and the transfer-line to the Proton Synchrotron Booster (PSB) were also tested with a peak beam current of up to 50 mA from the source resulting in 35 mA at the PSB injection.

This paper discusses the recent developments, tests, and future plans for the Linac4 H^- ion source.

INTRODUCTION

Linac4 is the proton beam injector for CERN's accelerator complex, including the Large Hadron Collider (LHC). It accelerates negative hydrogen ions, H^-, to 160 MeV and transfers them to the Proton Synchrotron Booster (PSB). The ions are stripped of their two electrons during the charge exchange injection process into the PSB. The low-energy part of Linac4 consists of a 45 keV ion source, a low-energy beam transport (LEBT), and a radio-frequency quadrupole (RFQ) that accelerates the beam to 3 MeV.

The previous Linac4 source version, the IS03 [1], produced a beam current of 35 mA, which resulted in 27 mA after the RFQ. Attempts to run with a higher intensity from the source did not result in a higher intensity out of the RFQ. This was mainly due to the extracted beam emittance exceeding the acceptance of the RFQ. The IS03 extraction design could work with a much higher co-extracted electron current, which allowed the source to operate without caesium. Now that caesiation is routinely used for surface H^- production, a new geometry of the Linac4 source extraction electrodes has been developed and optimised for higher beam currents, with the aim of decreasing the extracted beam emittance and increasing the beam current and transmission through the RFQ. The new source type, the IS04, has been studied in simulations and thoroughly tested at the Linac4 test stand [2].

† edgar.sargsyan@cern.ch

NEW EXTRACTION SYSTEM

The IS04 ion source is composed of a ceramic (Al_2O_3) plasma chamber with an external five-turn RF antenna. Hydrogen gas is injected via a pulsed valve and a 2 MHz RF amplifier provides 100 kW maximum power to ignite and sustain the plasma. The source is operated in surface H^- production mode, with a continuous caesium injection at 65 °C; during the source start-up process, initial caesiation is usually done at higher temperatures and can take up to a few days. In routine operation at Linac4, the ion source produces beam pulses with a length of 850 µs at a repetition rate of 0.83 Hz and is typically providing 35 mA of beam at 45 keV energy with about 30 kW of forward RF power.

The IS04 source extraction system has a simplified design [3] compared to IS03, with only three electrodes (see Fig. 1): plasma, puller, and ground, which makes the extraction region 6 cm shorter than in the IS03. The puller-dump and einzel lens causing undesired emittance growth were eliminated. The design voltage of the puller electrode is -22.5 kV. Co-extracted electrons are disposed of at 45 keV onto a dedicated dump after deflection by a permanent dipole magnet housed at the base of the dump itself. The dump can be biased with a voltage of up to +1 kV to contain secondary electrons produced on the dump and create a potential barrier for the positive compensation particles collected in the beam in the low-energy beam transport section.

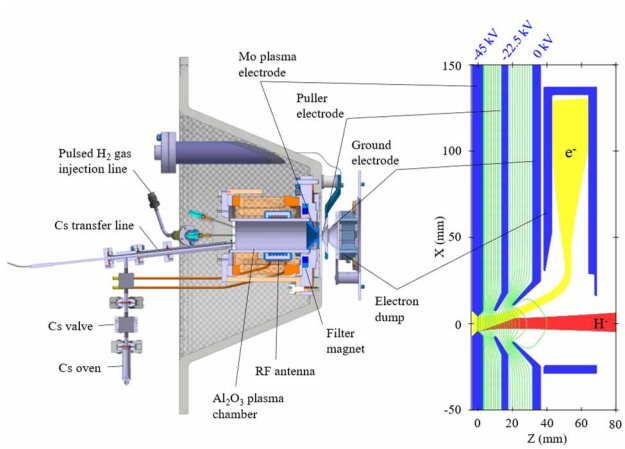

Figure 1: IS04 source 3D model (left) and extraction simulation model in IBSimu (right).

SIMULATIONS

Simulations have been carried out to characterise and improve the performance of the source, LEBT, and RFQ, as well as to help analysing the measurement results. Two simulation codes have been used. IBSimu [4], which is a computer simulation package for ion optics, plasma extraction and space charge dominated ion beam transport, is mainly used to model the plasma, and simulate ion beam

ISBN: 978-3-95450-253-0 ISSN: 2673-5571 doi:10.18429/JACoW-HB2023-WEA4C1

BEAM LOSS STUDIES IN THE CSNS LINAC*

J. Peng[1,†], Y. L. Han[1], Z. P. Li[1], Y. Li[1], Y. Yuan[1], X. B Luo[1], X. Y. Feng[1], X. G. Liu[1], M. Y. Huang[1], S. Y. Xu[1], H. C. Liu[1], S. Wang[1], S. N. Fu[1]
Institute of High Energy Physics, Chinese Academy of Sciences, Beijing, China
[1] also at Spallation Neutron Source Science Center, Dongguan, China

Abstract

The China Spallation Neutron Source（CSNS）accelerator consists of an 80 MeV linac and a 1.6 GeV rapid cycling synchrotron. It started operation in 2018, and the beam power delivered to the target has increased from 20 kW to 140 kW, step by step. Various beam loss studies have been performed through the accelerator to improve the beam power and availability. For the CSNS linac, the primary source of the beam loss is the halo generated by beam mismatches. In the upgrade plan of the CSNS, the beam current will increase five times, which requires more strict beam loss control. Much work is done during the design phase to keep the loss down to 1 W/m of loss limit. This paper will report results obtained from beam experiments and optimization methods applied to the CSNS linac upgrade design.

INTRODUCTION

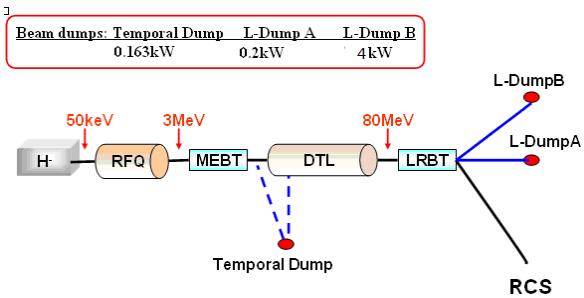

Figure 1: CSNS linac layout.

The CSNS is designed to accelerate proton beam pulse to 1.6 GeV at a 25 Hz repetition rate while striking a solid metal target to produce spallation neutrons. The accelerator aims to provide 100 kW of proton beam power with more than 90% reliability. The accelerator complex consists of an 80 MeV H- linac as the injector and a 1.6 GeV rapid cycling proton synchrotron (RCS), as shown in Fig. 1[1]. The linac consists of a 50 keV H- ion source, a 3 MeV RFQ, an 80 MeV DTL, and several beam transport lines. Table 1 shows the main parameters of the CSNS linac. The beam commission of the accelerator was started in 2015, and the first neutrons were produced in 2017. In the following year, the facility was put into user operation with a beam power of 20 kW. Over the next six years, the beam power was gradually improved from 20 kW to 140 kW, which is about 40% more than the design value. Figure 2 shows the beam power evolution of the CSNS accelerator since the beginning of operation in 2018. During the process of beam power ramping, the peak beam current transporting through the linac has been increased from 10 mA to 15 mA, and the pulse width has been widened from 100 μs to 540 μs. According to the latest measurement, residual radiation at 30 cm is less than 7mrem/hour throughout the linac, showing that the beam loss level keeps under 1 W/m. During beam commission and operation, several problems have been studied and solved, including ion source instability [2], quad failures in the DTL [3], chopping effect, and instability of the LLRF system [4]. These problems can induce beam transmission decline or create large beam loss spots along the linac. There are many H^- beam loss mechanisms for H^- accelerators, including residual gas stripping, H^+ capture and acceleration, intra-beam stripping mechanism, and so on [5]. For the CSNS linac, emittance growth arises from the mismatch, and the beam halo is the primary source of beam loss.

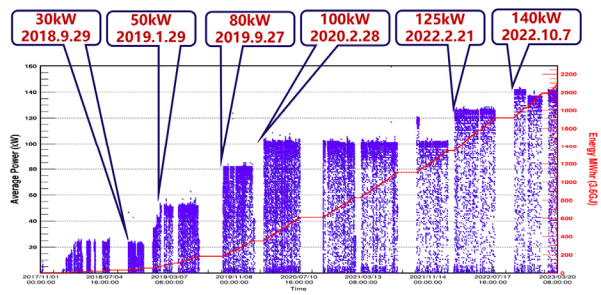

Figure 2: CSNS beam power evolution.

Table 1: Main Parameters of the CSNS Linac

	Ion Source	RFQ	DTL
Input Energy (MeV)		0.05	3.0
Output Energy (MeV)	0.05	3.0	80
Pulse Current (mA)	20	10	10
RF frequency (MHz)		324	324
Chop rate (%)		50	50
Duty factor (%)	1.3	1.05	1.05
Repetition rate (Hz)	25	25	25

BEAM LOSS STUDIES

Ion Source Instability

Before September 2021, the type of Penning IS was used for the CSNS accelerator to produce H^- beam. At the be-

*Work supported by National Natural Science Foundation of China (11505201)
†pengjun@ihep.ac.cn

ISBN: 978-3-95450-253-0 ISSN: 2673-5571 doi:10.18429/JACoW-HB2023-WEA4C2

BEAM LOSS SIMULATIONS FOR THE PROPOSED TATTOOS BEAMLINE AT HIPA

M. Hartmann*,[1], D. Kiselev, D. Reggiani, J. Snuverink, H. Zhang, M. Seidel[1]
Paul Scherrer Institut, 5232 Villigen PSI, Switzerland
[1]also at École Polytechnique Fédérale de Lausanne (EPFL), Lausanne, Switzerland

Abstract

IMPACT (Isotope and Muon Production with Advanced Cyclotron and Target Technologies) is a proposed initiative envisaged for the high-intensity proton accelerator facility (HIPA) at the Paul Scherrer Institute (PSI). As part of IMPACT, a radioisotope target station, TATTOOS (Targeted Alpha Tumour Therapy and Other Oncological Solutions) will allow the production of promising radionuclides for diagnosis and therapy of cancer in doses sufficient for clinical studies. The proposed TATTOOS beamline and target will be located near the UCN (Ultra Cold Neutron source) target area, branching off from the main UCN beamline. In particular, the beamline is intended to operate at a beam intensity of 100 µA (60 kW), requiring a continuous splitting of the main beam via an electrostatic splitter. Realistic beam loss simulations to verify safe operation have been performed and optimised using Beam Delivery Simulation (BDSIM), a Geant4 based tool enabling the simulation of beam transportation through magnets and particle passage through the accelerator. In this study, beam profiles, beam transmission and power deposits are generated and studied. Finally, a quantitative description of the beam halo is introduced.

INTRODUCTION

The High Intensity Proton Accelerator facility (HIPA) at the Paul Scherrer Institute (PSI) delivers a 590 MeV CW (50.6 MHz) proton beam with up to 1.4 MW beam power (2.4 mA) to spallation and meson production targets serving particle physics experiments and material research [1].

IMPACT (Isotope and Muon Production using Advanced Cyclotron and Target technologies) is a proposed upgrade project envisaged for HIPA [2]. As part of IMPACT two new target stations are foreseen to be constructed : HIMB (High Intensity Muon Beamline) focuses on increasing the rate of surface muons while TATTOOS (Targeted Alpha Tumour Therapy and Other Oncological Solutions), an online isotope separation facility, will allow to produce promising radionuclides for diagnosis and therapy of cancer in doses sufficient for clinical studies. The TATTOOS facility includes a dedicated beamline intended to operate at a beam intensity of 100 µA (60 kW beam power), requiring continuous splitting of the high-power main beam via an electrostatic splitter [4]. A realistic model of the complete TATTOOS beamline from splitter to target was established in Ref. [5] using Beam Delivery Simulation (BDSIM), a Geant4 based program simulating the passage of particles in a particle accelerator [6].

One of the primary concerns in the operation of high-power accelerators is machine component activation caused by uncontrolled beam losses [7]. With regards to the TATTOOS beamline, the splitter in particular has to withstand significant power deposition and the beam losses due to scattering are a major challenge to be evaluated. Within this context, beam profiles and power deposits are simulated and studied. Finally, a quantitative description of the beam halo is introduced.

PROTON BEAMLINE

Overview of HIPA Facility

An overview of the HIPA facility with the foreseen TATTOOS installation is shown in Fig. 1. The proton beam is extracted from the Ring cyclotron and delivered to two meson production targets, Target M and Target E, through a dedicated beamline (PK1), along with two spallation targets for thermal/cold neutrons (SINQ) and ultracold neutrons (UCN) [1]. A fast kicker magnets diverts the full intensity beam (henceforth named main beam) from Targets M, E and SINQ to the UCN beamline via macro-pulsed kicks. Finally, the splitter located downstream of the kicker magnet in the PK1 beamline can peel off a fraction of the main beam and send it continuously to the UCN target [8]. Importantly, the fast kicker magnet and splitter cannot operate simultaneously.

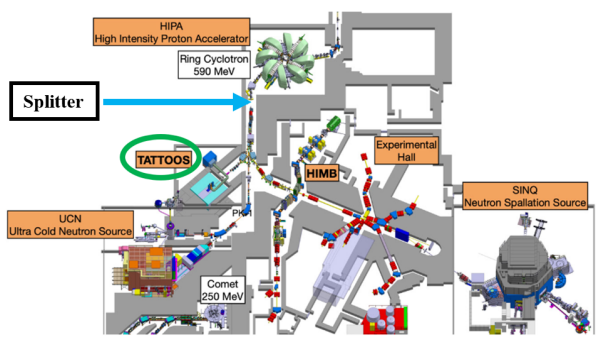

Figure 1: PSI's proton accelerator facility HIPA. The proposed TATTOOS installation is circled in green. The relative location of the splitter is also marked.

TATTOOS Beamline Description

Figure. 2 illustrates the simulated BDSIM model of the TATTOOS beamline. The beamline starts with the splitter

* marco.hartmann@psi.ch

ISBN: 978-3-95450-253-0 ISSN: 2673-5571 doi:10.18429/JACoW-HB2023-WEC4I1

RF SYSTEMS OF J-PARC PROTON SYNCHROTRONS FOR HIGH-INTENSITY LONGITUDINAL BEAM OPTIMIZATION AND HANDLING

Fumihiko Tamura*, Masanobu Yamamoto, Masahito Yoshii, Chihiro Ohmori, Yasuyuki Sugiyama, Hidefumi Okita, Kiyomi Seiya, Masahiro Nomura, Taihei Shimada, Katsushi Hasegawa, Keigo Hara, Ryosuke Miyakoshi
J-PARC Center, JAEA & KEK, Tokai-mura, Japan

Abstract

The application of magnetic alloy (MA) cores to the accelerating rf cavities in high intensity proton synchrotrons was pioneered for the J-PARC synchrotrons, the RCS and MR. The MA loaded cavities can generate high accelerating voltages. The wideband frequency response of the MA cavity enables the frequency sweep to follow the velocity change of protons without the tuning loop. The dual harmonic operation, where a single cavity is driven by the superposition of the fundamental and second harmonic rf voltages, is indispensable for the longitudinal bunch shaping to alleviate the space charge effects in the RCS. These advantages of the MA cavity are also disadvantages when looking at them from a different perspective. Since the wake voltage consists of several harmonics, which can cause bucket distortion or coupled-bunch instabilities, the beam loading compensation must be multiharmonic. The operation of tubes in the final stage amplifier is not trivial when accelerating very high intensity beams; the output current is high and the anode voltages also multiharmonic. We summarize our effort against these issues in the operation of the RCS and MR for more than 10 years.

INTRODUCTION

The Japan Proton Accelerator Research Complex (J-PARC) [1] is a high intensity proton facility, which consists of the 400 MeV linac, the 3 GeV Rapid Cycling Synchrotron (RCS) [2], and the 30 GeV Main Ring (MR) [3]. The high intensity output beams from the RCS and MR are used for generation of secondary particles at the Materials and Life Science Experimental Facility (MLF), the Hadron Hall, and the Neutrino Experimental Facility. The main parameters and their rf systems of the RCS and MR are listed in Table 1 and 2, respectively.

The application of magnetic alloy (MA) cores to the accelerating rf cavities in high intensity proton synchrotrons was pioneered for the J-PARC synchrotrons, the RCS and MR. The MA cavities can generate high accelerating voltage required for acceleration of high intensity proton beams. As shown in the tables, the maximum voltage of 440 kV is generated by twelve rf cavities in the RCS and 480 kV is generated by nine cavities in the MR. The MA cavity has wideband frequency response. The Q values of the cavities are set to 2 and 22 by an external inductor [4] and cut-core scheme for the RCS and MR, respectively. In both of the RCS and MR, the wideband responses enable the frequency sweep to follow the velocity change of the protons without tuning loops. The MR cavity is driven by the single harmonic rf. The Q value of the RCS cavity is set so that the dual harmonic operation [5], where a single cavity is driven by the superposition of the fundamental and the second harmonic rf voltages, is possible. The dual harmonic operation is indispensable for the longitudinal bunch shaping to alleviate the space charge effects in the beginning of acceleration in the RCS [6, 7].

On the other hand, the wideband frequency response has drawbacks. The wake voltage in the MA cavity is multiharmonic. In the case of the RCS cavity, the wake voltage consists of several higher harmonics. The rf bucket distor-

Table 1: Parameters of the J-PARC RCS and its RF System

Parameter	Value
Circumference	348.333 m
Energy	0.400–3 GeV
Beam intensity	8.3×10^{13} ppp
Output beam power	1 MW
Accelerating frequency	1.227–1.671 MHz
Harmonic number	2
Maximum rf voltage	440 kV
Repetition rate	25 Hz
No. of cavities	12
Q-value of rf cavity	2

Table 2: Parameters of the J-PARC MR and its RF System

Parameter	Value
Circumference	1567.5 m
Energy	3 – 30 GeV
Beam intensity	2.5×10^{14} ppp
Output beam power	(design) 750 kW
Accelerating frequency	1.67–1.72 MHz
Harmonic number	9
Maximum rf voltage	480 kV
Repetition period	1.16 – 5.2 s
No. of cavities (Fund. + 2nd)	9+2
Q-value of Fund. rf cavity	22

* fumihiko.tamura@j-parc.jp

ISBN: 978-3-95450-253-0 ISSN: 2673-5571 doi:10.18429/JACoW-HB2023-WEC4I2

DEVELOPMENT OF DUAL-HARMONIC RF SYSTEM FOR CSNS-II*

Xiao Li†, Bin Wu, Jian Wu, Xiang Li, Yang Liu, Wei Long, Chunlin Zhang
Institute of High Energy Physics, Chinese Academy of Science, Beijing, China

Abstract

The upgrade of the China Spallation Neutron Source (CSNS-II) encompasses the development of a dual harmonic RF system for the Rapid Cycling Synchrotron (RCS). The objective of this system is to achieve a maximum second harmonic voltage of 100 kV. To meet this requirement, a high gradient cavity is being used in place of the traditional ferrite loaded cavity. Magnetic alloy (MA) loaded cavities, which can attain very high field gradients, have demonstrated their suitability for high-intensity proton synchrotrons. As a result, designing an RF system with MA-loaded cavities has emerged as a primary focus. Over the past decade, substantial advancements have been made in the development of MA-loaded cavities at CSNS. This paper provides an overview of the RF system that incorporates the MA-loaded cavity and presents the high-power test results of the system.

INTRODUCTION

The China Spallation Neutron Source (CSNS) is advancing into its upgrade phase (CSNS-II), targeting a higher beam power up to 500 kW. The key parameters of CSNS-II can be found in Table 1. The most important thing for the transverse and longitudinal beam dynamics is to address the strong space charge effect arising from the higher beam intensity. To counteract this, the dual-harmonic acceleration mechanism [1,2], which has already demonstrated its efficacy in mitigating the space charge effect, is slated for introduction. Given the limited tunnel space in Rapid Cycling Synchrotron (RCS), only a high-gradient cavity can fulfill the needs for the second harmonic voltage. Consequently, ferrite-loaded cavities, constrained by their low saturation flux density, fall short in comparison.

MA-loaded cavities, celebrated for their standout saturation flux density and permeability [3,4], emerge as the top choice for high-gradient applications. Their low Q-value and broad bandwidth further position them as uniquely capable of providing both fundamental frequency and second harmonic voltages without the necessity of a tuning loop. Over the past decade, extensive advancements have been made in the development of MA-loaded cavities at CSNS. Concurrently, the power supply and the low-level RF (LLRF) control systems have seen considerable development.

In this paper, we provide an overview of the RF system, including the MA-loaded cavity, RF amplifiers, and the LLRF system, and present the test results from high-power tests.

* Work supported by the funds of National Natural Science Foundation of China (Fund No: 11875270, U1832210, 12205317), Youth Innovation Promotion Association CAS (2018015). Guangdong Basic and Applied Basic Research Foundation (2019B1515120046).
† email address: lixiao@ihep.ac.cn

Table 1: Key Parameters of the CSNS-II

Linac end energy	300 MeV
RCS extraction energy	1.6 GeV
Beam power	500 kW
RF cavities	8 (1^{st}) + 3 (2^{nd})
RF voltages	175 kV (1^{st})) + 100 kV (2^{nd})
Number of bunches	2
Number of protons	7.80×10^{13} ppp

OVERVIEW OF THE RF SYSTEM

MA-loaded Cavity

The MA-loaded cavity is composed of three λ/4 double-resonators, each linked by three accelerating gaps, spanning a total length of 1.8 m. These resonators function as water tanks filled with MA cores. Tanks on the same side of the gaps are interconnected in parallel. A visual representation of this configuration can be found in Fig. 1.

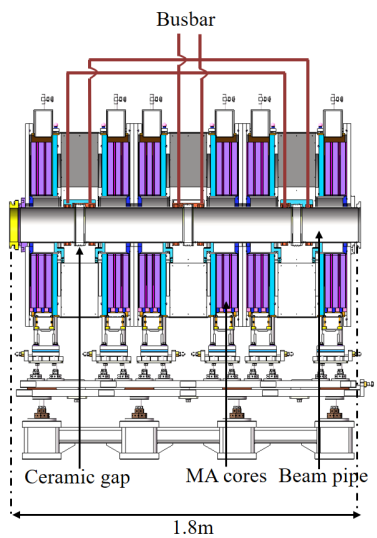

Figure 1: Schematic of the MA-loaded cavity.

The cavity incorporates a compact gap structure, engineered for robust voltage tolerance. It boasts a toroid constructed from alumina micro-powder, with stainless steel pipes embedded into the ceramic. This design minimizes the electric field exposure on the ceramic's surface and guarantees quick beam transit in the vacuum, facilitating efficient beam acceleration. To enhance the Q-value and amplify the operational prowess of the amplifier, two air inductors are aligned in parallel to the cavity. The impedance of the MA-loaded cavity, equipped with a 20 μH air inductor, is depicted in Fig. 2.

ISBN: 978-3-95450-253-0 ISSN: 2673-5571 doi:10.18429/JACoW-HB2023-WEC4C1

MAGNETIC ALLOY LOADED CAVITIES IN J-PARC AND CERN

C. Ohmori*, J-PARC, Tokai, Japan
M. Paoluzzi, CERN, Geneve, Switzerland

Abstract

Magnetic alloy loaded cavities have been used in seven synchrotrons at J-PARC and CERN. In this paper, we review various cavity technologies to satisfy the requirements for the beam acceleration, deceleration, manipulation, and instability damping. This paper also contains improvements of cavity cores by magnetic annealing scheme, quality control of cores during production, the cooling methods of magnetic alloy cores: direct water cooling and indirect one using copper discs, control of cavity bandwidths from broad to narrow bands, and the methods to drive RF cavities by tube and rad-hard solid-state amplifiers.

INTRODUCTION

The research and development of the wideband cavity without tuning circuit, began in 1995 [1]. Finemet, which is a nano-crystalline material that consists of $Fe_{bal.}Cu_1Nb_3Si_{15.5}B_7$, was used in the cavities [2, 3]. Thin amorphous ribbons coated with silica were wound to form a ring-core and annealed to form nano-crystal [4, 5]. One of the cavities was installed in the AGS tunnel in 1998 for a barrier bucket experiment [6]. The other was installed in HIMAC to demonstrate beam acceleration [7]. The cavity also exhibited a dual harmonic acceleration [8].

In 2002, KEK and CERN started collaborating on a wideband cavity for the heavy ion acceleration for lead-lead collisions in LHC [9–12]. J-PARC, which is a joint project of KEK and JAEA, used it as a high-gradient cavity for a high intensity beam acceleration [13–15].

After the beam operation of J-PARC began, a cavity core improvement program started [16]. Magnetic annealing was adopted to control the micro-structure of the magnetic domain of the material and to reduce the RF power loss caused by domain-wall displacement. J-PARC developed a large magnetic annealing oven to produce 80-cm diameter cores for the main ring cavities. The RF power loss in the cores was reduced to half by this technology. Two hundred and eighty cores were produced using the oven which was rent to the production company. Replacement of the cavities was completed in 2016 [17]. The available RF voltage of the cavities increases, which contributes to an increase in the beam intensity [18]. Magnetic-annealed cores were also adopted for a test cavity in the PS booster in CERN and MedAustron which was contributed by CERN [19, 20].

The LIU, LHC Injector Upgrade project, was launched at CERN [21, 22]. The project included a consolidation/upgrade of the PS booster RF system [23] as well as cure of longitudinal coupled bunch instability in PS [24]. In the PS, another wideband cavity was used to suppress several harmonic components of the instability simultaneously [25]. The beam-loading effects on the PS booster cavities were studied using test cavities in the PS booster and J-PARC [26]. Beam loadings on the wide-band cavity, including several harmonics, were also damped using a digital LLRF system [27–31]. The requirements for High Luminosity LHC project were satisfied by the combination of the cavity and another Landau one [32, 33]. Wideband technology was adopted to upgrade the PS booster RF system [34–36]. J-PARC-made magnetic annealing oven was also used to produce 324 cores for the booster. Two test-production cores before the mass production were used for a single-gap cavity of ELENA, Extra Low Energy Antiproton ring [37]. During the long shut down, LS2, all ferrite cavity systems were removed from the booster, and wideband systems were installed. The systems operated properly and have contributed to all the proton beam operations [38]. The test cavities in the booster were also removed in LS2, and one system was installed in the AD, Antiproton Decelerator. The wideband RF system also provided flexibilities for beam tunings and operations [39, 40].

J-PARC RCS demonstrated the beam acceleration beyond 1 MW [41]. RCS started replacing the present wideband systems with single-ended systems that use magnetic-annealed cores [42]. In this paper, we present key technologies for wideband RF systems, including the quality control and evaluation of core materials. The differences of the RF systems between CERN and J-PARC and between rings are also described.

CAVITY COOLING SCHEMES

CERN LEIR and J-PARC adopted a direct water-cooling scheme to cool their cores [9, 16]. The cores were waterproofed to protect the metal from corrosion. An advantage of this scheme is the large cooling power required for higher power loss. The three cores were placed in a water tank. Figure 1 shows the cores in the water tank of LEIR cavity. Two water tanks form a single cavity. In J-PARC, three or four cavity cells were combined to form a multi-gap cavity, and each gap was connected by bus bars as listed in Table 1. Indirect cooling was adopted in the other CERN cavities. Figure 2 shows the PS booster cavity which has 6 cells. The cell consists of two cores, two cooling disc, and an acceleration gap. Silicon paste was used on the side of core for a good heat transfer. A thin polyimide film was placed on the surface of a copper cooling disc. The film was used for insulation between the core and cooling disc. Each cell was driven by a solid-state amplifier [43]. A PT100 thermometer was placed on the core surface. The status of the cores was monitored externally. The indirect cooling

* chihiro.ohmori@kek.jp

ISBN: 978-3-95450-253-0 ISSN: 2673-5571 doi:10.18429/JACoW-HB2023-WEC4C2

MULTIHARMONIC BUNCHER FOR THE ISOLDE SUPERCONDUCTING RECOIL SEPARATOR PROJECT*

J. L. Muñoz†, I. Bustinduy, S. Varnasseri, P. González, A. Kaftoosian, L. Catalina-Medina
Consorcio ESS-Bilbao, Zamudio, Bizkaia, Spain
I. Martel, University of Huelva, Huelva, Spain

Abstract

The ISOLDE Superconducting Recoil Separator (ISRS) is based on a very compact particle storage ring of only 3.5 m in diameter. This instrument will be coupled with present and future detector systems of the HIE-ISOLDE facility. The injection of the HIE-ISOLDE beam into this ring requires a more compact bunch structure, so a Multi-Harmonic Buncher (MHB) device is proposed for this task. The MHB will operate at a frequency of 10.128 MHz, which is a 10% of the linac frequency, and would be installed before the RFQ. The MHB is desgined as a two electrodes system, and the MHB signal, composed for the first four harmonics of the fundamental frequency, is fed into the electrodes that are connected to the central conductor of a coaxial waveguides. The full design of the MHB is presented, including electromagnetic optimization of the electrode shape, optimization of the weights of each of the harmonic contribution, mechanical and thermal design of the structure. The RF generation and electronics to power up the device are also presented. A solution that generates directly the composed signal and is then amplified by a solid state power amplifier is also presented in this contribution.

INTRODUCTION

The HIE-ISOLDE [1] facility at CERN can accelerate more than 1000 isotopes of about 70 elements at collision energies up to 10 MeV/A, thus making it an ideal testbench to probe nuclear theories by selecting optimum (N, Z) combinations.

The "ISOLDE Superconducting Recoil Separator" (ISRS) [2,3] is a novel high-resolution spectrometer based on multifunction superconducting canted cosine theta magnets. This device will extend the physics program to more exotic isotopes produced in the secondary target. It will use focal plane spectroscopy with particle and photon detection using different detector devices at HIE-ISOLDE. The ISRS device consists on a ring composed of an array of iron-free superconducting multifunction magnets (SCMF) cooled by cryocoolers [4].

The HIE-ISOLDE linac operates at an RF frequency of 101.28 MHz, which results in a bunch separation of 9.87 ns. For operation of the ISRS, a longer separation is required. This can be achieved by inserting a pre-buncher before the RFQ. If the buncher operates at a frequency of 1/10th (f=10.128 MHz), then the bunch separation will be increased by a factor of ten, but at the same time the beam will be bunched at an exact fraction of the linac RF frequency, so it can be transmitted and accelerated by the RFQ and the rest of the linac.

Within the framework of the ISRS collaboration, a MHB prototype will be designed and built. The device will comply with ISOLDE specifications. At this stage of the project, the cavity will be tested in ESS-Bilbao injector, so diagnostics and other elements are also being developed [5].

MULTIHARMONIC BUNCHER DESIGN

The common technology for a buncher for radioactive beams in that frequency range is a Multi-Harmonic Buncher (MHB) [6–9]. To bunch a continuous beam to a certain RF frequency f, the optimum field time profile is a saw-tooth wave profile of frequency f [6], with a linear ramp of field centered at the middle of the bunch. The saw-tooth profile can be synthesized by summing up the first harmonics of its Fourier expansion. Usually, four harmonic terms are enough to generate an adequate approximation of the wave shape. In the MHB, this electric field is applied to two electrodes powered up with the combined multiharmonic RF wave. The field in the gap between the electrodes will be as uniform as possible, and it will be modulated by the MHB wave. In a real device the electric field between the electrodes depends on the electrode geometry and the aperture needed for the beam, so the actual performance of the MHB will be lower than the ideal one.

The buncher electrode geometry is usually designed by assuming a constant voltage [6–9]. In this way the field spatial distribution can be computed as an electrostatics problem. The field is taken as an amplitude that is then modulated by the four harmonic components, each one with the adequate weight, to obtain the composed saw-tooth profile in the time domain. Beam dynamics simulations are then run to evaluate the bunching efficiency. For low frequencies the differences in the electric field shape between an electrostatics and a RF calculations are very low. The design procedure and the computational tools used ha already been reported in [10].

Electrode Geometry

In Fig. 1 the electric field maps of two models are shown. The original model (named here Fraser model) is the one described in [7], while the wedge shaped model is a modification of this one. The gap in both cases is of 5 mm and the aperture is of 20 mm. The electric field profile along

* This research is funded by the Next Generation EU–Recovery and Resilience Facility (RRF).
† jlmunoz@essbilbao.org

ISBN: 978-3-95450-253-0 ISSN: 2673-5571 doi:10.18429/JACoW-HB2023-THA1I1

PERFORMANCE AND UPGRADE CONSIDERATIONS FOR THE CSNS INJECTION*

M. Y. Huang†,1,2,3,4, S. Y. Xu1,2,3, S. Wang1,2,3
[1]Institute of High Energy Physics, Chinese Academy of Sciences, Beijing, China
[2]Spallation Neutron Source Science Center, Dongguan, China
[3]University of Chinese Academy of Sciences, Beijing, China
[4]Key Laboratory of Particle Acceleration Physics &Technology, Institute of High Energy Physics, Chinese Academy of Sciences, Beijing, China

Abstract

For the proton synchrotron, the beam injection is one of the most important issues. In this paper, based on the China Spallation Neutron Source (CSNS), the injection methods have been comprehensively studied, including phase space painting and negative hydrogen stripping. By using the design scheme of the anti-correlated painting, the beam power has successfully reached 50 kW. However, some difficulties have been found in the higher power beam commissioning. In order to solve these key problems, flexibility in the CSNS design has been exploited to implement the correlated painting by using the rising current curve of the pulse power supply. The effectiveness of the new method has been verified in the simulation and beam commissioning. By using the new method, the beam power on the target has successfully risen to the design value. For the CSNS upgrade (CSNS-II), the injection energy is increased from 80 MeV to 300 MeV and the injection beam power is increased to about 19 times. Based on the CSNS experience and simulation results, it is hoped that the new painting injection scheme can not only greatly reduce the peak temperature of the stripping foil and the edge focusing effect of the chicane bump, but also need to be compatible with correlated and anti-correlated painting. After in-depth study, a new painting scheme has been proposed which not only achieves the design goals but also has many advantages.

INTRODUCTION

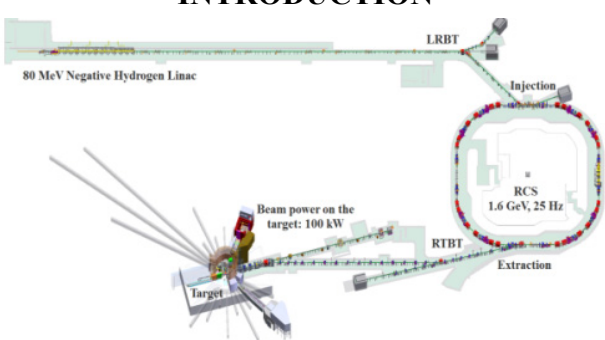

Figure 1: Layout of the CSNS.

The China Spallation Neutron Source (CSNS) accelerator [1, 2] consists of an 80 MeV negative hydrogen Linac and a 1.6 GeV rapid cycling synchrotron (RCS) with a repetition rate of 25 Hz. It accumulates an 80 MeV injection beam, accelerates the beam to the design energy of 1.6 GeV and extracts the high energy proton beam to the target [3]. Figure 1 shows the layout of the CSNS. The design goal of beam power on the target for the CSNS is 100 kW which has been achieved in Feb. 2020.

To increase the beam power on the target from 100 kW to 500 kW, the accelerator needs to be upgraded (CSNS-II), mainly including: Linac upgrade, injection system upgrade, and three dual harmonic cavities would be added to the RCS. Figure 2 shows the layout of the CSNS-II. It can be seen from the figure that the injection system upgrade is an important part of the CSNS-II. Table 1 shows the comparison of the injection beam parameters between the CSNS and CSNS-II.

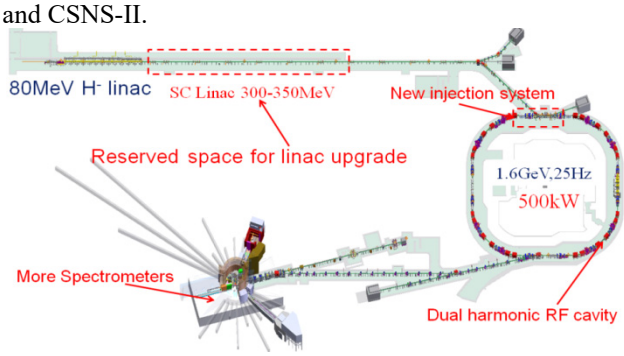

Figure 2: Layout of the CSNS-II.

Table 1: Comparison of the Injection Beam Parameters Between the CSNS and CSNS-II

Phase	CSNS	CSNS-II
Injection beam power (kW)	5	94
Linac energy (MeV)	80	300
Extraction beam energy (GeV)	1.6	1.6
Average beam current (μA)	62.5	312.5
Repetition frequency (Hz)	25	25
Proton number per pulse (10^{13})	1.56	7.8
Injection time (μs)	390	500
Injection beam size (mm/1σ)	1.0	1.5

The space charge effects are the core problem of the high intensity proton accelerator, and the main method to solve this problem is to use the phase space painting injection method. In addition, in order to break the restriction of Liouville's theorem, the negative hydrogen stripping method

* Work supported by the National Natural Science Foundation of China (No. 12075134) and the Guangdong Basic and Applied Basic Research Foundation (No. 2021B1515120021)
† huangmy@ihep.ac.cn

ISBN: 978-3-95450-253-0 ISSN: 2673-5571 doi:10.18429/JACoW-HB2023-THA1I2

HIGH-INTENSITY STUDIES ON THE ISIS RCS AND THEIR IMPACT ON THE DESIGN OF ISIS-II

R. E. Williamson*, D. J. Adams, H. V. Cavanagh, B. Kyle, D. W. Posthuma de Boer, H. Rafique, C. M. Warsop, ISIS Facility, Rutherford Appleton Laboratory, STFC, UK

Abstract

ISIS is the pulsed spallation neutron and muon source at the Rutherford Appleton Laboratory in the UK. Operation centres on a rapid cycling proton synchrotron (RCS) that accelerates 3×10^{13} protons per pulse from 70 MeV to 800 MeV at 50 Hz, delivering a mean beam power of 0.2 MW.

As a high-intensity machine, research at ISIS is predominantly focused on understanding, minimising and controlling beam-loss, which is central to sustainable machine operation. Knowledge of beam-loss mechanisms then informs the design of future high power accelerators such as ISIS-II.

This paper provides an overview of the R&D studies currently underway on the ISIS RCS and how these relate to ongoing work understanding and optimising designs for ISIS-II. In particular, recent extensive investigations into observed head-tail instabilities are summarised.

INTRODUCTION

The ISIS Neutron and Muon Facility has successfully been in operation for almost 40 years, providing neutron and muon beams to the user community for a broad spectrum of materials research [1]. Operation centres on an RCS with a 163 m circumference composed of 10 superperiods. It accelerates up to 3×10^{13} protons per pulse (ppp) from 70 MeV to 800 MeV on the 10 ms rising edge of a 50 Hz sinusoidal main magnet field, resulting in a mean beam power of 0.2 MW. Each beam pulse is extracted to one of two neutron targets (TS1 and TS2) and a small portion of the beam to TS1 interacts with an intermediary, carbon target to produce pions which decay into muons for condensed matter research.

Injection into the RCS is via charge-exchange of a 70 MeV, 25 mA H^- beam over ~130 turns with painting over both transverse acceptances, collimated at around 300 π mm mrad. The injected, essentially coasting, beam is bunched and accelerated by the ring dual harmonic RF system (h = 2, 4). The nominal betatron tunes are (Q_x, Q_y)=(4.31, 3.83) with peak incoherent tune shifts exceeding −0.5. Key ISIS RCS parameters are listed in Table 1. Beam intensity in the ring is loss-limited, with the main beam-losses coming from injection processes, longitudinal trapping, transverse space charge and the head-tail instability.

The main challenge for high-intensity operation of a hadron accelerator is minimising and controlling beam-losses which lead to activation of machine components, restricting hands-on maintenance. This paper presents an overview of R&D studies on the ISIS RCS focusing on the main drivers of beam-loss: building on our existing machine models to better understand the loss mechanisms, looking to methods of reducing beam-loss or increasing beam intensity, and thereby improving machine efficiencies. This paper also presents the impact of current R&D work on the design of a next generation, short-pulse neutron and muon facility, ISIS-II [2, 3].

Table 1: Important ISIS Synchrotron Parameters

Parameter	Value
Energy range	70 – 800 MeV
Beam intensity	3×10^{13} ppp
Gamma transition	5.034
Mean radius	26.0
No. superperiods	10
Dipole field	0.176 – 0.697 T
Nominal tunes (Q_x, Q_y)	4.31, 3.83
Chromaticity (ξ_x, ξ_y)	-1.1, -1.1
No. RF cavities (h = 2, 4)	6, 4
Machine accept. (A_x, A_y)	(540, 430) π mm mrad
Injection scheme	H^- charge-exchange
Extraction scheme	Fast, single-turn

Recent studies have been focused on benchmarking models of the ISIS accelerators to experimental data with a view to improving ISIS operations, through beam-loss reduction and control and increased efficiencies, and more reliable loss predictions for new accelerator designs. A detailed comparison of experimental measurements with a linear ORBIT [4] model of the ISIS RCS has been presented by Adams *et al.* [5]. This included dual harmonic RF, 3D injection painting, tune variation, real apertures and collimation, but without detailed magnet errors, and showed reasonable agreement on beam distributions and beam-loss as a function of time. Since then, in order to control and understand the machine better, and to allow more detailed R&D, there is a major effort to improve all aspects of machine modelling, as detailed below.

TRANSVERSE DYNAMICS MODELS

Magnet Models

Given the vintage of the accelerator, only limited data are available on ring lattice magnets: there are detailed measurements and OPERA [6] models of each lattice magnet type [7], but not each magnet. However, good agreement between measurements and models gives confidence in this "generic" data. The OPERA models and measurements are

* rob.williamson@stfc.ac.uk

ISBN: 978-3-95450-253-0 ISSN: 2673-5571 doi:10.18429/JACoW-HB2023-THA1I3

PREDOMINANTLY ELECTRIC STORAGE RING WITH NUCLEAR SPIN CONTROL CAPABILITY

R. M. Talman*, Laboratory for Elementary-Particle Physics, Cornell University, Ithaca, NY, USA

Abstract

A predominantly electric storage ring with weak superimposed magnetic bending is shown to be capable of storing two different nuclear isotope bunches, such as helion and deuteron, co-traveling with different velocities on the same central orbit. "Rear-end" collisions occurring periodically in a full acceptance particle detector/polarimeter, allow the (previously inaccessible) direct measurement of the spin dependence of nuclear transmutation for center of mass (CM) kinetic energies ranging from hundreds of keV up toward pion production thresholds. These are "rear-end" collisions occurring as faster stored bunches pass through slower bunches. An inexpensive facility capable of meeting these requirements is described, with nuclear channel $h + d \rightarrow \alpha + p$ as example.

INTRODUCTION

The proton is the only stable elementary particle for which no experimentally testable fundamental theory predictions exist! Direct p, p and p, n coupling is too strong for their interactions to be calculable using relativistic quantum field theory. Next-best: the meson-nucleon perturbation parameter (roughly 1/5) is small enough for standard model theory to be based numerically on π and K meson nucleon scattering. This "finesses" complications associated with finite size, internal structure, and compound nucleus formation.

These issues should be addressed experimentally, but this is seriously impeded by the absence of nuclear physics measurement, especially concerning spin dependence, for particle kinetic energies (KE) in the range from 100 keV to several MeV, comparable with Coulomb potential barrier heights. Even though multi-keV scale energies are easily produced in vacuum, until now spin measurement in this region has been prevented by space charge and negligibly short particle ranges in matter. In this energy range, negligible compared to all nucleon rest masses, the lab frame and the CM frame coincide.

To study spin dependence in nuclear scattering, one must cause the scattering to occur in what is (at least a weakly relativistic) moving frame of reference. This is possible using "rear-end" collisions in a predominantly electric with a weak magnetic field ring, a so-called E&m storage ring. Superimposed weak magnetic bending makes it possible for two beams of different velocity to circulate in the same direction, at the same time, in the same storage ring. "Rear-end" collisions occurring during the passage of faster bunches through slower bunches can be used to study spin dependence on nucleon-nucleon collisions in a moving coordinate frame.

* richard.talman@cornell.edu

Such "rear-end" collisions allow the CM KEs to be in the several 100 keV range, while all incident and scattered particles have convenient laboratory KEs, two orders of magnitude higher, in the tens of MeV range. Multi-MeV scale incident beams can then be established in pure spin states and the momenta and polarizations of all final state particles can be measured with high analyzing power and high efficiency. In this way the storage ring satisfies the condition that all nuclear collisions take place in a coordinate frame moving at convenient semi-relativistic speed in the laboratory, with CM KEs comparable with Coulomb barrier heights.

CO-TRAVELING ORBITS WITH SUPERIMPOSED E&m FIELDS

By symmetry, stable *all-electric* storage ring orbits are forward/backward symmetric and there are continua of different orbit velocities and radii, one of which matches the design ring radius in each direction. To represent the required bending force at radius r_0 being augmented by magnetic bending while preserving the orbit curvature we define "electric and magnetic bending fractions" η_E and η_M satisfying

$$\eta_E + \eta_M = 1, \text{ where } |\eta_M/\eta_E| \lesssim 0.5\,. \qquad (1)$$

The resulting magnetic force dependence on direction causes an $\eta_M > 0$ (call this "constructive") or $\eta_M < 0$ ("destructive") perturbation to shift opposite direction orbit velocities of the same radius, one up, one down, resulting in two stable orbits in each direction. For stored beams, any further $\Delta\eta_M \neq 0$ change causes beam velocities to ramp up in energy in one direction, down in the other. Our proposed E&m storage ring is ideal for investigating low-energy nuclear processes and, especially, their spin dependence.

Consider the possible existence of a stable orbit particle pair (necessarily of different particle type) such as deuteron/proton (d, p) or deuteron/helion (d, h), traveling with different velocities in the same direction. This periodically enables "rear-end" collisions events whose CM KEs can be tuned into the several 100 keV range by changing η_M. All incident and scattered particles will have laboratory KEs two orders of magnitude higher, in the tens of MeV range. (This symmetry argument is not effective for "same particle" pairs, such as p, p or d, d. The resultant co-traveling bunch velocities remain identical and no "rear-end" collisions ensue; treatment of the fundamentally most important case of identical particle scattering, has to be deferred for now.)

With careful tuning of E and B, such nucleon bunch pairs have appropriately different charge, mass, and velocity for their rigidities to be identical. Both beams can then co-circulate indefinitely, with different velocities.

ISBN: 978-3-95450-253-0 ISSN: 2673-5571 doi:10.18429/JACoW-HB2023-THA1C1

HIGH INTENSITY BEAM DYNAMICS CHALLENGES FOR HL-LHC

N. Mounet*, R. Tomás, H. Bartosik, P. Baudrenghien, R. Bruce, X. Buffat, R. Calaga, R. De Maria, C. Droin, L. Giacomel, M. Giovannozzi, G. Iadarola, S. Kostoglou, B. Lindström, L. Mether, E. Métral, Y. Papaphilippou, K. Paraschou, S. Redaelli, G. Rumolo, B. Salvant, G. Sterbini, CERN, Geneva, Switzerland

Abstract

The High Luminosity (HL-LHC) project aims to increase the integrated luminosity of CERN's Large Hadron Collider (LHC) by an order of magnitude compared to its initial design. This requires a large increase in bunch intensity and beam brightness compared to the first LHC runs, and hence poses serious collective-effects challenges, related in particular to electron cloud, instabilities from beam-coupling impedance, and beam-beam effects. Here we present the associated constraints and the proposed mitigation measures to achieve the baseline performance of the upgraded LHC machine. We also discuss the interplay of these mitigation measures with other aspects of the accelerator, such as the physical and dynamic aperture, machine protection, magnet imperfections, optics, and the collimation system.

INTRODUCTION

HL-LHC relies on a levelled luminosity reaching $5 \cdot 10^{34}\,\mathrm{cm}^{-2}\,\mathrm{s}^{-1}$ [1, 2] to be able to integrate $250\,\mathrm{fb}^{-1}$ per year of proton-proton luminosity in ATLAS and CMS [2]. In terms of beam properties, the luminosity $\mathcal{L} \propto \frac{n_\mathrm{b} N^2}{\varepsilon_\mathrm{n}}$ depends mainly on the number of colliding bunches n_b, the intensity per bunch N, and the normalised transverse emittance ε_n [1].

A high brightness N/ε_n for the initially injected beam, and its preservation through the machine cycle, are obviously critical ingredients to maximise luminosity. In view of HL-LHC, the entire LHC injector chain has undergone a campaign of improvements through the LHC Injectors Upgrade (LIU) project [3]. LIU was designed to provide HL-LHC with $N = 2.3 \cdot 10^{11}$ protons per bunch (p^+/b) within an emittance of 2.1 µm. Currently, nominal trains with up to $2.2 \cdot 10^{11}$ p^+/b within about 2 µm have been accelerated to 450 GeV/c in the CERN Super Proton Synchrotron (SPS), i.e. just before extraction into the LHC [4, 5]. Brightness preservation in HL-LHC is a subject in itself and will not be specifically considered in this article – we simply note that based on past experience, from injection to collision, losses are assumed to remain below 5% and an emittance blow-up of 20% is assumed (i.e., $\varepsilon_\mathrm{n} = 2.5$ µm is foreseen at the start of collisions, as a conservative estimate that takes into account some blow-up at injection, when ramping the energy, and when the separation between the two beams is collapsed).

The main focus of this paper will be on two crucial beam-dependent parameters that drive the machine performance, namely the bunch intensity and the number of bunches per beam. We will first discuss the limitations arising from electron-cloud (or e-cloud) effects, in particular, in terms of number of bunches, as well as their mitigation measures. Then we will focus on transverse impedance and stability, detailing the constraints imposed by the collimation system, the crab cavities and the dynamic aperture, as well as possible mitigation measures, before providing the global picture about beam stability. A few additional considerations with impact on intensity reach will then be listed, and our conclusion will follow.

THE ELECTRON-CLOUD CHALLENGE

Since the first LHC runs, the electron-cloud effect was found to significantly affect machine performance [6–9], essentially through its impact to the heat load on the magnet beam screens, which have to be maintained at a temperature of 20 K through an active cooling system whose capacity is limited. In addition, the electron cloud may also be responsible for emittance blow-up and instabilities.

The e-cloud is generally a self-healing phenomenon, i.e. it is gradually mitigated through a progressive conditioning of the inner surface of the vacuum pipe (or that of the beam screens, in the case of the superconducting magnets). Surface conditioning occurs during operation or in dedicated runs in the presence of e-cloud. This beam-induced scrubbing process effectively reduces the secondary electron emission yield (SEY), quickly at its beginning but then slowing down in an asymptotic way. It stops at a level that may depend on the surface properties and/or on the beam parameters. Unfortunately, the conditioning in the LHC became less and less effective for several sectors after being vented during successive long shutdowns. The reason has been identified in the degradation of the copper-plated surface of the beam screens, related to the unwanted formation of CuO oxide on conditioned surfaces exposed to air [10, 11]. This oxide increases the effective SEY value obtained after reconditioning compared to that of pure copper. As a consequence, the strong heat load in the most affected sector 78 [9, 12] has been limiting the number of bunches in LHC during Run 3. The degradation of the heat load from Run 2 to Run 3, for sector 78, is illustrated in Fig. 1.

For HL-LHC, several options are being studied to prevent the formation of an electron cloud, involving amorphous carbon coating (performed in situ), possibly after CuO reduction through surface treatment [14]. While these could be partially implemented already during long shutdown 3 (LS3, 2026–2029), it is likely that the first run of HL-LHC (Run 4) will still be limited by electron-cloud-induced effects, in particular the heat load, as in Run 3, and possibly

* nicolas.mounet@cern.ch

ISBN: 978-3-95450-253-0 ISSN: 2673-5571 doi:10.18429/JACoW-HB2023-THC1I2

FRIB BEAM POWER RAMP-UP: STATUS AND PLANS*

J. Wei†, C. Alleman, H. Ao, B. Arend, D. Barofsky, S. Beher, G. Bollen, N. Bultman, F. Casagrande, W. Chang, Y. Choi, S. Cogan, P. Cole, C. Compton, M. Cortesi, J. Curtin, K. Davidson, X. Du, K. Elliott, B. Ewert, A. Facco[1], A. Fila, K. Fukushima, V. Ganni, A. Ganshyn, T. Ginter, T. Glasmacher, J. Guo, Y. Hao, W. Hartung, N. Hasan, M. Hausmann, K. Holland, H. C. Hseuh, M. Ikegami, D. Jager, S. Jones, N. Joseph, T. Kanemura, S. H. Kim, C. Knowles, T. Konomi, B. Kortum, N. Kulkarni, E. Kwan, T. Lange, M. Larmann, T. Larter, K. Laturkar, R. E. Laxdal[2], J. LeTourneau, Z.-Y. Li, S. Lidia, G. Machicoane, C. Magsig, P. Manwiller, F. Marti, T. Maruta, E. Metzgar, S. Miller, Y. Momozaki[3], M. Mugerian, D. Morris, I. Nesterenko, C. Nguyen, P. Ostroumov, M. Patil, A. Plastun, L. Popielarski, M. Portillo, A. Powers, J. Priller, X. Rao, M. Reaume, S. Rogers, K. Saito, B. M. Sherrill, M. K. Smith, J. Song, M. Steiner, A. Stolz, O. Tarasov, B. Tousignant, R. Walker, X. Wang, J. Wenstrom, G. West, K. Witgen, M. Wright, T. Xu, Y. Yamazaki, T. Zhang, Q. Zhao, S. Zhao
Facility for Rare Isotope Beams, Michigan State University, East Lansing, MI, USA
P. Hurh, Fermi National Accelerator Laboratory, Batavia, IL, USA
S. Prestemon, T. Shen, Lawrence Berkeley National Laboratory, Berkeley, CA, USA
[1]also at INFN - Laboratori Nazionali di Legnaro, Legnaro (Padova), Italy
[2]also at TRIUMF, Vancouver, BC, Canada
[3]also at Argonne National Laboratory, Lemont, IL, USA

Abstract

This paper reports on the plans for a strategic ramp-up to high-beam-power operation of the Facility for Rare Isotope Beams, emphasizing challenges and solutions for beam-interception devices and targetry systems; radiation protection and controls; legacy systems renovation and integration; and automation and machine learning.

INTRODUCTION

The Facility for Rare Isotope Beam (FRIB) was completed in April 2022, ahead of the baseline schedule established about 10 years ago; the scientific user program started in May 2022 [1]. The ramp-up to the ultimate design beam power of 400 kW is planned over a six-year period (Fig. 1); 1 kW was delivered for initial user runs, and 5 kW was delivered as of February 2023. Primary beams delivered for rare isotope production include ^{36,40}Ar, ^{64}Zn, ^{48}Ca, ^{70}Zn, ^{82}Se, ^{86}Kr, ^{124}Xe, and ^{198}Pt. Test runs with 10 kW ^{36}Ar and ^{48}Ca beams were conducted in July 2023.

Extensive work has been done to prepare for high-power operation, including simultaneous acceleration of multiple charge states [2]; charge stripping of primary beams with liquid lithium [3]; commissioning of a superconducting electron-cyclotron-resonance ion source [4]; and operation of a rotating graphite target [5]. The superconducting radiofrequency (SRF) driver linac has been operating in continuous-wave (CW) mode as planned [6]. The linac setting is developed with a pulsed, low-average-power beam, while all experiments use a CW beam.

Although the driver linac is ready to deliver full-power beams, ramp-up of the average beam power requires facility-wide development. First, experience must be gained to safely handle increased radiological impact, including prompt radiation, activation in device materials and non-conventional utilities, and possible residual activation in ground water and exhaust air. Second, extensive machine studies and beam tuning are needed to minimize uncontrolled beam losses for the desired operating conditions. High-power targetry systems and beam-intercepting devices are in phased deployment along with ancillary systems, including non-conventional utilities and remote handling. Accelerator improvements and renovations to aging legacy systems are being implemented in parallel.

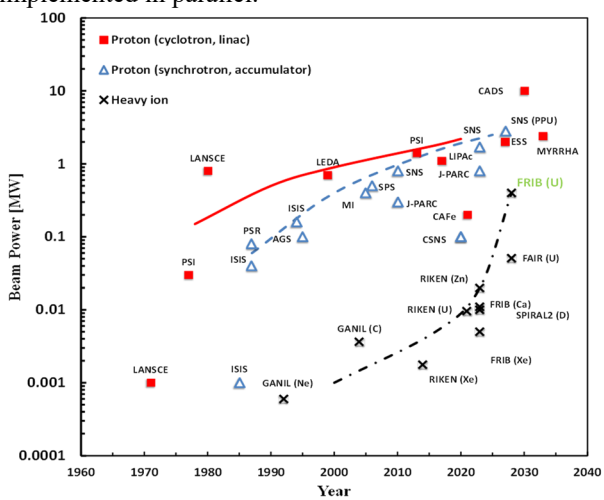

Figure 1: Beam power on target as a function of time for existing (as of August 2023) and planned power-frontier accelerator facilities.

* Work supported by the U.S. Department of Energy Office of Science under Cooperative Agreement DE-SC0023633, the State of Michigan, and Michigan State University.
† wei@frib.msu.edu

ISBN: 978-3-95450-253-0 ISSN: 2673-5571 doi:10.18429/JACoW-HB2023-THC1C1

TRANSVERSE EMITTANCE RECONSTRUCTION ALONG THE CYCLE OF THE CERN ANTIPROTON DECELERATOR

G. Russo*, B. Dupuy, D. Gamba, L. Ponce
CERN, Geneva, Switzerland

Abstract

The precise knowledge of the transverse beam emittances on the different energy plateaus of the CERN Antiproton Decelerator (AD) ring is important for assessing and optimising the machine performance as well as its setting-up. This paper presents a methodology for reconstructing transverse beam profiles from scraper measurements employing the Abel Transform (AT). The proposed methodology provides a precise, reproducible and user independent way of computing the beam emittance, as well as a useful tool to qualitatively track machine performance in routine operation. As discussed in this paper, its application has already been proven crucial for the operational setting-up of the stochastic cooling in AD. It also opens up the possibility for detailed benchmark studies of the cooling performance in different machine and beam conditions.

INTRODUCTION

The Antiproton Decelerator (AD) ring is the only operational facility worldwide where high brightness antiproton beams are produced. Nowadays the AD ring reaches a nominal intensity of $4.0 \times 10^7 \bar{p}$ in a single bunch, which are decelerated from the production momentum of 3.574 GeV/c to 100 MeV/c. Over the years, AD has undergone many significant changes and upgrades, however one of the main remaining challenges is the determination of the transverse emittance along the cycle. Conversely to accelerators, the geometric emittance adiabatically increases during the deceleration process by a factor proportional to the ratio between initial and final beam momentum; therefore, stochastic and electron cooling is applied on several energy plateaus. From here the need to be able to characterise the emittance along the AD cycle as a mean to control the performance of the cooling systems arises.

EMITTANCE MEASUREMENTS

Emittance along the AD cycle can be measured by means of a scraper and Ionization Profile Monitors (IPM). In this paper, only the former will be analysed since the latter is presently not operational. It is worth mentioning that, given the length of the AD cycle (≈ 110s) and given that a scraper measurement leads to a complete loss of the beam, the time needed to perform a complete set of emittance measurements in the horizontal (H) and vertical (V) plane at a few key moments along the cycle can take between 45 minutes and up to 2 hours, if no machine downtime occurs in the meantime.

* giulia.russo@cern.ch

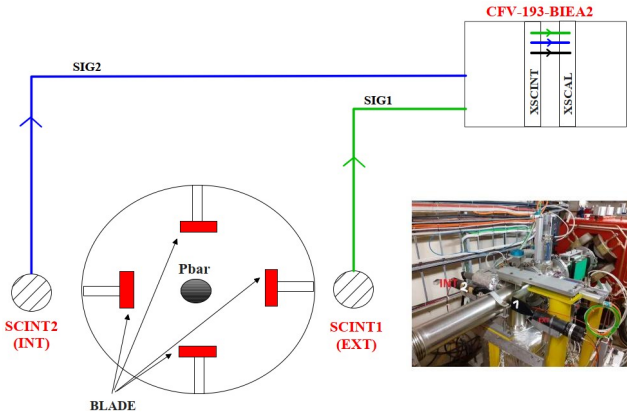

Figure 1: Schematic representation of the 4 blades systems used for scraper measurements as well as a photo of the system in the AD ring.

In AD four independent scraper blades (see Fig. 1), two per plane, are installed and each of them has its own moving mechanism. As the blade moves inside the beam, portions of the beam are scraped away. The interaction of $\bar{p}$ and the blade produces secondary particles that are detected by two scintillators (namely, SCINT1 and SCINT2) installed symmetrically outside the vacuum chamber in a horizontal arrangement, as shown in Fig. 1. The signal of one of the two scintillators is further processed by means of an electronic scalar board which provides a signal with a higher sampling rate

For a $4D$ Gaussian beam it is possible to analytically compute the profile of the losses during the scraping process. If the scraper is installed in a dispersion-free region (as in AD), the evolution of the losses as a function of the scraper position reads as:

$$\ell(u_s) = \frac{u_s - u_0}{\beta_u(s = s_s)\epsilon_{\mathrm{u,\,RMS}}} \exp\left(-\frac{1}{2}\frac{(u_s - u_0)^2}{\beta_u(s = s_s)\epsilon_{\mathrm{u,\,RMS}}}\right), \quad (1)$$

where u refers to x or y whether the Horizontal (H) or Vertical (V) plane is considered, respectively, and u_s indicates the scraper position and u_0 the beam closed orbit. This process can also be simulated numerically. If a fictitious scraper is moved along the H plane (and the same holds true for the V one) then it progressively removes particles with action J larger than $J_{\max}$:

$$2\epsilon_{\mathrm{RMS}} =< 2J_{\max} >=< X^2 + X'^2 >=< \frac{(x_s - x_0)^2}{\beta_x} >, \quad (2)$$

ISBN: 978-3-95450-253-0 ISSN: 2673-5571 doi:10.18429/JACoW-HB2023-THA2C1

MEASUREMENT OF TRANSVERSE BEAM EMITTANCE FOR A HIGH-INTENSITY PROTON INJECTOR*

D.-H. Kim †, H.-S. Kim, H.-J. Kwon, S. Lee, Korea Multipurpose Accelerator Complex, Korea Atomic Energy Research Institute, Gyeongju, Korea

Abstract

We propose a simple and fast diagnostics method for the transverse beam emittance using a solenoid magnet. The solenoid scan data is analysed employing the hard edge solenoid model and thick lens approximation. The analytical method is validated by beam dynamics simulations with varying input beam parameters. To address the space charge effect in a simplified manner, the space charge force is linearized and incorporated between segments of the drift-solenoid transfer matrix. For intense hadron injectors with higher beam current accounting for space charge prove to be more effective for correction. Building upon the method validated through beam simulation, experiments are conducted on space charge compensation at the beam test stand in the Korea Multipurpose Accelerator Complex (KOMAC). In a constant ion source operating condition, beam emittance is measured from solenoid scans while varying the flow rate of krypton gas injection. Notable shifts are observed in transverse beam emittance attributable to krypton gas injection, implying some optimal gas flow rate for mitigating emittance growth.

INTRODUCTION

In the low energy beam transport section, the method of measuring the transverse beam profile with a faraday cup or microchannel plate is preferred rather than wire or grid because the ion beam has a short range in the medium. In addition, various beam diagnostic systems have been developed to obtain transverse beam emittance, such as an Allison-type scanner [1] that electrically sweeps the beamlets, a pepperpot meter that passes the beamlets through a thin mask arranged with very fine holes, or a magnet scan technique that measures the change in beam size while scanning the intensity of the focusing magnet.

The magnet scan technique has advantages in that the beam measurement system is simpler to be implemented than the Allison scanner or pepperpot meter, and it utilizes focusing magnets that are essential to control beam optics. Quadrupole magnet is commonly used in magnet scan techniques in hadron machines, because magnetic quadrupole lattices is required for hadron beams above MeV with high magnetic rigidity. On the other hand, in the low energy beam transport (LEBT) of the high-intensity linear accelerator, solenoid magnet is often used to focus beams of low magnetic rigidity. In this study, the solenoid scan technique is verified with beam dynamics simulation data, especially by linearizing the space charge effect that greatly affects the high-intensity low energy proton beam, and applying it to beam experiments.

† one@kaeri.re.kr

RFQ-BASED BEAM TEST STAND

The Radio Frequency Quadrupole-based beam test stand (RFQ-BTS) is for studying the physical characterization and industrial applications of low energy high current beams ranging from a 50 keV, 30 mA proton injector to a 1 MeV/n RFQ [2]. It is a test facility with specifications similar to those of the 100-MeV proton linear accelerator at the Korea Multipurpose Accelerator Complex (KOMAC).

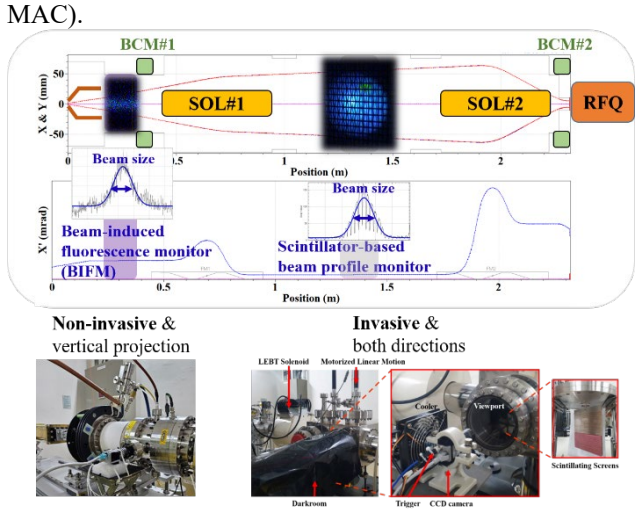

Figure 1: Layout of RFQ-based beam test stand and low energy beam diagnostics for transverse beam measurement.

The RFQ-based beam test stand has two low energy beam diagnostics for measuring the transverse beam profile as shown in Fig. 1 [3]. The beam-induced fluorescence monitor (BiFM) measures the emission light generated by interaction with the neural gas present in the beam pipe [4]. This method has the advantage of being non-invasive and enabling real-time measurement. This monitoring system is installed between the ion extraction system and the first beam optics element, the solenoid magnet, and is used to determine the initial envelope of the ion source extraction beam. The intensity of the emitted light is proportional to the product of the beam current and gas density of the ion source, assuming that the decay time of the fluorescence is much shorter than a millisecond, the normal beam pulse width of the beam test stand. Typically, the pressure of the plasma chamber corresponds to a few mTorr when generating hydrogen plasma in the microwave ion source, so the gas pressure around the beam extraction system is measured at a value close to 1 mTorr by the diffusion of hydrogen gas. Accordingly, sufficient emission light can be measured near the ion source of the high-intensity proton injector.

ISBN: 978-3-95450-253-0 ISSN: 2673-5571 doi:10.18429/JACoW-HB2023-THA2C2

COMPARISON OF LONGITUDINAL EMITTANCE OF VARIOUS RFQs

M. Comunian†, L. Bellan, A. Pisent
Istituto Nazionale di Fisica Nucleare Laboratori Nazionali di Legnaro, Legnaro, Italy

Abstract

In various projects a large variety of RFQs has been developed, for different application, with different average current, frequency, and energy range. On this article a comparison, in a scaled way, will be done, using the build RFQs of IFMIF, ESS, SPES, ANTHEM, PIAVE. On particular the beam dynamics characteristics will be analysed, like transmission, output longitudinal emittance and real performance versus simulation.

INTRODUCTION

Longitudinal emittance at the RFQ output is a very important parameter that define the beam quality in the subsequent accelerator. A low value of longitudinal emittance permits higher real state energy gain, so a more compact Linac. Achieving a small longitudinal output emittance is difficult because the initial bunching of the injected dc beam, initially emittance dominated for low current beam and space charge dominated for high current beam, tends to fill the evolving bucket separatrix in both cases. On the other hand, an external multi harmonic buncher do not guarantee high particles capture efficiency, especially for a high current beam.

A standard strategy is the use of slow of quasi-adiabatic bunching process that is highly nonlinear, this process requires tens of RFQ cells. The result from this slow adiabatic bunching process would require an unrealistically long RFQ to accommodate the several longitudinal phase space rotations needed.

An example of limits on longitudinal emittance optimization is reported in Fig. 1, where it is shown for each point a full multiparticle simulation obtained by the LANL chain of programs and a swarm optimization algorithm [1,2]. In this example the TRASCO RFQ [3] has been re-designed with the IFMIF voltage shape law, to check the possible improvements. The lower left part of the figure shows the lower peak RF power and longitudinal emittance, with respect to the TRASCO RFQ with a shorter RFQ if the dot colour is near to blue. The dashed lines are the actual characteristics of TRASCO RFQ. In this example to get a factor 2 lower longitudinal emittance is necessary to increase of about 1-meter the RFQ length, with a factor 2 increase on peak RF power.

Another way to look at the trade-off on the longitudinal emittance is the shaper length. Figure 2 shows the length of the shaper for the same TRASCO RFQ cases.

To get a factor 2 less longitudinal emittance, it is necessary to increase the shaper length of a factor 3, obtaining an increment of the total RFQ length of more than 1 meter.

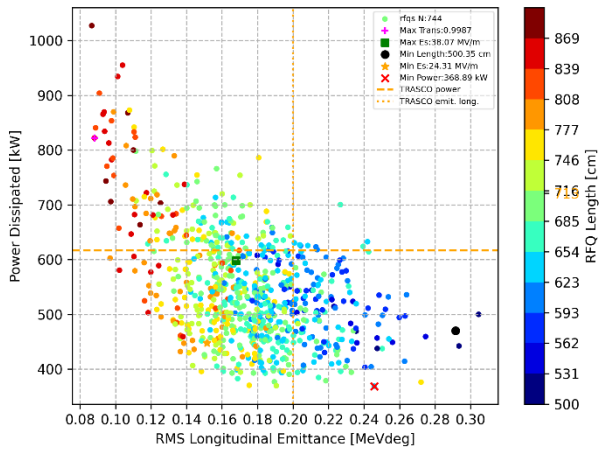

Figure 1: Longitudinal emittance as function of RF power and total RFQ Length.

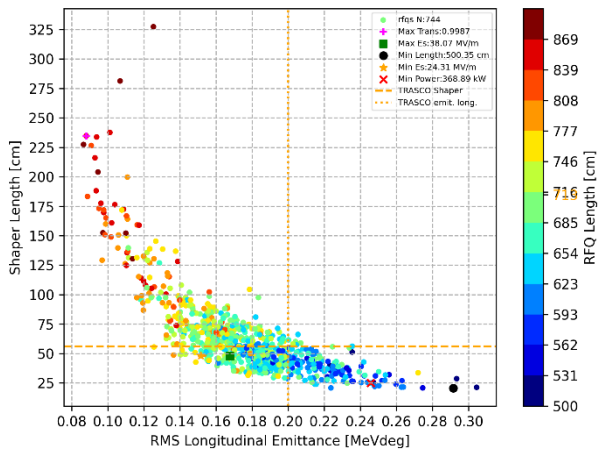

Figure 2: Longitudinal emittance as function of shaper length and total RFQ length.

RFQ SELECTIONS

In this context the analysed 4-vane type RFQs are already built; each of them is the result of several optimization processes which involve practical consideration such as realistic length, RF power, and manufacturing process. The selected RFQs for the comparison are: the TRASCO RFQ that now is used for the ANTHEM BNCT project; the IFMIF/EVEDA RFQ is high current CW RFQ now under commissioning in Rokkasho (Japan) [4]; the RFQ for the LNL RIBs beams project SPES also CW but for low current and able to handle a range of 3<A/q<7 [5]; the SPIRAL2 RFQ is CW for ions [6]. The ESS proton RFQ is a pulsed machine with 14 Hz as d.c [7].

In Table 1 is reported in summary the main parameters of the RFQs. Each RFQs has been designed with a specific

† email: michele.comunian@lnl.infn.it

ISBN: 978-3-95450-253-0 ISSN: 2673-5571 doi:10.18429/JACoW-HB2023-THA2C3

PERIODIC SOLUTION FOR TRANSPORT OF INTENSE AND COUPLED COASTING BEAMS THROUGH QUADRUPOLE CHANNELS

C. Xiao*, L. Groening,
GSI Helmholtzzentrum für Schwerionenforschung GmbH, Darmstadt, Germany

Abstract

Imposing defined spinning to a particle beam increases its stability against perturbations from space charge. In order to fully explore this potential, proper matching of intense coupled beams along regular lattices is mandatory. Herein, a novel procedure assuring matched transport is described and benchmarked through simulations. The concept of matched transport along periodic lattices has been extended from uncoupled beams to those with considerable coupling between the two transverse degrees of freedom. For coupled beams, matching means extension of cell-to-cell periodicity from just transverse envelopes to the coupled beam moments and to quantities being derived from these.

INTRODUCTION

Preservation of beam quality is of major concern for acceleration and transport especially of intense hadron beams. This aim is reached at best through provision of smooth and periodic beam envelopes, being so-called matched to the periodicity of the external focusing lattice. The latter is usually composed of a regular arrangement from solenoids or quadrupoles. For the time being, the quality of matching has been evaluated through the periodicity of spatial beam envelopes. This is fully sufficient as long as there is no coupling between the phase space planes (for brevity "planes"), neither in beam properties nor in lattice properties.

Spinning of beams is a very promising tool to further augment accelerator performance. It requires coupling between planes and thus imposes dedicated efforts for proper matching to periodic lattices. Beam matching with coupling between the horizontal and longitudinal planes has been investigated in [1]. Special cases of beams with zero four-dimensional emittances have been treated in [2] The present work is on the development and demonstration of a method to assure rms-matched transport of intense beams with considerable transverse coupling, an issue being addressed conceptually in [3]. It partially implements the early concept, i.e. tracking of moments, into a procedure to obtain full cell-to-cell four-dimensional (4D)-periodicity. Through simulations it is shown that the lattice periodicity is not just matched by the two transverse envelopes but also by the beam rms-moments that quantify coupling. To this end, an iterative procedure towards the periodic solution is applied. It starts from determining the solution with zero current, using a method that is applied later also to beams with current.

Coupled beams inhabit ten independent second-order rms-moments. They are summarized within the symmetric beam moments matrix

$$C := \begin{bmatrix} \langle xx\rangle & \langle xx'\rangle & \langle xy\rangle & \langle xy'\rangle \\ \langle x'x\rangle & \langle x'x'\rangle & \langle x'y\rangle & \langle x'y'\rangle \\ \langle yx\rangle & \langle yx'\rangle & \langle yy\rangle & \langle yy'\rangle \\ \langle y'x\rangle & \langle y'x'\rangle & \langle y'y\rangle & \langle y'y'\rangle \end{bmatrix} . \quad (1)$$

Four of its elements quantify beam coupling. Beams are *x-y* coupled if at least one of these elements is different from zero.

A simple way to impose spinning to a beam is to pass it through an effective half solenoid. Although half solenoids do not exist due to $\vec{\nabla} \cdot \vec{B} = 0$, their effect can be imposed by particle creation inside the solenoid or by changing the beam charge state inside the solenoid [4,5] and demonstrated experimentally in [6].

The first part of the transport matrix S^h of an effective half solenoid is given by the matrix $S_{\rightarrow}$ of the main body of the solenoid of effective length L, comprising just the pure longitudinal magnetic field B_s

$$S_{\rightarrow} = \begin{bmatrix} 1 & \frac{\sin(2KL)}{2K} & 0 & \frac{1-\cos(2KL)}{2K} \\ 0 & \cos(2KL) & 0 & \sin(2KL) \\ 0 & -\frac{1-\cos(2L)}{2K} & 1 & \frac{\sin(2KL)}{2K} \\ 0 & -\sin(2KL) & 0 & \cos(2KL) \end{bmatrix} , \quad (2)$$

with $K := B_s/[2(B\rho)]$ (Larmor wave number) and $(B\rho)$ as beam rigidity.

The second part of S^h is from the fringe field matrix $S_{\downarrow}$ of the solenoid exit

$$S_{\downarrow} = \begin{bmatrix} 1 & 0 & 0 & 0 \\ 0 & 1 & -K & 0 \\ 0 & 0 & 1 & 0 \\ K & 0 & 0 & 1 \end{bmatrix} , \quad (3)$$

and the total matrix of the half solenoid is the product of both matrices

$$S^h = S_{\downarrow} \cdot S_{\rightarrow} = \begin{bmatrix} S^h_{xx} & S^h_{xy} \\ S^h_{yx} & S^h_{yy} \end{bmatrix} . \quad (4)$$

The determinants of the diagonal sub-matrices S^h_{xx} and S^h_{yy} are different from 1.0, hence the projected rms-emittances are changed by S^h. Additionally, S^h_{xy} and S^h_{yx} are also different from zero, thus coupling will be imposed to an initially uncoupled beam. Although being non-symplectic, S^h has the determinant of 1.0 preserving the product of the two eigen-emittances.

The beam line being used to determine the periodic solution of an intense coupled beam along a periodic channel is sketched systematically in Fig. 1.

* c.xiao@gsi.de

ISBN: 978-3-95450-253-0 ISSN: 2673-5571 doi:10.18429/JACoW-HB2023-THA2C4

ALTERNATING PHASE FOCUSING UNDER INFLUENCE OF SPACE CHARGE DEFOCUSING

S. Lauber *[1,2] W. Barth[1,2,3], R. Kalleicher[2,3],
M. Miski-Oglu[1,2], S. Yaramyshev[1]
[1] GSI Helmholtzzentrum für Schwerionenforschung GmbH, Darmstadt, Germany
[2] HIM Helmholtz Institute Mainz, Mainz, Germany
[3] KPH Johannes Gutenberg-University Mainz, Mainz, Germany

Abstract

Alternating phase focusing (APF) recently emerged as a promising beam dynamics concept for accelerating bunched proton or ion beams in drift tube linear accelerators, eliminating the need for additional transverse focusing lenses. The performance of APF systems, similar to radio frequency quadrupoles, heavily relies on the employed focusing lattice, including the particle synchronous phase in each gap, as well as various hyperparameters such as the number of gaps, the focusing gradient, and the required beam acceptance. However, to fully utilize the cost advantages and mechanical simplicity of APF drift tube linacs, specialized software tools are necessary to streamline the accelerator development process. After successful development of the HELIAC-APF-IH-DTL for low current and continuous wave duty cycle, this paper presents the design concepts for APF cavities tailored for high-current applications, aiming to facilitate the design and implementation of APF-based accelerators.

INTRODUCTION

The method of alternating phase focusing (APF) [1–5] for compact and less costly linacs has been implemented in several projects within the last decade [6–13], enabled by the increase in computing power. The APF method aims to remove magnetic focusing lenses from inside the linacs (close to the radio frequency quadrupole (RFQ)). Some applications introducing external (thus easily accessible) magnetic focusing lenses have been also proposed and implemented.

Two resonance acceleration cavities, implementing the APF method for lower current continuous wave heavy ion beams, have been designed applying the beam dynamics simulation code DYNAMION [14, 15] for the Helmholtz Linear Accelerator (HELIAC) project [10, 16, 17]. The new accelerator will supply beam for material science and superheavy ion research at GSI Helmholtz Centre for Heavy Ion Research (GSI). The APF cavities are currently in production. Whilst the APF cavities will be later used as injector for HELIAC, the expertise from designing such cavities were used to create a software to deliver APF designs rapidly.

The former prototyping software was capable of delivering beam dynamics prototype designs within weeks. In contrast, the new, improved software is capable of delivering preliminary beam dynamics prototypes within hours. Nevertheless, the beam dynamics layout does not remove the need for careful 3D-CAD design, as well as radio frequency (RF) and thermal simulations. The development now enables the linac designer to study the influence of hyperparameters such as the number of cells, the input emittances, the matching parameters, input/output energy, the electric field gradient, the gap/cell ratio, and the aperture radius. At this point, a reasonable enhancement to this software is to include space charge effects, which thus becomes an investigatable hyperparameter as well.

METHOD

For the APF method, a set of alternating synchronous phases (the phase of the electromagnetic field when the bunch is in the center of a gap) along the linac has to be found for the particular project, providing sufficient beam focusing in all directions for the given boundary conditions, like emittance, number of gaps, etc. Therefore, a set of phases is optimized to find an adequate layout using beam dynamics simulations repeatedly.

The core of the beam dynamics simulation consists of well-known equations [18, 19], accounting for acceleration of each particle by its respective synchronous phase, in order to feature the longitudinal deformation of the beam by the sinusoidal RF. Furthermore, the beam defocusing due to the transverse electric field component in between the drift tubes is considered as well. The transit-time factor is calculated for each gap in dependence of the gap length and particle velocity, the radial dependence of the transit-time factor [18] is also considered by

$$T_{\mathrm{TTF}}(r,\beta,g) = I_0(Kr)\frac{J_0(2\pi a/\lambda)}{I_0(Ka)}\,T_{\mathrm{TTF}}(\beta,g), \quad (1)$$

using the zeroth order Bessel function J_0, the zeroth order modified Bessel function I_0 , the radial particle position r, the aperture radius a, the RF wavelength λ the particle velocity as fraction of speed of light β, the effective gap length g, and the constant $K = \frac{2\pi}{\gamma\beta\lambda}$.

The distance in between two drift tubes is derived during execution to map the set of synchronous phases along the linac to a geometric drift distance [10]. The voltage in each gap is derived by the gap- and cell-length at the current position, accounting for a non-flat electric field strength along the linac ($E_z(z) \propto \sin(\pi z/L)$).

* s.lauber@gsi.de

ISBN: 978-3-95450-253-0 ISSN: 2673-5571 doi:10.18429/JACoW-HB2023-THC2I2

EXTRACTION OF LHC BEAM PARAMETERS FROM SCHOTTKY SIGNALS

K. Lasocha*, D. Alves, C. Lannoy[1], N. Mounet, CERN, Geneva, Switzerland
T. Pieloni, EPFL, Lausanne, Switzerland
[1]also at EPFL, Lausanne, Switzerland

Abstract

Analysis of Schottky signals provides rich insights into the dynamics of a hadron beam, with well-established methods of deriving the betatron tune and machine chromaticity. In this contribution, we will report on recent developments in the analysis and understanding of the signals measured at the Large Hadron Collider during proton and Pb^{82+} fills. A fitting-based technique, where the measured spectra are iteratively compared with theoretical predictions, will be presented and compared with the previous methods. As a step beyond the classical theory of Schottky spectra, certain signal modifications due to the activity of the LHC machine systems will be discussed from the perspective of the applicability of the modified signal to the beam diagnostics.

INTRODUCTION

Schottky signals, that is fluctuations of the macroscopic beam characteristics due to the discrete motion of individual particles, can provide rich insights into their dynamics within the bunch. After the pioneering works of Simon van der Meer [1] and the first experimental observations at the Intersecting Storage Ring [2], Schottky signals have been used at many facilities as a source of information on the betatron tune, momentum spread, transverse emittance and chromaticity.

In the LHC the Schottky monitor was commissioned in 2011 [3] and underwent a major redesign during 2014-2015 [4]. Although the quality of the measured spectra during the Pb^{82+} runs is in general very good, for proton beams this is not the case. The signal is particularly difficult to analyze due to the presence of numerous coherent spectral components, enhanced by the high intensity of the proton beams.

The aim of this contribution is to summarize the recent progress in the analysis of LHC Schottky spectra. As described in Refs. [5–7], a new technique was developed, which allows for longitudinal and transverse beam parameter estimation by iterative simulation of fragments of the spectrum. A thorough revision of the theory describing Schottky signals resulted in a formal derivation of certain results, which were previously based mostly on empirical arguments. Finally, the analysis of the spectra acquired during LHC Runs 2 (2015-2018) and 3 (2022) allowed us to understand how various beam and machine conditions, not included in the theory of Schottky spectra, affect the beam.

* kacper.lasocha@cern.ch

LONGITUDINAL SCHOTTKY SIGNALS

Let us consider a single particle i, performing synchrotron oscillations around the ideal synchronous particle that travels around the synchrotron ring with angular frequency ω_0. We shall assume that the synchrotron motion is sinusoidal and that the time delay between particle i and the synchronous particle at a given location in the ring is given by:

$$\tau_i(t) = \widehat{\tau}_i \sin\left(\Omega_{s_i} t + \varphi_{s_i}\right),$$

with synchrotron frequency Ω_{s_i}, time amplitude $\widehat{\tau}_i$ and phase φ_{s_i}. The synchrotron frequency is related to the amplitude as predicted by the theory of the mathematical pendulum [8]:

$$\Omega_s = \frac{\pi}{2\mathcal{K}\left[\sin\left(\frac{h_{RF}\omega_0\widehat{\tau}}{2}\right)\right]}\Omega_{s_0}, \quad (1)$$

where Ω_{s_0} is the nominal synchrotron frequency, $h_{RF}\omega_0$ is the angular RF frequency and $\mathcal{K}$ denotes the complete elliptic integral of the first kind [9, p. 590].

At a given location in the ring, the current of a single particle i can be described, up to a scaling factor, in the following way [10]:

$$I_i(t) \propto \sum_{n=-\infty}^{\infty}\sum_{p=-\infty}^{\infty} J_p(n\omega_0\widehat{\tau}_i)e^{j([n\omega_0+p\Omega_{s_i}]t+p\varphi_{s_i})}, \quad (2)$$

where J_p denotes the Bessel function of the first kind.

The Power Spectral Density (PSD) of such a signal, as visible in Fig. 1, consists of a series of so-called synchrotron lines, symmetrically located around each harmonic of the revolution frequency ω_0. The distance between consecutive satellites is equal to the particle's synchrotron frequency.

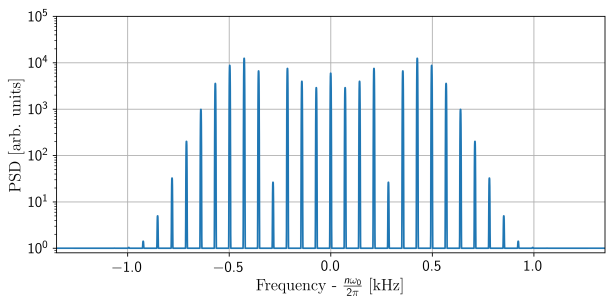

Figure 1: Simulated single particle longitudinal LHC Schottky spectrum.

The intensity signal of the whole bunch will preserve a similar structure but with a few significant differences.

ISBN: 978-3-95450-253-0 ISSN: 2673-5571 doi:10.18429/JACoW-HB2023-THC2C1

SHOWER SIMULATIONS FOR THE CERN PROTON SYNCHROTRON INTERNAL DUMP AND COMPARISON WITH BEAM LOSS MONITOR DATA

S. Niang*,[1], D. Domange[2], L. S. Esposito[1], M. Giovannozzi[1], C. Hernalsteens[1], A. Huschauer[1], T. Pugnat[1]
[1]CERN, Geneva, Switzerland
[2]Université libre de Bruxelles, Brussels, Belgium

Abstract

During the Long Shutdown 2 (LS2), two new internal dumps (TDIs) were installed and successfully put into operation in the CERN Proton Synchrotron (PS) to withstand the intense and bright beams produced for the High Luminosity LHC. TDIs serve as safety devices designed to rapidly enter the beam trajectory and stop the beam over multiple turns. Due to their design, the TDI only absorbs a fraction of the secondary particle shower produced by beam particles that impinge on it. Starting from impacts computed by multi-turn beam dynamics simulations, detailed shower simulations were performed with FLUKA to assess the radiation field's impact on the downstream equipment, with a particular emphasis on the dose measured by Beam Loss Monitors. The numerical data obtained from the simulations are compared with the experimental data collected during PS operation.

INTRODUCTION

The internal dumps of the PS ring, located in straight sections (SS) 47 and 48 of the accelerator, underwent a complete redesign to be installed during LS2 from 2019 to 2021. This was to make the internal dumps compatible with the increase in beam brightness as a result of the implementation of the LHC Injector Upgrade (LIU) project [1, 2]. Extensive studies were carried out to validate the thermomechanical limits of the new dump design [3, 4] and its efficiency in stopping the beams produced in PS after LS2 [5]. In the study [6], a standalone dump simulation was implemented in FLUKA [7, 8], along with a 5-dimensional matrix to transport beam particles throughout the rest of the accelerator. This matrix described the multi-passage of the beam particles by the dump location. Additionally, the movement of the dump was included during the revolution time.

In this study, our primary objective is to identify any energy deposition hot spots when utilising the dumps, and, if necessary, enhancing the shielding in these locations will be considered.

NUMERICAL SIMULATIONS

A significant difference from previous studies is the implementation in FLUKA of an extended and detailed model of the PS ring over the sections where the particle showers are absorbed. This required the input of the distribution of primary particles at the dump location obtained from a beam dynamic code, SixTrack [9, 10], in our case, coupled with FLUKA to describe in detail the mechanical aperture along the PS ring, while accurately accounting for the beam-matter interactions occurring in the moving internal dump [11] and the beam dynamics in the rest of the ring. The results of these simulations provide the position, direction, and energy of primary protons when they impact the dump at each turn. This distribution is loaded as source term into the FLUKA simulation, taking into account the dump's position at each turn. The tracking of the shower particles starts from SS47 and ends at SS69. Figure 1 shows a 3D visualisation of the geometry model. It should be noted that due to the dump speed of approximately 0.8 m s^{-1}, the beam is fully stopped after about a thousand turns, which corresponds to about a few ms in duration[1].

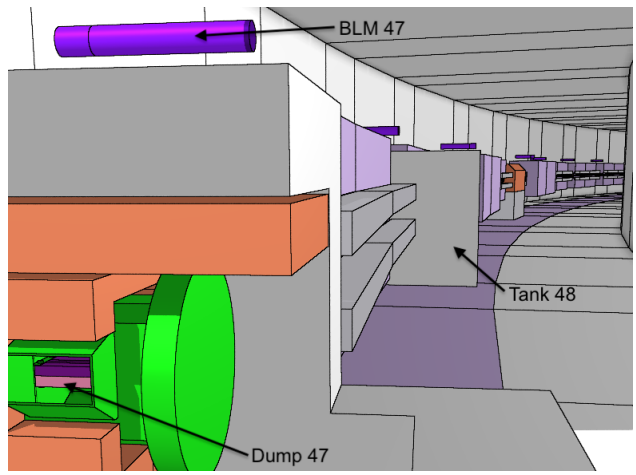

Figure 1: 3D visualisation of the PS ring FLUKA model using FLAIR [12].

We have considered three different operational scenarios:

- Activation of TDI.47 with the LHC beam at flat top, with a momentum of $p = 26.4\,\mathrm{GeV}/c$.
- Activation of TDI.48 with the same LHC beam.
- Activation of TDI.47 with the beam for the fixed-target programme at CERN's Super Proton Synchrotron (SPS) ring (SFTPRO), with a momentum of $p = 14.0\,\mathrm{GeV}/c$.

* samuel.niang@cern.ch

[1] Note that the revolution time is approximately 2.1 µs.

ISBN: 978-3-95450-253-0 ISSN: 2673-5571 doi:10.18429/JACoW-HB2023-THAFP01

PROBING TRANSVERSE IMPEDANCES IN THE HIGH FREQUENCY RANGE AT THE CERN-SPS

E. de la Fuente*,1, I. Mases†,2, H. Bartosik, G, Rumolo, C. Zannini
CERN, Geneva, Switzerland
[1]also at Polytechnic University of Madrid, Madrid, Spain
[2]also at Goethe University of Frankfurt, Frankfurt am Main, Germany

Abstract

The SPS transverse impedance model, which includes the major impedance contributions in the machine, can be benchmarked through measurements of the Head-Tail mode zero instability. Since the SPS works above transition energy, the Head-Tail mode zero is unstable for negative values of chromaticity. The measured instability growth rate is proportional to the real part of the transverse impedance. Studies performed after the LHC Injectors Upgrade (LIU) showed a relevant impedance around 2 GHz with high-gamma transition optics (Q26). This paper presents a comprehensive follow-up to probe the behavior of this beam coupling impedance contribution. Our studies include measurements of instability growth rates in both vertical and horizontal planes, spanning a broad spectrum of negative chromaticity values. To address the uncertainties in the high chromatic frequency range, the SPS Head-Tail monitor data is used to calculate the intrabunch chromatic content through a bi-dimensional frequency domain analysis.

INTRODUCTION

In accelerators operating above transition energy, the presence of negative chromaticity Q' leads to the occurrence of Head-Tail instability [1]. This instability is primarily driven by the non-zero machine impedance inherent to the accelerator system and is further magnified by the longitudinal oscillations performed by individual particles within the bunch [2]. The short-range wakefield produced by the leading part of a bunch (head) excites an oscillation of the trailing part (tail) of the same bunch, causing, after several turns, the characteristic exponential growth of the bunch's transverse centroid position [3].

The instability mode zero growth rate τ^{-1} is proportional to the real part of the effective driving impedance $Z^{\text{eff}}_{\perp,\text{dip}}$ as a function of relative chromaticity $\xi = Q'/Q$ [4]:

$$\tau^{-1}(\xi) = \pi^{-\frac{3}{2}} \frac{Re\left[Z^{\text{eff}}_{\perp,\text{dip}}(\xi)\right] N r_0 c^2}{8\pi^2 \gamma Q \sigma_z}, \qquad (1)$$

where N is the number of protons per bunch, r_0 is the electron radius, c is the speed of light, γ is the relativistic factor, Q is the betatron tune and σ_z is the RMS bunch length.

Chromaticity can be expressed in terms of chromatic frequency $f_\xi = \xi Q f_{\text{rev}}/\eta$. Therefore, studying the instability growth rate for a wide range of negative chromaticities provides information on the frequency dependence of the SPS transverse impedance. The smaller slip factor $\eta = 1/\gamma_t^2 - 1/\gamma^2$ of the high-gamma transition Q26 optics allows us to explore a wider spectrum of chromatic frequencies.

Pre-LS2 measurements of Head-Tail mode zero growth rates are reported in Ref. [5]. In the framework of the LHC Injectors Upgrade (LIU), a further benchmark of the present impedance model is required. Post-LS2 measurements reported in Ref. [6] showed a relevant impedance around 2 GHz. The trustworthiness of this impedance contribution was hampered by scarce data and the absence of consistent chromaticity measurements at highly negative values. In these studies, the measurements were replicated in the vertical plane and extended to the horizontal plane with a finer negative chromaticity scan. Finally, SPS Head-Tail monitor data is used to estimate the negative chromaticity values, in order to mitigate the uncertainty in the high-frequency regime.

GROWTH RATE MEASUREMENTS

The measurements were performed with a single-bunch beam with low intensity $2.8 \cdot 10^{10}$ p/b. Prior to performing the chromaticity scans, the tunes were set to the nominal operation values, measured, and adjusted with the SPS Laslett correction tool [7], the octupole strengths (LOF and LOD) were set to zero, and the transverse feedback was disabled. Chromaticity measurements were performed with the MultiQ procedure [8] to find the small offset between the set value Q'_{knob} and the real machine chromaticity, finding $\Delta Q'_V = 0.07$ and $\Delta Q'_H = 0.14$. The chromaticity function is defined following the methodology established in Ref. [6], applying a delay of 1000 ms to avoid sextupole current hysteresis and injection oscillations.

Figure 1 shows the main beam properties observed during the measurements. When a negative chromaticity value is applied at 1000 ms, the beam becomes unstable, showing sharp intensity losses (Fig. 1, upper-left). If the scan of negative chromaticity is performed in the vertical plane, the bunch vertical centroid position exhibits the expected exponential growth (upper-right). However, if coupling is present between transverse planes, some exponential growth can be observed also in the horizontal plane. To obtain the growth rate from the centroid turn-by-turn positions, the Moving Window Fourier Transform (MWFT) was used, as described in Refs. [1] and [6]. The final value of the growth rate τ^{-1}

* elena.de.la.fuente.garcia@cern.ch
† ingrid.mases.sole@cern.ch

ISBN: 978-3-95450-253-0 ISSN: 2673-5571 doi:10.18429/JACoW-HB2023-THAFP02

RESONANCE EXTRACTION RESEARCH BASED ON CHINA SPALLATION NEUTRON SOURCE

Yuwen An *[1], Liangsheng Huang[1], Shouyan Xu[1],Zhiping Li[1], Yaoshuo Yuan[1], Sheng Wang[1]
Institute of High Energy Physics, Chinese Academy of Sciences (CAS), Beijing, China
[1]also at Spallation Neutron Source Science Center, Dongguan, China

Abstract

Resonance extraction from the RCS ring is a crucial element in beam applications. This article presents a novel design for resonance extraction in the CSNS-RCS ring. Through parameter adjustments, including the skew sextupole magnet, beam working point, RF-Kicker, and more, simulation results highlight the capability to efficiently extract a significant number of protons within a few revolutions. This innovative design offers new insights and approaches towards achieving high-performance proton beam extraction.

INTRODUCTION

The CSNS accelerator is made up of a linear accelerator (LINAC) and a rapid cycling synchrotron (RCS) [1, 2]. In 2020, it achieved stable operation at a power level of 100 kW. CSNSII is a significant upgrade to the accelerator, incorporating a superconducting radiofrequency system to increase the energy of the LINAC to 300 MeV. Additionally, the number of injected particles will be multiplied by five, allowing the accelerator to reach a target power of 500 kW. Table 1 shows the upgrades schemes of the CSNS.

Table 1: Upgrades Schemes of the CSNS

	CSNS I	CSNS II
Beam power	100	500
Repetition Rate [Hz]	25	25
Inj. Energy [MeV]	80	300
Ext. Energy [GeV]	1.6	1.6
Beam Intensity [$*10^{13}$]	1.56	7.8
Harmonic number	2	4

The increase in power of the neutron scattering source opens up more possibilities for its widespread applications. Proton radiography is one potential application of the neutron scattering source, which requires the extraction of beam bunches with strict specifications. For example, the time interval between adjacent beam bunches should be 410 ns, and each beam bunch should contain a high number of particles, such as exceeding 1E11 particles. In the case of CSNSII, the total number of particles in the extracted beam bunches is 7.8E13. If these particles can be extracted through resonant extraction, the requirements can be met.

The article is structured as follows: the second section discusses the design of the lattice, the third section presents the simulation of resonant extraction, the fourth section discusses the parameters of the skew sextupole, septa and RF Kicker, and the final section provides a summary.

LATTICE DESIGN OF THE CSNSII

The lattice design of the CSNS-RCS is of utmost importance and has specific requirements to meet desired operational characteristics. One crucial requirement is the flexibility to adjust the working point of the optics. This adjustment allows for mitigating beam instability by varying the working point from 4.3/4.3 (horizontal/vertical) to 5.3/5.3 (horizontal/vertical), and it also enables easy adjustment of the working point to the third-order resonance for beam expansion and applications. Additionally, the magnets used in the lattice design should have relatively small apertures to reduce costs and provide longer straight sections. These straight sections are essential for accommodating high-frequency cavities, injection systems, collimators, and extraction devices.

Figure 1 provides a visualization of the twiss parameters for a single super-period in the RCS lattice. The CSNS-RCS lattice is constructed using a triplet cell configuration with a total circumference of 227.92 m. The linear lattice consists of 48 quadrupoles powered by five families of power supplies. Additionally, there are 24 dipoles powered by a single power supply.

Overall, the lattice design of the CSNS-RCS is carefully engineered to ensure flexibility in optics adjustment, cost-effectiveness, and the provision of suitable spaces for essential components and devices.

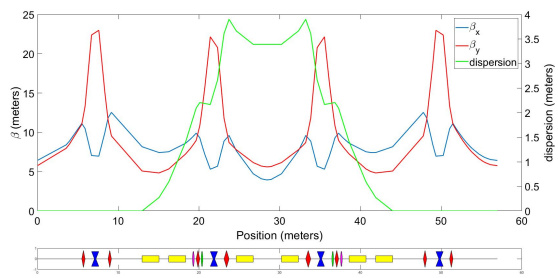

Figure 1: Twiss parameters of the RCS one super-period.

* anyw@ihep.ac.cn

ISBN: 978-3-95450-253-0 ISSN: 2673-5571 doi:10.18429/JACoW-HB2023-THAFP03

MEASUREMENT OF STABILITY DIAGRAM AT IOTA AT FERMILAB*

M.K. Bossard†, Y.-K. Kim, The University of Chicago, Chicago, IL, USA
R. Ainsworth, N. Eddy, O. Mohsen, Fermi National Accelerator Laboratory, Batavia, IL, USA

Abstract

Nonlinear focusing elements can enhance the stability of particle beams in high-energy colliders by means of Landau Damping, through the tune spread which is introduced. We propose an experiment at Fermilab's Integrable Optics Test Accelerator (IOTA) to investigate the influence of nonlinear focusing elements on the transverse stability of the beam. In this experiment, we employ an anti-damper, an active transverse feedback system, as a controlled mechanism to induce coherent beam instability. By utilizing the anti-damper, we can examine the impact of the nonlinear focusing element on the beam's transverse stability. The stability diagram, a tool used to determine the system's stability, will be measured using a recently demonstrated method at the LHC. This measurement is carried out experimentally by selecting specific threshold gains and measuring them for a range of phases. The experiment at IOTA adds insight towards the stability diagram measurement method by supplying a reduced machine impedance, to investigate the impedance's effect on the stability diagram, as well as a larger range of phase measurements.

MOTIVATION

Landau damping (LD) is the damping of the collective oscillation modes. In particle accelerators, Landau damping occurs due to the inherent variation in the betatron and synchrotron frequencies within the beam. Without Landau damping, intense particle beams would become unstable due to various collective unstable modes. These modes would negatively impact the quality of the beam in both its transverse and longitudinal directions. Therefore, understanding the magnitude of Landau Damping is crucial for predicting the stability of high-energy colliders.

Landau damping studies are commonly approached via stability diagram theory. Given the collective motion frequency $\Delta\omega$, the frequency in the presence of LD Ω is given by the following relation [1]:

$$\Delta\omega = -1 / \int \frac{J_x \partial F / \partial J_x}{\Omega + \delta\omega(J_x + J_y) + io} \, dJ_x dJ_y \,, \qquad (1)$$

where $F(J_x, J_y)$ is the beam's unperturbed distribution function, $\delta\omega$ is the action-dependent frequency shift, and io is a negligible imaginary number. To find Ω, one would need to solve Eq. (1) for all $\Delta\omega$. From this, a stability contour would be produced in the $\Delta\omega$ space when $\mathrm{Im}\Omega = 0$. Often to find the stability diagram, one would use beam transfer function (BTF) measurements through the frequency dependence of the response to forced beam oscillations.

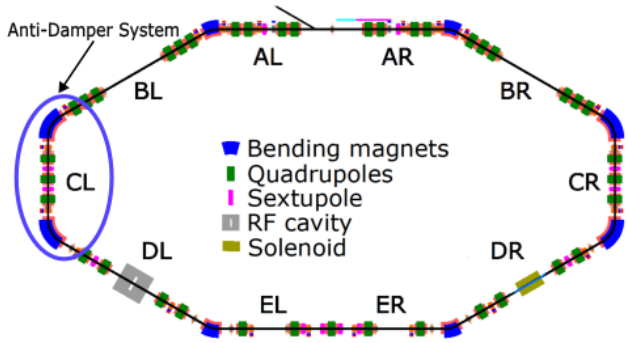

Figure 1: Schematic of the Integrable Optics Test Accelerator (IOTA). The anti-damper system elements are located in section CL, as circled in the figure.

There are limitations to the BTF method for obtaining stability diagrams, including that the measurement does not probe the actual strength of Landau damping but rather the BTF, and therefore relies on assumptions in Eq. (1). These assumptions include that the spread of synchtrotron frequency is negligible, the beam response to external excitations is linear, that the betatron frequency spread is sufficiently small, and that the coherent modes are uncoupled [1]. As there are multiple sources for error in the BTF method to obtain stability diagrams, an alternative method has been proposed by Alexey Burov. As proof-of-principle it has been initially studied at the LHC [1] using an anti-damper, and is now further being studied and quantified at the Integrable Optics Test Accelerator (IOTA) at Fermilab.

IOTA, shown in Fig. 1, is a 40 m re-configurable ring dedicated towards research of accelerator physics and beam dynamics. IOTA can circulate both electrons and protons, where this experiment is for when electrons are circulating. This experiment aims to measure the stability diagram using an anti-damper, where an anti-damper is an active feedback system, used as a controllable source of beam impedance.

METHODS

The IOTA transverse feedback system consists of a digital controller, a stripline kicker, two stripline BPMs, and a BPM analog nodule. A schematic of the experimental setup can be seen in Fig. 2.

The digital controller allows one to vary both the gain and the phase of the system. This provides the means to measure the full stability diagram. The beam first gets kicked by the kicker, where the total phase from the two BPMs is adjusted to supply the correct phase change as a virtual pickup. Once these elements are adjusted to produce the correct impedance, the stripline BPMs measure the beam

* Work supported by The University of Chicago and Fermi National Accelerator Laboratory
† mbossard@uchicago.edu

ISBN: 978-3-95450-253-0 ISSN: 2673-5571 doi:10.18429/JACoW-HB2023-THAFP04

INVESTIGATION OF TAIL-DOMINATED INSTABILITY IN THE FERMILAB RECYCLER RING

O. Mohsen*, A. Burov, R. Ainsworth
Fermi National Accelerator Laboratory, Batavia, IL, USA

Abstract

In the latest operational run at the Fermilab accelerator complex (22-23), a single bunch, tail-dominated instability was observed in the Recycler Ring (RR). This instability exclusively occurs in the vertical plane when the chromaticity is close to zero. In this work, we conduct a detailed analysis of this instability under different operational parameters. We investigate the impact of space-charge on the head-tail motion and propose potential interpretations of the underlying mechanism of the instability. Moreover, we explore methods to mitigate this instability in the future.

INTRODUCTION

Accelerators are vital instruments in the realm of particle physics, playing an indispensable role in our quest to unravel the fundamental constituents of matter and their interactions. As the need to increase beam power and intensity becomes more pressing, accelerators are often faced with operational challenges, most importantly beam instabilities, which often stand as a limitation to increasing beam intensity. These instabilities manifest as deviations from the desired beam trajectories in planes of motion, leading to beam loss, diminished beam quality, and increased beam emittance [1, 2].

The Transverse Mode Coupling Instability (TMCI) poses a significant obstacle to both current and future accelerator designs due to its stringent intensity threshold. Consequently, surmounting this instability is essential in attaining the desired energies and intensities required for future physics experiments. The effect of space-charge on TMCI threshold has been explored before [3–5]. It is shown that space-charge increases the TMCI threshold. However, recent theoretical and analytical frameworks suggest a different type of instabilities that take over at higher space-charge tune shifts, namely convective instabilities [6]. Such instabilities can occur at high space-charge tune shifts in the presence of a strong wake and differ from TMCI by having an asymmetrical transverse motion with a large head-to-tail amplification.

In this work, we describe our recent observation of transverse instabilities in the vertical plane that was recently found in the Fermilab Recycler Ring (RR). During our observation, we gathered evidence that this instability is not TMCI but rather convective. Nevertheless, the instability shows a tune dependence that is not yet well understood.

* omohsen@fnal.gov

INSTABILITIES STUDY

In the RR, we can study beam instabilities under several operational conditions. For this work, we use a single bunch for our studies with different beam intensities (N) at energy $E = 8$ GeV. Typically, we use a dedicated event that can be placed within our supercycle parasitically. This allows us to perform studies while having normal beam operation. Some of the RR parameters used in our studies are summarized in Table 1.

Table 1: Typical RR Parameters Used for the Instability Studies

Parameter	Symbol	Value
Energy	E	8 GeV
Radius	R	528 m
Betatrone tune	ν_x, ν_y	25.40, 20.44
Synchrotron tune	ν_s	0.0005
Chromaticity	ξ_x, ξ_y	−0.75, −0.16
Emittance	$\varepsilon_{N,\mathrm{rms}}$	2.5 π mm mrad

Our typical study event lasts for 2 seconds. During the event and following the injection of the beam from the upstream machine, we employ the RR gap-clearing kickers to partially batch the beam thus aborting 70-72 of the 84 bunches. Subsequently, a rebunching process is utilized to reconfigure the remaining 12-14 bunches from 53 MHz into a single 2.5 MHz bunch while allowing sufficient time for the beam to undergo this process adiabatically. Afterwards, we turn off the bunch-by-bunch dampers and tune the chromaticity to values close to zero; see Fig. 1. Following these processes, we initiate instabilities using a diverse range of techniques. To facilitate diagnostics, we employ Ion Profile Monitors (IPMs) and a wall current monitor to gauge transverse and longitudinal beam sizes, respectively. For the IPMs, we avoid changing the Micro Channel Plate (MCP) to avoid any uncertainties caused by the IPMs. Subsequently, our diagnostic includes a stripline Beam Position Monitor (BPM) to capture intra-bunch motion. The signal from the stripline BPM plates (A, B) is passed through a hybrid filter where the sum ($A + B$) and the difference ($A - B$) are outputted. The signal from the hybrid filter is then processed via an oscilloscope. The resulting signal must be integrated since the bunch length is much longer than the stripline. The processed $A + B$ signal is then related to the beam intensity $I(\zeta)$ along the bunch, where ζ is particle coordinates inside the bunch. Subsequently, the signal from $A - B$ is related to the dipole moment of the beam $I(\zeta) \times y(\zeta)$, where $y(\zeta)$ is the vertical displacement of particles along the bunch. The

ISBN: 978-3-95450-253-0 ISSN: 2673-5571 doi:10.18429/JACoW-HB2023-THAFP05

A WIRELESS METHOD FOR BEAM COUPLING IMPEDANCE MEASUREMENTS OF THE LHC GONIOMETER

C. Antuono*,[1], C. Zannini, CERN, Geneva, Switzerland
M. Migliorati, A. Mostacci, University of Rome "La Sapienza" and INFN, Rome, Italy
[1] also at University of Rome "La Sapienza", Rome, Italy

Abstract

The beam coupling impedance (BCI) of an accelerator component should be ideally evaluated exciting the device with the beam itself. However, this scenario is not always attainable and alternative methods must be exploited, such as the bench measurements techniques. The stretched Wire Method (WM) is a well established technique for BCI evaluations, although nowadays its limitations are well known. In particular, the stretched wire perturbs the electromagnetic boundary conditions. Therefore, the results obtained could be inaccurate, especially below the cut-off frequency of the beam pipe in the case of cavity-like structures. To overcome these limitations, efforts are being made to investigate alternative bench measurement techniques that will not require the modification of the device under test (DUT). In this framework, a wireless method has been identified and tested for a pillbox cavity. Its potential for more complex structures, such as the LHC crystal goniometer, is explored.

INTRODUCTION

The beam coupling impedance represents the electromagnetic interaction between a particle beam and the accelerating structure. As a driving term for collective effects, its vital function in the context of beam stability and quality is well-known and it is therefore crucial to be able to estimate it, either in simulations or measurements. Ideally, one should assess the beam impedance by directly stimulating the device with the beam. Nonetheless, in many instances, this approach proves unfeasible, requiring the use of alternative methods to account for the effect of the beam. Nowadays, various bench methods are employed, but their limitations are also known and documented, as in the case of the Wire method [1, 2]. Consequently, new techniques should be developed to overcome these limitations.

A possible solution, which will not require the modification of the Device Under Test (DUT), named Wireless method, is proposed in Refs. [3, 4]. An exact formula to obtain the longitudinal beam coupling impedance of the accelerator beam chambers is presented and validated. Its feasibility and possible extension to resonant structures is presented in this paper supported by simulations studies, with a possible application to a more complex device, the LHC crystal goniometer.

* chiara.antuono@cern.ch

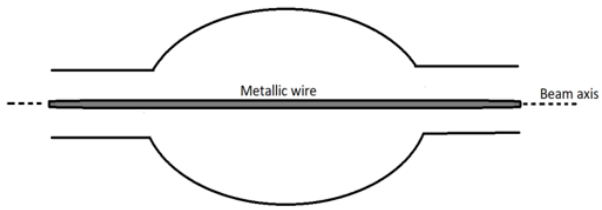

Figure 1: Wire method setup.

BEAM IMPEDANCE MEASUREMENTS: METHODS AND THEIR LIMITATIONS

The measurement of the longitudinal beam coupling impedance is usually performed using a standard technique: the stretched Wire Method (WM) [1], which implies the insertion of a metallic wire along the beam axis of the DUT as shown in Fig. 1.

In fact, the excitation produced by the relativistic beam, in particular its current pulse, can be approximated with a current pulse having the same temporal behavior but flowing through a wire stretched along the beam axis. However, one should note that the introduction of the stretched wire, and therefore of a metallic conductor along the device, modifies the Electro-Magnetic (EM) boundary conditions of the initial DUT. In such a structure, the propagation of Transverse Electro-Magnetic (TEM) modes with zero cut-off frequency is allowed, with the undesired consequence of depleting the resonant frequencies of the structure and introducing additional losses. This behavior occurs specifically below the cut-off frequency of the beam pipe of the device, as already demonstrated in Ref. [2]. As a result, the method gives inaccurate results for resonant structures in the aforementioned range. On the other hand, for resonant structures, a possible alternative technique is the bead-pull method, as described in Refs. [5–7]. It relies on a perturbation introduced by a small object that samples the field in the cavity and it can be related with the change in resonant frequency. Furthermore, the latter can be related to the shunt impedance of the cavity. Nonetheless, this approach requires the use of a pulling system, which may not be particularly convenient or straightforward to implement, especially when considering a portable general-purpose setup. To overcome those limitations and to avoid introducing undesired perturbations (e.g. a change in boundary conditions), the attention has been focused on the development of a Wireless method.

ISBN: 978-3-95450-253-0 ISSN: 2673-5571 doi:10.18429/JACoW-HB2023-THAFP06

BEAM DYNAMICS STUDY OF A 400 kW D^+ LINEAR ACCELERATOR TO GENERATE FUSION-LIKE NEUTRONS FOR BREEDING BLANKET TESTS IN KOREA

Y-L. Cheon, H. W. Kim, M. Y. Ahn, S. Y. Cho
Korea Institute of Fusion Energy, Daejeon, Republic of Korea
E. Cosgun, S-H. Moon, D. Kwak, M. Chung*
Dept. of Physics, Ulsan National Institute of Science and Technology, Ulsan, Republic of Korea

Abstract

Recently, a pre-conceptual design study was conducted in Korea for developing a dedicated linear accelerator (linac) for 400 kW (40 MeV, maximum 10 mA CW) deuteron (D+) beams to generate fusion-like neutrons. The accelerated beam hits a solid Beryllium target to produce fusion-like neutrons, which will be utilized for technical feasibility tests of the breeding blanket including tritium production and recovery. In this work, we present a detailed start-to-end simulation and machine imperfection studies with proper beam tuning, to access the target beam availability and validate the machine specifications. We have designed a 2.45 GHz ECR ion source and a 4-vane type 176 MHz RFQ by using IBSimu, Parmteq, and Toutatis simulation codes. We propose a super-conducting linac with HWR cavities and solenoid focusing magnets to accelerate the beam up to 40 MeV. In the HEBT line, we adopt two octupole magnets and subsequent quadrupoles to make a rectangular-shaped and uniform density beam with 20 cm × 20 cm footprint at the target. Extensive beam dynamics studies along the linac have been performed using the Tracewin simulation code.

FINAL LAYOUT

The Korea Institute of Fusion Energy (KFE) conducted a pre-conceptual design study for the Integrated Breeding Test Facility (IBTF), which serves as the central component of the Korea Fusion Engineering Advanced Test Complex (KFEAT) [1]. The primary objective of this facility is to assess the technical feasibility of a Breeding Blanket (BB), including tritium production and recovery. In order to generate neutrons suitable for these tests, we also performed a pre-conceptual design study of a linear accelerator (linac) aimed at delivering a 40 MeV deuteron beam (D^+) with a maximum average current of 10 mA [2].

The final layout of the pre-conceptual design of the 40 MeV D^+ linear accelerator in Korea is summarized in Fig. 1. In this study, we have mainly benchmarked the SARAF-PHASE2 facility [3] for the Superconducting RF (SRF) linac section to accelerate the beam up to 40 MeV. Additionally, we have optimized the High Energy Beam Transport (HEBT) line based on the IFMIF/IFMIF-DONES facility [4] to create a rectangular-shaped and uniform density beam cross-section in the transverse space at the target. The 40 MeV deuteron beam will impact a solid Beryllium (Be) target of 22 cm × 22 cm spot size under the continuous wave (CW) mode to produce fusion-like neutrons (14.1 MeV), which have similar characteristics to those generated by the D-T fusion reaction.

The detailed design structures of the Electron Cyclotron Resonance Ion Source (ECR IS), Low Energy Beam Transport (LEBT) line, and Radio Frequency Quadrupole (RFQ) are depicted in Fig. 2. A 2.45 GHz ECR IS generates over 12 mA of D^+ beam at a total output energy of 40 keV, for which the extraction has been simulated with IBSimu. For low-energy beam bunching and acceleration, we have designed the 4-vane type 176 MHz RFQ using Parmteq and Toutatis simulation codes, which accelerates the beam from 40 keV to 3 MeV.

BEAM DYNAMICS STUDY

The start-to-end simulation result along the Medium Energy Beam Transport (MEBT) line, SRF linac and HEBT line is shown in Fig. 3. It has been carried out by using TraceWin simulation code [5]. In the MEBT, the beam from the RFQ is matched to the SRF linac section by using two rebunchers (3-gap structure with an effective length of 280 mm and an aperture of 40 mm) and 7 quadrupoles, which focus the beam in the longitudinal and transverse directions, respectively. The effective voltages of the two rebunchers are 69 kV and 87 kV, respectively.

To achieve a beam power of 400 kW in CW mode, with the capability for long-term operation, we have adopted the SRF linac structure with Half-Wave Resonator (HWR) cavities and solenoid focusing magnets. This choice is motivated by the SARAF-PHASE2 design. The SRF linac is composed of 4 cryomodules; the first two are for low-beta (0.091) cavities (effective length: 0.155 m, maximum accelerating gradient: 6.1 MV/m) and the last two are for high-beta (0.181) cavities (effective length: 0.308 m, maximum accelerating gradient: 7.2 MV/m). The maximum solenoid magnetic field strength is 6.6 T. In this work, a design study of RF cavities in the MEBT and Superconducting linac has been conducted using the CST simulation code. The goal is to optimize machine specifications such as effective length and maximum electromagnetic field strength to meet the design requirements. We integrated the 3-dimensional field-map structures of the designed rebunchers and HWR cavities into the TraceWin simulation code to analyze beam dynamics and verify the target beam availability.

* mchung@unist.ac.kr

ISBN: 978-3-95450-253-0 ISSN: 2673-5571 doi:10.18429/JACoW-HB2023-THAFP07

PRELIMINARY RESULTS ON TRANSVERSE PHASE SPACE TOMOGRAPHY AT KOMAC

S. Lee*, H.-S. Kim, D.-H. Kim, S.-P. Yoon, H.-J. Kwon, Korea Multipurpose Accelerator Complex, Korea Atomic Energy Research Institute, Gyeongju, Korea
J.-J. Dang, Korea Institute of Energy Technology, Naju, Korea

Abstract

Beam loss is a critical issue to be avoid in the high power proton accelerators due to machine protection from radiation. Nonlinear processes add higher order moments and cause halo and tail structures to the beam. It eventually causes beam losses. Hence it becomes more important to characterize beams for the high power accelerators. Conventional beam diagnostic methods can measure only approximate elliptical features of the beam and are not suitable for high power beams. Tomography method reconstructs a multi-dimensional phase space distribution from its lower-dimensional projections. At the Korea Multipurpose Accelerator Complex (KOMAC), we used this method to tomographically reconstruct the transverse (x-x′) and (y-y′) phase space distributions of the beam from the 100 MeV proton linac by utilizing a wire scanner for x and y beam profiles. In this paper, we describe the tomography measurement system and present the preliminary results of phase space reconstruction obtained from the 100 MeV proton linac.

INTRODUCTION

Beam diagnostics research for measuring high power beam distribution becomes more important and is studied in several laboratories [1–4]. Tomographic techniques has been considered to be a useful technique for measuring high power beam distribution. We have a 100 MeV proton linac which is planned to be upgraded for higher energy. For the stable operation and machine protection from radiation in the high power proton linac, we developed Computational Tomography (CT) method to characterize beams. A set of one-dimensional beam profile data (x or y) obtained under various strengths of a quadrupole magnet placed in front of the wire-scanner are converted to two-dimensional phase space distribution (x-x′ or y-y′) using the CT method. In this paper, we describe the experimental setup, CT method and the tomography measurement system developed at KOMAC, and present the preliminary results of phase space reconstruction obtained from the dump beamline in the 100 MeV proton linac.

EXPERIMENTAL SETUP

Current 100 MeV proton linac operating at 350 MHz consists of a microwave ion source (IS) for 20 mA beam current, a low energy beam transport (LEBT), a radiofrequency quadrupole (RFQ), a 20 MeV drift tube linac (DTL I), a medium beam transport (MEBT) and a 100 MeV drift tube linac (DTL II). The described schematics is shown in Fig. 1. After the DTL II, we have a straight beamline to a dump, called dump beamline. Dump beamline is used for the reconstruction of the beam phase space distribution using the CT method. We used first four quadrupole magnet (QM1-QM4) and a wire scanner (WS-1) in the beamline for the experiment shown in Fig. 1. The QM1, QM2, QM3 and QM4 are operated at the current of 60 A, 50 A, -110 A-110 A, and 0 A - 80 A respectively to change the phase advance angle of the beam. The wire scanner (WS-1) measures the beam profile in x and y for every setting of QM1-QM4 during the measurement.

COMPUTATIONAL TOMOGRAPHY METHOD FOR BEAM PHASE SPACE RECONSTRUCTION

The beam distributions in x-x′ (i.e. horizontal direction) and y-y′ (i.e. vertical direction) phase spaces were reconstructed in this study [5, 6]. Beam profiles in x and y are obtained for all the QM1-QM4 settings and are used for the reconstruction of the transverse beam distribution. In CT method, a filtered back projection algorithm is introduced to reconstruct the beam distribution in the phase space. This algorithm is widely used in medical imaging technique. In the CT imaging system, a detector rotates around the object of interest. However, in this study, the object, i.e. a beam rotates by some beam optics such as QM1-QM4 and a detector, i.e. WS-1, keeps its position. The beam right before the QM1 has a beam distribution at z_0 in Fig 1 is assumed as an ellipse. Then, the beam ellipse at z_1 is determined by the beam matrix at z_0 and a transfer matrix from QM1 to WS-1. Two points, $(x_{p0}, 0)$ and $(0, x'_{q0})$, at z_0 rotates to (x_{p1}, x'_{p1}) and (x_{q1}, x'_{q1}) at z_1 through the transfer matrix, M shown in Fig 2 and expressed in Eq. (1).

The relation between the points defined on different planes is mathematically expressed as follows;

$$\begin{pmatrix} x_{p1} & x_{q1} \\ x'_{p1} & x'_{q1} \end{pmatrix} = \boldsymbol{M} \begin{pmatrix} x_{p0} & 0 \\ 0 & x'_{q0} \end{pmatrix} = \begin{pmatrix} M_{11} & M_{12} \\ M_{21} & M_{22} \end{pmatrix} \begin{pmatrix} x_{p0} & 0 \\ 0 & x'_{q0} \end{pmatrix} = \begin{pmatrix} M_{11}x_{p0} & M_{12}x'_{q0} \\ M_{21}x_{p0} & M_{22}x'_{q0} \end{pmatrix} \quad (1)$$

$$\tan\theta = \frac{x_{p0}}{x'_{q0}} = \frac{M_{12}}{M_{11}} \quad (2)$$

$$a = \frac{x_{p1}}{s} = \frac{M_{11}x_{p0}}{s} = \frac{M_{11}}{\cos\theta} \quad (3)$$

* shl@kaeri.re.kr

ISBN: 978-3-95450-253-0 ISSN: 2673-5571 doi:10.18429/JACoW-HB2023-THAFP08

PERFORMANCE OF THE ION CHAIN AT THE CERN INJECTOR COMPLEX AND TRANSMISSION STUDIES DURING THE 2023 SLIP STACKING COMMISSIONING

M. Slupecki*, R. Alemany-Fernandez, S. Albright, M. Angoletta, T. Argyropoulos, H. Bartosik, P. Baudrenghien, G. Bellodi, R. Bruce, M. Bozzolan, C. Carli, J. Cenede, H. Damerau, A. Frassier, D. Gamba, G. Hagman, A. Huschauer, V. Kain, G. Khatri, D. Kuchler, A. Lasheen, K. Li, E. Mahner, G. Papotti, G. Piccinini, A. Rey, R. Scrivens, M. Schenk, A. Spierer, G. Tranquille, D. Valuch, F. Velotti, R. Wegner, CERN, Geneva, Switzerland
E. Waagaard, EPFL, Lausanne, Switzerland

Abstract

The 2023 run has been decisive for the Large Hadron Collider (LHC) Ion Injector Complex. It demonstrated the capability of producing full trains of momentum slip stacked lead ions in the Super Proton Synchrotron (SPS). Slip stacking is a technique of interleaving particle trains, reducing the bunch spacing in SPS from 100 ns to 50 ns. This bunch spacing is needed to reach the total ion intensity requested by the High Luminosity LHC (HL-LHC) project, as defined by updated common LHC Injectors Upgrade (LIU/HL-LHC) target beam parameters, and it cannot be provided by the PS (SPS injector). This paper reviews the lead beam characteristics across the Ion Injector Complex, including transmission efficiencies and beam quality up to the SPS extraction. It also documents the difficulties found during the commissioning and the solutions put in place.

INTRODUCTION

The first full-length lead collision production period at the Large Hadron Collider (LHC) in Run 3 is taking place between 26 September and 29 October 2023 at a beam energy of 6.8Z TeV. In 2022, the lead ions collided for two days at the LHC at the same energy, but at low beam intensity and interaction rate [1] as a test of the accelerator and experiments' equipment upgraded during Long Shutdown 2 (LS2). The last full-fledged lead collision period was in 2018 when lead beams collided at 6.5Z TeV. The previous comprehensive transmission and emittance study was done for the p-Pb period in 2016 [2].

This paper summarizes the performance of the ion injector complex at the start of the 2023 LHC ion physics run. It presents the main acceleration schemes and associated ion beam structure. It lists the issues encountered during beam commissioning and the solutions implemented to reach the performance required by the LHC.

ION BEAM PRODUCTION SCHEME

The CERN ion injector complex is shown in Fig. 1. The lead ion beam is produced through evaporation from a solid sample of lead and consequent ionization in the Electron Cyclotron Resonance (ECR) ion source [3, 4]. Only Pb^{29+} is transported through Linac3 where the beam reaches a kinetic energy of 4.2 MeV/nucleon and the ions are stripped to Pb^{54+}. Linac3 produces a 200 µs long pulse every 200 ms. Up to seven of these pulses are injected into the Low Energy Ion Ring (LEIR), which employs several techniques to facilitate charge accumulation, such as multiturn injection and electron cooling [5]. The coasting beam is then bunched into two bunches, accelerated to 72 MeV/nucleon and extracted towards the Proton Synchrotron (PS). Here, each bunch is split in two and their separation is reduced to 100 ns. They are accelerated to 6 GeV/nucleon and longitudinally squeezed using bunch rotation to fit within the radio-frequency (RF) bucket of the Super Proton Synchrotron (SPS). The ions are fully stripped to Pb^{82+} in the TT2 transfer line between PS and SPS (see Fig.1). Up to fourteen injections are accumulated in the SPS at injection energy. Each injection consists of a 4-bunches batch from the PS, with 100 ns bunch spacing, amounting to 56 bunches at maximum. The beam is then accelerated to the slip stacking intermediate energy plateau at 300Z GeVwhere the bunch spacing is reduced to 50 ns, and further accelerated to 450Z GeV or 177 GeV/nucleon. Slip stacking is a technique that permits two particle beams of different momenta (and therefore different RF frequencies) to slip longitudinally relative to each other, in the same beam pipe [6, 7]. When the two beams are in the correct longitudinal position, the full beam is recaptured with a non-adiabatic voltage jump at the average RF frequency. The LHC takes on the order of 40 injections from the SPS, which corresponds to about 1200 bunches in each LHC ring. The bunch scheme evolution is sketched in Fig. 2.

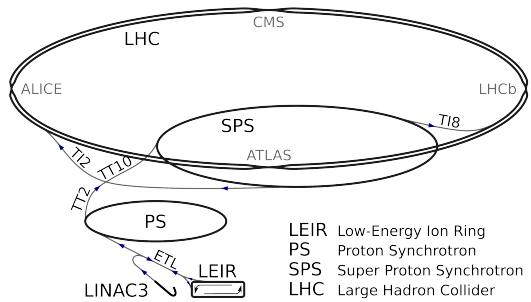

Figure 1: Layout of accelerators and transfer lines used for ion beam production for LHC.

* maciej.slupecki@cern.ch

ISBN: 978-3-95450-253-0 ISSN: 2673-5571 doi:10.18429/JACoW-HB2023-THAFP09

OPTIMIZING BEAM DYNAMICS IN LHC WITH ACTIVE DEEP LEARNING

D. Di Croce[1,*], M. Giovannozzi[2], E. Krymova[3], T. Pieloni[1], M. Seidel[1,4], F. F. Van der Veken[2]
[1]École Polytechnique Fédérale de Lausanne, Lausanne, Switzerland
[2]CERN, Geneva, Switzerland
[3]The Swiss Data Science Center, Zurich, Switzerland
[4]Paul Scherrer Institut, 5232 Villigen PSI, Switzerland

Abstract

The Dynamic Aperture (DA) is an important concept for the study of non-linear beam dynamics in a circular accelerator. It refers to the region in phase space where a particle's motion remains bounded over a given number of turns. Understanding the features of DA is crucial for operating circular accelerators, like the CERN Large Hadron Collider, as it provides insights on non-linear beam dynamics and the phenomena affecting beam lifetime. The standard approach to calculate the DA requires accurate numerical simulations to perform tracking of initial conditions distributed in phase space over a sufficient number of turns in a circular machine to understand the beam dynamics. This process is very computationally intensive. In our study, we aim at determining the evolution of beam stability for a set of machine parameters, like betatron tune, chromaticity, and Landau octupole strengths, i.e., the values that maximise the DA, using a Deep Neural Network (DNN) model. To enhance its performance, we integrated the DNN model into an innovative Active Learning (AL) framework. This framework not only enables the retraining and updating of the DNN model but also facilitates efficient data generation through smart sampling.

INTRODUCTION

The study of dynamic aperture (DA), defined as the extent of the connected phase-space region in which the single-particle dynamic is bounded, offers valuable insight into the non-linear beam dynamics of single particles and the underlying mechanisms contributing to beam losses [1]. The numerical calculation of the DA involves tracking a large number of initial conditions in phase space for many turns. This method is computationally demanding, especially for large accelerators such as the CERN Large Hadron Collider (LHC) [2, 3], and for this reason, analytical scaling laws have been studied for several years [4, 5].

In recent years, we have developed a Machine Learning (ML) model to quickly and accurately predict DA for unknown machine configurations [6]. To achieve this, we trained a Deep Neural Network (DNN) on a substantial dataset of simulated initial conditions, enabling it to capture the intricate relationship between the initial conditions and the resulting DA.

In this study, we integrate machine learning techniques into an Active Learning (AL) framework. Additionally, we introduce an error estimator alongside the DA model to gauge the uncertainty in the predictions. This enables the AL algorithm to perform smart sampling, i.e., it can determine which new machine configuration to simulate first, based on the size of the predicted DA error. This approach aims to facilitate the rapid estimation of DA and its associated error for new machine parameters. At the same time, it aims to expand the initial dataset, eventually improving the performance of the ML model in an efficient manner.

SIMULATED SAMPLES

To train the DNN, we simulated several accelerator configurations using MAD-X [7] and the 2023 LHC lattice at the injection configuration at 450 GeV. We varied six accelerator parameters, namely the betatron tunes Q_x, Q_y, chromaticities Q'_x, Q'_y, strength of the Landau octupoles (using the current, I_{MO}, powering them) and the realisations (also called seeds) of the magnetic field errors assigned to the various magnet families. Furthermore, both Beam 1 and Beam 2 have been considered in these studies. We performed a random uniform grid search of the following parameters: $Q_x \in [62.1, 62.5]$ and $Q_y \in [60.1, 60.5]$ both with steps of size 5×10^{-3}, 15 Q' values in $[0, 30]$, 17 I_{MO} in $[-40, 40]$, and 60 random realisations of the magnetic errors for both Beam 1 and Beam 2. The final dataset is made up of 10459 machine configurations.

The phase space was probed by tracking with XSuite [8, 9] for 10^5 turns. To speed up the tracking, we perform an initial scan of the initial conditions uniformly distributed in 8 polar angles in $[0, \pi/2]$ and 33 radial amplitudes in $[0.0, 20\sigma]$, to identify the value of the last stable amplitude for that angle (limit of the stable zone), as well as the first amplitude where the particle does not survive more than 10^3 turns (limit of the fast-loss zone). Then a finer scan of the initial conditions between the stable zone -2σ and the fast-loss zone $+2\sigma$ was performed, along with 44 polar angles in $[0, \pi/2]$ and 330 radial amplitudes in $[0.0, 20\sigma]$. An example of the results of these computations in the $x - y$ space is shown in Fig. 1 for a specific accelerator configuration.

The target of the ML regressor is the last stable amplitude for every angle (angular DA). To prevent extreme angular DA values from affecting the regressor [10], we cap values above 18 σ, as they are outliers in a distribution ranging from 0 σ to 20 σ. To gain insight into the evolution of beam stability,

* davide.dicroce@epfl.ch

ISBN: 978-3-95450-253-0 ISSN: 2673-5571 doi:10.18429/JACoW-HB2023-THAFP10

STRIPLINE DESIGN OF A FAST FARADAY CUP FOR THE BUNCH LENGTH MEASUREMENT AT ISOLDE-ISRS*

S. Varnasseri†, I. Bustinduy, J.L. Muñoz, P. González, R. Miracoli,
ESS-Bilbao, Zamudio, Spain

Abstract

In order to measure the bunch length of the beam after Multi Harmonic Buncher (MHB) of ISOLDE Superconducting Recoil Separator (ISRS) [1] and characterize the longitudinal structure of bunches of MHB, installation of a Fast Faraday Cup (FFC) is foreseen. Several possible structures of the fast faraday cup are studied and due to timing characteristics of the beam, a microstrip design is selected as the first option. The beam is collected on the biased collector of the microstrip with a matched impedance and transferred to the RF wideband amplification system. The amplified signal then can be analysed on the wideband oscilloscope or acquisition system to extract the bunch length and bunch timing structure with precision. The design of the microstrip FFC and primary RF measurement of the prototype are discussed in this paper.

INTRODUCTION

ESS-Bilbao is designing a Multi Harmonic Buncher (MBH) for the ISOLDE-ISRS [2]. In order to measure the functionality and characteristics of the MBH bunches, some diagnostics have been foreseen. They include ACCT current measurement, energy measurement, and a Fast Faraday Cup (FFC) for bunch length measurement. Prior to delivery of MHB to its final location at ISOLDE-ISRS, it will be tested with ion source beam at ESS-Bilbao with a β equal to 0.00328. The operational RF frequency of MHB is 10.126 MHz and the low velocity bunch length after MHB could converge down-to 1 ns. The maximum proton energy is 50 keV, the beam current could reach up to 40 mA and the maximum pulse width is 3 ms. The beam repetition rate varies from 1 to 30 Hz. It should be mentioned the beam species, energy and current at ISOLDE-ISRS are different than ESS-Bilbao injector.

BUNCH LENGTH MEASUREMENT PRINCIPLES

The measurement of bunch length involves capturing the temporal distribution of charged particles within a bunch. There are methods which rely on the interaction of the bunch with a transverse radiofrequency (RF) field, leading to longitudinal deflection, which is then measured using downstream diagnostics. A commonly used instrument for bunch length measurements is the Feschenko bunch shape monitor (BSM), which relies on the time-to-space conversion of electrons emitted when the beam interacts with a wire [3]. However, there are also methods which can interact directly with the beam and measure the bunch induced signal temporal distribution directly. In the latter case the fast faraday cups (FFC) are developed and inserted in the beam trajectory in order to collect the signal and transmit it via coaxial cable to the broadband amplifiers before acquisition system.

The performance of these fast faraday cups mainly affected by the bandwidth of the overall system, from the FFC signal to amplification and acquisition system. The required bandwidth of FFC usually depends on the bunch longitudinal size and its frequency spectrum.

FAST FARADAY CUP DESIGN

Two types of fast faraday cups are studied namely coaxial type and stripline type. In both cases the bunch incident signal is collected and propagated in the FFC structure, which is matched to the cables and amplification system. However, for the required operational frequency range of the MBH, a coaxial type also can be realized without problems, but foreseeing future projects we decided to design a stripline type with higher frequency bandwidth. The main advantage of the stripline type FFC is the high frequency bandwidth, and its main drawback is the reduced beam thermal capacity.

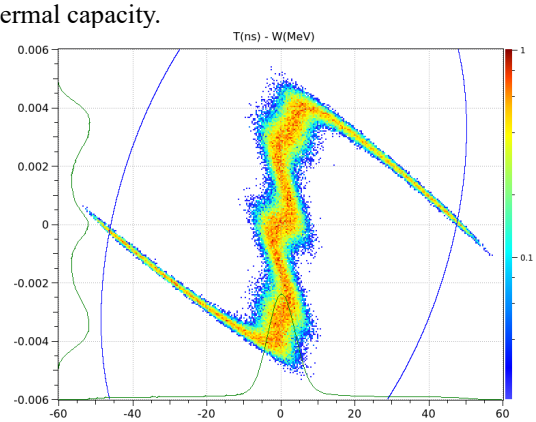

Figure 1: Bunch formation development at a distance of 1m from MHB. Horizontal axis corresponds to time (ns) and vertical axis to energy (MeV).

Figure 1 shows a TRACEWIN simulation of a specimen with β=0.00328 at a distance of 1m after MHB. Figure 2 shows the estimated shortest Gaussian bunch temporal distribution and the frequency spectrum of the bunches after MHB in the location of FFC. The Gaussian bunch has a

*This research is funded by the Next Generation EU–Recovery and Resilience Facility (RRF).
† svarnasseri@essbilbao.org

ISBN: 978-3-95450-253-0 ISSN: 2673-5571 doi:10.18429/JACoW-HB2023-THAFP11

FPGA-BASED DIGITAL IQ DEMODULATOR USED IN THE BEAM POSITION MONITOR FOR HIAF Bring

F. Ni†, Z. Li, Y. Wei, R. Tian, J. Wu#
Institute of Modern Physics, Chinese Academy of Sciences, Lanzhou, China
School of Nuclear Science and Technology, Univ. of Chinese Academy of Sciences, Beijing, China

Abstract

A digital beam position monitor processor has been developed for the High Intensity heavy ion Accelerator Facility (HIAF). The digital IQ demodulator is used in the Beam Position Monitor (BPM) signal processing. All data acquisition and digital signal processing algorithm routines are performed within the FPGA. In the BPM electronics system, a 250 MHz sample rates ADC was used to digitize the pick-up signal. In the FPGA, the digital signal is filtered by ultra-narrow bandpass filters, then the digital IQ demodulator is used to calculate the beam position with a difference-over-sum algorithm. The heavy ion synchrotron CSRm revolution frequency changes from 0.2 MHz to 1.78 MHz when charged particles. In this design, a Direct Digital Synthesizer (DDS) whose output frequency changes over time is applied to generate the in-phase and quadrature components in the digital IQ demodulator. The performance of this designed BPM processor was evaluated with the online HIRFL-CSRm.

INTRODUCTION

Beam Position Monitor (BPM) is a common non-intercepted beam measurement device used to measure the lateral position of beams in vacuum tubes and is widely used in cyclotrons, linear accelerators, and synchrotrons[1–3], especially in the synchrotrons these monitors are distributed around the ring and used to calculate the closed orbit. HIAF is a high-intensity heavy ion accelerator complex designed by the Institute of Modern Physics, CAS, China. It can provide intense primary and radioactive ion beams for studies in nuclear physics, atomic physics, and related research fields[4]. As shown in Figure 1 it mainly consists of a superconducting electron cyclotron resonance ion source (SECR), a superconducting ion Linac accelerator (iLinac), a booster ring (BRing), high-energy fragment separator (HFRS), and a storage ring spectrometer (SRing). BRing is the main part of HIAF, it could accelerate the proton beam from 48 MeV to 9.3 GeV with an intensity of up to 6.0e12 ppp (particles per pulse)[5]. The ramping rate of BRing dipole magnet is up to 12 T/s and the beam particles are accelerated to the top level energy of less than 300 ms, which means that the revolution frequency of BRing would be changed from 0.2 MHz to 1.78 MHz within this short period[5]. In HIAF, about 40 BPM pich-ups would be distributed around the BRing and the resolution of the BPM should be better than 0.1 mm. An independent research and development full digital prototype of the BRing beam position calculation system was designed. Because the HIAF is under construction, the prototype of the BPM algorithm would first tested and estimated on the HIRFL-CSRm (the main cooling storage ring in the Heavy Ion Research Facility in Lanzhou) which has a similar range of revoluation frequency.

* This work was supported by the NSFC No. E911010301, Y913010GJ0
† nifafu@impcas.ac.cn, #wujx@impcas.ac.cn

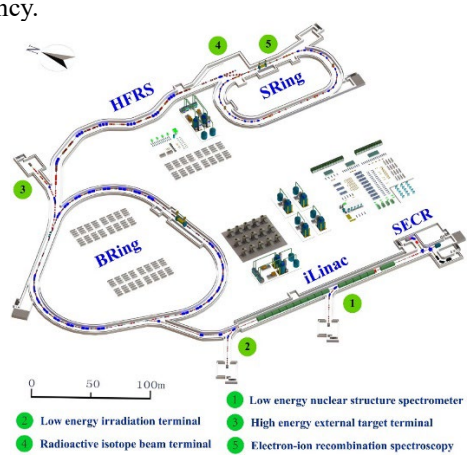

Figure 1: The layout of HIAF.

SYSTEM ARCHITECTURE

The block diagram of the BPM data acquisition is shown in Figure 2. The signal on the pick-up first passes through the front-end amplifier with a gain of about 40 dBm and then travels over a long coaxial cable to the BPM data processing electronics and data acquisition system. In the BPM electronics, high-speed ADCs (analog to digital converter) are employed, and the sample rate is 250 Msps. The main digital signal processing is implemented by a System-on-Chip (SoC) device ZYNQ UltraScale+(ZU15) series. By using the SoC, the data from FPGA to ARM could be easily acquired. Figure 2 is the digital platform of the BPM system architecture.

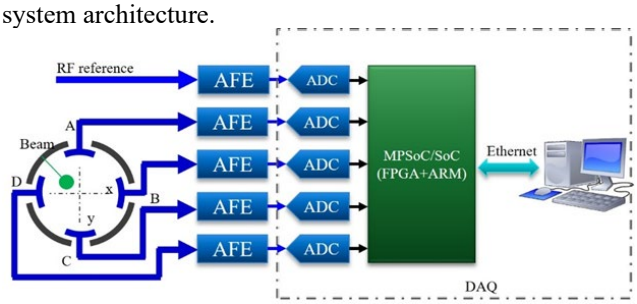

Figure 2: System architecture.

DIGITAL SIGNAL PROCESSING

The sampling frequency of 250 MHz is the main clock frequency in the FPGA. After the ADC sampling the amplified signal from pick-ups, the acquired signal is first passed through a narrow band-pass filter that cuts off high-

ISBN: 978-3-95450-253-0 ISSN: 2673-5571 doi:10.18429/JACoW-HB2023-THBP01

ESS-BILBAO RFQ POWER COUPLER: DESIGN, SIMULATIONS AND TESTS

I. Bustinduy*, J. L. Muñoz, N. Garmendia, A. Kaftoosian, P. J. González,
J. Martín, A. Conde, D. Fernández-Cañoto, G. Harper, ESS-Bilbao, Zamudio, Spain
A. Letchford, STFC/RAL/ISIS, Chilton, Didcot, UK

Abstract

ESS-Bilbao RFQ (Radio Frequency Quadrupole) power coupler is presented. The RFQ operates at 352.2 MHz and will accelerate the 32 mA proton beam extracted from the ion source up to 3.0 MeV. The RFQ will complete the ESS-Bilbao injector, that can be used by the ARGITU neutron source or as a stand-alone facility. The machining of the RFQ is finished, and vacuum tests as well as low power RF measurements have been carried out. The presented power coupler is a first iteration of the device, designed to be of easier and faster manufacturing than what might be needed for future upgrades of the linac. The coupler does not have active cooling and no brazing has been needed to assemble it. It can operate at the RF power required by the RFQ but at lower duty cycles. The dielectric window is made of polymeric material, so it can withhold the assembly using vacuum seals and bolts. Design and manufacturing issues are reported in the paper, as well as the RF tests that have been carried out at medium power. Multipacting calculations compared to measured values during conditioning are also reported. High power tests of the coupler have also been performed in the ISIS-FETS RFQ and are also described here.

INTRODUCTION

ESS Bilbao is involved in developing a local project that includes the study of a multi-purpose light ion linear accelerator for a 30 MeV proton beam [1]. The first part of the linac comprises an Electron Cyclotron Resonance (ECR) proton ion source and Low Energy Beam Transport (LEBT) which can provide a proton beam of up to 40 mA at an energy of 45 keV. These are already on operation at the ESS Bilbao premises. The next section, the Radio Frequency Quadrupole (RFQ), is under manufacturing [2]. In parallel, we need to feed the RF power to the RFQ. In the last year, two couplers have been designed, manufactured and tested in low and high power. In the following sections we will describe the current status.

The power coupler of an RF accelerator cavity is the device that allows the injection of RF power into the cavity. To do so, it must excite the adequate resonant mode in the cavity and transmit the required RF power with as minimum losses as possible. In the case of the ESS-Bilbao RFQ, the coupler connects a 4-1/2 inch EIA coaxial waveguide that comes from the RF power chain to a loop that is inserted into the RFQ body through the RFQ coupler/tuners ports

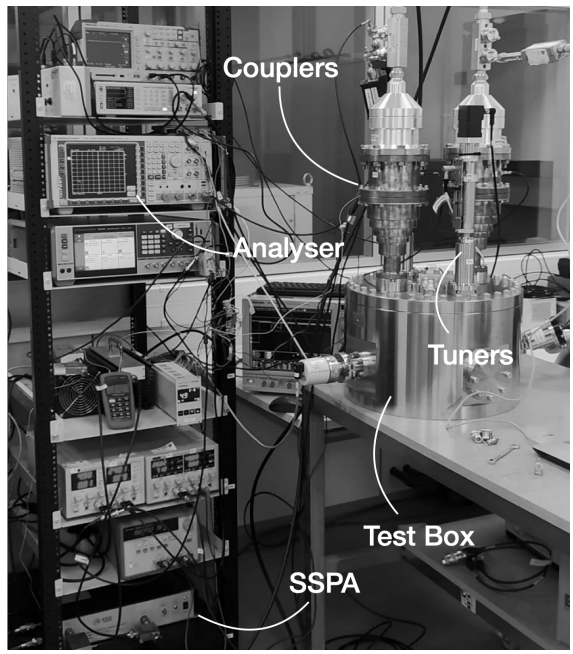

Figure 1: Test-bench for the RFQ couplers conditioning.

(close to DN40). Table 1 summarizes design parameters of the coupler. From the DC point of view, the loop is itself a short-circuit between the external and internal coaxial conductors. The design of a RF coupler is a challenge since it needs to provide a separation between air (waveguide) and vacuum (cavity) and transmit the RF power efficiently.

Table 1: RFQ and Coupler Design Specifications

Parameter	Value
Specimen	H^+
Beam current	32 mA
Beam energy	45 keV (3 MeV)
RF Frequency	352.2 MHz
Pulse Operation	30 Hz, 1.5 ms, 4.5 %
Intervane Voltage	85 kV
Kilpatrick	1.85
Input emittance	0.25 π mm mrad
Window Material	PEEK
RF Coaxial Interface	4-1/2" EIA
Inner/Outer Radius	4.6 / 10.58 mm

To overcome the difficulties a first version has been designed [2] that does not need water cooling. Also, the fabrication was simplified, and no brazing was needed for the

* ibustinduy@essbilbao.org

ISBN: 978-3-95450-253-0 ISSN: 2673-5571 doi:10.18429/JACoW-HB2023-THBP02

FFA MAGNET FOR PULSED HIGH POWER PROTON DRIVER

J.-B. Lagrange*, C. Jolly, D. Kelliher, A. Letchford, S. Machida, I. Rodriguez, C. Rogers, J. Speed
STFC/RAL, UK
T.-J. Kuo, Imperial College, UK
S. Brooks, BNL, USA

Abstract

Fixed Field Alternating gradient (FFA) accelerator is considered as a proton driver for the next generation spallation neutron source (ISIS-II). To demonstrate its suitability for high intensity operation, an FFA proton prototype ring is planned at RAL, called FETS-FFA. The main magnets are a critical part of the machine, and several characteristics of these magnets require attention, such as doublet spiral structure, essential operational flexibility in terms of machine optics and control of the fringe field extent from the nonlinear optics point of view. This paper will discuss the design of the prototype magnet for FETS-FFA ring.

INTRODUCTION

ISIS-II is a major upgrade of the ISIS facility [1], and is under study with an established roadmap [2]. One of the considered options for the proton accelerator is the use of FFA (Fixed Field alternating gradient Accelerator). This arrangement has several advantages. First, it brings longitudinal flexibility and so allows beam stacking [3]. It is also more reliable, and more sustainable from an energy consumption point of view, as a whole accelerator system since the main magnets are operated in DC mode. Third, as long as acceleration voltage is sufficient, high repetition rate (more than 100 Hz) can be achieved. However, no high intensity pulsed FFA has been built so far. An FFA test ring called FETS-FFA is proposed [4] to confirm these features experimentally and to build engineering experience, using the 3 MeV beam from RAL's R&D injector, FETS [5]. As a critical part of the hardware a magnet prototype is being designed. Essential features for this magnet are

- zero-chromaticity during acceleration,
- dynamic aperture larger than physical aperture to avoid uncontrolled losses,
- flexibility in terms of tune point to allow different operation as a function of intensity.

The scaling law keeps zero-chromaticity during acceleration by following the equation

$$B_z = B_0 \left(\frac{r}{r_0}\right)^k \mathcal{F}\left(\theta - \tan\xi \ln\left(\frac{r}{r_0}\right)\right), \qquad (1)$$

with B_0 the field at the reference radius r_0, ξ the logarithmic spiral angle, k the constant geometrical field index and $\mathcal{F}$ the arbitrary longitudinal function. Other solutions can be used to retain the zero-chromaticity of the lattice [6].

A reverse bend magnet (D-magnet) is included to allow a change in vertical tune, while the k-value must be able to vary to change the horizontal tune. It leads to large change of beam excursion as seen in Fig. 1, that needs to be taken into account in the magnet design.

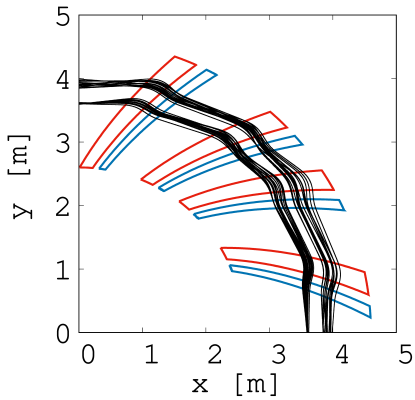

Figure 1: Closed orbits (3 MeV and 12 MeV) in black in one superperiod of the lattice for different tune points.

MAGNET SPECIFICATIONS

The magnet specifications are presented in Table 1. They are based on the 4-fold symmetry lattice design of the prototype ring [4]. The fourth doublet (lowest in Fig. 1) has been chosen as a prototype magnet.

Table 1: Magnet Specifications from Lattice Design

Parameter	Value
Cell type	FD spiral
Spiral angle	30.0 deg.
k-value range (central scenario)	6 – 9 (7.5)
Injection, Extraction proton energy	3, 12 MeV
F Magnet opening angle	4.50 deg.
D Magnet opening angle	2.25 deg.
Short drift opening angle	2.25 deg.
Full gap size	100 mm
Good field region excursion	738 mm
Maximum vertical field in GFR	1.5 T
Fixed injection radius	3.6 m

The lattice design computes a physical acceptance of ±32 mm, corresponding to a normalised 40 π mm mrad emittance. A closed orbit distorsion of 8 mm is added to this,

* jean-baptiste.lagrange@stfc.ac.uk

ISBN: 978-3-95450-253-0 ISSN: 2673-5571 doi:10.18429/JACoW-HB2023-THBP03

ESS-BILBAO RFQ STATIC TUNING ALGORITHM AND SIMULATION

J. L. Muñoz*, I. Bustinduy, N. Garmendia, A. Conde, J. Martin, V. Toyos, P. González,
Consorcio ESS-Bilbao, Zamudio, Spain

Abstract

The ESS-Bilbao RFQ operates at 352.2 MHz. The machining of the four RFQ segments has finished and the assembly and tuning operations will follow shortly. The static tuning and field flatness are provided by an array of 60 plunger tuners, distributed along the 3.2 meters length of the structure. There are four tuners per segment per quadrant, except for one of the segments where the ports are used by the power couplers. A bead-pull setup will provide the measurements of the field profiles, that will be collected in a matrix built up with the contributions of individual tuners. The conventional approach of inverting the matrix to get the optimum tuners distribution is explored, as well as additional optimization method. Particularly, a genetic optimization algorithm provides a very successful tuning of the RFQ. The solution provided by this approach will be used as the initial configuration of the tuners before the bead-pull measurements are carried out.

INTRODUCTION

The ESS-Bilbao RFQ [1, 2] is currently under fabrication. It will be part of the injector for the ARGITU compact accelerator-based neutron source [3]. The RFQ will accelerate protons from 45 keV to 3.0 MeV. It is a pulsed linac that operates at 352.2 MHz, and up to a duty cycle of 5 %. In order to meet the acceleration and transmission characteristics, the RFQ needs to be precisely machined and assembled. It is worth pointing out that each of the RFQ four segments, that are themselves an assembly of four components named vanes, are not brazed together. Polymeric vacuum gaskets and RF contact elements are used instead (see [1, 2] for details). The 3.12 meters long structure of the RFQ has to be tuned up so it not only resonates at the required frequency, but also has the correct field profile. This is achieved by the combined action of a set of 60 plunger tuners. The field profile along the cavity length, measured using a bead-pull technique, will be modified by the action of the tuners. The tuning of the RFQ is then the procedure of modifying the measured field profile so it becomes flat. The algorithms to do this in an optimal way, for ESS-Bilbao RFQ, are described in this paper.

RFQ TUNING

The ESS-Bilbao RFQ is designed to have a uniform intervane voltage of $V(z)$ =85 kV along all its length. In operation, the magnitude of this voltage will be determined by the RF power delivered into the cavity. The 2D cross-section of the RFQ (see Fig. 1) represents a perfect LC resonator, with a single frequency and a single value for the intervane voltage at a certain power. In the 3D cavity, the modulation of the RFQ vane tips (Fig. 2), that allows its bunching and accelerating characteristics, as well as other features of the resonant structure will modify the local capacitance per unit length, resulting in a non uniform voltage $V(z)$. Mechanical fabrication or alignment issues will also contribute to this non-uniformity.

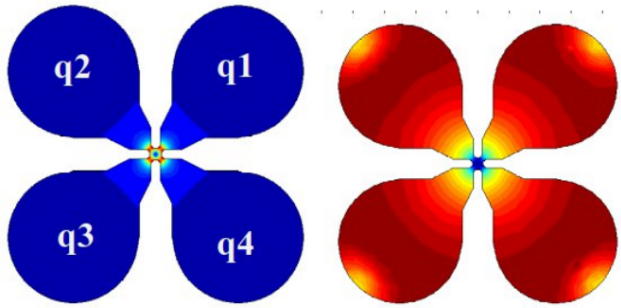

Figure 1: Electric (left) and magnetic (right) field maps for the cross section of the RFQ, with the quadrant naming specified in the electric field map.

The effect of the modulation can be calculated using a conventional perturbation approach to the transmission line model of the RFQ (see, for example, [4]). The effect of the 3D structure features, as well as the effect of geometrical deviations of the cavity, can be computed using FEM models of the RFQ. The combined effect of all deviations is a non-uniform voltage $V(z)$, that if is not corrected will affect the operation of the cavity.

These perturbations are compensated by the action of the plunger tuners. The field profiles are obtained by bead-pull measurements or are extracted from computer simulations. As described in [5], from the values along the 4 quadrants (q_1, q_2, q_3, q_4, Fig. 1), the combined magnitudes 1 are derived. From the measurements, a set of P values along z are selected. The field profile values for these selected coordinates are grouped in a vector V of size $3P$. Then, each one of the N tuners is moved a specific distance inside the cavity from the initial setup, and the curves are measured again. The perturbation caused by each tuner is assumed to be linear. In this way we can arrange the field perturbations caused by each tuner in the form of a matrix equation, Eq. (2) that includes all individual changes. This equation is the basis of all the tuning methods described here.

$$\begin{aligned} Q &= (q_1 - q_2 + q_3 - q_4)/4 \\ D_1 &= (q_1 - q_3)/2 \\ D_2 &= (q_2 - q_4)/2 \end{aligned} \tag{1}$$

$$V = MT \tag{2}$$

* jlmunoz@essbilbao.org

ISBN: 978-3-95450-253-0 ISSN: 2673-5571 doi:10.18429/JACoW-HB2023-THBP04

MACHINE PROTECTION SYSTEM FOR THE PROPOSED TATTOOS BEAMLINE AT HIPA

J. Snuverink*, P. Bucher, R. Eichler, M. Hartmann, D. Kiselev, D. Reggiani, E. Zimoch
Paul Scherrer Institut, 5232 Villigen PSI, Switzerland

Abstract

IMPACT (Isotope and Muon Production with Advanced Cyclotron and Target Technology) is a proposed upgrade project for the High Intensity Proton Accelerator (HIPA) at the Paul Scherrer Institute (PSI). As part of IMPACT, a new radioisotope target station, TATTOOS (Targeted Alpha Tumour Therapy and Other Oncological Solutions) is planned. The TATTOOS beamline and target will be located near the UCN (Ultra Cold Neutron source) target area, branching off from the main UCN beamline. In particular, the 590 MeV proton beamline is designed to operate at a beam intensity of 100 μA (60 kW), requiring a continuous splitting of the main beam by an electrostatic splitter. The philosophy of the machine protection system (MPS) for the TATTOOS beamline will not differ significantly from the one already implemented for HIPA. However, it is particularly important for TATTOOS to avoid damage to the target due to irregular beam conditions. We will show the diagnostic systems involved and how the requirements of the machine protection system can be met. Emergency scenarios and protective measures are also discussed.

INTRODUCTION

The High Intensity Proton Accelerator facility (HIPA) at the Paul Scherrer Institute (PSI) delivers a 590 MeV proton beam with up to 1.4 MW beam power (2.4 mA) to spallation and meson production targets serving particle physics experiments and material research [1].

IMPACT (Isotope and Muon Production using Advanced Cyclotron and Target technologies) is a proposed upgrade project envisaged for HIPA [2]. IMPACT proposes two new target stations: HIMB (High Intensity Muon Beamline) replaces an existing target and focuses on increasing the rate of surface muons while TATTOOS (Targeted Alpha Tumour Therapy and Other Oncological Solutions), an online isotope separation facility, will allow to produce promising radionuclides for diagnosis and cancer therapy in doses sufficient for clinical studies. The TATTOOS facility includes a dedicated beamline intended to operate at a beam intensity of 100 µA (60 kW beam power), requiring continuous splitting of the high-power main beam via an electrostatic splitter [3, 4]. A realistic model of the complete TATTOOS beamline from splitter to target was established [5, 6].

OVERVIEW HIPA

An overview of the HIPA facility with the foreseen TATTOOS installation is shown in Fig. 1. HIPA consists of a Cockcroft-Walton pre-accelerator (870 keV) followed by two isochronous cyclotrons, the Injector II (72 MeV) and the Ring cyclotron (590 MeV). After extraction from the Ring cyclotron the high intensity, up to 2.4 mA, proton beam interacts with two rotating graphite target wheels, target M and E, to produce pions and muons. After collimation the remaining beam with roughly 1 MW power is used to produce neutrons in a spallation target (SINQ). In addition, a pulsed source for ultracold neutrons (UCN) is in operation as well. A fast kicker magnet can divert the full intensity beam to the UCN beamline and target for up to 8 seconds. Finally, an electrostatic splitter (EHT) located downstream of the kicker magnet in the PK1 beamline can peel off a fraction of the main beam and send it continuously to the UCN target. Another electrostatic splitter (EXT) [7, 8] can peel off a few tens of microamperes from the main 72 MeV (2.4 mA) beam to produce radionuclides in the IP2 irradiation station [9].

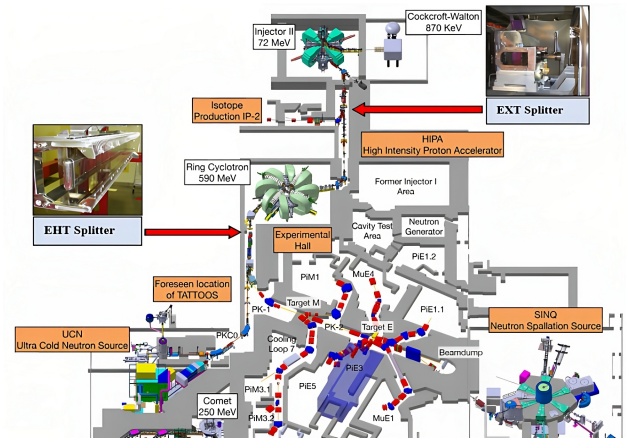

Figure 1: Overview of the high intensity proton accelerator HIPA. The proposed TATTOOS beamline and the location of the EHT splitter is also indicated.

Machine Protection System

When handling a beam of over 1 MW power, the protection and control of the facility become crucial and require reliable protection mechanisms as well as appropriate diagnostics and controls. In particular the high dynamic range needed for currents between less than 1 and up to 2400 µA is a big challenge for the beam diagnostics and has to be accounted for by the control system.

The well established HIPA machine protection system (MPS) [10–13] guarantees safe operation of the accelerator facility protecting the machine from severe instantaneous beam losses and from prohibitive activation generated by large integrated losses.

* jochem.snuverink@psi.ch

ISBN: 978-3-95450-253-0 ISSN: 2673-5571 doi:10.18429/JACoW-HB2023-THBP05

CERN SPS DILUTION KICKER VACUUM PRESSURE BEHAVIOUR UNDER UNPRECEDENTED BEAM BRIGHTNESS

F. M. Velotti*, M. J. Barnes, W. Bartmann, H. Bartosik, E. Carlier, G. Favia, I. Karpov, K. S. Bruce Li, N. Magnin, L. Mether, V. Senaj, C. Zannini, P. Van Trappen
CERN, Geneva, Switzerland

Abstract

The Super Proton Synchrotron (SPS) is the second largest synchrotron at CERN and produces high-brightness beams for the Large Hadron Collider (LHC). Recently, the dilution kicker (MKDH) of the SPS beam dump system (SBDS) has demonstrated unanticipated behaviour under high beam brightness conditions. During the 2022 and 2023 beam commissioning, the MKDH, which is routinely pulsed at high voltage, was subjected to intensities of up to 288 bunches of 2×10^{11} protons per bunch and bunch lengths as low as 1.5 ns. Under these conditions, all the SPS kickers and septa exhibited a rapid vacuum pressure rise and a significant temperature increase with the MKDH playing the dominant effect in restricting the maximum line density that can be attained. This paper presents the results of the collected data, emphasizes the dependence on beam parameters, and introduces a probabilistic model to illustrate the effect of MKDH conditioning observed to forecast the pressure behaviour. Finally, potential countermeasures and outlook are discussed.

INTRODUCTION

The CERN Super Proton Synchrotron (SPS) serves as the final acceleration stage for the LHC beams. Protons are accelerated from 26 GeV to 450 GeV before being delivered to the LHC through two distinct extraction systems. Within the framework of the LHC Injectors Upgrade (LIU) program, the SPS underwent several modifications, including the introduction of a new internal dump system. This updated dump system was conceived to facilitate the internal disposal of 25 ns beams with intensities up to 2.3×10^{11} p/b, accommodating a maximum of 320 bunches with potential emittances as low as 1.37 mm mrad [1].

Relocating the SBDS to Long Straight Section (LSS) 5 from LSS1 necessitated the incorporation of an additional vertical kicker (MKDV) and the development of a completely new absorber block to handle the augmented brightness. The existing dilution system, denoted as MKDH and comprising three 1.6 m tanks, remained unchanged but was relocated to the new dump position. This system's primary function is to diminish the particle density at the absorber block's front face.

The MKDH kickers are constructed using laminated steel plates and are available in two variants, differentiated by their lamination thickness. They possess a magnetic length of 1.256 m and are designed to achieve a magnetic field strength up to 1.5 T.

Following the resumption of operations after Long Shutdown (LS) 2, during which the SBDS received its upgrade, the LHC-type beam intensities were progressively increased during specialised measurement sessions. A notable observation was that as the intensity per bunch increased and the bunch length reduced, the vacuum pressure at the MKDH rose rapidly at every cycle, and in many cases went beyond the limit allowed for the safe operation of the kicker system, stopping machine operation.

Although this phenomenon has been noted in earlier instances with different kickers [2], it has yet to be replicated in simulations. The observed threshold effects related to both the intensity per bunch and bunch length remain unexplained by current models. A comparable behaviour was documented at RHIC [3], but one must exercise caution when drawing parallels due to significant disparities in beam type and energy.

This paper provides a comprehensive review of the observations gathered pre and post the SBDS upgrade. We delve into the specifics of the beam parameters recorded in the SPS and the corresponding response of the MKDH. Lastly, we outline the conditioning rate and detail the peak parameters achieved.

OBSERVATIONS PRE-LS2

The LHC demands a beam consisting of up to 288 bunches with a spacing of 25 ns, organised into 4 batches, or 6 batches

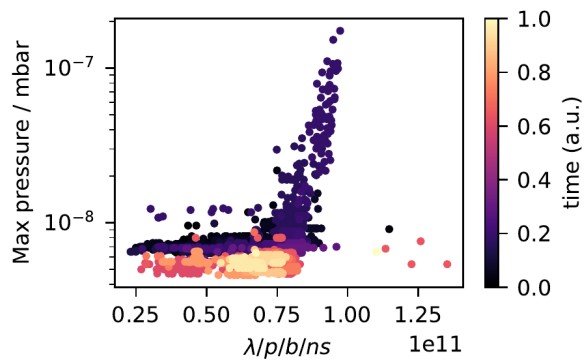

Figure 1: Maximum vacuum pressure recorded among all MKDH tanks as a function of the line density at 450 GeV for 72 bunches. The relative time with respect to the beginning of the year 2023 is shown as colour code.

* francesco.maria.velotti@cern.ch

ISBN: 978-3-95450-253-0 ISSN: 2673-5571 doi:10.18429/JACoW-HB2023-THBP06

RFQ UPGRADES FOR IFMIF-DONES

M. Comunian†, L. Bellan, A. Palmieri, A. Pisent
Istituto Nazionale di Fisica Nucleare Laboratori Nazionali di Legnaro, Legnaro, Italy

Abstract

In the framework of IFMIF-DONES (International Fusion Materials Irradiation Facility- DEMO-Oriented Neutron Early Source) a powerful neutron irradiation facility for studies and certification of materials to be used in fusion reactors is planned as part of the European roadmap to fusion electricity. A possible RFQ upgrade has been designed. In this article the beam dynamics of an RFQ able to handle CW 200 mA of Deuterium, based on experience of IFMIF RFQ, will be presented.

INTRODUCTION

The IFMIF-DONES facility [1] will serve as a fusion-like neutron source (1×10^{14} neutrons/cm2/s) for the assessment of materials damage in future fusion reactors. The neutron flux will be generated by the interaction between the lithium curtain and the deuteron beam from an RF linear accelerator at 40 MeV and nominal CW current of 125 mA. As far as the RFQ is concerned, the mainstream idea is the use of a copy of IFMIF RFQ [2] for the DONES facility. Nevertheless, a possible RFQ upgrade can handle more current and absorb the experience of the IFMIF RFQ. The experience of the IFMIF/EVEDA commissioning suggests the design of a higher acceptance RFQ, to deal with different than standard distribution, which results in a higher 99% emittance and increase the lifetime of RFQ due to the possible electrodes erosion. The last point has an important impact on maintenance activity that needs to be considered, that can potentially stop the machine for months to exchange the eroded modules.

DESIGN PARAMETERS

Based on the IFMIF RFQ experience the new RFQ for the upgrade of DONES can be:

- Input energy range from 110 keV to 150 keV.
- Output energy=5 MeV
- Input emittance RMS=0.3 mm·mrad (norm.)
- Frequency=175 MHz
- Max surface field of 25.2 MV/m (1.8 kp – 1.88 kp)
- Input Current=200 mA
- Particle=Deuteron

The increase of input energy can help to reduce the beam size, and the space charge effects. The input emittance is a possible realistic value with a LEBT transport of more than 200 mA. The limits on the RFQ design come from the total length (less than 10 meters as IFMIF RFQ) and maximum surface field of 1.8 - 1.9 kp.

DESIGN METHOD

The design is based on a new tool called VeRDe (Venetian RFQ Design), an optimization toolkit for the RFQ Beam Dynamics design developed at the Legnaro National Laboratories [3]. The core program is given by the Los Alamos RFQ codes [4]: PARMTEQM, PARI, RFQuick and CURLI. VeRDe allows to manage the parameters needed for each RFQ cell definition: the transvers focusing term, the voltage, the modulation, and the synchronous phase. RFQuick estimates the longitudinal capture efficiency, given the current limit by CURLI, through the study of the buncher section characteristics; the PARI designs the RFQ cells based on the RFQuick output (that uses the Crandall tables to estimate the multipoles of the cells); VeRDe also implement on PARI the voltage law shape on the designed RFQ, PARMTEQM performs the simulations based on the PARI output.

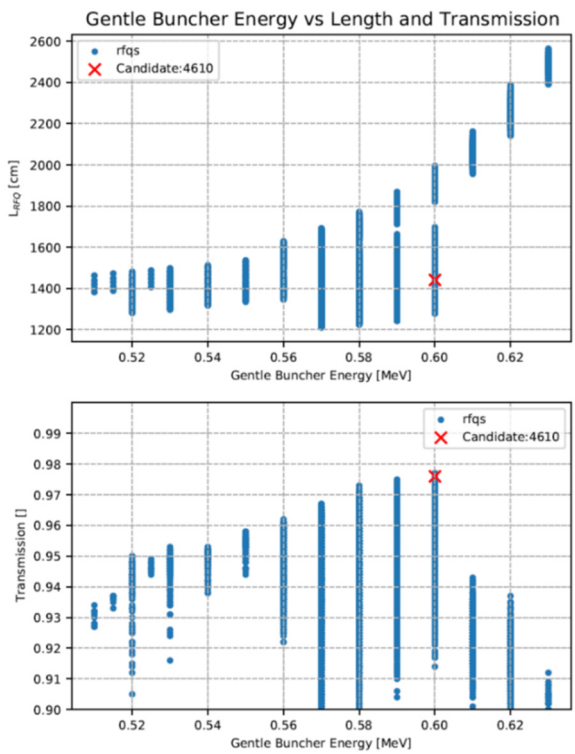

Figure 1: RFQ length (above) and transmission (below) as a function of Gentle Buncher energy.

Considering that the RFQ is composed of 3 sections, Shaper, Gentle Buncher and Accelerator, each composed of several tens of cells, it is straightforward to understand that the degrees of freedom of the process is very large. From hundreds to thousands of RFQ candidates may be produced in parallel on several computers. Each single case is a full

† email: michele.comunian@lnl.infn.it

ISBN: 978-3-95450-253-0 ISSN: 2673-5571 doi:10.18429/JACoW-HB2023-THBP08

SIMULATION STUDIES ON THE LOW ENERGY BEAM TRANSFER (LEBT) SYSTEM OF THE ISIS NEUTRON SPALLATION SOURCE

S. Ahmadiannamin, A. Letchford, S. R. Lawrie, D. Faircloth, O. Tarvainen, T. M. Sarmento,
ISIS, STFC, Rutherford Appleton Laboratory, Oxfordshire, UK

Abstract

The transmission efficiency and beam dynamic parameters of the low-energy beam transfer (LEBT) section of proton accelerators, serving as a neutron spallation source, have a critical impact on beam loss in subsequent sections of the linear accelerator. Due to variations and mismatches, the beam parameters at the entrance of the radio-frequency quadrupole (RFQ) change, significantly affecting the transmission efficiency of the RFQ and the matching between RFQ and drift tube linac (DTL) structures. Recognizing the importance of this concept, particle-in-cell studies were conducted to optimize the LEBT section of the ISIS accelerator. This study presents the results of simulations.

INTRODUCTION

Nowadays, proton or H^- linear accelerators find a wide range of applications, with one of the most significant being neutron spallation sources. The ISIS neutron spallation source stands as a renowned research centre, having provided neutrons to the user community for almost 40 years. Beam parameters are matched between the ion source and RFQ by the LEBT and is planned between the RFQ and DTL by a new MEBT sections [1, 2].

Two types of H^- Penning ion sources are currently in use, one on the existing ISIS machine, and one on (Front End Test Stand) FETS. The high output current of these ion sources necessitates use of caesium which limits the lifetime and typically results in replacement every two weeks. Recently, RF ion sources are being developed at ISIS, offering greater reliability and longer lifetimes, albeit with lower current density compared to their predecessors [3].

In the current configuration of the machine, it is desirable to extract higher currents out of the ion source and transport to the end of RFQ, accepting poor transmission into the DTL to obtain 25 mA for injection into the RCS. Following the machine's upgrade with the MEBT section, the required current at the output of RFQ will be 25 mA instead of 35 mA for the current RCS operation. The MEBT design also includes a chopper which will be synchronised to the ring RF system to place beam directly into the RF bucket, removing beam losses associated with RF capture [4, 5].

Figure 1 depicts the LEBT section, while Table 1 reports the simulation beam parameters at the output of the Penning and RF ion sources, along with the matched beam parameters at the entrance of the 665 keV RFQ.

The unnormalized rms beam emittances is $\varepsilon_x = \varepsilon_y = 34.24\ \pi$ mm mrad. The ISIS and FETS ion sources are 35 keV and 65 keV respectively.

In every scenario, it is imperative to achieve complete matching between the ion source and RFQ to attain the maximum possible transmission of the H- ion beam. Besides ensuring the correct settings for solenoid magnets and drift distances, it is crucial to take into account the process of space charge compensation (SCC). For this investigation, we have focused solely on the pure reduction of beam current and conducted simulations using TRACE beam envelope and Parmila PIC codes for the ISIS LEBT section [6,7].

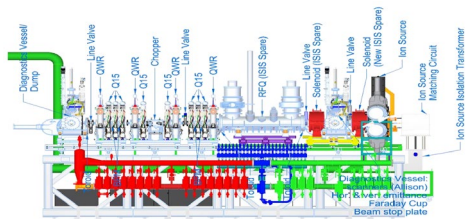

(b)

Figure 1: Drawing of ISIS low energy section including ion Source, LEBT, RFQ and MEBT.

STUDY OF LEBT PARAMETERS

The LEBT section of ion accelerators typically comprises a pumping section, diagnostic box, solenoid magnets, and collimators. The parameters of the LEBT section have been optimized using the TRACE-3D code. The simulation layout and parameters of the LEBT section are illustrated in Fig. 2. The solenoid fields for different beam currents after compensation are presented in Fig. 3. It is noteworthy that the variations in magnetic field strength in both solenoid-1 and solenoid-2 remain linear during the process of matching beam parameters between the ISIS RF ion source and RFQ in LEBT/MEBT arrangement.

When adjusting the solenoids to achieve a complete 90% beam space charge compensation for a 35-mA beam, any deviation in the level of compensation can lead to changes in the beam Twiss parameters and subsequent variations in beam emittance. This variation becomes particularly significant during the transition to 100% compensation. The maximum achievable level of compensation is contingent upon the vacuum conditions and the combination of gases present within the ion source and LEBT section.

To better understand the effects of compensation with solenoid adjustments, a study was conducted for a 3.5 mA (90% beam compensation), exploring different compensation percentages ranging from 85% to 100%. This analysis estimated the Twiss parameters α and β, considering the degree of mismatch. Notably, the change in α was found to be linear, while β exhibited a nonlinear response. These results are presented in Fig. 4. These results pertain to a uniform charge distribution, and it is noted that for other types of charge distributions such as Waterbag and Gaussian, the

ISBN: 978-3-95450-253-0 ISSN: 2673-5571 doi:10.18429/JACoW-HB2023-THBP09

PUSHING HIGH INTENSITY AND HIGH BRIGHTNESS LIMITS IN THE CERN PSB AFTER THE LIU UPGRADES

F. Asvesta*, S. Albright, H. Bartosik, C. Bracco, G. P. Di Giovanni, T. Prebibaj
CERN, Geneva, Switzerland

Abstract

After the successful completion of the LHC Injectors Upgrade (LIU) project, the CERN Proton Synchrotron Booster (PSB) has produced beams with up to two times higher brightness. However, the efforts to continuously improve the beam quality for the CERN physics experiments are ongoing. In particular, the high brightness LHC beams show non-Gaussian tails in the transverse profiles that can cause losses in the downstream machines, and even at LHC injection. As a result, alternative production schemes based on triple harmonic capture are being investigated in order to preserve brightness and reduce transverse tails at the same time. In addition, in view of a possible upgrade to the ISOLDE facility that would require approximately twice the number of protons per ring, the ultimate intensity reach of the PSB is explored. In this context, injection schemes using painting both transversely and longitudinally in order to mitigate the strong space charge effects are developed.

INTRODUCTION

The PSB is the first synchrotron of the proton injectors chain at CERN. The most challenging beams in terms of brightness are the ones for LHC and its upgrade, the High-Luminosity LHC [1]. After the successful implementation of the LIU project [2], the PSB has managed to reach the brightness target [3], while issues of beam quality, in particular non-Gaussian tails in the transverse distributions, have been identified [4]. However, the LHC beams are not the most demanding in terms of intensity, as the ISOLDE facility [5] requires almost a factor 3 higher intensity for day to day operations, reaching >800 × 10^{10} Protons Per Ring (ppr). In addition, in the context of the Physics Beyond Colliders (PBC) study [6] and a possible upgrade of the ISOLDE experimental area, intensities up to >1500 × 10^{10} ppr need to be investigated. On the other hand, the beams for the ISOLDE facility are not very demanding in terms of brightness, as the transverse beam size does not pose limitations for the experiments.

The main performance limitations at the PSB for the production of high brightness and high intensity beams are discussed in the following sections. Also alternative operational scenarios to overcome these challenges are proposed.

SPACE CHARGE MITIGATION TECHNIQUES

The main performance limitation for the challenging high brightness and high intensity beams is due to space charge, especially at the injection energy of 160 MeV. In particular, space charge introduces an incoherent tune shift that depends on both transverse and longitudinal beam characteristics. For Gaussian beam distributions the maximum tune shift, corresponding to particles at the center of the beam, is obtained as [7]:

$$\Delta Q_{x,y} = -\frac{r_0 \lambda}{2\pi e \beta^2 \gamma^3} \oint \frac{\beta_{x,y}(s)}{\sigma_{x,y}(s)(\sigma_x(s)+\sigma_y(s))} ds \,, \quad (1)$$

where r_0 is the classical particle radius, λ the longitudinal line density, e the particle charge, $\beta\gamma$ the relativistic factors,

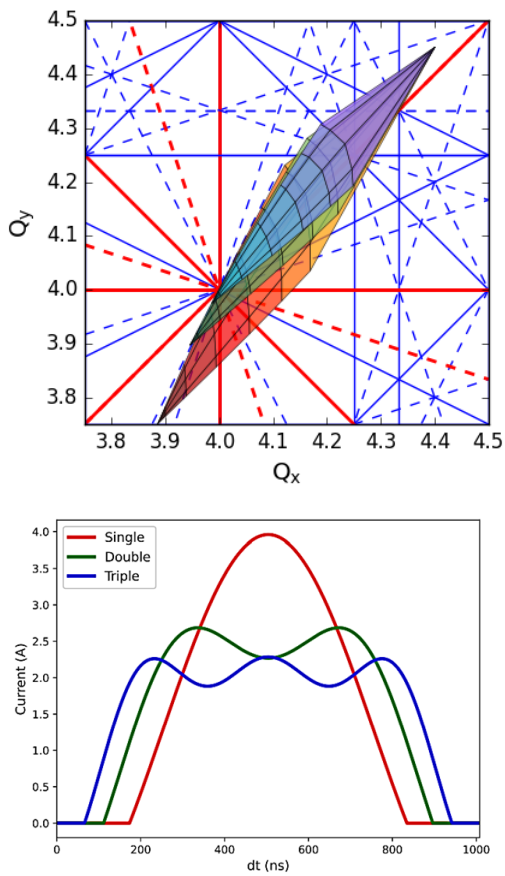

Figure 1: Analytically estimated space charge tune spread [8] at PSB injection for the operational high brightness beams for the single (red), double (green) and triple (blue) cases (bottom). Resonance lines up to 4th order plotted, normal in solid and skew in dashed, systematic in red and non-systematic in blue. Longitudinal line density for the cases of single, double and triple harmonic system (top).

* foteini.asvesta@cern.ch

ISBN: 978-3-95450-253-0 ISSN: 2673-5571 doi:10.18429/JACoW-HB2023-THBP10

A LINEARIZED VLASOV METHOD FOR THE STUDY OF TRANSVERSE e-CLOUD INSTABILITIES

S. Johannesson*,[1], G. Iadarola, CERN, Geneva, Switzerland
M. Seidel[1], Paul Scherrer Institut, 5232 Villigen PSI, Switzerland
[1] also at École Polytechnique Fédérale de Lausanne, Lausanne, Switzerland

Abstract

Using a Vlasov approach, e-cloud driven instabilities can be modeled to study beam stability on time scales that conventional Particle In Cell simulation methods cannot access. The Vlasov approach uses a linear description of e-cloud forces that accounts for both the betatron tune modulation along the bunch and the dipolar kicks from the e-cloud. Forces from e-clouds formed in quadrupole magnets as well as dipole magnets have been expressed in this formalism. In addition, the Vlasov approach can take into account the effect of chromaticity. To benchmark the Vlasov approach, it was compared with macroparticle simulations using the same linear description of e-cloud forces. The results showed good agreement between the Vlasov approach and macroparticle simulations for strong e-clouds, with both approaches showing a stabilizing effect from positive chromaticity. This stabilizing effect is consistent with observations from the LHC.

INTRODUCTION

Electron clouds, also known as e-cloud, in circular accelerator beam chambers can induce coupled and single-bunch instabilities [1, 2]. While the former can usually be controlled using standard transverse feedback systems, mitigating single-bunch instabilities, caused by fast intra-bunch motion, requires wide-band feedback systems, which are typically out of reach in accelerators operating with short bunches [3]. Alternatively, these instabilities can often be mitigated by large chromaticity and/or octupole magnets to introduce amplitude detuning [4].

The study of e-cloud instabilities heavily relies on numerical simulations. Conventional simulations, which employ macroparticle tracking and the Particle-In-Cell method for e-cloud-beam interaction, are computationally intensive, which makes evaluation of slow instabilities challenging [5]. Alternatively, the Vlasov equation, describing multi-particle systems under conservative forces, can be used to simulate beam instabilities due to collective effects, particularly through the linearized Vlasov equations derived from perturbation theory [6, 7].

The Vlasov equation is applicable when simulating instabilities driven by beam-coupling impedances [8]. Efforts have also been made to extend this approach to simulate e-cloud-driven instabilities, where e-cloud forces are represented as impedances. However, both dipolar forces and the betatron tune modulation along the longitudinal coordinate are required to describe the e-cloud forces in the Vlasov approach [9, 10].

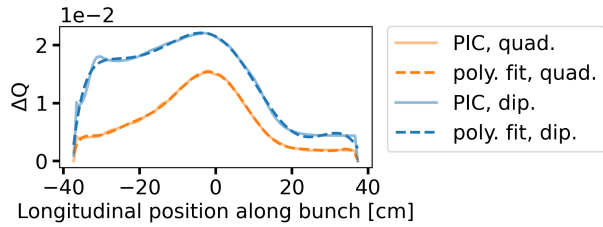

Figure 1: The betatron tune introduced by the e-cloud in the LHC quadrupoles, orange, and the LHC dipoles, blue, at high e-cloud conditions.

e-CLOUD IN VLASOV

Linearized Description of e-Cloud Forces

Quadrupolar forces When a bunch passes through an e-cloud, it attracts electrons, increasing the electron density at the beam's location, which alters the betatron tune along the bunch. This detuning can be characterized with single-pass PIC simulations. Fig. 1 shows the resulting tune modulation for the parameters in Table 1.

Table 1: The table presented here lists the simulation parameters that exert the strongest influence on the characteristics of the e-cloud-driven instability.

Parameter	Value
SEY	2.0
Bunch Intensity	1.2e+11
interaction points per turn	8
element with e-cloud	quadrupoles or dipoles
beam energy	450 GeV (injection)

To model the betatron tune modulation caused by the e-cloud, a polynomial is used:

$$\Delta Q(z) = \sum_{n=0}^{N_p} A_n z^n \,. \tag{1}$$

The results in Fig. 1 demonstrate that a realistic model can be obtained by truncating the sum at $N_p = 10$. There is the flexibility to incorporate detuning from e-cloud in quadrupoles, dipoles, or both into the simulations.

Dipolar forces To model the dipolar forces from e-cloud, a set of sinusoidal bunch distortions are selected,

* sofia.carolina.johannesson@cern.ch

ISBN: 978-3-95450-253-0 ISSN: 2673-5571 doi:10.18429/JACoW-HB2023-THBP11

MKP-L IMPEDANCE MITIGATION AND EXPECTATIONS FOR MKP-S IN THE CERN-SPS

C. Zannini*, M. Barnes, M. Beck, M. Diaz, L. Ducimetière, G. Rumolo, D. Standen, P. Trubacova
CERN, 1211 Geneva, Switzerland

Abstract

Beam coupling impedance mitigation is key in preventing intensity limitations due to beam stability issues, heating and sparking. In this framework, a very good example is the optimization of the SPS kickers beam-coupling impedance for beam-induced heating mitigation. After the optimization of the SPS extraction kickers, the SPS injection kickers became the next bottleneck for high intensity operation. This system is composed of three MKP-S tanks and one MKP-L tank. To accommodate LIU beam intensities, it was necessary to mitigate the beam induced heating of the MKP-L, using a shielding concept briefly reviewed in this paper. Moreover, temperature data from the 2023 run are analyzed to qualify the accuracy of the models and assess the effectiveness of the impedance mitigation. Finally, the expected limitations from the MKP-S, foreseen to become the next bottleneck in terms of beam induced heating, are discussed.

INTRODUCTION

The beam coupling impedance describes how a particle beam interacts with an accelerator component. As the beam passes through the accelerator, it generates electromagnetic fields that can impact its stability and induce power to be dissipated on the accelerator wall [1] causing heating of specific devices. For instance, in ferrite kicker magnets, this heating can risk damage or malfunction if not addressed during the design phase. Historically, beam coupling impedance was not systematically considered in accelerator component design due to typically forgiving beam performance requirements. Consequently, the original SPS ferrite-loaded kicker design was not optimized for beam-induced heating.

For example, due to heating issues [2], the original design of the SPS extraction kickers (MKEs) had to be modified [3]. Serigraphy, which introduces a parallel impedance, was applied directly to the ferrite. Proper engineering of this serigraphy significantly reduced the beam coupling impedance across a broad frequency range without affecting kicker rise time or High Voltage (HV) performance [3–8]. Following the SPS extraction kicker optimization [9], the SPS injection kicker (MKP-L) became the primary bottleneck for CERN-SPS beam induced heating [10].

MKP-L BEAM-INDUCED HEATING MITIGATION

The SPS injection kicker system is composed of four tanks (three MKP-S and one MKP-L tank): the MKP-L tank contains four modules [11]. The MKP-L, due to the wider aperture, has a higher impedance than the MKP-S at lower frequency. This causes a stronger interaction with the beam spectrum and hence higher beam induced power loss [12, 13].

The need to mitigate the MKP-L beam induced power loss in order to accommodate HL-LHC beam intensities was identified already in 2013 and reported in [14]. Consequently, potential solutions to mitigate the beam induced heating were investigated. Based also on the SPS extraction kicker experience, a design with silver fingers was developed. However, due to the shorter length of the MKP-L ferrite cells, 31 mm in comparison with 235 mm, applying the fingers directly on an MKP-L ferrite, as done for the MKEs, was not a viable solution. It was found that significantly longer fingers, extending over several cells, would be needed to efficiently shield the impedance. This was achieved by applying silver fingers on the beam side of ceramic (Al_2O_3) plates, with the fingers connected to the module end ground plates, to ensure isolation from the ferrite and HV plates. Figure 1 shows a sketch of the concept.

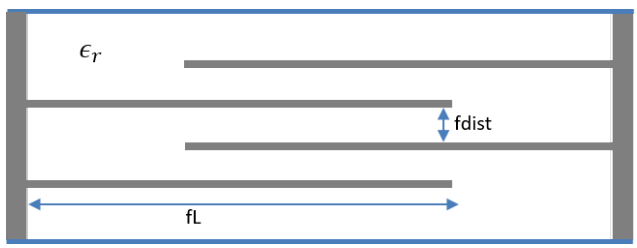

Figure 1: Sketch of the silver fingers applied to Al_2O_3 with electrical permittivity ϵ_r: 'fL' indicates the finger length, and 'fdist' represents the finger separation. The resonance frequency resulting from the serigraphy increases as 'fdist' increases (smaller capacitance) and decreases as the finger length 'fL' increases (higher inductance).

Details about the first version of the impedance shielding of the MKP-L can be found in [15]. This initial beam coupling impedance mitigation solution was successfully verified with bench measurements [13]. Unfortunately, this first version was not a good solution at high voltage [16]. After several investigations, the connection of the fingers to the HV end-plates was chosen as the best solution [16]. As previously mentioned, the serigraphy leads to a significant reduction of the broadband impedance. However, resonances are introduced in the low frequency range. The design of the shielding has been optimized, with the HV constraints in mind [16], to place the dangerous impedance resonance as far as possible from the 40 MHz, 25 ns, beam spectrum line maximizing also the distance from 8b4e additional lines.

* carlo.zannini@cern.ch

ISBN: 978-3-95450-253-0 ISSN: 2673-5571 doi:10.18429/JACoW-HB2023-THBP12

SLOW VS FAST LANDAU DAMPING THRESHOLD MEASUREMENTS AT THE LHC AND IMPLICATIONS FOR THE HL-LHC

X. Buffat*, L. Giacomel and N. Mounet, CERN, Geneva, Switzerland

Abstract

The mechanism of Loss of Landau Damping by Diffusion (L2D2) was observed in dedicated experiments at the LHC using a controlled external source of noise. Nevertheless, the predictions of stability threshold by L2D2 models are plagued by the poor knowledge of the natural noise floor affecting the LHC beams. Experimental measurements of the stability threshold on slow and fast time scales are used to better constrain the model. The improved model is then used to quantify requirements in terms of Landau damping for the HL-LHC.

INTRODUCTION

At the LHC flat top, the Landau octupoles are usually powered with about twice the current predicted by the stability diagram theory [1] based on an unperturbed Gaussian distribution and complex tune shifts predicted by DELPHI [2] following on the LHC impedance model [3]. When performing dedicated experiments to assess the instability threshold by varying the octupole strength, it seemed that the agreement between experimental data and model was good when the octupole was varied on the time scale of minutes. While the (twice) higher threshold was seen when varying the octupoles on the scale of tens of minutes. This slow time scale is the relevant one for operation, since few tens of minutes are usually elapsed between the arrival at top energy and the establishment of collisions. Once in collision, the tune spread is dominated by the contributions of beam-beam interactions, providing large stability margins.

In this slow time scale, the diffusion induced by external sources of noise changes the particle distribution and thus affects Landau damping. The existence of coherent modes stabilised by Landau damping leads to local diffusion depleting the areas of phase space which are generating damping for the coherent modes. Eventually, the distorted distribution no longer provides Landau damping, thus leading to an instability through a Loss of Landau Damping by Diffusion (L2D2) [4,5]. We present here an experiment which directly compares the result of an instability threshold measurement using either a slow or fast octupole scan in identical conditions. The results and the caveat of this experiment are then discussed based on comparison with numerical simulations of L2D2 using the code PyRADISE [6]. Finally, the implications for HL-LHC and possible mitigation strategies are discussed.

MEASUREMENT

In two consecutive cycles, 3 bunches per beam were brought to top energy (6.8 TeV) and kept with a fixed optics ($\beta^* = 1.33$ m). The bunches were placed such that they never meet in common chambers, thus preventing beam-beam effects. They were spaced longitudinally with more than 10 μs, thus preventing electron cloud effects and limiting the effect of long-range wakefields to the minimum. After the instability threshold measurement, the chromaticity was measured to 11 ± 1 units using an energy modulation.

The octupoles [7] were ramped down in steps of 20 A every 15 minutes for the slow scan and every 1.5 minutes for the fast one, as shown in Fig. 1a. First instabilities during the slow scan are observed at 177 A. Three bunches became unstable in the next two steps (157 and 137 A). During the fast scans, all bunches became unstable at 79 A. The evolution of the beam parameters are shown in Figs. 1b, 1c and 1d. In this regime, the horizontal stability threshold is proportional to the bunch intensity and inversely proportional to the bunch length and the vertical emittance [8]. By scaling the obtained threshold with the relevant measured quantities of each bunch, we find that the ratio between the slow and fast threshold is 2.0 ± 0.2, which is compatible with the operational experience discussed in the introduction.

DISCUSSION

We use the code PyRADISE [6] to simulate the evolution of the transverse distribution and of the stability diagram under the impact of an external noise source and the resulting diffusion due to electromagnetic wakefields. We define the instability latency as the time elapsed between the start of the simulation with an unperturbed Gaussian distribution until the point when the stability diagram reaches the complex tune shift of one of the coherent modes.

The instability latency for different detuning and noise amplitude is shown in Fig. 2. The detuning is expressed in units of the detuning on the threshold with an unperturbed Gaussian distribution. We find that a noise amplitude of $(6 \pm 2) \cdot 10^{-4}\ \sigma_{x'}$ is compatible with a threshold measured at 2.0 ± 0.2 times the unperturbed detuning for a latency below 15 minutes. This noise amplitude is 5 to 10 times higher than the one inferred from emittance growth in collision [9]. While this measurement through the emittance growth also suffers from important uncertainties, it is likely that our present measurement overestimates the amplitude of the noise experienced by the beam. We discuss two possible causes for this overestimation.

The unperturbed instability threshold obtained with the impedance model of the LHC is about 120 A, which is significantly higher than the observed threshold of 77 A in the fast scan. This difference cannot be attributed to the uncertainty on the impedance model itself, since other observables sug-

* xavier.buffat@cern.ch

ISBN: 978-3-95450-253-0 ISSN: 2673-5571 doi:10.18429/JACoW-HB2023-THBP13

RECENT DEVELOPMENTS WITH THE NEW TOOLS FOR COLLIMATION SIMULATIONS IN Xsuite

F. F. Van der Veken*,1, A. Abramov[1], G. Broggi[1,2], F. Cerutti[1], M. D'Andrea[1], D. Demetriadou[1], L. S. Esposito[1], G. Hugo[1], G. Iadarola[1], B. Lindström[1], S. Redaelli[1], V. Rodin[1], N. Triantafyllou[1]
[1]CERN, Geneva, Switzerland, [2]Sapienza University of Rome, Italy

Abstract

Simulations of single-particle tracking involving collimation systems need dedicated tools to perform the different tasks needed. These include the accurate description of particle-matter interactions when a tracked particle impacts a collimator jaw; a detailed aperture model to identify the longitudinal location of losses; and others. One such tool is the K2 code in SixTrack, which describes the scattering of high-energy protons in matter. This code has recently been ported into the Xsuite tracking code that is being developed at CERN. Another approach is to couple the tracking with existing tools, such as FLUKA or Geant4, that offer better descriptions of particle-matter interactions and can treat lepton and ion beams. This includes the generation of secondary particles and fragmentation when tracking ions. In addition to the development of coupling with Geant4, the SixTrack-FLUKA coupling has recently been translated and integrated into the Xsuite environment as well. In this paper, we present the ongoing development of these tools. A thorough testing of the new implementation was performed, using as case studies various collimation layout configurations for the LHC Run 3.

INTRODUCTION

Xsuite is a modern Python toolkit developed at CERN to simulate particle behaviour in an accelerator [1, 2]. It aims at integrating existing tools for different applications into one framework, and as such currently consists of 6 individual Python packages: Xobjects, Xdeps, Xpart, Xtrack, Xfields, and Xcoll. The focus of this paper lies on the latter, which is dedicated to integrating collimation simulations featuring particle-matter interactions into this new framework [3].

Simulations that study how beam-intercepting devices like collimators influence the performance of an accelerator make use of two different types of software, namely a dedicated tool to track the 6D motion of a charged particle in an accelerator lattice, and a Monte Carlo simulation package for the interaction and transport of particles (including leptons and nuclei) in matter. For the former, SixTrack [4–12] has been the standard at CERN for many years, while for the latter two tools are principally used at CERN, namely FLUKA [13–19] and Geant4 [20–22]. Next, one needs to construct a communication that guarantees the adequate exchange of particles from the tracking code to the material interaction code and back. In the case of FLUKA this is managed by the FlukaIO coupling [23–26] which uses a network protocol for reliable transmission, while in the case of Geant4, this communication is handled by the BDSIM interface [27–30] which acts as a dedicated API to the Geant4 engine. Additionally, for simulations involving only protons without fragmentation, SixTrack has a built-in scattering engine called K2 to simulate proton-matter interactions [4, 31–33]. It greatly simplifies both the initial setup and final post-processing, while vastly reducing the necessary computation time, with excellent results when its output is used as input to FLUKA for energy deposition. All three scattering engines have been thoroughly benchmarked against experiment and each other.

A NEW APPROACH

With the advent of Xsuite and its move to Python and its modular approach, adapting the collimation code to the same environment is a logical step. Due to the complicated nature of this type of simulation, in particular the internal scattering engine and the coupling to external tools, this migration is quite challenging. Significant progress has been made, and we are nearing a complete integration into Xsuite. Furthermore, thanks to its design based on JIT (just-in-time) compilation to C, Xsuite is constructed to be compatible with many different architectures including GPUs [34]. The migration to Xsuite hence opens the road to high-performance computing for collimation as well.

Most tools needed to perform collimation studies in Xsuite are collected into the Xcoll Python package [3]. These include, but are not limited to:

- The management of collimator settings in a lattice via a database on file or in memory, and the automatic conversion of the collimator jaw openings in units of the transverse beam size into physical units;
- The generation of matched particle distributions, such as an annular halo or a pencil beam [35] at a given location, for a CPU-efficient simulation of the first particle encounters with the collimators (Xpart);
- An interpolation of losses on the aperture, to precisely define their location along the lattice (Xtrack);
- The logging of particles that are scattered by and absorbed in collimators and the aperture, in order to create a longitudinal histogram of losses (a loss map);
- The inclusion of and connection to adequate scattering engines to describe particle-matter interactions.

These capabilities were already present in the SixTrack environment, however, due to the modular nature of Python they become much more flexible in use and are easily expandable.

* frederik.van.der.veken@cern.ch

ISBN: 978-3-95450-253-0 ISSN: 2673-5571 doi:10.18429/JACoW-HB2023-THBP14

LHC OPTICS MEASUREMENTS FROM TRANSVERSE DAMPER FOR THE HIGH INTENSITY FRONTIER

T. Nissinen*, F. Carlier, M. Le Garrec, E. H. Maclean, T. H. B. Persson, R. Tomás,
A. Wegscheider, CERN, Geneva, Switzerland

Abstract

Current and future accelerator projects are pushing the brightness and intensity frontier, creating new challenges for turn-by-turn based optics measurements. Transverse oscillations are limited in amplitude due to particle losses. The LHC Transverse Damper (ADT) is capable of generating low amplitude ac-dipole like transverse coherent beam oscillations. While the amplitude of such excitations is low, it is compensated by the excitation length of the ADT which, in theory, can last for up to 48h. Using the ADT, it is possible to use the maximum BPM acquisition length and improve the spectral resolution. First optics measurements have been performed using the ADT in the Large Hadron Collider in 2023, and the results are presented in this paper. Furthermore, some observed limitations of this method are presented and their impact on ADT studies are discussed.

INTRODUCTION

Optics measurements from transverse turn-by-turn data are generally carried out with a single low intensity bunch to limit particle losses from the ac-dipole forced betatron oscillations [1]. This is particularly important for high energy accelerators where machine protection constraints are tight. Under such conditions the effects of high bunch intensities and large number of bunches on the optics are not measured. As bunch intensities are pushed further, the resulting optics perturbations become more relevant. Optics measurements under these conditions can yield valuable insights and provide new paths for machine optimisation.

Optics measurements in the Large Hadron Collider (LHC) are mostly performed by exciting coherent transverse oscillations using an ac-dipole [2–8]. These oscillations are measured at Beam Position Monitors (BPMs) around the ring. The spectral analysis of such signals provides amplitude and phase information of the main modes of oscillation from which the optics functions are calculated, as described in Refs. [9–11]. In the LHC, the ac dipole generates large amplitude, 6600 turns flattop excitations. In this paper, the ADT is used in an ac dipole-like mode, as an alternative excitation method to provide low amplitude coherent oscillation with a duration close the maximum recording limit of the BPMs. While lower in amplitude, the increase in number of turns provides an important improvement in the spectral resolution. Most importantly, the ac dipole may not be used with more than 3 low intensity bunches, while the ADT is considered safe for using during nominal operational conditions. It should be mentioned that in operation large chromaticity and Landau octupoles are used to mitigate coherent instabilities. These have an impact in the optics measurement technique that requires further studies [5, 6, 8, 11]. The ADT therefore opens up the possibility to perform optics measurements at the LHC intensity limit.

This paper describes the progress in performing linear and non-linear optics measurements using the LHC ADT in ac dipole mode. The first optics measurements are presented at injection energy with pilot bunches. Lastly, an analysis of the observed sidebands on the ADT excitation resulting from 50 Hz noise is presented.

PHASE RESOLUTION FROM TURN-BY-TURN DATA

The phase error on the main betatronic oscillation has been calculated from the spectral analysis of single BPM turn-by-turn data for different excitation conditions. Figure 1 shows the phase error obtained from turn-by-turn data of ac dipole and ADT excitations as a function of oscillation amplitude. A clear reduction of phase errors is observed for increasing oscillation amplitudes. Figure 1 also shows the measured betatron spectral phase error for ADT excitations with larger number of turns considering a single excitation per point. The phase resolution from ADT driven oscillations matches that from the ac dipole at injection energy.

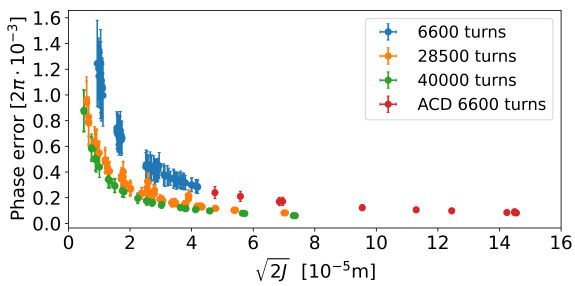

Figure 1: Phase error from ADT and ac dipole (ACD) excitations as a function of oscillation amplitude for different number of turns.

OPTICS MEASUREMENTS WITH THE ADT

Since the end of Run 2 the ADT is used for calculating coupling corrections during the nominal physics cycle in the LHC [12], and they are part of the operational procedure at the start of each fill. The aim of the current studies is to demonstrate the feasibility of performing optics measurements using the ADT, with the future goal of integrating this feature in the operational tools. Optics measurements were performed using the ADT with pilot bunches at injection

* tnissine@cern.ch

ISBN: 978-3-95450-253-0 ISSN: 2673-5571 doi:10.18429/JACoW-HB2023-THBP15

OPTIMIZING RESONANCE DRIVING TERMS USING MAD-NG PARAMETRIC MAPS

L. Deniau*, S. Kostoglou, E.H. Maclean, K. Paraschou, T. Persson, R. Tomás
CERN, Geneva, Switzerland

Abstract

In 2023, a review of the LHC octupolar resonance driving terms at injection was carried out, motivated by two observations: (i) unwanted losses during the injection process with strongly powered octupoles and (ii) an expected reduction in emittance growth from e-cloud effects in simulations with weaker octupolar resonances. The MAD-NG code was used to simultaneously optimize the main octupolar resonances: 4Qx, 4Qy, and 2Qx-2Qy by adjusting 16 quadrupole families and 16 octupole families, for a total of 32 parameters. These knobs were introduced as parameters in the transfer map, allowing the Jacobian required by the optimizer to be calculated in a single pass, saving 32 additional optics evaluations and avoiding finite difference approximations. Constraints on tunes, amplitude detuning, and optics around the machine were also considered as part of the optimization process. This paper reviews the parametric optimization with MAD-NG and compares the results with MADX-PTC.

INTRODUCTION

The review of the LHC octupolar resonance driving terms (RDTs) at injection was carried out in 2023 [1–4], motivated by the observation of undesirable losses during injection related to strongly powered octupoles, and by the will to reduce the emittance growth from e-cloud effects with weaker octupolar resonances. The MAD-NG code [5, 6] was used to simultaneously optimize the main octupolar resonances: 4Qx, 4Qy, and 2Qx-2Qy by adjusting 16 quadrupole families and 16 octupole families, for a total of 32 parameters.

To avoid any confusion, the following acronyms are used throughout this paper: MAD-X refers to the CERN code [7, 8], MADX-PTC refers to E. Forest's PTC/FPP library [9–11] embedded into MAD-X, and the keyword `MADX` refers to the special environment within MAD-NG that emulates the behavior of the global workspace of MAD-X.

To ease optimization with many knobs, MAD-NG offers a unique feature called *parametric differential maps* build from the generalized truncated power series algebra (GTPSA) [12], which combined with other well-designed features helps simplify the overall process:

1. Load MAD-X files of LHC sequences and injection optics into `MADX` environment with appropriate setup.
2. Create a parametric phase-space and *link* the knobs, e.g., magnet strengths, to the phase-space parameters.
3. Optimize the constraints by varying the knobs using the derivatives of relevant quantities versus these knobs.
4. Restore the knobs as scalars with optimized values.

* laurent.deniau@cern.ch

Each of these steps will be detailed in the following sections, starting from the preliminary setup performed by the script snippet below, where the `LHCB1` and `LHCB2` sequences and the optics file of MAD-X are directly read, translated and loaded into the special `MADX` environment in MAD-NG. The sequences are modeled with thick lens elements and a proton injection beam is created and attached to them:

```
local pb450=beam{particle='proton',energy=450}
MADX:load'lhc_seq.madx'
MADX:load'inj_optics.madx'
MADX.lhcb1.beam = pb450
MADX.lhcb2.beam = pb450
MADX.lhcb2.dir  = -1 -- set LHCB2 as reversed
```

PARAMETRIC MAPS

Setting up parametric phase-space in MAD-NG is simple, even when everything has been loaded inside the `MADX` environment. For convenience, we start by defining the lists of variable and parameter names of the 6D parametric phase-space such that they can be accessed by name everywhere:

```
local vars = { -- variable names (strings)
  -- 6 canonical variables of phase-space
  'x','px','y','py','t','pt'
}
local prms = { -- param./knob names (strings)
  -- 16 strengths of trim quadrupoles families
  'kqtf.a12b1','kqtf.a23b1',…,'kqtf.a81b1',
  'kqtd.a12b1','kqtd.a23b1',…,'kqtd.a81b1',
  -- 16 strengths of octupoles families
  'kof.a12b1' ,'kof.a23b1' ,…,'kof.a81b1',
  'kod.a12b1' ,'kod.a23b1' ,…,'kod.a81b1',
}
```

From these lists, we can define the parametric phase-space with `nv=6` variables of order `mo=5` and `np=32` parameters of order `po=1` named after the knobs in the optics file, and where the list of names must satisfy `#vn=nv+np`. The order of the *variables* must be `mo=4+1` as we want to optimize octupolar resonances at order 4 using their derivatives versus the knobs from order 5.

```
-- DA map representing parametric phase-space
local X0 = damap {nv=#vars,np=#prms,mo=5,po=1,
                  vn=tblcat(vars,prms)}
```

The next step is to link the knobs defined in the optics file to the parameters defined in the phase-space by replacing the knobs (scalars) in the `MADX` environment with their corresponding parameters (GTPSA) from the phase-space. Thanks to MAD-NG's deferred expressions and physics support for polymorphism, which simplifies the whole process through automatic handling by the `track` and `twiss` commands. This is achieved by the loop hereafter that replaces the knobs in `MADX` by the sum of knobs and parameters with

ISBN: 978-3-95450-253-0 ISSN: 2673-5571 doi:10.18429/JACoW-HB2023-THBP16

EMITTANCE GROWTH FROM ELECTRON CLOUDS FORMING IN THE LHC ARC QUADRUPOLES

K. Paraschou*, H. Bartosik, L. Deniau, G. Iadarola, E. H. Maclean, L. Mether, Y. Papaphilippou, G. Rumolo, R. Tomás, CERN, Geneva, Switzerland,
T. Pieloni, J. Potdevin, EPFL, Lausanne, Switzerland.

Abstract

Operation of the Large Hadron Collider with proton bunches spaced 25 ns apart favors the formation of electron clouds. In fact, a slow emittance growth is observed in proton bunches at injection energy (450 GeV), showing a bunch-by-bunch signature that is compatible with electron cloud effects. The study of these effects is particularly relevant in view of the planned HL-LHC upgrade, which relies on significantly increased beam intensity and brightness. Particle tracking simulations that take into account both electron cloud effects and the non-linear magnetic fields of the lattice suggest that the electron clouds forming in the arc quadrupoles are responsible for the observed degradation. In this work, the simulation results are studied to gain insight into the mechanism which drives the slow emittance growth. Finally, it is discussed how optimizing the optics of the lattice can allow the mitigation of such effects.

INTRODUCTION

Simulations of incoherent electron cloud (e-cloud) effects for the Large Hadron Collider (LHC) in its typical injection energy configuration were described in Refs. [1–3]. The results showed that incoherent emittance growth can be caused by the e-clouds forming in the main quadrupoles. This can be understood from the fact that the e-cloud forming in the main quadrupoles shows a significant electron density at the beam's location. Contrary to that, the e-clouds forming in the dipoles have electron densities that are concentrated at distances far away from the center of the beam.

This contribution is focused on the analysis of the beam dynamics for LHC e-cloud simulations, in order to gain information on the mechanism driving the emittance growth. In the first part of the paper, the effect of synchro-betatron resonances is identified to be present in the dynamics of the protons, through the Frequency Map Analysis (FMA) [4] method. This observation led to an effort to improve the LHC optics through a change in the arc-by-arc phase advance, which minimizes the excitation of fourth-order resonances by the lattice octupoles and of synchro-betatron resonances from the e-clouds [5,6]. In the second part of this paper, long-term tracking simulations are presented, showing that the emittance growth from e-cloud effects improves significantly as a result of the optics modification.

* konstantinos.paraschou@cern.ch

SIMULATION METHOD

The analysis of the beam dynamics is done through turn-by-turn particle tracking simulations using the Xsuite software [7], where the elements of the LHC lattice and the e-cloud interactions are modelled with thin lenses. Strong non-linearities with sextupolar and octupolar magnets are induced on purpose during the typical operation of the LHC. These non-linearities are necessary to prevent coherent beam instabilities caused by the electron clouds themselves. Normally, during the 2022 and the 2023 runs, the sextupole magnets were powered to achieve chromaticity values of $Q'_x = Q'_y = 25$, while the octupole magnets were powered to approximately 40 A, inducing an amplitude detuning characterized by the detuning coefficients $\alpha_{xx} = 0.31\,\mu\text{m}^{-1}$, $\alpha_{yy} = 0.32\,\mu\text{m}^{-1}$, $\alpha_{xy} = \alpha_{yx} = -0.22\,\mu\text{m}^{-1}$ [8].

The effect of the e-cloud is simulated by using a scalar potential that has been generated with the PyECLOUD multipacting simulation code [9], under the effect of a quadrupolar magnetic field (12.1 T/m) and bunches spaced by 25 ns, each with $1.2 \cdot 10^{11}$ protons per bunch, normalized transverse emittances equal to 2 µm and an r.m.s. bunch length equal to 9 cm. The surface of the beam chamber is assumed to have a uniform Secondary Emission Yield (SEY) with a maximum equal to 1.4 and the e-cloud interaction is modelled as a thin-lens following the formalism in Ref. [10]. Moreover, a tricubic interpolation scheme is employed to ensure that the

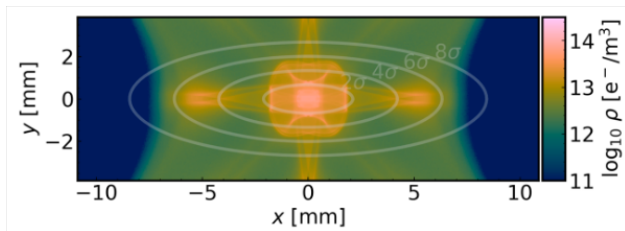

Figure 1: Snapshot of an electron cloud forming in a main quadrupole of the LHC.

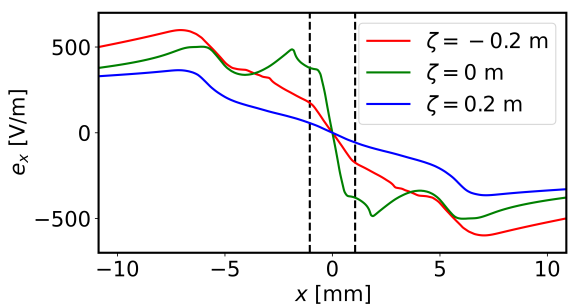

Figure 2: Normalized horizontal force at $y = 0$ for different times during the bunch passage.

ISBN: 978-3-95450-253-0 ISSN: 2673-5571 doi:10.18429/JACoW-HB2023-THBP17

TRANSVERSE COHERENT INSTABILITY STUDIES FOR THE HIGH-ENERGY PART OF THE MUON COLLIDER COMPLEX*

D. Amorim†, F. Batsch, L. Bottura, D. Calzolari, C. Carli, H. Damerau, A. Grudiev, A. Lechner, E. Métral, D. Schulte, K. Skoufaris, CERN, Geneva, Switzerland
T. Pieloni, EPFL, Lausanne, Switzerland
A. Chancé, CEA-IRFU, Saclay, France

Abstract

The International Muon Collider Collaboration (IMCC) is studying a 3 TeV center-of-mass muon collider ring as well as a possible next stage at 10 TeV. Current studies focus mainly on the 10 TeV collider and its injector complex. Muons being 200 times heavier than electrons, limitations from synchrotron radiation are mostly suppressed, but the muon decay drives the accelerator chain design. After the muon and anti-muon bunches are produced and 6D cooled, a series of Linacs, recirculating Linacs and Rapid Cycling Synchrotrons (RCS) quickly accelerate the bunches before the collider ring.

A large number of RF cavities are required in the RCS to ensure that over 90 % of the muons survive in each ring. The effects of cavities higher-order modes on transverse coherent stability have been investigated in detail, including a bunch offset in the cavities, along with possible mitigation measures.

In the collider ring, the decay of high-energy muons is a challenge for heat load management and radiation shielding. A tungsten liner will protect the superconducting magnet from decay products. Impedance and related beam stability have been investigated to identify the minimum vacuum chamber radius and transverse damper properties required for stable beams.

INTRODUCTION

A muon collider could reach high luminosity and multi-TeV center-of-mass (c.o.m) energy collisions with leptons. The muon mass being 200 times larger mass than the electron, limitations from synchrotron radiation encountered with electron-positron colliders are suppressed [1]. The goal of the International Muon Collider Collaboration [2, 3] and the MuCol program [4] is to study a 3 TeV c.o.m $\mu^+ - \mu^-$ collider, with the option of a following 10 TeV c.o.m stage.

Maximum instantaneous luminosities of $1.8 \times 10^{34}\,\mathrm{cm^{-2}\,s^{-1}}$ for the 3 TeV collider and $20 \times 10^{34}\,\mathrm{cm^{-2}\,s^{-1}}$ for the 10 TeV collider are targeted. Reaching these high luminosities requires to minimize the decay of of both the muon and the anti-muon bunch. With a 10 km circumference for the 10 TeV collider, the revolution period of a beam traveling at the speed of light is 33 µs, much longer than the muon lifetime at rest of $\tau_0 = 2.2$ µs. However, thanks to relativistic time dilation, the muon lifetime in the laboratory frame τ increases with the Lorentz factor γ as $\tau = \gamma\tau_0$. In the 10 TeV collider, with $\gamma = 47323$, the muon lifetime reaches $\tau = 104$ ms.

The US MAP project [5] developed a muon/anti-muon production and acceleration concept, schematized in Fig. 1. Muons are first produced by hitting a target with a high power proton beam. Then both longitudinal and transverse emittances are reduced through a ionization cooling stage. Afterwards an acceleration stage provides a fast energy increase to the muon beams to quickly increase their γ.

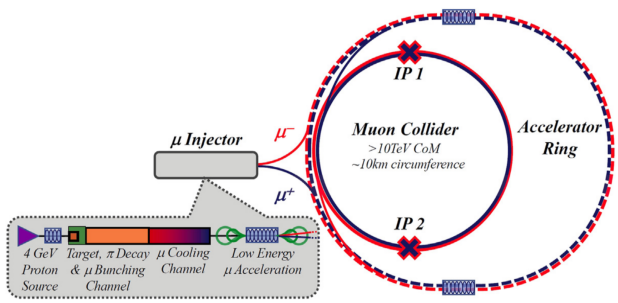

Figure 1: Proposed layout of a muon collider and its muon production and acceleration stages. Picture from Ref. [6].

Emittance preservation through the acceleration stages are fundamental to obtain the target luminosity in the absence of synchrotron radiation damping mechanism. Transverse beam coupling impedance models were developed for the first Rapid Cycling Synchrotron and the 10 TeV collider, and are then used to simulate coherent beam stability effects in these two accelerators.

IMPEDANCE AND STABILITY STUDIES FOR THE RCS

The last acceleration stage before the 3 TeV collider ring comprises three Rapid Cycling Synchrotrons that increase the muon and anti-muon beam energy from ~60 GeV to 1.5 TeV. For the 10 TeV collider, a fourth RCS would further accelerate the muon beams from 1.5 TeV to 5 TeV.

In each of these RCS, the targeted muon survival rate is at least 90 %. For the first RCS of the chain (RCS 1), whose parameters are summarized in Table 1, an energy increase of 14.8 GeV per turn is required, which in turn requires a total of 20.9 GV RF voltage for the ring [7].

* Work funded by the Swiss Accelerator Research and Technology program (CHART) and by the European Union (EU). Views and opinions expressed are however those of the authors supported only and do not necessarily reflect those of the EU or European Research Executive Agency (REA). Neither the EU nor the REA can be held responsible for them.
† david.amorim@cern.ch

ISBN: 978-3-95450-253-0 ISSN: 2673-5571 doi:10.18429/JACoW-HB2023-THBP18

REVISED COLLIMATION CONFIGURATION FOR THE UPDATED FCC-hh LAYOUT

A. Abramov*, R. Bruce, M. Giovannozzi, G. Perez-Segurana, S. Redaelli, T. Risselada
CERN, 1211 Meyrin, Switzerland

Abstract

The collimation system for the hadron Future Circular Collider (FCC-hh) must handle proton beams with an unprecedented nominal beam energy and stored beam energy in excess of 8 GJ, and protect the superconducting magnets and other sensitive equipment while ensuring a high operational efficiency. The recent development of the 16-dipole lattice baseline for the FCC-hh, and the associated layout changes, has necessitated an adaptation of the collimation system. A revised configuration of the collimation system is presented, considering novel high-beta optics in the betatron collimation insertion. Performance is evaluated through loss map studies, with a focus on losses in critical areas, including collimation insertions and experimental interaction regions.

INTRODUCTION

The hadron Future Circular Collider (FCC-hh) [1] is a design study for a 91 km circumference energy frontier hadron collider, providing 84 TeV to 120 TeV centre of mass proton-proton collisions by using advanced magnet technology. One of the challenges for the collider is the stored beam energy of up to 8.3 GJ for the Conceptual Design Report (CDR) [1] reference 50 TeV energy per beam, which is a factor 21 higher than the achieved stored beam energy in the CERN Large Hadron Collider (LHC) [2], and a factor 12 higher than in the High-Luminosity LHC (HL-LHC) design [3]. The stored beam energy could be even higher, 10 GJ, for the upper end 60 TeV per beam if the CDR beam intesnity is considered. A highly efficient collimation system is required to ensure safe operation of the collider and avoid the risk of superconducting magnet quenches during regular operation and accidental loss scenarios, while tolerating instantaneous loss power of up to 11.6 MW in design loss scenarios for the CDR beam energy, based on the LHC design loss scenarios. The first design of the FCC-hh collimation system, based on a scaled version of the system installed in the LHC, was developed for the CDR [1, 4], where a comprehensive study campaign found that the system was adequate for operation with nominal proton and heavy-ion beams [5, 6]. The current focus of FCC-hh studies is to align the ring layout and infrastructure to the first-stage lepton collider, FCC-ee, and to explore new design concepts. As a result of the post-CDR studies, there have been significant changes in the ring layout and optics, which affect the collimation performance and must be studied in detail. This paper provides an outline of the configuration of the latest FCC-hh baseline, the adaptations required for the collimation system, and preliminary results from collimation tracking studies.

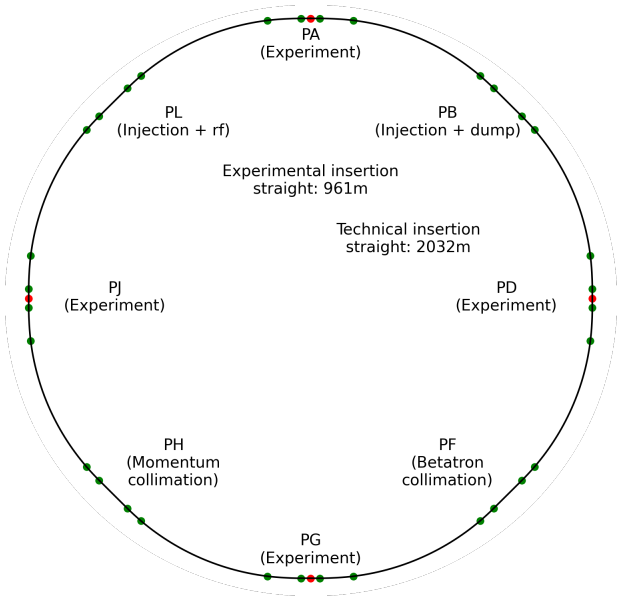

Figure 1: Layout of the FCC-hh, showing the experimental insertions PA, PD, PG, PJ, and the technical insertions PB, PF, PH, and PL. Interaction points are shown as red dots, and dispersion suppressor boundaries with green dots.

LAYOUT AND OPTICS CHANGES

The first major redesign of the FCC-hh layout after the CDR was completed in 2023 [7] and featured a significant change of the ring geometry, to match the tunnel layout and the FCC-ee collider rings, as well as changers to the optics. The first collimation studies for the new FCC-hh configuration were carried out with an early iteration of the design [8], and showed that the changes impact the performance of the collimation system. The latest development of the FCC-hh layout and optics have resulted in a new stable baseline, which implements further design changes. The layout of the ring is shown in Fig. 1.

The main differences include a change in circumference to 90.66 km, down from 91.17 km in the previous iteration and 97.75 km in the CDR, shortening of the technical insertions from 2160 m to 2032 m, and changes to the geometry of the interaction region (IR) to displace the interaction points (IPs) radially outwards to match the FCC-ee IPs, leading to IR shortening from 1400 m to 936 m. The experimental IRs also feature new dogleg geometry, due to the use of superconducting separation and recombination dipoles, as well as a new dispersion suppressor (DS) geometry. There

* andrey.abramov@cern.ch

ISBN: 978-3-95450-253-0 ISSN: 2673-5571 doi:10.18429/JACoW-HB2023-THBP19

EXPERIMENTAL INVESTIGATIONS ON THE HIGH-INTENSITY EFFECTS NEAR THE HALF-INTEGER RESONANCE IN THE PSB

T. Prebibaj*, F. Antoniou, F. Asvesta, H. Bartosik, CERN, Geneva, Switzerland
G. Franchetti, GSI Helmholtzzentrum für Schwerionenforschung, Darmstadt, Germany

Abstract

Space charge effects are the main limitation for the brightness performance of the Proton Synchrotron Booster (PSB) at CERN. Following the upgrades of the LHC Injectors Upgrade (LIU) project, the PSB delivered unprecedented brightness even exceeding the projected target parameters. A possibility for further increasing the brightness is to operate above the half-integer resonance $2Q_y = 9$ in order to avoid emittance blow-up from resonances at $Q_{x,y} = 4$ due to the strong space charge detuning. The half-integer resonance can be compensated to a great extent using the available quadrupole correctors in the PSB, and also deliberately excited in a controlled way. The control of the half-integer resonance and the flexibility of the PSB to create a variety of different beam and machine conditions allowed the experimental characterization of space charge effects near this resonance. This contribution reports the experimental observations of the particle trapping during the dynamic crossing of the half-integer resonance, as well as systematic studies of the beam degradation from space charge induced resonance crossing.

INTRODUCTION

The brightness performance of the PSB is limited by space charge effects at injection. At high beam intensities, emittance growth is induced by the interaction of the beam with the resonances around the integer tunes $Q_{x,y} = 4.0$ due to the large space charge tune spread. Studies demonstrated that operation with high working points at injection, i.e. $4.40 < Q_{x,y} < 4.5$, far from $Q_{x,y} = 4.0$, mitigate this emittance growth and increase the beam brightness [1]. An injection at even higher working points, i.e. above the half-integer resonance $2Q_y = 9$ ($Q_y > 4.5$), could further mitigate the undesired emittance growth. However, in this scenario, to reach the extraction working point $(Q_x, Q_y) = (4.17, 4.23)$, the half-integer resonance needs to be dynamically crossed during the acceleration cycle. The dynamic crossing of (compensated) third and fourth order resonances is a common practice during the PSB operation [2]. However, the half-integer resonance is much stronger and thus more difficult to control to avoid particle losses and/or emittance growth.

In this context, a series of studies were initiated in order to characterize the effects of space charge when crossing the half-integer resonance with tunes $Q_y > 4.5$ (from above). These effects can change depending on the resonance strength, the crossing speed and the space charge tune spread. The eventual goal is to experimentally study and understand the beam behaviour under these conditions and to find ways to increase the achievable beam brightness.

Operationally, the high-brightness beams in the PSB have space charge tune spreads that can exceed $\Delta Q_{x,y} = -0.5$ and thus overlap multiple resonances. In addition, the synchrotron oscillations induce a modulation in the local line density of the particles and therefore a modulation in their space charge tune-shift, which can lead to periodic resonance crossing and associated beam degradation [3]. To remove some of the operational complexities, the starting point of the studies presented here was the use of a relatively lower intensity, unbunched (coasting) beam in a non-accelerating cycle. This contribution will focus only on the half-integer crossing under these special beam conditions.

EXPERIMENTAL SETUP

The half-integer resonance $2Q_y = 9$ has been characterized experimentally in the PSB [4]. In the bare machine, the resonance is excited by residual quadrupole errors in the machine and can be compensated by two families of orthogonal quadrupole correctors, namely QNO412 and QNO816. A controlled excitation of the resonance can be performed by slightly varying the strengths of the correctors with respect to their compensating value. In this way, the resonance stopband has a finite width that is strong enough to have a measurable effect on the beam, but not too strong (like the uncompensated resonance) so that the beam is fully lost and cannot be measured. For the purposes of these experiments the half-integer resonance is excited by changing the current of the QNO816 family by $\delta I_{816} = -2$ A from its compensation value (integrated focusing strength of $\delta k_1 l_{816} = -6.2 \times 10^{-4}$ m^{-1}). This corresponds to a stopband width of smaller than $\delta Q = 0.004$ [4].

Beams with different intensities and transverse emittances can be used in the PSB. The coasting beam is created by injecting a long pulse from Linac4, that almost fills the PSB circumference, and keeping all RF cavities switched off. The beam fully debunches after only 500 turns. In addition, the vertical chromaticity has been corrected close to zero using the available sextupole correctors. Therefore, the chromatic tune spread can be considered negligible.

PARTICLE TRAPPING

The stability of the particle motion near a resonance depends on the distance of the working point from the resonance and the amplitude detuning. Here, the detuning of the particles comes mainly from the space charge defocusing which is amplitude dependent: particles at low amplitude (near the beam core) receive the strongest detuning while

* tirsi.prebibaj@cern.ch

ISBN: 978-3-95450-253-0 ISSN: 2673-5571 doi:10.18429/JACoW-HB2023-THBP20

OPTICS FOR LANDAU DAMPING WITH MINIMIZED OCTUPOLAR RESONANCES IN THE LHC

R. Tomás*, F. Carlier, F. Chudoba, L. Deniau, J. Dilly, S. Horney, M. Hostettler, J. Keintzel, S. Kostoglou, M. Le Garrec, E.H. Maclean, T. Nissinen, K. Paraschou, T. Persson, M. Solfaroli, F. Soubelet, A. Wegscheider and J. Wenninger, CERN, Geneva, Switzerland

Abstract

Operation of the Large Hadron Collider (LHC) requires strong octupolar magnetic fields to suppress coherent beam instabilities. The amplitude detuning that is generated by these octupolar magnetic fields brings the tune of individual particles close to harmful resonances, which are mostly driven by the octupolar fields themselves. In 2023, new optics were deployed in the LHC at injection with optimized betatronic phase advances to minimize the resonances from the octupolar fields without affecting the amplitude detuning. This paper reports on the optics design, commissioning and the lifetime measurements performed to validate the optics.

INTRODUCTION

In 2022 losses driven by the Landau octupoles and chromaticity were observed in the LHC at injection [1]. In addition, e-cloud simulations showed that the LHC Landau octupoles drive emittance growth that could be mitigated by reducing resonance driving terms [2]. These observations motivated the quest for a new injection optics in the LHC aiming to suppress the main resonances driven by the Landau octupoles via parametric optics matching in the LHC [3]. To minimize the changes between 2022 and 2023 only arc trim quadrupoles would be used in the optimization with the only constraints of keeping the same tunes and a β-beating below 5% in the Insertion Regions (IRs), with respect to the 2022 optics. Therefore, the phase advances between the different arcs are the key parameters in the optimization.

In the arc12 of Beam 1 there is a total of 21 octupoles, 13 of them are defocusing and are placed in 13 consecutive FODO cells with a phase advance of about $\pi/2$. The remaining 8 focusing octupoles are interleaved with the defocusing octupoles, extending over 10 consecutive FODO cells but skipping 2 cells. In arc23 the same structure is present but swapping the focusing and defocusing roles of the octupoles. These two structures alternate along the 8 arcs of both beams with the exception of arc56 in Beam 1, where instead of 13 defocusing octupoles there are only 10 available. Within one arc the focusing octupoles drive the $4Q_x$ resonance in-phase and the defocusing octupoles drive the $4Q_y$ resonance in-phase too. The resonance $2Q_x - 2Q_y$ is driven by all focusing and defocusing octupoles within one arc with similar phases. The resonance driving terms (RDTs) f_{2002}, f_{4000}, f_{0004} drive the resonances $2Q_x - 2Q_y$, $4Q_x$ and $4Q_y$, respectively.

* rogelio.tomas@cern.ch

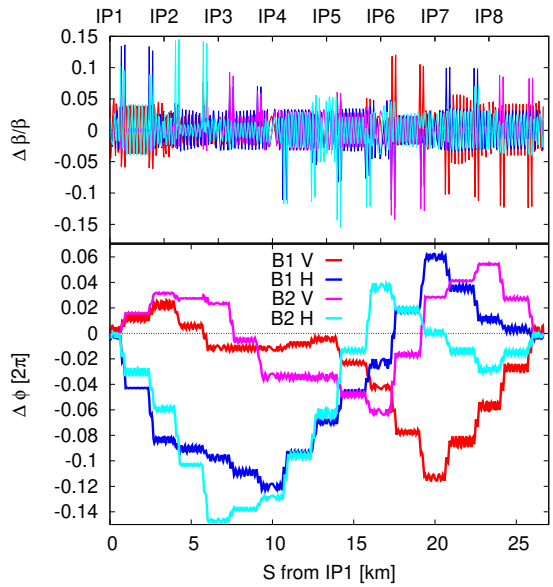

Figure 1: Relative β-function and phase advance deviations between the 2023 and 2022 optics at $Q_{x,y} = (62.270,\ 60.295)$.

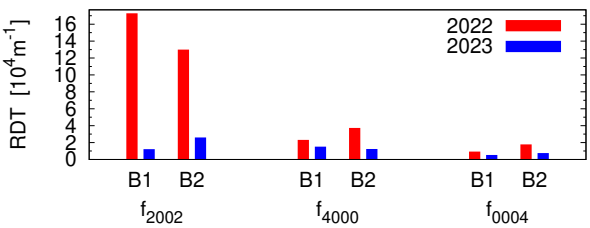

Figure 2: Average octupolar RDTs in the 2023 and 2022 optics at $Q_{x,y} = (62.270,\ 60.295)$ for both beams.

Figure 1 shows the resulting β-beating and phase advance shift between the 2023 and the 2022 design optics. A peak β-beating of about 5% is seen in the IRs with spikes of up to 15% at the location of the trim quadrupoles in the arcs. Phase advance shifts up to 50° are induced. Figure 2 shows a comparison between the RDTs in the two optics with Landau octupoles powered at 40 A and chromaticities of $Q'_{x,y} = 25$. All RDTs are reduced between 2022 and 2023, achieving large factors above 5 for the $2Q_x - 2Q_y$ resonance in both beams. Dynamic aperture simulations show a remarkable improvement by more than 1σ for both beams, see Ref. [3].

OPTICS COMMISSIONING

Optics measurements and corrections are necessary in LHC to meet tolerances. During Run 1 optics corrections

ISBN: 978-3-95450-253-0 ISSN: 2673-5571 doi:10.18429/JACoW-HB2023-THBP21

INCREASING HIGH LUMINOSITY LHC DYNAMIC APERTURE USING OPTICS OPTIMIZATIONS*

R. De Maria†, Y. Angelis[1], C. Droin, S. Kostoglou, F. Plassard,
G. Sterbini, R. Tómas, CERN, Geneva, Switzerland
[1]also at Aristotle University of Thessaloniki, Thessaloniki, Greece

Abstract

CERN's Large Hadron Collider (LHC) is expected to operate with unprecedented beam current and brightness from the beginning of Run 4 in 2029. In the context of the High Luminosity LHC project, the baseline operational scenarios are currently being developed. They require a large octupole current and a large chromaticity throughout the entire cycle, which drives a strong reduction of dynamic aperture, in particular at injection and during the luminosity production phase. Despite being highly constrained, the LHC optics and sextupole and octupole corrector circuits still offer a few degrees of freedom that can be used to reduce resonances and the extent of the tune footprint at constant Landau damping, thereby leading to an improvement of the dynamic aperture. This contribution presents the status of the analysis that will be used to prepare the optics baseline for LHC Run 4.

INTRODUCTION

The HL-LHC project [1] aims at upgrading the insertion regions of the high luminosity experiments and ancillary systems all around the LHC run, enabling the collection of over 3000 fb^{-1} proton-proton luminosity in ATLAS and CMS and, at the same time, providing collisions to the ALICE and LHCb experiments.

Run 4 is the first run with the new HL-LHC hardware, notably Nb_3Sn triplet magnets, crab cavities (CC), full remote alignment system, new collimation system, and additional cryogenic plants. The first year is expected to be mostly dedicated to commissioning activities, with luminosity production reaching the yearly integrated luminosity target of 250 fb^{-1} by the end of Run 4, while still integrating a substantial amount of luminosity (750 fb^{-1}) in the first 4 operational years [2–4].

OPTICS CHALLENGES

The Run 4 optics for protons should accommodate numerous challenges spanning very different aspects, among which the dynamic aperture is one of them. Before addressing the dynamic aperture, it is useful to recall the optics challenges.

Run 4 will use for the first time magnets based on the novel Nb_3Sn technology, in particular the triplets in IP 1 and 5, that could be critical for optics control and correction. Therefore, the lowest β^* at the end of the luminosity levelling is expected to be difficult to commission [5]. At the same time, the population of the bunch is expected to be lower than the HL-LHC baseline to match the bunch charge achieved during Run 3 [1, 3]. Similarly, in the first year of Run 4 it is planned to use β^* values close to those already achieved in Run 3. It is also important to prepare an optics cycle that allows pushing β^* during Run 4 and even further for the machine studies in preparation for Run 5. In this respect, Run 4 optics should be prepared to support a large range of β^* at the flat top and the end of levelling.

Table 1: Critical phase advance in degrees (modulo 360°) for the end-of-levelling optics ($\beta^* = 15$ cm) without optimizations. The values are marked red when close to the worst possible case, orange when not yet ideal, and black for those close to the best case. Red values are not a blocking issue but require mitigation, such as relaxing the collimator hierarchy and thus limiting the optimum β^* reach. Crab-cavities (CC) to tertiary collimators (TCP) phase advance should be smaller than 30° mod 180°. Dilution kickers (MKD) to TCT phase advance should be smaller than 30° mod 180°. The primary collimators (TCP) to TCT should be either below 30° or in between 70 – 110° mod 180°.

CC-TCP	**B1 Left**	**B1 Right**	**B2 Left**	**B2 Right**
CC1 H	88.21	86.76	28.77	29.93
CC5 V	21.19	19.74	-52.65	-36.87
MKD-TCT	**A.B1**	**O.B1**	**A.B2**	**B.B2**
TCTH1	-4.85	1.35	-18.7	-14.74
TCTH5	-29.87	-23.67	-30.97	-27
TCTH8	3.55	9.74	57.16	61.12
TCP-TCT	**B1 H**	**B1 V**	**B2 H**	**B2 V**
TCT1	23.75	-81.71	81.78	-31.38
TCT5	-1.27	-85.69	69.52	-13.25
TCT8	32.14	77.75	-22.36	-82.54

One of the key ingredients to obtain low-β^* in ATLAS and CMS is to run with the tightest possible hierarchy of collimators. The minimum gap of collimators is limited by several constraints of various origins. These constraints can be mitigated by special optics design. The primary and secondary collimator gaps are limited by impedance. New special optics [6] are being studied and tested to increase the β-functions and thereby the gap at the collimator, during the ramp and flat top, as the geometrical emittance reduces. Furthermore, the phase advance from the TCP to the TCT must be optimised to avoid an increase in background [7] and the phase advance from the CCs to the TCPs should be

* Work supported by the High Luminosity LHC Project
† riccardo.de.maria@cern.ch

ISBN: 978-3-95450-253-0 ISSN: 2673-5571 doi:10.18429/JACoW-HB2023-THBP22

ON LIOUVILLIAN HIGH POWER BEAM ACCUMULATION

J.-M. Lagniel[1,2], N. Milas[1,*], M. Eshraqi[1]
[1]European Spallation Source ERIC, Lund, Sweden
[2]Grand Accélérateur National d'Ions Lourds (GANIL), Caen, France

Abstract

It is acknowledged that the injection of high power proton beams into synchrotrons must be done using stripping injection of H^- beams which are accelerated by an injector, as done in many facilities worldwide such as ISIS, JPARC, SNS and CERN. However, this technique is not necessarily the only way of accumulation and in some cases might not represent the best choice. For example in the case of the ESSνSB Accumulator Ring, injecting the protons into the ring could represent savings in capital cost, reduced risk of losses in the linac and transfer lines and simplification to the overall project. This work presents the development of a method allowing to optimize the 4D Liouvillian accumulation of high-power proton and heavy ion beams.

INTRODUCTION

The European Spallation Source (ESS) [1], presently under construction in Lund, Sweden, will be the world's brightest neutron source, powered by a 5 MW proton linac. The linac accelerates proton pulses to 2 GeV, at a repetition rate of 14 Hz and a duty cycle of 4 %, before transport to the target station. The RF cavities at ESS can accept up to 10 % duty cycle, which means that it has the capability to provide an additional 5 MW of beam power. To this end, the ESS linac can, with moderate modifications, be used for the production of a very intense neutrino beam [2]. The ESSνSB project studies this possibility and a possible upgrade to the facility, which includes adding a H^- source and extra accelerating cavities for the linac, a transfer line and an accumulator ring (AR) that would then provide short proton pulses to the neutrino targets.

The main goal of this study is to analyse the possibility to inject protons from the linac directly into the accumulator using a 4D Liouvillian multi-turn accumulation process. The motivation is to analyse the advantages and drawbacks of such a choice in the ESS-specific case, considering the added complexity of the dual source front-end, issues with H^- source reliability and lifetime, losses due to H^- stripping in the linac and transfer line to the ring and the substantial increase in complexity of the control and safety system. Also, an accumulation at higher energy, which is the case of the ESSνSB project at 2.5 GeV, has the advantages to be done with lower emittances and lower space-charge effects compared with its counterparts in US (SNS) and Japan (J-PARC).

* natalia.milas@ess.eu

METHOD

The code developed for Liouvillian Injection Optimization (LIO) uses a formalism similar to the one used in MISHIF [3]. While the goal of MISHIF is to optimize the multiturn injection parameters in order to accumulate a maximum of beam in a given ring acceptance the goal of LIO is to minimize the ring acceptance needed for no losses, in short, to get 100 % accumulation efficiency in an emittance as small as possible. In other words, the ring acceptance is an input parameter for MISHIF while it is an output parameter for LIO. The reason for this choice looks obvious since the objective is to accumulate a 5 MW beam, with no loss budget considering this huge beam power.

100 % Emittance

LIO is built to optimize the injection parameters considering that 99.999 % of the injected beam should be stored without loss (50 W loss budget). To avoid the need for particle tracking and heavy simulations at this exploratory phase, the calculations are then done considering un-normalized transverse emittance of $\varepsilon_{100} = 26 \cdot \varepsilon_{rms} = 2.8$ mm mrad in both planes [4]. One can notice that this emittance is defined by the far halo particles for which the space charge effects from the beam core are very weak.

Optimized Injection Parameters

The link between the injected (index i) and stored (index r) beam parameters to obtain an optimized 4D injection (see Refs. [3] and [4]) is given by the equations below:

$$\frac{\beta_{r,i}}{\alpha_{r,i}} = \frac{\beta_{i,x}}{\alpha_{i,x}} = \frac{x_i}{x'_i} = -\frac{x_i - x_{co}(n)}{x'_i - x'_{co}(n)}, \quad (1)$$

$$\frac{\beta_r}{\beta_i} = \left(\frac{\varepsilon_r}{\varepsilon_i}\right)^{1/3}, \quad (2)$$

with similar equations also valid for the vertical plane. α and β are the Courant-Snyder (C-S) parameters, ε the emittances, (x_i, x'_i) the injected beam position and angle in the closed-orbit coordinate system, $(x_{co}(n), x'_{co}(n))$ the closed-orbit position and angle at turn n.

Choices for the ESSnuSB AR

To have a complete accumulation in ESSνSB AR we need to inject and store ε_{100} for a total of 600 turns with no loss. In order to investigate this possibility few choices are needed. The first choice is to work with fixed injected beam parameters to allow the use of collimators to precisely define the injected beam transverse emittances with some freedom on the C-S parameters in the transfer line (injected beam control).

ISBN: 978-3-95450-253-0 ISSN: 2673-5571 doi:10.18429/JACoW-HB2023-THBP23

EXPLORING SPACE CHARGE AND INTRA-BEAM SCATTERING EFFECTS IN THE CERN ION INJECTOR CHAIN

E. Waagaard, H. Bartosik, CERN, Geneva, Switzerland

Abstract

As of today, the LHC ion physics programme is mostly based on Pb ion collisions. For the future, the ALICE3 detector proposal requests significantly higher nucleon-nucleon luminosities, as compared to today's operation. This improved performance could be potentially achieved with ion species that are lighter than Pb. In this respect, the CERN Ion Injector chain (consisting of LINAC3, LEIR, PS and SPS) will need to provide significantly higher beam intensities with light ion beams as compared to Pb, whereas operational experience with such beams is limited. We present space charge and intra-beam scattering studies across the Ion Injector chain to identify the relative impact of these effects. This is the first step for identifying the ideal ion isotopes and charge states for maximised LHC luminosity production.

INTRODUCTION

The Large Hadron Collider (LHC) ion physics programme is mostly based on heavy-ion collisions using lead (Pb) ion beams [1]. The ion injector chain consists of the ion source, LINAC3, the Low-Energy Ion Ring (LEIR), the Proton Synchrotron (PS) and the Super Proton Synchrotron (SPS), as described in detail in [2]. The present CERN ion injector chain is shown in Fig. 1, with the path of Pb ions, their charge state and associated stripper foils highlighted.

Injector optimizations have been undertaken along the years for maximising the beam intensities within the LHC Injector Upgrade (LIU) project [2, 3]. Two alleged intensity limitations that remain are space charge (SC) and intra-beam scattering (IBS) effects [4]. SC and IBS have been studied extensively in the context of resonances [5–7] and to increase extracted bunch intensity from LEIR [9], but the combined impact of SC and IBS still remains as one of the main bottlenecks to higher bunch intensity injected into the LHC.

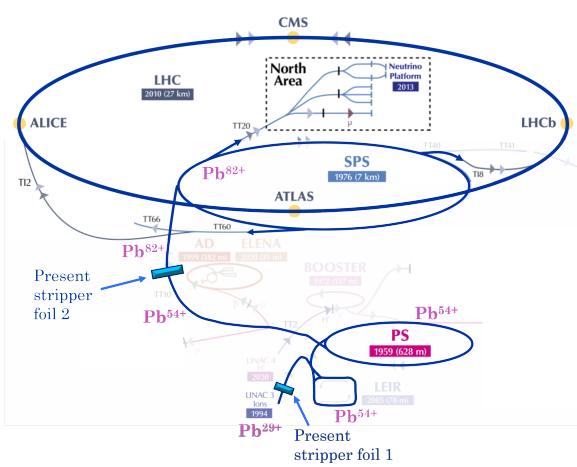

Figure 1: The CERN Ion Injector Chain [8].

These beam-degrading effects are important in the light of future CERN ion programmes, first to be tested with an upcoming short oxygen $^{16}O^{8+}$ pilot run for the LHC in 2024 [10]. Working Group 5 (WG5) of the HL/HE-LHC Workshop presented in 2018 a report to extend the LHC ion programme beyond Run 4 with ions lighter than Pb for higher beam intensities and nucleon-nucleon luminosities in the LHC [11], also highlighted by the 2022 Letter of Intent of the ALICE3 collaboration [12]. Also the NA61/SHINE experiment at the CERN North Area (NA) has requested ion species such as O, magnesium (Mg) and boron (B) beams [13], most of them untested in the CERN accelerator complex. In this article, we present a first mapping of the SC and IBS effects based on measured beam parameters throughout the Pb cycles in LEIR, PS and SPS.

SPACE CHARGE AND INTRA-BEAM SCATTERING

Space charge is a fundamental collective effect, referring to the Coulomb forces between charged particles in a high-intensity beam. This effect results in a non-linear defocusing force [14], introducing a tune spread of the beam particles. Space charge does not by itself cause beam losses, but can excite resonances far away from the set tune if the tune spread is large enough, or in combination with resonances excited by magnetic imperfections, leading to emittance growth and beam losses [15]. In this study, we calculate the maximum SC-induced tune shift $\Delta Q_{x,y}$ from the lattice integral in Eq. (18) in [14]. $\Delta Q_{x,y}$ is larger for smaller emittances, higher bunch intensities and lower energy.

Intra-beam scattering is a stochastic process of small-angle multiple Coulomb scattering of charged particles in a beam that leads to momentum exchange between the planes and emittance growth. The IBS emittance growth rates $1/T_{\mathrm{IBS},\,u}$ $(u = x, y, z)$ depend mainly on the machine optics, the bunch intensity N_b, the geometric emittance ϵ_u, bunch length σ_z and the beam energy. Higher N_b and smaller ϵ_u generally lead to stronger growth rates. The first IBS theory for accelerators was presented by Piwinski in 1974 [16], then generalised by Bjorken and Mtingwa (BM) for strong-focusing lattices in 1983 [17]. In 2005, Nagaitsev presented a faster numerical evaluation of the BM elliptic integrals [18], which we use to estimate $T^{-1}_{\mathrm{IBS},\,u}$ numerically.

In order to calculate $\Delta Q_{x,y}$ and $T^{-1}_{\mathrm{IBS},\,u}$, we measure beam parameters across typical Pb cycles in LEIR, PS and SPS: bunch intensity N_b, relativistic gamma factor γ and bunch

ISBN: 978-3-95450-253-0 ISSN: 2673-5571 doi:10.18429/JACoW-HB2023-THBP24

RCS AND ACCUMULATOR RING DESIGNS FOR ISIS II

D. J. Adams, H. V. Cavanagh, B. Kyle, H. Rafique, C. M. Warsop, R. E. Williamson,
I. S. K. Gardner, ISIS Facility, STFC, Rutherford Appleton Laboratory, Oxfordshire, UK

Abstract

ISIS is the spallation neutron source at the Rutherford Appleton Laboratory in the UK, which provides 0.2 MW of beam power via a 50 Hz, 800 MeV proton RCS. Detailed studies are now underway to find the optimal configuration for a next generation, short-pulsed neutron source that will define a major ISIS upgrade, with construction beginning ~2031. Determining the optimal specification for such a facility is the subject of an ongoing study involving neutron users, target and instrument experts. The accelerator designs being considered for the MW beam powers required, include proposals exploiting FFA rings as well as conventional accumulator and RCS rings. This paper summarises work on physics designs for the conventional rings. Details of lattice designs, injection and extraction systems, correction systems as well as detailed 3D PIC simulations used to ensure 0.1% losses and low foil hits are presented. Designs for a 0.4 to 1.2 GeV RCS and 1.2 GeV AR are outlined. Work on the next stages of the study are also summarised to benchmark and minimise predicted losses, and thus maximise the high intensity limit of designs.

INTRODUCTION

The present working specification for the proposed ISIS II Facility requires 1.3×10^{14} protons per pulse (ppp) at 1.2 GeV and a repetition rate of 50 Hz. This 1.25 MW beam will supply multiple user targets to produce neutrons and muons for condensed matter research [1]. Consultation with the user communities and evaluation of accelerator technology, cost and sustainability are ongoing and may change the accelerator technologies and beam parameters.

The options outlined here are a 0.4 – 1.2 GeV Rapid Cycling Synchrotron (RCS) and a 1.2 GeV Accumulator Ring (AR) which represent conventional machine options delivering the high power, 1 μs pulse length proton beams required. Both can be positioned on the RAL site adjacent to, and run in parallel with, the existing facility. Options to site the accelerator within existing accelerator halls would require unacceptable interruptions to the experimental program.

Each machine option has its own challenges in meeting the physics specification. The RCS, at lower injection energy, has higher space charge effects whilst the AR, with thicker foils, has higher foil heating. To sustainably operate these high power beams it is necessary to limit total ring losses to ~0.1% to prevent machine damage and allow hands-on maintenance. Main parameters are summarised in Table 1.

Table 1: Summary of main RCS and AR parameters

Parameter	RCS	AR
Energy (GeV)	0.4 – 1.2	1.2
Intensity (ppp)	1.3×10^{14}	1.3×10^{14}
Repetition Rate (Hz)	50	50
Mean Power (MW)	1.25	1.25
Circumference (m)	282	282
No Super Periods	4	4
Magnet Excitation	Sinusoidal	DC
Dipole Fields (T), L (m)	0.42–0.84, 3	0.84, 3
Quad Max Field (T), L (m)	0.44, 0.5	0.43, 0.5
Betatron Tunes (Q_x, Q_y)	6.40, 6.32	6.40,6.32
Gamma Transition	5.21	5.21
Peak RF Volts (h=2, 4) (kV/turn)	300, 150	50, 28
RF Frequency (h=2)(MHz)	1.52 – 1.91	1.91
Acceptances: painted, collimated, aperture (π mm mr unnorm.) ($\Delta p/p$ ±0.01)	400, 600, 750	300, 350, 500
Carbon Foil μg/cm^2, eff. %	300, 99.4	500, 99.4
Injection Septum (T), L(m)	0.49, 2	0.27, 4.5
Inj. Dump, L (m), P (kW)	170, 2.6	790, 5.9

RING AND LATTICE DESIGN

The same lattice design is used for both the RCS and AR. It is similar in structure to the SNS lattice [2] but with additional drift lengths in the arcs to accommodate RF in the RCS. The ring has four super periods, a 282.3 m circumference, comprising of four-cell FODO achromatic arcs and two-cell reverse doublets for the straights. The straight is optically symmetric, hence a central waist with small (β_x, β_y) = (4.20, 6.99) m, chosen as the ring injection point, see Fig. 1. Drift lengths of 4.32 m in the arc sections and 7.29 m, 9.82 m in the straights provide ample room for RF, injection and extraction systems. The lattice transition gamma is 5.21, well above γ_{max}=2.27 at 1.2 GeV. The nominal working point is (Q_x, Q_y)=(6.40, 6.32). This gives reasonable space for incoherent tune spreads of up to −0.3 and avoids structural resonances. As established on the existing ISIS ring, a flexible working point is a very important feature in high-intensity operation. The addition of 4 trim quadrupoles in each straight provide working point control between 6.2 and 6.5 in both planes. Chromaticity correction is achieved using sextupoles in the arc sections. Lattice magnets have been sized to keep fields below 1 T, considered a limit for 50 Hz RCS ramping rates.

ISBN: 978-3-95450-253-0 ISSN: 2673-5571 doi:10.18429/JACoW-HB2023-THBP27

EXPERIMENTAL INVESTIGATION OF NONLINEAR INTEGRABLE OPTICS IN A PAUL TRAP*

J. A. D. Flowerdew†, S. L. Sheehy, University of Oxford, Oxford, UK
D. J. Kelliher, S. Machida, STFC Rutherford Appleton Laboratory, Oxford, UK

Abstract

Octupoles are often used to damp beam instabilities caused by space charge. However, in general the insertion of octupole magnets leads to a nonintegrable lattice which reduces the area of stable particle motion. One proposed solution to this problem is Quasi-Integrable Optics (QIO), where the octupoles are inserted between a specially designed lattice called a T-insert. An octupole with a strength that scales as $1/\beta^3(s)$ is applied in the drift region to create a time-independent octupole field, leading to a lattice with an invariant Hamiltonian. This means that large tune spreads can be achieved without reducing the dynamic aperture. IBEX is a Paul trap which confines low energy ions with an RF voltage, simulating the transverse dynamics of an alternating gradient accelerator. IBEX has recently undergone an upgrade to allow for octupole fields to be created in the trap in addition to quadrupole focusing. We present our first experimental results from testing QIO with the IBEX trap.

INTRODUCTION

In order to push the limits of the intensity frontier in accelerators, we must be prepared to address the problems associated with space charge and collective effects, which are the result of the interactions between the charged particles in a beam. It is important that we understand these collective effects because they can lead to resonant behavior and beam loss. These instabilities caused by space charge prevent accelerators from reaching their desired intensities. Achieving higher-intensity accelerators will require studying possible mitigation techniques to limit the effects of space charge. For example, the theory of Nonlinear Integrable Optics (NIO) [1] proposes a design for a nonlinear lattice that could damp the coherent resonances caused by space charge, without exciting the higher order resonances associated with the insertion of nonlinear elements. The challenge with testing these techniques experimentally is that studying beam loss in accelerators risks activating and damaging components. Thus, simulations are often relied upon instead to study collective effects. However, these simulations require large amounts of computational power to replicate the multiple Coulomb forces between particles and can never fully replace experimental validation. In order to circumvent these practical obstacles, linear Paul traps have been developed, to experimentally study beam dynamics without the large amounts of computational power needed for high-intensity simulations. A number of linear Paul traps have been created to study transverse dynamics such as the Simulator for Particle Orbit Dynamics (S-POD), Japan [2], the Paul Trap Simulator Experiment (PTSX), US [3], and the Intense Beams Experiment (IBEX), UK [4]. The transverse Hamiltonian in a Paul trap is equivalent to that of an alternating gradient accelerator [2]. Thus, these traps allow for the transverse effects in accelerators to be simulated without the risk of activating components and without the granularity of time steps, macro-particles, and grid sizes assumed in simulation. This paper presents the design and commissioning of a nonlinear upgrade to the IBEX Paul trap in order to enable experimental testing of a lattice designed according to the theory of Quasi Integrable Optics (QIO). We discuss the results from the successful trapping of ions in a quasi-integrable lattice and the promising potential contributions that the theories of NIO and QIO could make to the future of high-intensity beams.

NONLINEAR INTEGRABLE OPTICS

Current designs for accelerators such as synchrotrons and linacs are generally based on a system of alternating focusing and defocusing quadrupole magnets which confine the beam of charged particles. For an ideal system, a lattice constructed of these linear components would be fully integrable — in other words, the Hamiltonian of a single particle would be time-independent and hence conserved. However, in reality small misalignments between magnets and space charge forces create perturbations that require the use of nonlinear components like sextupoles and octupoles to make higher-order corrections. The addition of these components means that the system becomes nonintegrable, which has the effect of limiting the available phase space in which the motion of the particles is bounded. It would therefore be beneficial to be able to design a lattice that remained integrable even with the inclusion of nonlinear components, so that the system stays close to an integrable solution despite magnet misalignment and space charge.

Nonlinear Integrable Optics (NIO) proposes a method for using nonlinear components in a lattice while maintaining integrability. First proposed by Danilov and Nagaitsev in 2010 [1], NIO prescribes constructing a lattice that consists of a linear T-insert section and a drift region designed for a nonlinear magnet insert. A fully integrable solution in 2D requires a nonlinear insert with a complex elliptical potential which is being tested at the Integrable Optics Test Accelerator (IOTA) [5]. However, a quasi-integrable lattice, with one invariant of motion (the Hamiltonian), can be achieved with a scaling octupole field as the nonlinear insert. The conditions of the quasi-integrable lattice are as

* Work supported by Royal Society grants.
† jake.flowerdew@physics.ox.ac.uk

ISBN: 978-3-95450-253-0 ISSN: 2673-5571 doi:10.18429/JACoW-HB2023-THBP28

A PHASE TROMBONE FOR THE FERMILAB PIP-II BEAM TRANSFER LINE*

M. Xiao†, J-F. Ostiguy, D. Johnson
Fermilab, Batavia, IL, USA

Abstract

The PIP-II beam transfer line (BTL) transports the beam from the PIP-II Linac to the Booster synchrotron ring. A crucial aspect of the BTL design is the collimation system which play a vital role in removing large amplitude particles that may otherwise miss the horizontal and vertical edges of the foil at the point of injection into the Booster. To ensure the effectiveness of the collimators, simulations were conducted to determine optimal placement within the BTL. These simulations revealed that precise control of the accumulated phase advances between the collimators and the foil is critical. To achieve fine-tuning of the phase advance, a phase trombone was incorporated within the BTL. This paper presents the design and implementation details of this phase trombone.

INTRODUCTION

The Proton Improvement Plan II, or PIP-II, is an essential enhancement to the Fermilab accelerator complex, powering the world's most intense high-energy neutrino beam on its journey from Illinois to the Deep Underground Neutrino Experiment in South Dakota – 1,300 kilometres (800 miles) [1]. At the heart of PIP-II is a new 800 MeV linear accelerator, the Linac, based on superconducting radio-frequency technology. The linac accelerates H- ions for injection into the existing Booster ring, where they converted into protons and accumulated by multi-turn charge exchange using a stripping foil. The protons are then accelerated to 8 GeV before being transferred into another ring downstream. Figure 1 shows the layout of the PIP-II Linac complex.

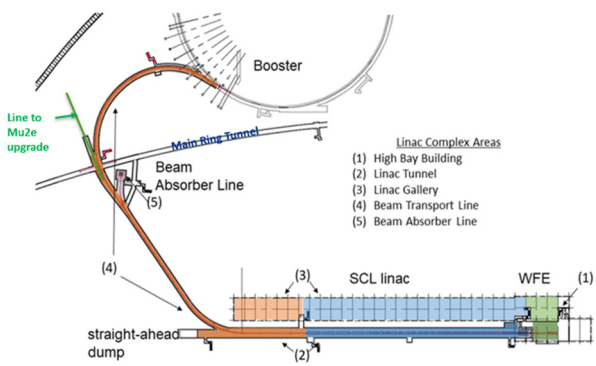

Figure 1: Layout of the PIP-II Linac Complex.

*Work supported by Fermi Research Alliance, LLC under Contract No. De-AC02-07CH11359 with the United States Department of Energy
†meiqin@fnal.gov.

The PIP-II Beam Transfer Line (BTL) transports the beam from the PIP-II Linac to the Booster ring. The optics of the BTL has recently been finalized [2]; a 3D CAD model is shown in Fig. 2. The lattice is based on 90-deg FODO cells. Four achromatic arcs, each comprising four cells are joined by an 8-cell straight section. The design meets requirements for civil construction and avoids mechanical interference with existing components. In an earlier design iteration, rolled dipoles in the second arc were used to bend the beam vertically; this feature has been eliminated and the reference trajectory now lies in a single plane. A switched magnet and corresponding septum are in Cell 3 and Cell 4 of the straight section and deflects the beam that would have gone to Booster into the Beam Absorber Line (BAL). A similar setting of a switched magnet and Septum will be located in Cell 7 and Cell 8 for a future upgrade which converts the 2-way split into a 3-way split providing the option of delivering beam to a Mu2e experiment.

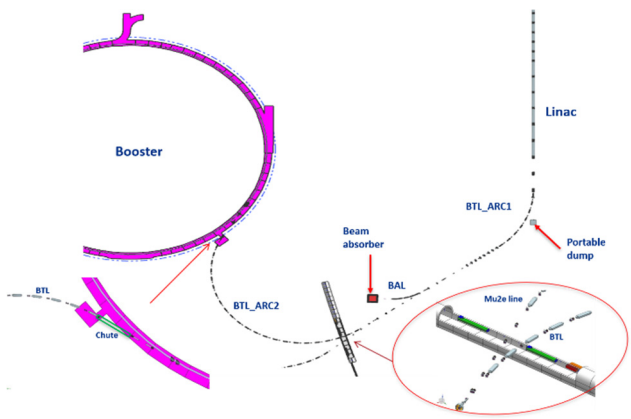

Figure 2: 3D CAD Model of the PIP-II complex layout.

COLLIMATION IN THE BTL

A crucial aspect of the BTL design is the collimation system [3]. To minimize the number of parasitic hits, the beam must be positioned as close as possible to the lower corner of the injection stripping foil. The minimal achievable distance is a compromise between the number of parasitic hits on the injection foil and the losses in the Booster injection absorber due to particles populating the distribution tails missing the foil.

The role of the collimators is to remove large amplitude particles that might otherwise miss the horizontal and vertical edge of the foil at the point of the Booster injection. By collimating the far tails of the beam transverse spatial distribution in a controlled manner one can move the beam closer to the foil edge without causing an increase in losses. This illustrated in Fig. 3.

ISBN: 978-3-95450-253-0 ISSN: 2673-5571 doi:10.18429/JACoW-HB2023-THBP29

EFFECTS OF CAVITY PRE-DETUNING ON RF POWER TRANSIENTS AT INJECTION INTO THE LHC

B. E. Karlsen-Baeck*,[1], T. Argyropoulos, A. Butterworth, R. Calaga,
I. Karpov, H. Timko, M. Zampetakis, CERN, Geneva, Switzerland
[1]also at the Department of Physics, Sapienza Università di Roma, Rome, Italy

Abstract

At injection into the LHC, the RF system is perturbed by beam-induced voltage resulting in strong RF power transients and the instant detuning of the cavities. The automatic tuning system, however, needs time for the mechanical compensation of the resonance frequency to take place. Acting back on the beam, the transients in RF power are expected to limit the maximum injected intensity by generating unacceptable beam loss. Reducing them is therefore essential to reach the target intensity during the High Luminosity (HL) LHC era. At LHC flat bottom, the cavities are operated using the half-detuning beam-loading compensation scheme. As implemented today, the tuner control algorithm starts acting only after the injection of the first longer bunch train which causes the bunches for this injection to experience the largest power spikes. This contribution presents an adapted detuning scheme for the RF cavities before injection. It was proposed as a path to decrease the transients, hence increasing the available intensity margin for the available RF power. The expected gain is evaluated in particle tracking simulations and measurements acquired during operation.

INTRODUCTION

Strong RF power transients occur due to the incoming beam during SPS to LHC injection [1]. The maximum possible injected bunch intensity, for bunch trains with lengths comparable to the cavity filling time, is limited by the size of these transients. The strongest transient occurs for the first of these bunch trains, because the RF system goes from steady state without beam to a new equilibrium with beam, passing through a transient state. The detuning of the RF cavity voltage due to beam-induced voltage is compensated by a tuner [2, 3], which tunes the cavity half-way between being resonant with and without beam, the so-called half-detuning beam-loading compensation scheme [4]. The tuner needs several seconds to act compared to the time scale of the injection transient and its effect is not present immediately after the first injection. Pre-detuning the eight cavities per beam before injecting the first batch into beam 1 (clockwise) and beam 2 (counterclockwise), was therefore proposed as a way to significantly reduce the transients and increase the maximum bunch intensity possible to capture.

This contribution details the predicted benefit of this scheme based on simulation using the Beam Longitudinal Dynamics (BLonD) code [5]. Additionally, results from measurements from operation during the summer of 2023 are shown and compared with the simulations.

BEAM-LOADING IN THE LHC

The relation between the cavity gap voltage, V_{ant}, the generator current, I_{gen}, and the RF beam current, $I_{\text{b,rf}}$, can be described by the following relation [6]

$$I_{\text{gen}} = \frac{V_{\text{ant}}}{2R/Q}\left(\frac{1}{Q_L} - 2i\frac{\Delta\omega}{\omega_{\text{rf}}}\right) + \frac{dV_{\text{ant}}}{dt}\frac{1}{\omega_{\text{rf}}R/Q} + \frac{I_{\text{b,rf}}}{2}\,. \quad (1)$$

Here, (R/Q) is the R upon Q, ω_{rf} is the RF angular frequency, Q_L is the loaded quality factor and $\Delta\omega$ is the detuning in frequency defined as $\Delta\omega \equiv \omega_r - \omega_{\text{rf}}$, where ω_r is the resonant frequency of the cavity. The RF power needed to supply the cavity is [6]

$$P_{\text{gen}}(t) = \frac{1}{2}R/QQ_L\left|I_{\text{gen}}(t)\right|^2\,. \quad (2)$$

During flat bottom in the LHC, the cavities are operated in half-detuning [4]. In this scheme, the required RF power is minimized through setting $\Delta\omega_{\text{opt}} = (R/Q)\, I_{\text{b,rf}}\omega_{\text{rf}}/(4V_{\text{ant}})$ and $Q_{L,\text{opt}} = 2V_{\text{ant}}/\left[(R/Q)\, I_{\text{b,rf}}\right]$, while keeping the gap voltage constant in both amplitude and phase. The average steady-state generator power then becomes

$$P_{\text{gen,opt}} = \frac{1}{8}\frac{V_{\text{ant}}^2}{R/QQ_L} + \frac{R/QQ_L}{32}I_{\text{b,rf}}^2 = \frac{V_{\text{ant}}I_{\text{b,rf}}}{8}\,. \quad (3)$$

In operation, the cavities are tuned via a mechanical tuner moved by a step motor which is controlled through firmware [7]. A steepest-descent algorithm is programmed, which minimizes the average of the maximum and minimum of the 2-dimensional cross-product between V_{ant} and $I_{\text{b,rf}}$ [3]. In the complex plane, the cross-product can be expressed as $\Im\left\{V_{\text{ant}}I_{\text{b,rf}}^*\right\} = x$, which is down-sampled with a cascaded integrator-comb (CIC) filter. The algorithm computes the correction

$$\left(\frac{\Delta\omega}{\omega_r}\right)_{n+1} = \left(\frac{\Delta\omega}{\omega_r}\right)_n - \frac{\mu}{2}\frac{x_{\max} + x_{\min}}{|V_{\text{ant}}|^2} \quad (4)$$

turn-by-turn and gradually moves ω_r. Here μ is a coefficient which determines how fast the tuner acts and is always negative. In the LHC this constant is set to a value such that the algorithm converges on the order of a second. It also follows from Eq. (4) that the tuner only acts when $I_{\text{b,rf}} \neq 0$, i.e. when there is already beam in the ring. The pre-detuning is implemented by adding a static phase-offset $\phi_{\Delta\omega}$ in the

* birk.beck@cern.ch

ISBN: 978-3-95450-253-0 ISSN: 2673-5571 doi:10.18429/JACoW-HB2023-THBP30

LINEAR MODELLING FROM BETATRON PHASE MEASUREMENTS AT THE FERMILAB RECYCLER NOvA RING*

M. Xiao†, M-J. Yang, K. J. Hazelwood, R. Ainsworth
Fermilab, Batavia, IL, USA

Abstract

Utilizing the measurement of coherent betatron oscillation phase has emerged as a fast and precise approach for identifying and rectifying errors in achieving a desired lattice in CESR (Cornell Electron Storage Ring), using TAO analysis program and BMAD subroutines. One key advantage of betatron phase measurement over β measurement is its sensitivity to phase variations between detectors. This software package has been successfully implemented for the Recycler Ring at Fermilab, with the adaptation of different hardware installations. By employing this technique, a linear model of the bare Recycler ring was established, enabling the correction of quadrupole errors.

INTRODUCTION

The Recycler Ring (RR), located at Fermilab, is an 8 GeV permanent magnet storage ring specifically designed for antiproton storage with electron cooling during the Tevatron Era [1] to improve luminosity. A phase trombone, located in RR60 straight section, is used to adjust phase advances, i.e., tunes in the ring [2]. In 2012 the ring was converted to a proton storage ring to stack 12 batches of beam from Booster, to be injected into Main Injector in one single transfer. This is necessary for delivering over 900kW of beam power to the NUMI target by Main Injector. The upgrade included the installation of modified end-shims to change focussing of ARC gradient dipole magnets and the replacement of e-cool high beta straight section at RR30 with regular straight section lattice, and with a second phase trombone [3] to add flexibility in tune compensations. With cycle time of only 1.13 seconds, for slip stacking 12 proton batches, the closed orbit response using LOCO (Linear Optics from Closed orbit) [4] technique is no longer suitable. Instead, the console application program R92 for lattice measurement [5] has been used. By fitting Turn-By-Turn (TBT) data to sine functions, phase and amplitude at each BPM can be determined. In addition, this program utilizes TBT orbit to fit beam phase space coordinates. By tracking TBT phase space coordinates the beta function can be calculated.

The objective of lattice measurement for the RR is to construct a predictive model that can accurately represent machine behaviour. At CESR (Cornell Electron Storage Ring) [6] utilizing the measurement of coherent betatron oscillation phase has been used as a fast and precise approach for identifying and rectifying errors. For this analysis TAO (Tool for Accelerator Optics) was developed at Cornel University [7]. The same software package has been successfully implemented for the present Recycler ring at Fermilab with adaptations. With the customized TAO program for the RR, we were able to turn measured phases and beta functions into quadrupole errors from design lattice. The adaptations of TAO program for the RR are presented in this paper.

*Work supported by Fermi Research Alliance, LLC under Contract No. De-AC02-07CH11359 with the United States Department of Energy † meiqin@fnal.gov.

ADAPTING AND BENCHMARKING TAO

TAO is a general purposed program for simulating high energy particle beams in accelerators and storage rings. The simulation engine that TAO uses is the Bmad software library [8]. Bmad subroutine library were written in FORTRAN95, for relativistic charged–particle and X-Ray simulations in high energy accelerators and storage ring. It was developed at Cornell University's Laboratory for Elementary Particle Physics and has been in use since 1996. Both TAO program and Bmad subroutines were compiled using FORTRAN 95 compiler and installed here at Fermilab. The input lattice for Bmad was converted from a MAD8 RR lattice.

The technique utilized at CESR is to shake the beam at betatron sideband and then measure the phase of the oscillations at the beam position detectors around the ring. This yields the betatron phases $\phi_{x,y}$ at the detectors which can then be related to the beta function via:

$$\frac{1}{\beta_{h,v}} = \frac{d\phi_{h,v}}{ds} \qquad (1)$$

An AC-dipole was used as shaker at CESR and Program TAO was used to locate isolated errors from the measured data by analysing the betatron phases [6]. In the Recycler ring at Fermilab, we could only ping the beam with one-shot kicker, and record the TBT orbit oscillation data. In the RR a gap clearing kicker was programmed to also work as horizontal pinger, and during summer shutdown of 2018 a vertical pinger was installed to facilitate collection of vertical plane TBT data. Program R92, after collecting TBT data from all BPM systems, does two independent analyses. The first is to perform sinusoidal fit to each individual BPM TBT data (104 in Horizonal and 104 in vertical plane). This gives betatron phases and oscillation amplitudes at BPM detectors. The second analysis is to: (1) use each turn of TBT data to construct TBT orbit data. (2) use beam line transfer matrix calculated based on lattice model, each turn orbit data is fitted to obtain TBT beam phase space coordinates (x, x') and (y, y'), as well as $\Delta p/p$. (3) resulted TBT coordinates, (x, x') or (y, y'), will exhibit betatron oscillation and populate the phase space around an elliptical trace. By fitting for the parameters of this elliptical trace we obtain the lattice function β, α, and the emittance associated with the betatron oscillation. (4) export phase and amplitude data, as well as the lattice functions. The output will then be available as input to TAO program for analysis.

ISBN: 978-3-95450-253-0 ISSN: 2673-5571 doi:10.18429/JACoW-HB2023-THBP31

ELECTRON CLOUD EFFECTS IN THE CERN ACCELERATORS IN RUN 3

L. Mether*, H. Bartosik, E. de la Fuente Garcia, L. Giacomel, G. Iadarola,
S. Johannesson, I. Mases Sole, K. Paraschou, G. Rumolo, L. Sabato, C. Zannini
CERN, Geneva, Switzerland

Abstract

Several of the machines in the CERN accelerator complex, in particular the Large Hadron Collider (LHC) and the Super Proton Synchrotron (SPS), are prone to the build-up of electron clouds. Electron cloud effects are observed especially when the machines are operated with a 25 ns bunch spacing, which has routinely been used in the LHC since the start of its second operational run in 2015. After the completion of the LHC Injectors Upgrade program during the latest long shutdown period, the machines are currently operated with unprecedented bunch intensity and beam brightness. With the increase in bunch intensity, electron cloud effects have become one of the main performance limitations, as predicted by simulation studies. In this contribution we present the experimental observations of electron cloud effects since 2021 and discuss their implications for the future operation of the complex.

INTRODUCTION

Electron clouds are caused by the avalanche multiplication of electrons that can occur as a consequence of their acceleration by the beam field and the subsequent emission of further electrons upon impact on the chamber surface, as defined by its secondary emission yield (SEY). They are typically manifested as transverse instabilities, emittance growth, pressure rise, heat load in cryogenic regions, incoherent beam losses and RF stable phase shift [1]. Since electron cloud (e-cloud) build-up is most prominent with closely spaced bunches, in the CERN accelerators, e-cloud effects are observed mainly for the LHC beam with its nominal bunch spacing of 25 ns [2]. They occur to a varying degree in the LHC and its injectors, starting from the Proton Synchrotron (PS), where the 25 ns bunch structure is first produced, and continuing through the SPS to the LHC.

So far, the main strategy for e-cloud mitigation in the CERN accelerators has been to rely on beam-induced conditioning, or scrubbing, in which the SEY of the beam chamber surface is reduced due to the bombardment by the e-cloud itself [3, 4]. In practise, this is often done with dedicated scrubbing runs, during which the amount and duration of beam, as well as the beam parameters, are regularly adjusted to systematically maximize e-cloud production while keeping its effects just within the acceptable limits. However, the SEY that can be achieved through scrubbing is limited to an extent that depends on the surface material and broader machine conditions. This is evident in particular in the LHC, where e-cloud effects, after initially reducing with scrubbing, remained present and significant throughout its second operational run (Run 2), even though they did not significantly limit the performance [5, 6]. In the injectors, scrubbing has been more successful. In the SPS, the 25 ns LHC beams initially suffered from strong pressure rise, transverse instabilities and emittance growth, which could be successfully mitigated with systematic scrubbing runs over a decade, in preparation for delivery to the LHC [7].

The High-Luminosity LHC (HL-LHC), expected to start in 2029, foresees a reduction in the transverse beam emittances along with a doubling of the bunch intensity from Run 2 to 2.3×10^{11} p in Run 4 [8]. To be able to produce such beams for the LHC, the injectors underwent a major consolidation, which was finalised during the previous long shutdown period (LS2) [9]. Among the new installations was an upgrade of the SPS RF system, allowing to significantly increase the total intensity that can be accelerated to 450 GeV/c and extracted to the LHC. During the current run, the injectors are expected to fully prepare the HL-LHC beam and are already on a good path towards this goal with $2.2{\times}10^{11}$ p/b (protons per bunch) accelerated in the SPS [10]. The operational bunch intensity in the LHC is foreseen to be ramped up to an intermediate value of 1.8×10^{11} p, with 1.6×10^{11} p reached in 2023 [11]. With the significant increase in bunch intensity since Run 2, new limitations from e-cloud have been encountered, in particular in the SPS and the LHC, as will be discussed below.

INJECTORS

The RF manipulations that give the LHC beams their 25 ns structure take place in the PS at the top energy of 26 GeV/c, shortly before beam extraction [12]. During this period, transverse instabilities, baseline distortion on pick-up signals and pressure rise have been observed after air exposure since 2001, but have quickly conditioned with machine operation [2, 13]. After the PS restart in 2021, pressure rise due to e-cloud was again observed in large parts of the machine and initially hindered normal operation by interlocking the pulsing of the injection kicker. The pressure rise could be conditioned by a dedicated period of scrubbing over several days, after which no further limitations from e-cloud have appeared, even with bunch intensities as high as 2.9×10^{11} p.

When the SPS resumed operation later in 2021, extensive scrubbing was needed, since much of the machine had been opened during the shutdown. Whereas transverse instabilities and emittance growth could be mitigated with chromaticity, the main limitation setting the scrubbing pace came from the vacuum pressures around the ring. One of the main bottlenecks was a vertical kicker magnet (MKDV1) for the upgraded beam dump system that was found to ex-

* lotta.mether@cern.ch

ISBN: 978-3-95450-253-0 ISSN: 2673-5571 doi:10.18429/JACoW-HB2023-THBP32

Xobjects AND Xdeps: LOW-LEVEL LIBRARIES EMPOWERING BEAM DYNAMICS SIMULATIONS

S. Łopaciuk*, R. De Maria, G. Iadarola, CERN, Geneva, Switzerland

Abstract

Xobjects and Xdeps are Python libraries included in the Xsuite beam dynamics simulation software package. These libraries are crucial to achieving two of the main goals of Xsuite: speed and ease of use. Xobjects allows users to run simulations on various hardware in a platform-agnostic way: with little user intervention single- and multi-threading is supported as well as GPU computations using both CUDA and OpenCL. Xdeps provides support for deferred expressions in Xsuite. Relations among simulation parameters and functions driving properties of lattice elements can be defined or indeed imported from other tools such as MAD-X and then easily updated before or during the simulation.

INTRODUCTION

Xsuite [1, 2] is a relatively recent collection of tools for conducting beam dynamics simulations in particle accelerators. The main focus in the development of Xsuite has been to create a versatile tool allowing the users to easily, and with high performance, conduct particle tracking simulations. Xsuite's ease of use comes from the fact that it is a framework that can be interfaced with in Python 3, and, optionally, C. The former of the two languages is regarded as particularly user-friendly and already well-known in the community, while the latter is used for writing parts of Xsuite where performance is critical. Xsuite aims to be performant by relying on hardware-accelerated computation contexts (GPU and CPU multi-threading), which is complemented by the ease of set-up of a simulation: e. g. an existing lattice model defined in MAD-X can often be directly imported into Xsuite.

A particle accelerator lattice model consists of a series of beam elements (collectively referred to as a 'line'), each of which abstracts a real-life machine element. The parameters of each of the elements (e. g. the strength of a magnet) can depend on various factors, and can be driven by hyper-parameters of the simulation (as an example of a hyper-parameter consider the crossing angle of two beams in a collider); these hyper-parameters are often referred to as 'knobs'. The relationships between all of the parameters are preserved in Xsuite thanks to the Xdeps package. With Xdeps the user can inspect the simulation parameters, as well as efficiently change them before or during a simulation. Simulation runs are themselves enabled by the Xobjects package which is responsible for memory management, tracking code generation and its execution regardless of the chosen computation context.

In this paper we explore these two packages to give a more in-depth overview of their design and capabilities.

* szymon.lopaciuk@cern.ch

XOBJECTS

Beam elements can be naturally divided into two categories: *non-collective*, where the computation of the new coordinates of the tracked particles depend solely on its previous coordinates and the element itself, and *collective*, where the computed coordinates are linked to the coordinates of other particles in the bunch. Tracking a bunch through a non-collective element can be easily accelerated through the application of parallelisation: for every particle the same computation is performed independently.

Parallelisation can be achieved through CPU or GPU-based multi-threading; however, the development of portable parallelisable code is non-trivial, as there are currently different, sometimes competing, technologies, while hardware vendors tend to support some, but not all of them. In addition to the conventional serial CPU execution context, Xobjects aids in writing procedures that simultaneously support CPU-based multi-threading through OpenMP [3], as well as GPU platforms compatible with CUDA [4] or OpenCL [5].

Universal API

In essence, Xobjects provides a simple object-oriented programming interface which allows for defining binary objects in Python, and for defining their methods in an extended C syntax. Xobjects comes with a set of built-in types:

- the standard collection of integer types (signed and unsigned; 8, 16, 32, and 64 bit),
- floating-point types (32 and 64 bit real; 64 and 128 bit complex),
- multi-dimensional array types (fixed and dynamic shape; support for arbitrary strides),
- structure types, union types, references, strings.

For any compound type (i. e. structure or array) Xobjects can generate a C API that can be used to interact with the 'Xobject' from a C 'method'. Consider the following example of a structure representing an array of vectors (`xo.Float64[:]` is an dynamic-length array of double-precision real numbers):

```
import xobjects as xo
class Vectors(xo.Struct):
    x = xo.Float64[:]
    y = xo.Float64[:]
```

Xobjects can be used to automatically generate methods for getting the size of the arrays comprising our object, as well as getters and setters for their individual elements:

ISBN: 978-3-95450-253-0 ISSN: 2673-5571 doi:10.18429/JACoW-HB2023-THBP34

PSI INJECTOR II AND THE 72 MeV TRANSFER LINE: MinT-SIMULATION vs. MEASUREMENTS

C. Baumgarten*, H. Zhang, Paul Scherrer Institut, 5232 Villigen PSI, Switzerland

Abstract

PSI's Injector II cyclotron is the only cyclotron worldwide that makes use of the so-called "Vortex effect", in which the space charge force leads to the counter-intuitive effect to "roll up" bunches, thus keeping them longitudinally compact. The effect has been confirmed by bunch shape measurements and the PIC-simulations with OPAL. However, PSI's new fast matrix code MinT allows to reproduce the Vortex effect by a linear matrix model which is computational much cheaper than PIC simulations, and is suitable for "online use" in Control rooms. Furthermore it provides the second moments σ_{ij} of matched distributions.

We compare results of various measurements with MinT calculations which show that the linear model works well and provides excellent initial conditions to fit the beam profiles of the 72 MeV transfer line to the Ring cyclotron.

INTRODUCTION

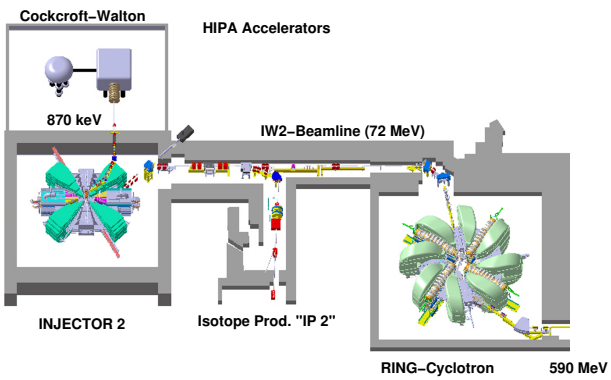

Figure 1: Accelerator part of PSI's high intensity accelerator facility (HIPA).

Figure 1 shows PSI's High Intensity Proton Accelerator (HIPA): A Cockcroft-Walton DC pre-accelerator provides a 870 keV proton beam of typically 10 mA DC current. Two (first and third harmonic) bunchers are used to generate 50 MHz CW bunch structure before the beam is axially injected into the first turn of Injector II as shown in Fig. 2. Due to the Vortex effect the bunches remain almost round. The beam is extracted at 72 MeV from Injector II and transported with the IW2-beamline towards the PSI's Ring cyclotron. The 590 MeV beam is used to generate pions and muons at two graphite targets and for neutron production in the Swiss spallation source SINQ [1].

* christian.baumgarten@psi.ch

THE VORTEX EFFECT

The Vortex effect [2] (or "negative mass instability" [3]) is due to strong space charge of bunches in the isochronous regime of circular accelerators. The space charge force induces coupling terms between the longitudinal and the transverse-horizontal beam motion [4, 5]. This coupling leads to a dense and matched core bunch and (typically) a halo with two tails [6, 7]. In the bunch core the space charge force is approximately linear and the linear matching conditions can be computed, if beam current and core emittances are known [5, 8]. The halo tails of the bunches

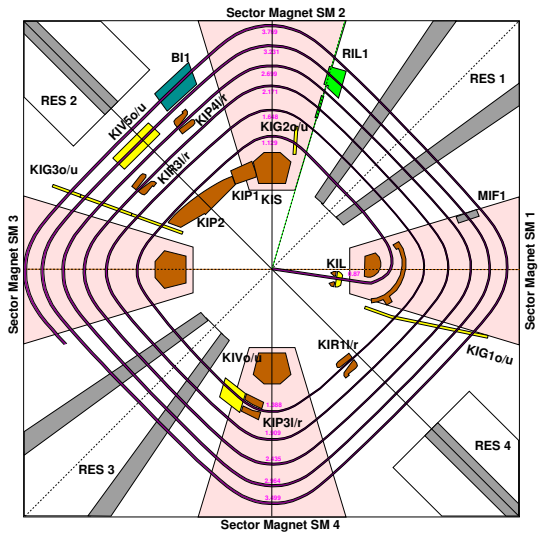

Figure 2: Central region of the Injector II cyclotron. Several movable collimators (KIP3, KIR1, KIP4) allow to remove halo in support of a clean bunch formation. The first few turns of the beam path are shown as well.

are cleaned by horizontal collimators if the orientation of the tails is transverse. However, the orientation of the halo tails depends on the details of the bunch formation and the strength of the space charge force, i.e. the beam current. As shown in Fig. 2, the first turns of Injector II are equipped with several sets of movable collimators. The radial position of the "KIP2" collimator is used to control the beam current. The other collimators allow for a setup with low losses at extraction.

However, if the orientation of the halo tails depends on the beam current, then the extraction losses caused by the halo tails will also depend on the bunch charge. Figure 3 shows the losses of the ionization chamber "MII6" located at the extraction of Injector II versus beam current, measured with current monitor "MXC1". The losses show a strongly non-linear, almost periodic, dependency on the current. In case of a strong Vortex effect, one expects that filamentation

ISBN: 978-3-95450-253-0 ISSN: 2673-5571 doi:10.18429/JACoW-HB2023-THBP35

ANALYSIS TOOLS FOR NUMERICAL SIMULATIONS OF DYNAMIC APERTURE WITH Xsuite

T. Pugnat[1,*], D. Di Croce[2], M. Giovannozzi[1], F. F. Van der Veken[1]
[1] CERN, Geneva, Switzerland
[2] EPFL, Lausanne, Switzerland

Abstract

Recently, several efforts have been made at CERN to develop a new tracking tool, `Xsuite`, which is intended to be the successor to `SixTrack`. In this framework, analysis tools have also been prepared with the goal of providing advanced post-processing techniques for the interpretation of dynamic aperture simulations. The proposed software suite, named `Xdyna`, is meant to be a successor to the existing `SixDesk` environment. It incorporates all recent approaches developed to determine the dynamic aperture for a fixed number of turns. It also enables studying the time evolution of the dynamic aperture and the fitting of rigorous models based on the stability-time estimate provided by the Nekhoroshev theorem. These models make it possible to link the dynamic aperture to beam lifetime, and thus provide very relevant information for the actual performance of particle colliders. These tools have been applied to studies related to the luminosity upgrade of the CERN Large Hadron Collider (HL-LHC), the results of which are presented here.

INTRODUCTION

The dynamic aperture (DA), i.e., the extent of the connected region in phase space where the bounded motion occurs for a finite number of turns $N_{\max}$, is a key quantity characterising the nonlinear beam dynamics and in particular the performance of high-energy storage rings and colliders. In fact, with the advent of superconducting magnets, which feature unavoidable magnetic field errors, the dynamics of charged particles in a circular accelerator turned intrinsically nonlinear. DA poses a challenge to accelerator physicists in terms of theoretical understanding of its features and computational evaluation. In the first domain, several studies were devoted to determine the appropriate models to describe how DA evolves as a function of $N_{\max}$. Several solutions to this problem have been found [1–3] using the stability time estimate provided by the Nekhoroshev theorem [4–6]. The interest of this approach consists in the fact that once the DA evolution over time has been determined with a set of numerical simulations, the analytical model describing such an evolution can be fitted to the numerical data, and the resulting function can be used to extrapolate or predict the DA value for a number of turns beyond that used in actual numerical simulations. The advantage of this approach with respect to a plain brute-force computation is clear, in particular for the large high-energy colliders and even more so for the future ones, such as the Future hadron Circular Collider under study at CERN [7–10]. These new developments in the field require a sophisticated post-processing of the tracking data, which was initially partially implemented for the `SixTrack` code [11, 12].

The new Python modular simulation package `Xsuite` [13–16] has the ambition to combine previous single-particle simulation tools developed at CERN during the past decade, such as `SixTrack`, as well as collective effects codes, such as `PyHEADTAIL` [17, 18]. Therefore, new efforts have been devoted to the implementation of DA techniques developed in the recent past using the new computational paradigm, and all this has been incorporated in the new `Xdyna` module.

BRIEF DESCRIPTION OF `XDYNA`

`Xdyna` [19] has been developed with the idea of providing a user-friendly environment for beam stability simulations and all the necessary tools for dynamic aperture (DA) analysis. The tools developed are capable of performing analyses similar to those implemented in `SixDesk`, also providing new tools such as the evaluation of DA versus turn and machine learning techniques to optimise the selection of initial conditions for DA computation. The development of `Xdyna` is also an opportunity to review the definition of DA and to provide new reflection paths on this topic. A brief description of the functionalities of this package is outlined in the following:

1. **Creation of a study:**

   For each study, a configuration file is created, which contains all the information about the working units such as: the study name, the normalised emittances, the turn number used, the number of realisations of the magnetic field errors (also called seeds), as well as information about the `MAD-X` [20] scripts that need to be used.

2. **Generate a distribution of particles:**

   `Xdyna` can generate different types of initial distribution of particles: a Cartesian grid, a polar grid, or a random grid. By default, and for the sake of backward compatibility, the radial distribution is the same as that generated by `SixTrack`. Note that `Xdyna` also manages pairs of particles, similar to `SixTrack`. Furthermore, the user can also specify a custom distribution of initial conditions. The post-processing will be performed similarly to that for a random distribution of particles.

* thomas.pugnat@cern.ch

ISBN: 978-3-95450-253-0 ISSN: 2673-5571 doi:10.18429/JACoW-HB2023-THBP36

STUDY OF THE PERFORMANCE OF THE CERN PROTON SYNCHROTRON INTERNAL DUMP

T. Pugnat[1,*], D. Domange[2], L. S. Esposito[1], M. Giovannozzi[1], E. Gnacadja[2], C. Hernalsteens[1], A. Huschauer[1], S. Niang[1], R. Tesse[2]
[1] CERN, Geneva, Switzerland
[2] Université libre de Bruxelles, Brussels, Belgium

Abstract

In the framework of the LHC Injector Upgrade project, a new internal dump for the CERN Proton Synchrotron (PS) has been designed, installed, and successfully commissioned. This device is meant to move rapidly into the beam and stop charged particles over several turns to provide protection to the PS hardware against beam-induced damage. The performance of the dump should ensure efficient use throughout the PS energy range, i.e., from injection at 2 GeV (kinetic energy) to flat top at 26 GeV (total energy). In this paper, detailed numerical simulations are presented, carried out with a combination of sophisticated beam dynamics and beam-matter interaction codes, assessing the behaviour of stopped or scattered particles. The results of these numerical simulations are compared with the data collected during the routine operation of the PS and its internal dump.

INTRODUCTION

During the second long shutdown of the CERN accelerator complex (2019-2021), the internal dumps of the PS ring, installed in straight sections (SS) 47 and 48, have been replaced. This was part of the LHC Injector Upgrade (LIU) [1, 2] project. In fact, the increase in beam brightness imposed a redesign and an upgrade of the dumps. Several studies have been carried out to check the thermomechanical properties of the new dump design [3, 4] as well as its ability to shave the beams [5]. In Ref. [5] a simplified model of beam dynamics in the PS ring was studied with the goal of accessing the multiturn effects in the beam-dump interaction.

The goal of this paper is to further develop the approach presented in Ref. [5] by using a beam dynamics code coupled with a code that simulates the beam-matter interaction. This enables considering the distribution of beam losses along the ring circumference, which is a key observable to assess whether additional shielding might be needed to protect the accelerator hardware. The typical parameters used in the simulations are listed in Table 1. Note that the column "LHC" refers to the proton beam used for the physics at the LHC, a high-brightness beam, while the column "SFTPRO" refers to the proton beam for the fixed-target programme at the CERN Super Proton Synchrotron (SPS) ring, a high-intensity beam. The ultimate goal is to compare the results of the simulation with the beam-based measurements [6].

* thomas.pugnat@cern.ch

Table 1: Typical beam and optics parameters used in the simulations for the PS internal dump, which are taken from the specifications [7, 8].

Parameter	Unit	LHC	SFTPRO
E_t	[GeV]	26.4	14
$\epsilon_x^*/\epsilon_y^*$	[mm mrad]	2.3	9/5
Q_x		6.217	6.247
Q_y		6.280	6.298
Q'_x		1.67	3.93
Q'_y		0.44	1.91
σ_δ	[10^{-3}]	0.4	0.1

MODEL OF THE PS RING

The studies presented in this paper require an accurate representation of the beam dynamics and aperture model along the PS ring as well as the beam-matter interactions occurring in the internal dump and the dynamic change of the dump position must be implemented with care.

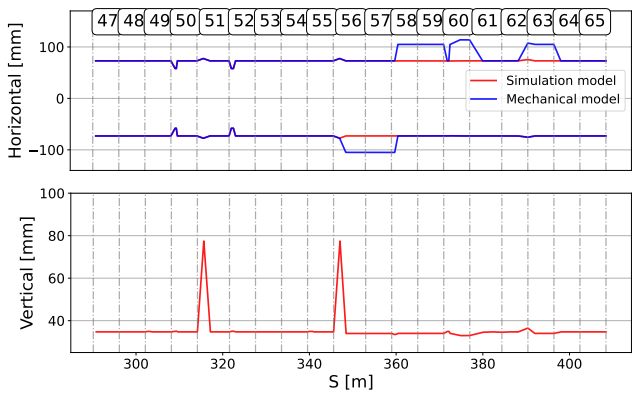

Figure 1: Evolution of the horizontal (top) and vertical (bottom) dimensions of the beam pipe (blue) and of the approximation used in the simulations (red). Note that the vertical aperture is always symmetric around zero and both curves are superposed.

Several chains of simulation codes can be used to achieve the required configuration. `MAD-X` [9], combined with `PTC` [10], is used to generate the optics input for `SixTrack` [11, 12] for which an active coupling [13, 14] with the `FLUKA` code exists [15, 16]. The alternatives consist of using the newly developed tracking code `Xsuite` [17–19], which includes already scattering modules, inherited

ISBN: 978-3-95450-253-0 ISSN: 2673-5571 doi:10.18429/JACoW-HB2023-THBP37

REFINING THE LHC LONGITUDINAL IMPEDANCE MODEL*

M. Zampetakis†, T. Argyropoulos, Y. Brischetto, R. Calaga, L. Giacomel
B. E. Karlsen-Baeck[1], I. Karpov, N. Mounet, B. Salvant, H. Timko
CERN, Geneva, Switzerland
[1]also at the Department of Physics, Sapienza Università di Roma, Rome, Italy

Abstract

Modelling the longitudinal impedance for the Large Hadron Collider (LHC) has been a long-standing effort, especially in view of its High-Luminosity (HL) upgrade. The resulting impedance model is an essential input for beam dynamics studies. Increased beam intensities in the HL-LHC era will pose new challenges like RF power limitations, beam losses at injection and coupled-bunch instabilities throughout the acceleration cycle. Starting from the existing longitudinal impedance model, effort has been made to identify the main contributing devices and improve their modelling. Loss of Landau damping (LLD) simulations are performed to investigate the dependence of the stability threshold on the completeness of the impedance model and its broad-band cut-off frequency. Plans to perform beam measurements to estimate the cut-off frequency, by investigating the LLD threshold in operation, are also discussed.

INTRODUCTION

In the design phase of the Large Hadron Collider (LHC), first estimations for its impedance were performed [1] to ensure beam stability in the transverse and longitudinal planes. In the longitudinal plane, the main limitation is single-bunch loss of Landau damping. Coupled-bunch instabilities have not been observed so far [2, 3]. Following design changes of several devices, the impedance was re-evaluated and the final estimations were published in the the LHC Design Report [4]. After the construction phase of the LHC, the impedance model has been continuously updated with more accurate calculations and measurements of the numerous accelerator components [5, 6] while beam measurements were performed to verify the validity of the model [7, 8].

The present impedance model of the LHC is implemented using the *Python Wake and Impedance Toolbox (PyWIT)* [9] and the *Impedance Wake 2D (IW2D)* code [10]. This model is built considering the devices that have a high impact on the impedance in the transverse planes. As the beam intensities are being increased, especially in view of the High-Luminosity (HL) LHC, the longitudinal impedance can affect the stability of the beam. For instance, undamped injection oscillations have been observed to lead to losses for single bunches at injection [11]. Thus, a realistic longitudinal impedance model is crucial to study the dynamics of the beam in simulations.

An important parameter for all the broad-band (BB) contributions is the cut-off frequency. In the model, the cut-off frequency is chosen to be at 50 GHz, to stay conservative for instability predictions at high chromaticity in the transverse planes. In the longitudinal plane, this cut-off frequency led to artificial beam losses observed in tracking simulations at injection [12]. Beam-based measurements are proposed to estimate the effective cut-off frequency of the BB impedance in the longitudinal plane, through the loss of Landau damping (LLD) mechanism [13].

In this contribution, the present longitudinal impedance model will be briefly presented and some ongoing improvements will be discussed. First LLD simulation results will be shown comparing a constant BB impedance with the full impedance model. The proposed method to estimate the BB cut-off frequency with beam measurements of the LLD threshold will be introduced.

PREVIOUS AND REFINED IMPEDANCE MODEL

Since the conceptual design of the LHC, its impedance model has seen several iterations and refinements. It includes most of the relevant LHC devices, e.g., collimators, vacuum chambers, beam screens with their pumping holes, Y-chambers, experimental chambers, as well as RF cavities with their higher-order modes (HOMs), and the design BB impedance [4], containing the BB contributions from collimators, pumping slots, Y-chambers, BPMs, bellows, etc. The model was built prioritizing the elements with the largest impact on transverse beam stability.

Figure 1 shows the complete and the BB models of the longitudinal impedance, Z, divided by the harmonics of the revolution frequency, $n = f/f_{\mathrm{rev}}$, as a function of the frequency, f. In the longitudinal plane, the real part of the impedance produces energy losses, while the imaginary part can cause instabilities. Many HOM impedances that could potentially lead to coupled-bunch instabilities are observed in the range of about 1 GHz. For lower frequencies there is a resistive-wall behavior, while for higher frequencies a BB behavior is observed. The comparison with a BB resonator with $Q = 1$, $Z/n = 0.076\,\Omega$ and a cut-off frequency of $f_c = 5$ GHz shows very good agreement, as indicated in Fig. 1. This BB behavior has often been used as an approximation for analytical estimations and simulations [7].

The relevant beam spectrum in the LHC is about 1 GHz wide. The main impedance contributions in this frequency range for the present model, normalized to unity, are illustrated in Fig. 2a. The dominant device for this frequency appears to be the beam screen that contributes about 50 % of the total impedance. The design BB impedance and the

* Research supported by HL-LHC project
† michail.zampetakis@cern.ch

ISBN: 978-3-95450-253-0 ISSN: 2673-5571 doi:10.18429/JACoW-HB2023-THBP38

TWO-DIMENSIONAL LONGITUDINAL PAINTING AT INJECTION INTO THE CERN PS BOOSTER

S. Albright*, F. Asvesta, C. Bracco, B. Bielawski, R. Wegner, P. Skowronski
CERN, Geneva, Switzerland

Abstract

To inject highest beam intensities at the transfer from Linac4 into the four rings of the PS Booster (PSB) at CERN, protons must be accumulated during up to 148 turns in total. With the conventional, fixed chopping pattern this process results in an approximately rectangular distribution in the longitudinal phase space. As the bucket shape in the PSB does not correspond to this distribution, the process leads to longitudinal mismatch, contributing to emittance growth and reduced transmission. The field in the last accelerating cavity of Linac4 can be modulated, which leads to fine corrections of the extracted beam energy. At the same time, the chopping pattern can be varied. Combining both allows injecting a near uniform longitudinal distribution whose boundary corresponds to an iso-Hamiltonian contour of the RF bucket, hence significantly reducing mismatch. In an operational context, the longitudinal painting must be controlled in a way that allows easy intensity variation, and can even require different painting configurations for each of the four PSB rings. This contribution presents the first demonstration of longitudinal painting in the PSB, and its impact on beam performance.

INTRODUCTION

The Proton Synchrotron Booster (PSB) is the first synchrotron in the CERN proton accelerator complex, its injector is the H^- accelerator Linac4. To meet the requirements of the downstream accelerators and experimental facilities, the beam parameter space covers approximately three orders of magnitude in intensity (from 10^{10} to 10^{13} protons per bunch) and more than an order of magnitude in longitudinal emittance (from 0.1 eVs to 3 eVs). As part of performance optimisation following the implementation of the LHC Injectors Upgrade (LIU) project, efforts are ongoing to maximise the available intensity from the PSB [1, 2].

In accelerators with strong space charge, tailoring the longitudinal distribution to reduce the tune spread is standard practice, and can be achieved in multiple ways. Controlled longitudinal emittance blow-up is applied in the PSB to increase the emittance of LHC-type beams to 3 eVs before injecting to the PS, which allows an increase in beam brightness [3, 4]. In the CERN Low Energy Ion Ring (LEIR), the RF frequency is modulated during capture to intentionally increase the longitudinal emittance, allowing higher transmission [5]. An intentional energy offset at injection has been studied as a potential mechanism to increase transmission in the J-PARC RCS [6].

* simon.albright@cern.ch

The objective of longitudinal painting is to provide a well matched distribution from injection, avoiding filamentation and reducing space charge by maximising the longitudinal emittance. Conventional techniques, such as adiabatic capture or injecting a larger emittance are not applicable to the PSB, and using intentional mismatch to increase emittance would negatively affect performance.

Longitudinal painting is of most interest for high intensity beams. This is because the painting process requires a relatively long injection. The following section explains how painting is achieved, and what operational limits must be considered.

CONTROL OF LINAC BEAM IN TIME AND ENERGY

The PSB uses multi-turn charge-exchange injection of H^- ions accelerated by Linac4. The H^- is stripped at injection and protons are accumulated over up to 148 turns into each of the four PSB rings. The number of turns is defined by the maximum Linac4 pulse length and the time required to switch between PSB rings. Transverse painting during injection is applied to control and optimise the transverse emittance [7].

In standard operation, each injected turn is overlapped with the previous turns in longitudinal phase space. After filamentation, the beam will then fill some area in longitudinal phase space. Figure 1 shows a typical longitudinal separatrix at PSB injection in blue, in red is an iso-Hamiltonian contour containing 80% of the bucket area, the target contour to be filled after injection and filamentation. The key parameters related to longitudinal painting are also indicated.

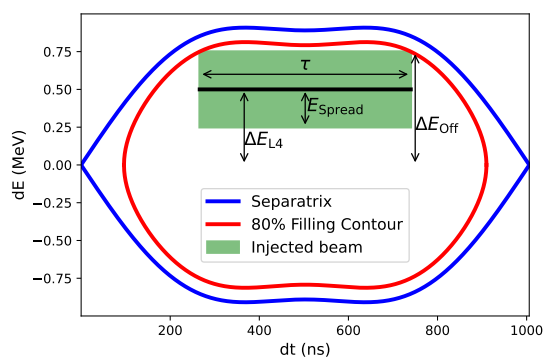

Figure 1: A typical longitudinal separatrix at PSB injection (blue) with the iso-Hamiltonian contour encircling 80% of the bucket area (red). The green box shows a beam injection with positive energy offset, representing an injected turn during longitudinal painting, with key parameters indicated.

ISBN: 978-3-95450-253-0 ISSN: 2673-5571 doi:10.18429/JACoW-HB2023-THBP39

ADVANCES ON LHC RF POWER LIMITATION STUDIES AT INJECTION*

H. Timko†, T. Argyropoulos, R. Calaga, N. Catalan Lasheras, K. Iliakis,
B. E. Karlsen-Baeck[1], I. Karpov, M. Zampetakis, CERN, Geneva, Switzerland
[1]also at the Department of Physics, Sapienza Università di Roma, Rome, Italy

Abstract

The average power consumption of the main RF system during beam injection in the High-Luminosity Large Hadron Collider is expected to be close to the maximum available klystron power. Power transients due to the mismatch of the beam and the action of control loops will exceed the available power. This paper presents the most recent estimations of the injection voltage and steady-state power needed for HL-LHC intensities, taking also beam stability into account. It summarises measurement and simulation efforts ongoing to better understand power transients and beam losses, and describes the operational margin to be taken into account for different equipment.

INTRODUCTION

The LHC is equipped with eight radio-frequency (RF) lines per beam. Each line consists of a high-power klystron, a single-cell superconducting cavity, and an independent cavity controller. The cavity controller comprises a one-turn-delay and a direct RF feedback, the latter having a low- and a high-pass branch.

For proton operation at the injection plateau, a dominant portion of the forward RF power is required to compensate beam loading. During the injection process, the RF voltage has to be kept constant over one turn, both in amplitude and phase, to efficiently capture SPS trains of bunches, which arrive with an equi-distant bunch spacing. With the voltage vector kept constant, the lowest power consumption is achieved using the half-detuning beam loading compensation scheme [1]. After the injection process, an adiabatic transition to the full-detuning beam-loading compensation scheme [2, 3] takes place, in which only the voltage amplitude is kept constant and the RF phase is modulated over the turn. This allows for a significant reduction in the RF power, providing the required voltage during the energy ramp and flattop, which would otherwise be beyond the reach of the present system.

For the LHC superconducting cavities, we apply the circuit model of the cavity-transmitter-beam interaction as derived in [4], where the generator current I_{gen} can be related to the cavity voltage V, the cavity detuning $\Delta\omega \equiv \omega_r - \omega_{\mathrm{rf}}$ from the resonant ω_{r} to the RF angular frequency ω_{rf}, the loaded quality factor Q_L and the RF beam current $I_{\mathrm{b,rf}}$ as follows:

$$I_{\mathrm{gen}}(t) = \frac{V(t)}{2R/Q}\left(\frac{1}{Q_L} - 2i\frac{\Delta\omega}{\omega_{\mathrm{rf}}}\right) + \frac{dV(t)}{dt}\frac{1}{R/Q\,\omega_{\mathrm{rf}}} + \frac{1}{2}I_{\mathrm{b,rf}}(t)\,, \tag{1}$$

where $R/Q = 45\,\Omega$ [5]. The half-detuning scheme optimises the detuning and the loaded Q to

$$\Delta\omega_{\mathrm{opt}} = \frac{R/Q\, I_{\mathrm{b,rf}}\omega_{\mathrm{rf}}}{4V} \quad \text{and} \quad Q_{L,\mathrm{opt}} = \frac{2V}{R/Q\, I_{\mathrm{b,rf}}}\,. \tag{2}$$

Under steady-state conditions, this results in the minimum average klystron forward power of

$$P_{\mathrm{gen,opt}} = \frac{1}{8}\frac{V^2}{R/Q\,Q_L} + \frac{1}{32}R/Q\,Q_L I_{\mathrm{b,rf}}^2 = \frac{V I_{\mathrm{b,rf}}}{8}\,. \tag{3}$$

At high bunch intensities towards the HL-LHC target, RF power limitations are expected (i) during the injection process and (ii) along the flat bottom [6]. This is because the SPS RF bucket has twice the length of the LHC bucket, and the SPS extracted bunch length[1] τ is long compared to the LHC bucket; for HL-LHC intensities, the bunch length spread over one bunch train is expected to be (1.65 ± 0.15) ns compared to the 2.5 ns RF period. Both capture and flat bottom losses are highly undesired as they hit the accelerator aperture at the start of the ramp. They can trigger a beam dump if they exceed the machine protection limits, in which case a roughly two-hour magnetic cycle is needed before beam can be injected again. Thus, on one hand, a higher the capture voltage is desirable to lower the losses from the tails of the bunches. On the other hand, a lower injection voltage reduces the power consumption. At injection, the maximum power consumption occurs in turn-by-turn and bucket-by-bucket transients that are due to the mismatched bunch, energy and phase errors at injection, and the action of global and local control loops. In steady state, bucket-by-bucket transients remain due to the regulation of the LHC cavity control loop.

RF POWER LIMITATIONS

Based on the LHC 2018 (Run 2) operational experience and the expected future SPS beam parameters, detailed RF power and voltage estimates for Run 3 and HL-LHC were given and refined [7–9]; see Table 1. In 2018, the capture voltage in the LHC was reduced stepwise over a period of about one month. The minimum voltage operationally acceptable was found to be 4 MV, as start-of-ramp losses occasionally reached up to 60 % of the beam dump threshold [10]. At that time, SPS-LHC energy matching and energy errors varied between -60 MeV to +90 MeV (or -1.3×10^{-4} to $+2.0\times10^{-4}$ in relative momentum offset) [10]. The largest

* Research supported by HL-LHC project
† helga.timko@cern.ch

[1] The bunch length is defined as a scaled full-width-half-maximum (FWHM) bunch length $\tau \equiv 2/\sqrt{2\ln 2}\,\mathrm{FWHM}$. For a Gaussian bunch, this results in a four-sigma bunch length.

ISBN: 978-3-95450-253-0 ISSN: 2673-5571 doi:10.18429/JACoW-HB2023-THBP40

MITIGATION STRATEGIES FOR THE INSTABILITIES INDUCED BY THE FUNDAMENTAL MODE OF THE HL-LHC CRAB CAVITIES

L. Giacomel*, P. Baudrenghien, X. Buffat, R. Calaga, N. Mounet
CERN, Geneva, Switzerland

Abstract

The transverse impedance is one of the potentially limiting effects for the performance of the High-Luminosity Large Hadron Collider (HL-LHC). In the current LHC, the impedance is dominated by the resistive-wall contribution of the collimators at typical bunch-spectrum frequencies, and is of broad-band nature. Nevertheless, the fundamental mode of the crab cavities, that are a vital part of the HL-LHC baseline, adds a strong and narrow-band contribution. The resulting coupled-bunch instability, which contains a strong head-tail component, requires dedicated mitigation measures, since the efficiency of the transverse damper is limited against such instabilities, and Landau damping from octupoles would not be sufficient. The efficiency and implications of various mitigation strategies, based on RF feedbacks and optics changes, are discussed, along with first measurements using crab cavity prototypes at the Super Proton Synchrotron (SPS).

INTRODUCTION

The crab cavities are a fundamental component of the HL-LHC project, which allow colliding with a large crossing angle without a major loss of luminosity [1]. These special radio-frequency (RF) cavities act as transverse deflectors, therefore their fundamental mode has a strong transverse component. The main parameters of the fundamental mode are summarized in Table 1 (the fundamental frequency is the instantaneous RF frequency) In the crabbing plane, the beam-coupling impedance of the fundamental mode of the crab cavities has a peaked dipolar component which is modelled through the formula

$$Z_\perp(f) = \frac{f_r}{f}\frac{R_\perp}{1 - iQ_L\left(\frac{f_r}{f} - \frac{f}{f_r}\right)}.$$

The resulting impedance curve is shown in Fig. 1, and the total transverse impedance model [2] including the crab cavities contribution, in Fig. 2. In the total impedance curves, the fundamental crabbing mode stands out due to its high shunt impedance. Weighted by the beta function at the cavities, it is more than three orders of magnitude higher than the LHC impedance at the fundamental frequency f_r. It is important to notice that the fundamental frequency is at a $\sim$ 3 kHz offset with respect to the closest critical betatron side-band. In these proceedings, we study the flat-top machine configuration as it is the most critical phase for stability. We use the $\beta^* = 1$ m optics, which will be used before the beams are brought in collision. During the collision phase, the bunches colliding head-on in IP1 and IP5 experience such a strong Landau Damping because of the beam-beam interactions that the impedance-induced instabilities are not harmful.

* lorenzo.giacomel@cern.ch

Table 1: Crab Cavities Fundamental Mode Parameters

Parameter	Value
Shunt impedance, $R_\perp$	$0.9024\,\mathrm{G\Omega\,m^{-1}}$
Loaded Quality factor, Q_L	$5 \cdot 10^5$
Fundamental frequency, f_r	400.789 MHz

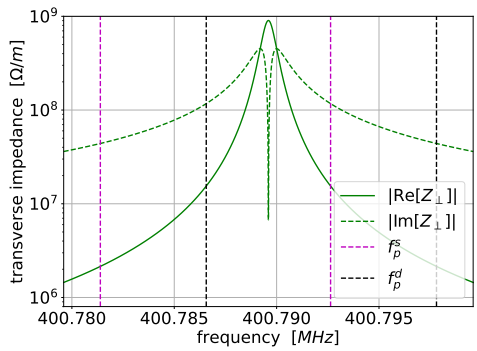

Figure 1: Beam-coupling impedance of the crab cavities fundamental mode. The dashed lines represent the betatron frequencies.

FUNDAMENTAL MODE AND

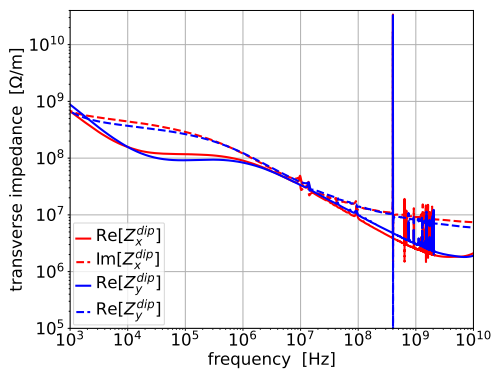

Figure 2: LHC dipolar impedances including the crab cavities fundamental mode.

ISBN: 978-3-95450-253-0 ISSN: 2673-5571 doi:10.18429/JACoW-HB2023-THBP42

LONGITUDINAL LOSS OF LANDAU DAMPING IN DOUBLE HARMONIC RF SYSTEMS BELOW TRANSITION ENERGY

L. Intelisano*,[1], H. Damerau, I. Karpov, CERN, Geneva, Switzerland
[1]also at Sapienza Università di Roma, Rome, Italy

Abstract

Landau damping plays a crucial role in ensuring single-bunch stability in hadron synchrotrons. In the longitudinal plane, loss of Landau damping (LLD) occurs when a coherent mode of oscillation moves out of the incoherent synchrotron frequency band. The LLD threshold is studied for a purely inductive impedance below transition energy, specifically considering the common case of double harmonic RF systems operating in counter-phase at the bunch position. The additional focusing force due to beam-induced voltage distorts the potential well, ultimately collapsing the bucket. The limiting conditions for a binomial particle distribution are calculated. Furthermore, the contribution focuses on the configuration of the higher-harmonic RF system at four times the fundamental RF frequency operating in phase. In this case, the LLD threshold shows a non-monotonic behavior with a zero threshold where the derivative of the synchrotron frequency distribution is positive. The findings are obtained employing semi-analytical calculations using the MELODY code.

INTRODUCTION

In the longitudinal plane, Landau damping [1] is established by the synchrotron frequency spread of individual particles caused by the non-linear voltage of the RF system [2–14]. A common technique to enhance beam stability is employing multiple RF systems, which can enlarge the synchrotron frequency spread.

This work focuses on the common case of a double-harmonic RF (DRF) system and considers a pure inductive impedance below the transition energy or, equivalently, capacitive impedance above it.

DRF systems are based on employing a higher harmonic RF system, typically working at a multiple of the fundamental RF frequency. In this configuration, the total voltage experienced by the particles is given by

$$V_{\mathrm{rf}}(\phi) = V_0[\sin(\phi + \phi_{s0}) + r\sin(n\phi + n\phi_{s0} + \Phi_2)]\,, \quad (1)$$

where V_0, r, and ϕ_{s0} are the voltage magnitudes of the main harmonic RF system, the voltage ratio between the higher and the fundamental harmonic number, and the phase of the synchronous particle. As far as ϕ, n, and Φ_2 are concerned, they represent the phase offset with respect to the synchronous particle, the harmonic number ratio, and the relative phase between the two RF systems. Two distinct operational modes can be distinguished depending on the relative phase Φ_2. Bunch shortening mode (BSM) occurs when the RF systems are in phase at the bunch position, leading to shorter bunches. On the contrary, when the RF systems are in counter-phase, it is referred to as bunch lengthening mode (BLM). Figure 1 illustrates the synchrotron frequency distributions for different orders of RF harmonic number ratio, n, in both configurations.

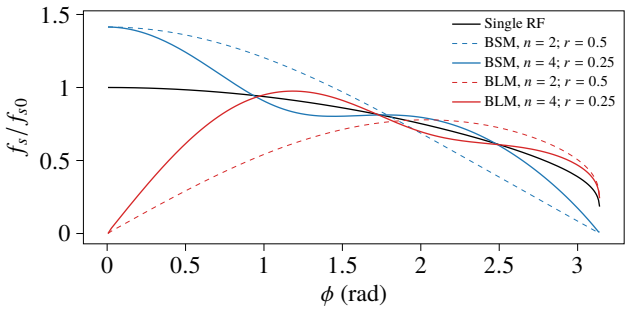

Figure 1: Synchrotron frequency distribution, normalized to small-amplitude synchrotron frequency, f_{s0}, in a single-harmonic RF system (black), BSM (blue) and BLM (red), as a function of the maximum phase deviation of the particle. No acceleration and collective effects are considered.

The studies presented in this contribution have been conducted with semi-analytical calculations using the code MELODY [15], based on the Oide-Yokya method [16]. To allow a direct comparison with the analysis for single RF [12] and BSM above transition [17], the same accelerator parameters outlined in Table 1 have been considered.

Table 1: Main RF Parameters of the LHC

Parameter	Unit	Value
Circumference, $2\pi R$	m	26658.86
Main harmonic number, h		35640
Main RF frequency, f_{rf}	MHz	400.79
Beam energy at injection, E_0	TeV	0.45
Main RF voltage V_0	MV	6
Effective impedance, $\mathrm{Im}Z/k$	Ω	−0.07

MAIN EQUATIONS AND DEFINITIONS

For convenience, the analysis is performed with the set of variables $(\mathcal{E}, \psi)$ to describe the longitudinal beam dynamics, which correspond to the energy and phase of the synchrotron oscillations:

$$\mathcal{E} = \frac{\dot{\phi}^2}{2\omega_{s0}^2} + U_t(\phi)\,,$$
$$\psi = \mathrm{sgn}(\eta\Delta E)\frac{\omega_s(\mathcal{E})}{\sqrt{2}\omega_{s0}}\int_{\phi_{\max}}^{\phi}\frac{\mathrm{d}\phi'}{\sqrt{\mathcal{E} - U_t(\phi')}}\,, \quad (2)$$

* leandro.intelisano@cern.ch

ISBN: 978-3-95450-253-0 ISSN: 2673-5571 doi:10.18429/JACoW-HB2023-THBP43

INTENSITY EFFECTS IN A CHAIN OF MUON RCSs

F. Batsch*,[1], H. Damerau[1], I. Karpov[1],
D. Amorim[1], A. Chancé[2], A. Grudiev[1], E. Métral[1], D. Schulte[1], S. Udongwo[3]
[1]CERN, Geneva, Switzerland
[2]CEA, Paris-Saclay, France
[3]University of Rostock, Germany

Abstract

The muon collider offers an attractive path to a compact, multi-TeV lepton collider. However, the short muon lifetime leads to stringent requirements on the fast energy increase. While extreme energy gains in the order of several GeV per turn are crucial for a high elevated muon survival rate, ultra-short and intense bunches are needed to achieve large luminosity. The longitudinal beam dynamics of a chain of rapid cycling synchrotrons (RCS) for acceleration from around 60 GeV to several TeV is being investigated in the framework of the International Muon Collider Collaboration. Each RCS must have a distributed radio-frequency (RF) system with several hundred RF stations to establish stable synchrotron motion. In this contribution, the beam-induced voltage in each RCS is studied, assuming a single high-intensity bunch per beam in each direction and ILC-like 1.3 GHz accelerating structures. The impact of single- and multi-turn wakefields on longitudinal stability and RF power requirements is analysed with particle tracking simulations. Special attention is moreover paid to the beam power deposited into the higher-order modes of the RF cavities.

INTRODUCTION

The recent improvements in accelerator technologies like superconducting magnets with fields beyond 8 T or high-gradient radio-frequency (RF) structures led to a strong interest in the development of a muon collider facility in the multi-TeV regime. The International Muon Collider Collaboration (IMCC) works towards a design proposal for a staged facility with 3 TeV to 10 TeV collision energy [1, 2] based on the US Muon Acceleration Program (MAP) [3, 4]. Luminosities of $2 \cdot 10^{35}\,\mathrm{cm}^{-2}\mathrm{s}^{-1}$ (at 10 TeV) are reached by colliding single high-intensity μ^+ and μ^- bunches with populations of $1.8 \cdot 10^{12}$ muons per bunch at the time of injection into the collider ring. The muon bunches are formed by depositing protons on a target, followed by 6-dimensional cooling. The subsequent accelerator complex consists of a low-energy part for an initial acceleration to an energy of about 60 GeV, and a high-energy part on which this paper focuses. A chain of rapid cycling synchrotrons (RCS) is foreseen to accelerate two counter-rotating bunches in stages of 0.30 TeV, 0.75 TeV and 1.5 TeV to finally 5 TeV at a repetition rate of 5 Hz, before injecting them into the separate collider ring. The accelerator chain is sketched in Fig. 1.

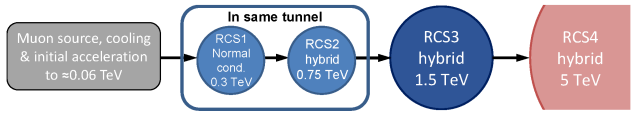

Figure 1: Schematic of the chain of rapid cycling-synchrotrons for the high-energy acceleration complex.

This design is fully driven by the muon decay. The muon lifetime at rest of $\tau_\mu = 2.2\,\mu\mathrm{s}$ is time-dilated by the extremely fast acceleration which extends the lifetime by the relativistic Lorentz factor γ, which reaches $4.7 \cdot 10^4$ at an energy of 5 TeV. A further challenge besides the fast acceleration is the high bunch population. Around $2.7 \cdot 10^{12}$ muons per bunch at the beginning of the RCS chain have to be accelerated to meet the target beam parameters [2] in the collider. Strong transient beam loading is expected due to the large peak current. For the studies, we extended the longitudinal macro-particle tracking code BLonD [5, 6] to the regime of multi-turn wakefields in multiple RF stations per ring. We observe the impact of these intensity effects on the longitudinal stability and the resulting RF power requirements. Single- and multi-turn wakefields are analyzed for the single bunches. We cover both the fundamental mode (FM) and higher-order modes (HOMs) of the RF cavities, including the beam power deposited into these HOMs.

BEAM AND RF PARAMETERS

A selection of preliminary parameters for the RCSs is listed in Table 1. Since the different RCSs are foreseen to use the same cavity type, our studies focus on the first RCS where the bunch population is highest. The RCS1 and RCS2

Table 1: Example parameters for the muon RCSs assuming a 90 % survival rate per RCS and an RF system at 1.3 GHz. Values for RCS4 are draft parameters.

	RCS1	RCS2	RCS3	RCS4
Circumference [m]	5990	5990	10700	35000
Injection energy [TeV]	0.06	0.30	0.75	1.50
Ejection energy [TeV]	0.30	0.75	1.50	5.00
Acceleration time [ms]	0.34	1.10	2.37	6.4
Revolution period [μs]	20.0	20.0	35.7	117
Number of turns	17	55	66	55
ΔE per turn [GeV]	14.8	7.9	11.4	64
Bunch intensity [10^{12}]	2.7	2.43	2.2	2.0
Bunch length [1σ, ps]	<45	<33	<28	<17
Bunch current [mA]	21.7	19.5	9.9	3.0
Target ε_L (4σ) [eVs]	0.31	0.31	0.31	0.31

* fabian.batsch@cern.ch

ISBN: 978-3-95450-253-0 ISSN: 2673-5571 doi:10.18429/JACoW-HB2023-THBP44

ImpactX MODELING OF BENCHMARK TESTS FOR SPACE CHARGE VALIDATION*

C. Mitchell†, A. Huebl, J. Qiang, R. Lehe, M. Garten, R. Sandberg, J-L. Vay
Lawrence Berkeley National Laboratory, Berkeley, CA, USA

Abstract

The code ImpactX represents the next generation of the particle-in-cell code IMPACT-Z, featuring s-based symplectic tracking with 3D space charge, parallelism with GPU acceleration, adaptive mesh-refinement, and modernized language features. With such a code comes a renewed need for space charge validation using well-defined benchmarks. For this purpose, the code is continuously checked against a test suite of exactly-solvable problems. The suite includes field calculation tests, dynamical tests involving coasting or stationary beams, and beams matched to periodic focusing channels. We evaluate the code performance on documented space charge benchmarks appropriate for high-intensity bunched beams.

CODE DESIGN

ImpactX [1, 2] is a GPU-capable C++ successor to the code IMPACT-Z [3], built on the AMReX software framework [4], for modeling relativistic charged particle beams in linacs or rings. Similar to IMPACT-Z, tracking is performed with respect to the path length variable s, and space charge is included using a second order operator splitting [5]. All tracking methods are symplectic by design, and maps are used where possible for efficient particle pushing. The 3D space-charge fields are computed with an iterative Multi-Level Multi-Grid (MLMG) Poisson solver [4], providing support for adaptive mesh refinement. The code is continuously benchmarked (after every code change) against a suite of >20 test problems, designed to validate each feature of the code. The space charge benchmarks, to be described, are valid for bunched beams in the presence of open boundary conditions.

BENCHMARK PROBLEMS

The code was used to reproduce the space charge benchmark problems described in Refs. [6] and [7]. However, the first problem in [7], involving a matched K-V beam in a periodic focusing channel (appropriate for beams with 2D space charge), has been replaced by a Kurth beam in a periodic focusing channel [8] (appropriate for bunches with 3D space charge). In each case, the boundary used by the Poisson solver is placed sufficiently far from the beam to reproduce the free-space space charge fields.

Space Charge Fields in a Gaussian Bunch

This benchmark is described in detail in Ref. [6]. In Fig. 1, the space charge fields within a 1 nC Gaussian electron bunch (at rest) produced by ImpactX are compared against the exact results for several values of the beam aspect ratio. Some visible discrepancy appears in the values of E_x for large aspect ratio ($r \leq 0.2$). In the future, the case of large aspect ratio will be addressed more efficiently using integrated Green function techniques [9].

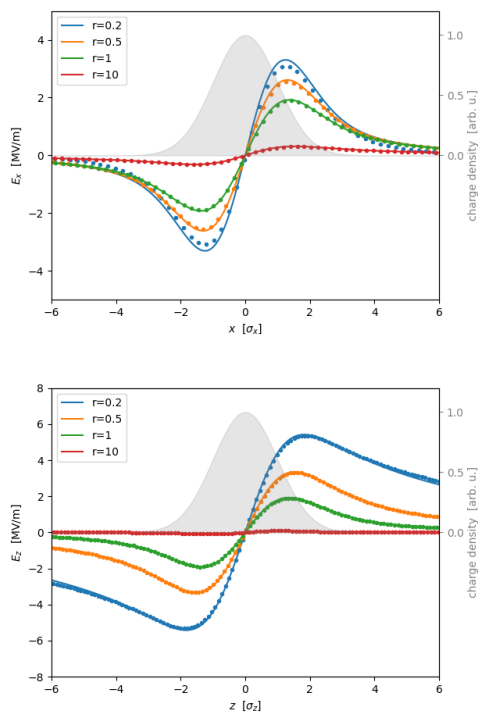

Figure 1: Electric field in a Gaussian bunch using ImpactX, 1 M particles and [128, 128, 256] grid (dots) and from Eq. (1) of Ref. [6] (lines) for various aspect ratios $r = \sigma_z/\sigma_\perp$. The bunch charge is 1 nC, with $\sigma_x = \sigma_y = \sigma_\perp = 1$ mm. (Upper) Along the line $y = 0$, $z = 0$. (Lower) Along the line $x = 0$, $y = 0$. Compare Fig. 1 of Ref. [6].

Figure 2 shows the phase space of an initially cold Gaussian 1 nC electron bunch after drifting a distance of 1 m, comparing the final particle populations of ImpactX and

* This work was supported by the Director, Office of Science of the U.S. Department of Energy under Contracts No. DE-AC02-05CH11231 and DE-AC02-07CH11359. This material is based upon work supported by the CAMPA collaboration, a project of the U.S. Department of Energy, Office of Science, Office of Advanced Scientific Computing Research and Office of High Energy Physics, Scientific Discovery through Advanced Computing (SciDAC) program. This research used resources of the National Energy Research Scientific Computing Center, a DOE Office of Science User Facility supported by the Office of Science of the U.S. Department of Energy under Contract No. DE-AC02-05CH11231 using NERSC award HEP-ERCAP0023719. Robert Ryne provided helpful clarification for problems described in Ref. [7].
† ChadMitchell@lbl.gov

ISBN: 978-3-95450-253-0 ISSN: 2673-5571 doi:10.18429/JACoW-HB2023-THBP45

LONGITUDINAL COLLECTIVE EFFECTS AT BEAM TRANSFER FROM PS TO SPS AT CERN

A. Lasheen*, H. Damerau, I. Karpov, G. Papotti, E. Vinten, CERN, Geneva, Switzerland

Abstract

The hardware upgrades of the LHC Injectors Upgrade (LIU) project at CERN were completed during the Long Shutdown 2 (2019-2021) to prepare the injectors for the beams required by the High Luminosity (HL) LHC. Doubling the bunch intensity leads to new challenges due to collective effects. Although many bottlenecks were already solved, a remaining limitation is the important loss of particles at transfer from the Proton Synchrotron (PS) to the Super Proton Synchrotron (SPS). The maximum transmission achieved since the restart in 2021 is in the order of 90%, yet leading to unnecessary activation of the SPS. The losses are distributed at various instants of the SPS cycle: fast intensity decay right after injection, slow losses along the injection plateau while waiting for multiple injections from the PS, and uncaptured beam removed at start of acceleration. In this contribution, the focus is on longitudinal aspects of transfer losses and more specifically on intensity effects during the non-adiabatic bunch shorting performed in the PS prior to extraction, as well as on the longitudinal mismatch at injection due to misaligned bunch phases in the SPS caused by transient beam loading.

INTRODUCTION

The design and improvements of the transfer of LHC-type beams from the PS to the SPS is a long standing topic of study. The main challenge resides in transferring long bunches from the PS (with longitudinal emittance $\varepsilon_l = 0.35$ eVs), to the short RF buckets in the SPS. A non-adiabatic bunch shortening is performed in the PS by applying a fast voltage increase with two pairs of cavities at 40 MHz and 80 MHz [1, 2]. The corresponding RF voltage program as set in operations in 2023 is displayed in Fig. 1 (left). This process brings the bunch length from about $\tau_l = 4\sigma = 11$ ns to $\tau_l = 3.8$ ns, allowing the bunches to fit in the 5 ns SPS RF bucket (Fig. 1 middle, σ is the RMS bunch length). One drawback are longitudinal tails which do not rotate entirely due to the non-linearity of the RF bucket, and are then lost at capture in the SPS (Fig. 1, right).

Extensive studies were conducted in view of doubling the beam intensity for the High-Luminosity (HL) LHC [3]. These studies included beam measurements [4] and simulations to investigate potential for improvements (in the PS [5] and in the SPS [6–8]). Following the LHC Injector Upgrade project [9] completed in 2021, the best achieved transmission in 2022 was 90% with injection of multiple trains in the SPS [10] at the baseline intensity of $N_b = 2.6 \times 10^{11}$ protons per bunch (ppb) and 25 ns bunch spacing. From the present losses, about 20% are occurring at the start of acceleration and can be measured as longitudinally uncaptured beam. These appear to increase overproportionnally above $N_b = 2.0 \times 10^{11}$ ppb pointing towards collective effects. In this paper, we present advancements of the simulation on the PS side to better represent collective effects during the bunch rotation, as well as recent observations in the SPS measured at highest beam intensity.

TRANSIENT BEAM LOADING DURING BUNCH ROTATION IN THE PS

An important effort was invested to update the PS longitudinal impedance model to improve the treatment of RF systems with feedback loops [11]. To build this model, a thorough survey of all equipment in the ring was done, complemented by the representation of the impedance through RF measurements or simulations. The most important contributions are the RF systems (25 systems tuned at six different frequencies). Simulations using the BLonD tracking code [12]

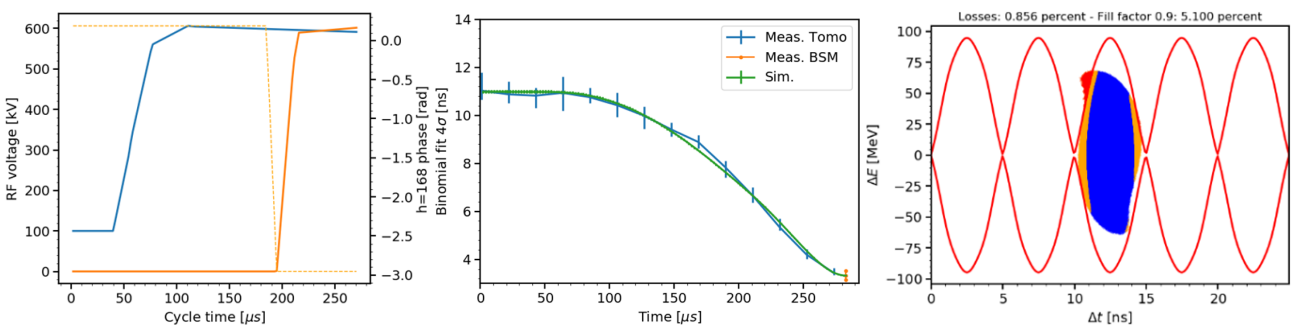

Figure 1: The RF voltage program during the bunch rotation before extraction of the LHC-type beams from the PS (left), the corresponding bunch length evolution (middle, measured and simulated), and the simulated longitudinal phase space distribution at extraction (right). The losses are evaluated in simulations by considering particles outside of the SPS RF bucket as lost (in red), as well as the particles too close to the separatrix (orange, 90% in amplitude from separatrix).

* alexandre.lasheen@cern.ch

ISBN: 978-3-95450-253-0 ISSN: 2673-5571 doi:10.18429/JACoW-HB2023-THBP46

SIMULATION OF THE ESS PROTON BEAM WINDOW SCATTERING

E. Fackelman, K. Sjobak*, H. Gjersdal, E. Adli, University of Oslo, Oslo, Norway
C. Thomas, Y. Levinsen, A. Takibayev, European Spallation Source, Lund, Sweden

Abstract

The European Spallation Source produces neutrons used for science by delivering a 5 MW proton beam to a tungsten target. The proton beam parameters must remain within a well-defined range during all phases of facility exploitation. The proton beam parameters are measured and monitored by an instrumentation suite, among which are two beam imaging systems. Parameters such as position and beam current density can be calculated from the images, supporting beam tuning and operation. However, one of the two systems may be affected by beam scattering. In this paper, we will focus on modelling the impact of the scattering on the beam on target distribution. The modelling process, involving simulation codes such as Geant4 and two-dimensional convolution in Matlab, is described. Initially, Geant4 simulates a scattered pencil beam. The resulting distribution is fitted and can be used similarly to an instrument response in image processing to model any possible beam distribution. Finally, we discuss the results of the scattered beam imaging model, showing the range of applications of the model and the impact of scattering on the beam parameters.

BACKGROUND

Before hitting the tungsten target of the European Spallation Source (ESS), the beam passes through the Proton Beam Window (PBW), which separates the accelerator vacuum from the target vacuum, as illustrated in Fig. 1. This passage through matter scatters the beam, increasing the footprint size on the front surface of the target. The footprint of each bunch is already enlarged using magnetic quadrupoles, and each bunch is placed at different locations on the target by fast rastering kicker magnets [1]. If the footprint is smaller than expected due to, e. g. a magnet failure, it can damage the target and the PBW. Furthermore, if the beam is larger than expected, it can damage equipment surrounding the target and beamline components. For this reason, the Target Imaging System (TIS) continuously produces images of the beam at the target and the PBW, which are coated with a luminescent material. The TIS will help the operators, and eventually automatic systems, detect and react to errant beam conditions before they damage the target region. However, the particle distribution during nominal beam conditions must be known for this to work well. Describing this distribution is part of the goal of the work described in this paper, which will also help in understanding abnormal scenarios.

* k.n.sjobak@fys.uio.no

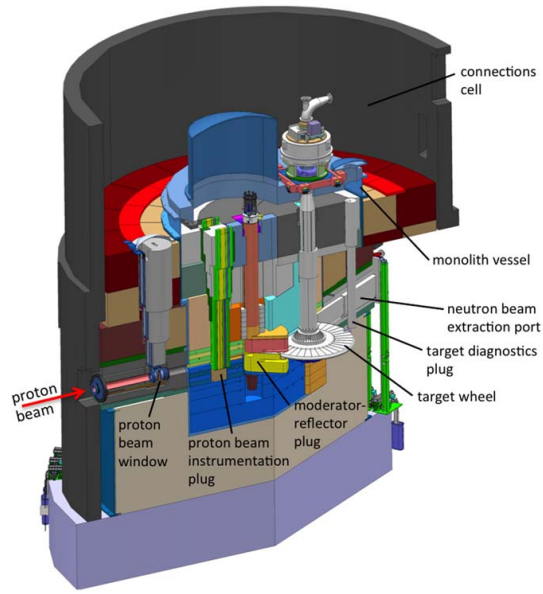

Figure 1: Illustration of the layout of the ESS target region. The beam comes in from the left, passing through the PBW and through the aperture of the proton beam instrumentation plug and also between the "wings" of the neutron moderator/reflector, before hitting the target wheel. Image from Ref. [2].

SETUP

Simulation with Geant4/MiniScatter

The main simulation tool used in this work is MiniScatter [3]. This is an application built on Geant4 [4–6] with a Python wrapping which makes it easy to create or load particle distributions, setup simple geometries, and extract information in the form of ROOT [7] histograms and trees. For this simulation, the QGSP_BERT_EMZ physics list was used with a production cut of 100 µm.

Geant4 handles the tracking of particles through the experiment, until they either exit the simulation volume or lose all their energy. For each step a particle makes, the energy loss, scattering angle, and whether to do secondary particle generation is decided via the Monte Carlo method, taking the particle and material properties into account.

The Proton Beam Window was modelled as shown in Fig. 2 (a), with a 1.25 mm thick front surface made from aluminum, a 2 mm water cooling channel, and a 1 mm back surface of aluminum. The radius of curvature of the downstream surface is 88 mm, and the horizontal/vertical size is $200 \times 160\ \mathrm{mm}^2$. The model is based on the design model [8, 9].

The overall geometry used for the MiniScatter simulation is shown in Fig. 2 (b), indicating the plane where the particles

ISBN: 978-3-95450-253-0 ISSN: 2673-5571 doi:10.18429/JACoW-HB2023-THBP47

STUDIES ON THE EFFECT OF BEAM-COUPLING IMPEDANCE ON SCHOTTKY SPECTRA OF BUNCHED BEAMS

C. Lannoy*,[1], D. Alves, K. Lasocha, N. Mounet, CERN, Geneva, Switzerland
T. Pieloni, EPFL, Lausanne, Switzerland
[1]also at EPFL, Lausanne, Switzerland

Abstract

Schottky monitors can be used for non-invasive beam diagnostics to estimate various bunch characteristics, such as tune, chromaticity, bunch profile or synchrotron frequency distribution. However, collective effects, in particular beam-coupling impedance, can significantly affect Schottky spectra when large bunch charges are involved. In such conditions, the available interpretation methods are difficult to apply directly to the measured spectra, thus preventing the extraction of beam and machine parameters, which is possible for lower bunch charges. To study the impact of impedance on such spectra, we perform here time-domain, macro-particle simulations and apply a semi-analytical method to compute the Schottky signal for various machine and beam conditions, including those corresponding to typical physics operation at the Large Hadron Collider. This study provides preliminary interpretations of the impact of beam-coupling impedance on Schottky spectra by incorporating longitudinal and transverse resonator-like impedance models into the simulations.

INTRODUCTION

Schottky spectra are a powerful diagnostic tool for investigating the longitudinal and transverse dynamics of charged particle beams. However, the accurate interpretation of these spectra becomes particularly challenging when collective effects such as beam-coupling impedance become significant as can be the case for proton bunches in the Large Hadron Collider (LHC). While theoretical frameworks for Schottky spectrum reconstruction exist [1–4], they do not include impedance effects which can strongly affect the spectra in certain conditions. In Ref. [5], we started investigating the effect of impedance on the longitudinal spectrum and addressed some of the gaps in existing theories.

The following section focuses on the effects of a longitudinal broad-band (BB) resonator on the Schottky spectrum and investigates, both theoretically and through simulations, the impact of such an impedance. Then, in the third section we explore through simulations how a transverse broad-band resonator affects the Schottky spectrum. Our concluding remarks then follow.

LONGITUDINAL BROAD-BAND RESONATOR

The equation of motion for the radio frequency (RF) phase ϕ of a given particle in the presence of longitudinal beam-coupling impedance was derived in Ref. [5] and is given by

$$\ddot{\phi} + \Omega_0^2 \sin\phi = \Omega_0^2 \frac{I}{\widehat{V}\cos\phi_s} \sum_{p=-\infty}^{\infty} Z_\parallel(p)\widehat{\lambda}(p) e^{j\frac{p}{h}\phi}, \quad (1)$$

with the nominal synchrotron frequency Ω_0, the average bunch current I, the amplitude of the RF voltage $\widehat{V}$, the synchronous phase ϕ_s, the revolution frequency ω_0, the longitudinal impedance $Z_\parallel(p) \equiv Z_\parallel(p\omega_0)$, the bunch spectrum $\widehat{\lambda}(p) \equiv \widehat{\lambda}(p\omega_0)$, and the RF harmonic number h. By expanding the sine and exponential functions into their Maclaurin series, the previous equation can be written in the compact form

$$\ddot{\phi} + \Omega_0^2 \sum_{n=0}^{\infty} S_n \phi^n = 0, \quad (2)$$

with the coefficients S_n defined by

$$S_n = \begin{cases} -Z_n & : n \text{ even}, \\ \frac{j^{n-1}}{n!} - Z_n & : n \text{ odd}, \end{cases}$$

and

$$Z_n = \frac{I j^n}{\widehat{V}\cos\phi_s\, n! h^n} \sum_{p=-\infty}^{\infty} \widehat{\lambda}(p) p^n \times \begin{cases} Re[Z_\parallel(p)] & : n \text{ even}, \\ j\, Im[Z_\parallel(p)] & : n \text{ odd}. \end{cases}$$

In order to derive an analytical relation between the amplitude of the synchrotron oscillation and its frequency, we assumed in Ref. [5] that the even terms in Eq. (2) can be neglected. In the following, we present how one can assess if this approximation is valid for a given impedance $Z_\parallel(p)$.

The complex exponential in Eq. (1) can also be expanded with the trigonometric functions

$$\ddot{\phi} + \Omega_0^2 \sin\phi = \frac{\Omega_0^2 I}{\widehat{V}\cos\phi_s} \sum_{p=-\infty}^{\infty} Z_\parallel(p)\widehat{\lambda}(p) \left(\cos(\frac{p}{h}\phi) + j\sin(\frac{p}{h}\phi)\right).$$

The cosine term is an even function and corresponds to the sum of all the even terms from Eq. (2). A first approximation of the RF phase shift for a particle of given synchrotron time-amplitude $\widehat{\tau}$ is given by the time average of the sum of the even terms:

$$\Delta\phi_s(\widehat{\tau}) = \frac{1}{S_1} \sum_{n=0}^{\infty} S_{2n} \left\langle \phi^{2n}(t) \right\rangle_t = \frac{I}{S_1 \widehat{V}\cos\phi_s} \sum_{p=-\infty}^{\infty} Re\left[Z_\parallel(p)\right] \widehat{\lambda}(p) \left\langle \cos\left(\frac{p}{h}\phi(t)\right)\right\rangle_t, \quad (3)$$

* christophe.lannoy@cern.ch

ISBN: 978-3-95450-253-0 ISSN: 2673-5571 doi:10.18429/JACoW-HB2023-THBP48

LATEST ADVANCES IN TARGETRY SYSTEMS AT CERN AND EXCITING AVENUES FOR FUTURE ENDEAVORS

R. Franqueira Ximenes*, M. Calviani†, O. Aberlee, R. Esposito, J.-L. Grenard,
T. Griesemer, A. Romero Francia, C. Torregrosa
CERN - European Organization for Nuclear Research, Geneva, Switzerland

Abstract

CERN's accelerator complex offers a variety of target systems to meet diverse scientific objectives, encompassing different beam energies, intensities, pulse lengths, and goals. The objective of future high-intensity fixed target experiments is to further advance this field. This contribution emphasises enhanced operational target systems, which significantly boost CERN's physics pursuits. An illustrative example is the third-generation n_TOF spallation neutron target, employing a nitrogen-cooled pure lead system impacted by a 20 GeV/c proton beam. Another example focuses on recent upgrades to antiproton production targets, where a high-intensity 26 GeV/c beam collides with a thin-air-cooled iridium target. Looking ahead, there are plans for new high-power target systems. One of the goals is to discover hidden particles utilizing a 350 kW high-Z production target, while another aims to enhance kaon physics through a 100 kW low-Z target. This article provides an overview of the current target systems at CERN, detailing beam-intercepting devices and engineering aspects. Additionally, it offers a preview of upcoming facilities that are on under consideration for implementation at CERN.

INTRODUCTION

CERN's accelerator complex provides a diverse spectrum of fixed target experiments to serve scientific objectives, encompassing different beam energies, intensities, pulse lengths, and goals. Addressing the design of target systems holistically is crucial to effectively support the physics program, ensure the reliability of its materials and mechanical system, and ensure that the best ALARA radiation protection practices are employed. Generally, beam-intercepting devices, and specifically production targets, are among the most radioactive devices at CERN.

During CERN's Long-Shutdown 2 (2018-2021), the two highest power target facilities of the Proton Synchrotron (PS) complex underwent extensive consolidation programs. The Antiproton Decelerator Target (AD-T) area and the Neutron-Time-Of-Flight (n_TOF) Target Facilities saw comprehensive upgrades to their production targets to maintain reliable and safe operation. In both cases, matching pre-LS2 physics performance was the baseline. However, a significant aspect of this initiative was to enhance mechanical system reliability and, notably, mitigate concerns regarding radiation protection. Additionally, extensive efforts were undertaken to refurbish the facilities and auxiliary services.

* rui.franqueira.ximenes@cern.ch
† marco.calviani@cern.ch

CERN's efforts in targetry extend beyond the consolidation of existing infrastructure. Looking ahead, plans are underway for new high-power target systems. An exciting project, the High Intensity ECN3 (HI-ECN3), is set to commence a Technical Design phase (TDR) in 2024, with implementation and operation targeted for 2030 (midway through CERN's Run 4). The project will deliver a high intensity and power beam to one of two competitive and compelling experimental candidates, which will be selected by the end of 2023 from the Physics Beyond Collider (PBC) Study Group proposals [1, 2]: The Beam Dump Facility (BDF) [3] together with the Search for the Hidden Particle Experiment (SHiP) [4], and the High-Intensity Kaon Experiments (HIKE) [5] together with the Search for Hidden And Dark Objects With the SPS (SHADOWS) [6].

This article provides an overview of some of the current target systems at CERN, detailing beam-intercepting devices and engineering aspects enhancing CERN's physics endeavours. Notably the main outcomes of LS2 consolidation works for the AD-Target and n_TOF Target facilities and possible future plans for these. Additionally, it also previews upcoming target facilities that may soon be implemented at CERN.

n_TOF TARGET

The n_TOF facility employs about 15 % of the complex protons to carry out neutron induced capture, fission and charge-particle cross-section measurements for astrophysics and basic nuclear physics research, as well as multidisciplinary measurements in medical applications and hadron therapy [7]. During LS2, the second generation water-cooled target has been removed and replaced by a new N_2-cooled pure lead spallation target, optimised for both the horizontal (EAR1) and vertical (EAR2) experimental neutron beamlines [8]. A complete new cooling station has been installed at the surface, and a new mobile shielding in the target pit. The latter opened the door for a new material irradiation facility named NEAR [9, 10].

The new n_TOF spallation Target (3rd generation) moves away from past water-cooled designs by employing N_2 cooling gas and significantly modifies the mechanical design [8, 11]. The target core consists of six slices of pure lead (> 99.99 % Pb) totalling approximately 1.5 tonnes, held in place by an aluminium EN AW-6082 T6 alloy cradle incorporating intermediate anti-creep plates. This aluminium structure serves a dual purpose: optimising N_2 flow distribution to efficiently cool the Pb hottest surface spots, and preventing creep of the lead blocks. The precise design

ISBN: 978-3-95450-253-0 ISSN: 2673-5571 doi:10.18429/JACoW-HB2023-THBP49

COLLIMATION OF 400 MJ BEAMS AT THE LHC: THE FIRST STEP TOWARDS THE HL-LHC ERA*

S. Redaelli, A. Abramov, D. Baillard, R. Bruce, M. D'Andrea, R. Cai, F. Carra, M. Di Castro, L. Giacomel, P. Hermes, B. Lindström, N. Mounet, F.-X. Nuiry, D. Mirarchi, A. Perillo Marcone, F. Van der Veken, A. Vella, CERN, Geneva, Switzerland

Abstract

An important upgrade programme is planned for the collimation system of the CERN Large Hadron Collider (LHC) in order to meet the challenges of the upcoming High-Luminosity LHC (HL-LHC) project. The first upgrade stage was already deployed during the last LHC Long Shutdown, offering improvements in the collimation cleaning, a significant reduction of the impedance contribution and better cleaning of collisional losses, in particular for ion-ion collisions. A new crystal collimation system was also deployed to improve the halo cleaning for heavy-ion beams. This upgrade provides the opportunity to explore the intensity limits during the LHC Run 3 and collect crucial feedback to refine upgrade plans and operational scenarios in the HL-LHC era. This paper describes the performance of the LHC Run 3 collimation system that has already enabled record stored beam energies above 400 MJ for protons at 6.8 TeV, and reviews further upgrade plans to reach 700 MJ beams at the HL-LHC.

INTRODUCTION

The Large Hadron Collider (LHC) at CERN is a 27 km-long circular collider for protons and heavy ions [1] designed to accelerate beams up to 7 TeV per charge. The LHC is presently in its third run (Run 3) that will last until 2025, followed by the third Long Shutdown (LS3) that will be dedicated to the deployment of the High-Luminosity LHC (HL-LHC) [2]. One of the key HL-LHC upgrade targets is to increase the beam current by nearly a factor of two, bringing the proton stored beam energy to about 700 MJ to be compared to the LHC design value of 362 MJ. This poses obvious challenges for beam collimation [3]. During LS2 (2019-2021), several important upgrade items were already installed to improve various aspects of the collimation system and to test new technologies planned for HL-LHC. This provides a unique opportunity to push the beam parameters already during Run 3. Presently, the LHC is colliding beams at 6.8 TeV and accelerates up to about 2500 bunches of 1.6×10^{11} protons each. It reached a record stored beam energy of 430 MJ and deployed already complex operational scenarios planned at the HL-LHC, such as luminosity levelling schemes using either β^* and transverse-offset. The rapid deployment of these unprecedented beam parameters is illustrated in Fig. 1, where the stored beam energy achieved in the first commissioning month of 2023 is shown. In this paper, the LS2 collimation upgrades are reviewed and their measured performances during Run 3 are discussed. The next steps of the collimation upgrade for HL-LHC are recalled before drawing some conclusions.

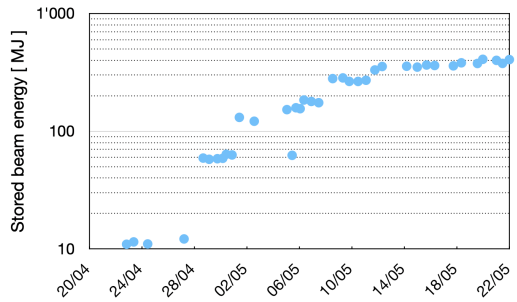

Figure 1: Average stored beam energy of the two LHC beams at the start of collision during the first month of operation in 2023.

LHC COLLIMATION SYSTEM IN RUN 3

The main collimation upgrades in LS2 are summarized [4]: (1) 12 new low-impedance collimators were installed in the insertion region 7 (IR7, betatron collimation): four primary collimators (TCPs) and 8 secondary collimators (TCS). Their jaws are made of the novel molybdenum-graphite (MoGr) material [5]: TCPs use bulk MoGr while TCSs have a 5 µm thick layer of Mo coating (Mo-MoGr); (2) two new collimators (TCLD) were installed in the dispersion suppressor (DS) regions around the ALICE experiment to protect superconducting magnets from heavy-ion collisional losses, to digest the requested luminosity following the ALICE detector upgrade [6]; (3) four new crystal primary collimators (TCPCs) were installed in IR7 and replaced previously used test devices [7, 8] to improve the betatron cleaning of heavy-ion beams for the operational ion runs starting in Run 3; (4) two new passive absorbers (TCAPM) were installed in IR7 to reduce the radiation wear of warm quadrupoles exposed to the loads from TCPs [9]. All new TCP, TCS and TCLD collimators embed in-jaw beam position monitors (BPMs) for fast beam-based alignment and continuous orbit measurements. This design [10, 11] was already successfully deployed for the LHC Run 2 (2015-2018) in the tertiary collimators around each experiment (16 TCT devices) and in 2 dump-protection collimators in IR6.

All new collimators were integrated into the LHC system and are available for Run 3 operation [12]. The upgrade items (2) and (3) target improvements to the heavy-ion beam operation. They have also been successfully commissioned with proton beams [13] and in a heavy-ion test in 2022 [14].

* Work supported by the HL-LHC project.

ISBN: 978-3-95450-253-0 ISSN: 2673-5571 doi:10.18429/JACoW-HB2023-THBP50

FERMILAB MAIN INJECTOR AND RECYCLER OPERATIONS IN THE MEGAWATT ERA

A. P. Schreckenberger*, Fermi National Accelerator Laboratory, Batavia, IL, USA

Abstract

Significant upgrades to Fermilab's accelerator complex have accompanied the development of LBNF (the Long-Baseline Neutrino Facility) and DUNE (Deep Underground Neutrino Experiment). These improvements will facilitate 1-MW operation of the NuMI (Neutrinos at the Main Injector) beam for the first time this year through changes to the Recycler slip-stacking procedure and shortening of the Main Injector ramp time. The modifications to the Recycler slip-stacking and efforts to reduce the duration of the Main Injector ramp will be discussed. Additionally, details regarding further shortening of the ramp time and the subsequent impacts on future accelerator operations are presented.

FERMILAB MOTIVATIONS

The Fermilab accelerator complex, illustrated in Fig. 1, delivers protons and consequent collision decay products to various physics experiments that include studies of accelerator stability, beam dynamics, muons, low- and high-energy neutrino interactions, neutrino oscillations, and the fixed-target program.

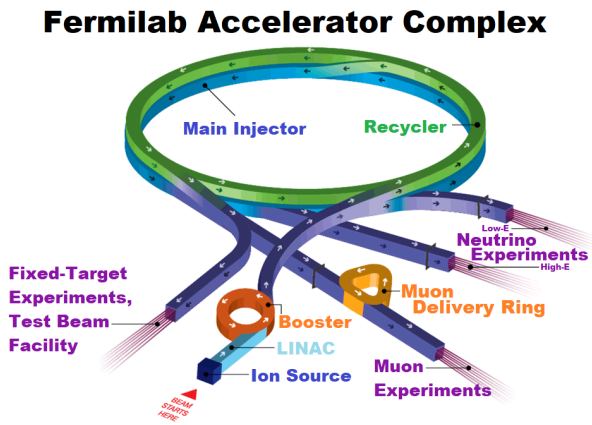

Figure 1: Illustration of the current Fermilab accelerator complex.

Fermilab's highest priority in the coming decade will be the development and construction of LBNF and DUNE [1]. DUNE's large liquid-argon-based detectors will provide unprecedented measurement precision of the neutrino oscillation parameters and sensitivity to CP-violation in the neutrino sector [2], paving a critical path to probing one of the Universe's fundamental questions.

Maximizing the neutrino flux produced by LBNF will improve the physics reach of DUNE. This goal is directly tied to the beam power delivered from the Main Injector (MI) and the efficiency of the accelerator complex. Many components in the proton accelerator chain have been in operation for decades and have exceeded their intended lifetimes.

The Fermilab linear accelerator (LINAC) was commissioned in 1970 and reached an upgraded design energy of 400 MeV in 1993. Construction has already begun on a new superconducting RF LINAC as part of the Proton Improvement Plan II (PIP-II) that will replace the original machine [3]. Likewise, the Booster synchrotron, responsible for accelerating protons to 8 GeV, reached its designed running in 1971. The existing proton source and downstream components operate at 15 Hz, but the PIP-II accelerator will operate at 20 Hz, further pushing the capabilities of the 52-year-old Booster.

The Recycler is an 8-GeV permanent magnet storage ring designed to accumulate antiprotons during Tevatron operations. Presently, the accelerator delivers beam to the Muon Campus and facilitates slip-stacking, which doubles the bunch intensity prior to delivery to the Main Injector. Occupying the same tunnel enclosure as the Recycler, the Main Injector accelerates the input 8-GeV beam to 120 GeV and provides protons to high-energy neutrino and test-beam experiments.

Beam power can be represented as:

$$P = |e|E\frac{N}{T}, \tag{1}$$

where e is the elementary charge, E is the particle energy, N is the number of particles per pulse, and T is the cycle duration. The Main Injector will continue to deliver protons at 120 GeV, so increases in beam power must be driven by increasing the beam intensity or decreasing the cycle duration. The slip-stacking process preloads an intensity increase into the Main Injector. However, additional increases do not come without incurring risks. Slip-stacking itself; the rise of fast-transverse, convective, and transverse mode coupling instabilities (TMCI); electron cloud accumulation, and space charge tune shifts are a few mechanisms that can yield additional beam losses as beam intensity grows. Recent slip-stacking optimization was an essential step for megawatt and LBNF/DUNE operations.

Decreasing the cycle duration is achievable by reducing the MI ramp time. During nominal NuMI running, this duration is 1.2 s, and megawatt operations are reached via a reduction to 1.067 s. As part of the Accelerator Complex Evolution (ACE) initiative, we aim to reduce the ramp time to 0.65 s to produce a multi-megawatt neutrino beam for LBNF. The advantages and requirements of this approach are discussed in this manuscript.

* wingmc@fnal.gov

ISBN: 978-3-95450-253-0 ISSN: 2673-5571 doi:10.18429/JACoW-HB2023-THBP52

A PYTHON PACKAGE TO COMPUTE BEAM-INDUCED HEATING IN PARTICLE ACCELERATORS AND APPLICATIONS

L. Sito*,[1], E. de la Fuente†,[2], F. Giordano, G. Rumolo, B. Salvant, C. Zannini
European Organization for Nuclear Research (CERN), Geneva, Switzerland
[1]also at University of Naples Federico II, Naples, Italy
[2]also at Polytechnic University of Madrid, Madrid, Spain

Abstract

High-energy particle beams interact electromagnetically with their surroundings when they travel inside an accelerator. These interactions may cause beam-induced heating of the accelerator's components, which could eventually lead to outgassing, equipment degradation and physical damage. The expected beam-induced heating can be related to the beam coupling impedance, an electromagnetic property of every accelerator device. Accounting for beam-induced heating is crucial both at the design phase of an accelerator component and for gaining an understanding of devices' failures. In this paper, an in-house developed Python tool to compute beam-induced heating due to impedance is introduced. The different features and capabilities will be showcased and applied to real devices in the LHC and the injector chain.

INTRODUCTION

A high-energy beam of charged particles traveling inside an accelerator component will generate electromagnetic wake-fields in the vacuum chamber that hosts it. This electromagnetic interaction can be described, in the frequency domain, through the concept of beam-coupling impedance: a complex quantity that is function of the beam chamber's geometry and material properties [1]. Wake-fields, and hence the impedance, other than affecting beam dynamics can be the source of energy deposited on accelerator components. This last phenomenon is impedance-related beam-induced heating (BIH) and may lead to a number of issues: outgassing, pressure spikes, unwanted beam dumps, and, potentially, permanent damage to the devices [2]. Thus, in many cases a good understanding of BIH is mandatory to push the performance of the machine.

In this proceeding, a python package that allows to easily compute the dissipated power due to BIH is presented [3]. The package named BIHC collects various methods to do this computation. More specifically, it is tailored for usage in the LHC and in the injector chain with two main applications:

1. During feasibility studies in the design phase of accelerator components.

2. To understand impedance-related issues that can occur during machine operation and investigate potential mitigation solutions.

* leonardo.sito@cern.ch
† elena.de.la.fuente.garcia@cern.ch

Following the introduction of the analytical formalism, two applications to the central beam pipe of the CMS experiment in the LHC and the beam wire scanners in the SPS will be shown to demonstrate the code's capabilities.

BEAM-INDUCED HEATING

The tool implements the equations for computing impedance related BIH for two scenarios: a single beam traveling in the vacuum chamber and two counter-rotating beams traveling through the same vacuum chamber.

Single Beam Scenario

The power dissipated due to a circulating beam into an accelerator component can be expressed as [1]:

$$P = 2(f_0 e M N_b)^2 \cdot \sum_{p=0}^{+\infty} |\Lambda(p\omega_0)|^2 \mathrm{Re}[Z_z(p\omega_0)]. \quad (1)$$

To compute Eq. (1), one characteristic quantity of the accelerator component (the real part of the longitudinal beam-coupling impedance $\mathrm{Re}[Z_z]$) and several characteristic quantities of the particle beam are needed.

The beam considered in the formalism is composed of a repetition of M bunches of N_b charged particles, each with charge e, that are circulating in the accelerator with revolution frequency f_0. The bunches have a certain longitudinal charge profile (for instance Gaussian or q-Gaussian) and they are spaced in time following a predetermined filling scheme. This is shown in Fig. 1 for a real fill of the LHC machine.

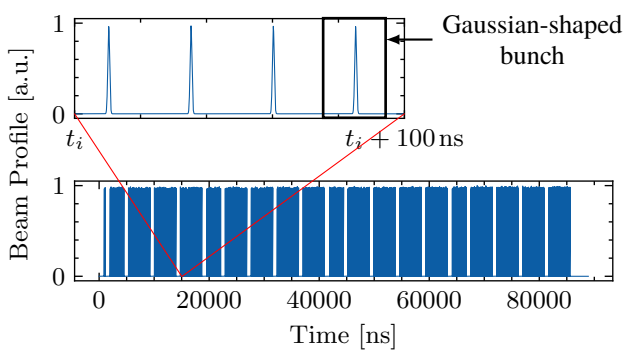

Figure 1: Normalized longitudinal beam profile of one 25 ns LHC fill with Gaussian bunch shape. The code allows to define as bunch shapes also q-Gaussian, binomial and cosine squared.

ISBN: 978-3-95450-253-0 ISSN: 2673-5571 doi:10.18429/JACoW-HB2023-THBP53

COMMISSIONING AND OPERATION OF THE COLLIMATION SYSTEM AT THE RCS OF CSNS

Shouyan Xu[1, 2, †], Kai Zhou[1, 2], Jianliang Chen[1, 2], Mingyang Huang[1, 2], Sheng Wang[1, 2]
[1]Institute of High Energy Physics, Chinese Academy of Sciences (CAS), Beijing, China
[2]Spallation Neutron Source Science Centre, Dongguan, China

Abstract

In high-intensity proton synchrotrons, minimizing particle losses during machine operation is crucial to prevent radiation damage. Uncontrolled beam loss is a major obstacle to achieve higher beam intensity and power in these synchrotrons. The beam collimation system plays a vital role in removing halo particles and localizing beam loss. It serves as a critical tool for controlling uncontrolled beam loss in high-power proton accelerators. To address the issue of uncontrolled beam loss, a transverse collimation system was designed for the RCS of CSNS. Initially, the design included a two-stage collimator. However, during the beam commissioning of CSNS, it was found that the collimation efficiency was compromised due to insufficient phase advance between the primary and secondary collimators. As a result, the designed two-stage collimator was modified to a one-stage collimator. Through optimization of the collimation system, the beam loss was effectively localized within the collimator area, resulting in a significant reduction in uncontrolled beam loss. As a result, CSNS achieved the design power of 100 kW with minimal uncontrolled beam loss.

INTRODUCTION

The China Spallation Neutron Source (CSNS) is designed to accelerate proton beam pulses to 1.6 GeV kinetic energy, striking a solid metal target to produce spallation neutrons. CSNS has two major accelerator systems, a linear accelerator (80 MeV Linac) and a 1.6 GeV rapid cycling synchrotron (RCS). The DTL raises the H^- beam energy to 80 MeV, and after the H^- beam is converted to a proton beam via a stripping foil, the RCS accumulates and accelerates the proton beam to 1.6 GeV. The 1.6 GeV proton beam is extracted to the target at a repetition rate of 25 Hz. The RCS is designed to extract a beam power of 100 kW, corresponding to 1.56×10^{13} protons per pulse in two bunches. The lattice of the RCS is a four-fold structure based on triplet cells. The entire ring comprises 16 triplet cells, with a circumference of 227.92 m. In each super-period, an 11 m long drift space is available between two triplet cells, providing uninterrupted space for accommodating the injection, extraction, acceleration, and transverse collimation system, as shown in Fig. 1. Table 1 provides the primary parameters of the RCS [1, 2].

For high-intensity proton synchrotrons, minimizing particle losses during machine operation is essential to avoid radiation damage. The use of collimation system is an important means of controlling uncontrolled beam loss in high-power proton accelerators. The beam collimation system can remove halo particles and to localize the beam loss. The design transverse collimator is a two-stage collimator. During the beam commissioning of CSNS, the designed two-stage collimator has been changed to one-stage collimator to overcome the problem of low collimation efficiency caused by insufficient phase shift between the primary and secondary collimators. By optimizing the collimation system, the beam loss is well localized in the collimator area, effectively reducing uncontrolled beam loss. This paper introduces the process of collimation system optimization at the RCS of CSNS.

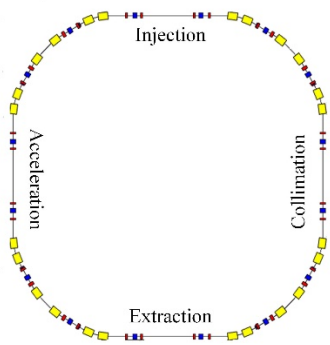

Figure 1: The schematic layout of the RCS of CSNS.

Table 1: The Primary Parameters of the RCS of CSNS

Parameters	Value
Output Beam Power (kW)	100
Injection Energy (MeV)	80
Extraction Energy (GeV)	1.6
Pulse repetition rate (Hz)	25
Ramping Pattern	Sinusoidal
Acceleration Time (ms)	20
Circumference (m)	227.92
Number of Dipoles	24
Number of Quadrupoles	48
Lattice Structure	Triplet
Nominal Betatron Tunes (H/V)	4.86/4.80
Natural Chromaticity (H/V)	-4.0/-8.2
Ring Acceptance (π·mm·mrad)	540
Number of Bunches	2

† email address: xusy@ihep.ac.cn

ISBN: 978-3-95450-253-0 ISSN: 2673-5571 doi:10.18429/JACoW-HB2023-THBP55

COMMISSIONING OF NICA INJECTION COMPLEX

O. I. Brovko, A. V. Butenko, E. E. Donets, B. V. Golovenskiy, E. B. Gorbachev, S. A. Kostromin, K. A. Levterov, V. A. Lebedev†, I. N. Meshkov, A. Yu. Ramsdorf, A. S. Sergeev, A. O. Sidorin, M. M. Shandov, V. C. Shpakov, V. L. Smirnov, E. M. Syresin, A. V. Tuzikov

Abstract

The Nuclotron-based Ion Collider fAcility (NICA) is under construction at JINR. The goal of the first stage of NICA project is to provide colliding beams for studies of collisions of heavy fully stripped ions at energies up to 4.5 GeV/u. The paper discusses results of recent commissioning run (Run IV) of NICA injection complex and plans for its further development.

INTRODUCTION

The NICA [1] injection complex has been under commissioning for more than 2 years. Its Run IV was carried from October 2022 to February of 2023. It was aimed at the injection complex preparation for the collider operations in the heavy ion mode. Additionally, the slowly extracted 3.9 GeV/u xenon beam was delivered to the BM&N experiment resulting in $2.5 \cdot 10^8$ events recorded by the detector. While major goals of Run IV were achieved its results revealed that an upgrade of the injection complex is required to support collider operation starting in about 2 years.

The injection complex includes:

- a new Electron String Ion Source (ESIS) (Krion-6T) generating highly charged heavy ions [2] and installed at a high voltage platform to make 16.6 keV/u ion energy for the targeted ion charge,
- 600 keV/u RFQ [3],
- 3.2 MeV/u linac (HILAC) [3],
- 600 MeV/u (A/Z=6) superconducting booster synchrotron (Booster) [4] and
- modernized main superconducting synchrotron (Nuclotron), kinetic energy up to 3.9 GeV/u (A/Z=2.5) [5].

Complete stripping of the ions is produced at the beam extraction from Booster at the very beginning of the Booster-Nuclotron transfer line. The schematic of the injection complex for the heavy ion operations in the collider mode and its main parameters are presented in Fig. 1. The reliability of the complex was low at the run beginning and was improving to its end. Overall, the complex operated 53% of time for the beam commissioning and 21% for data acquisition by BM@N [6].

ION SOURCE AND LINAC

The ion source produces highly charged heavy ions. At the Run IV beginning, for the ion source commissioning, we used $^{40}Ar^{13+}$ ions, which then were replaced by $^{124}Xe^{28+}$. The magnetic field of source solenoid is equal to 5 T while its value at the cathode is 0.25 T. That results in a reduction of the primary electron beam diameter from 1.2 mm to 0.27 mm. The electron beam energy is 6 keV. The reflex mode of operation requires the electron string being formed [7]. That yields the cathode current in the range of 4-6 mA. For operation with xenon the targeted ion charge was chosen to be 28. That required 18 ms ionization time and resulted in the total ion charge of 2.4 nC. About 20-25% of these ions had the targeted charge. That coincides well with CBSIM code predictions yielding 23% [8].

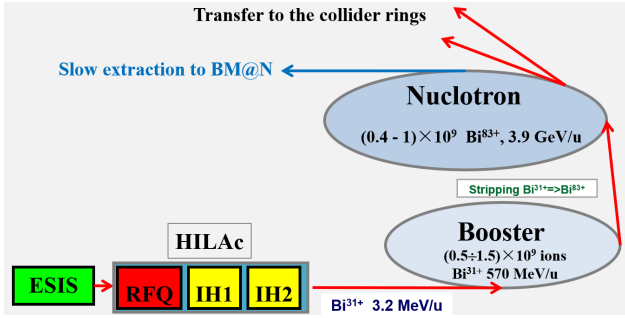

Figure 1: Schematic of the NICA injection complex.

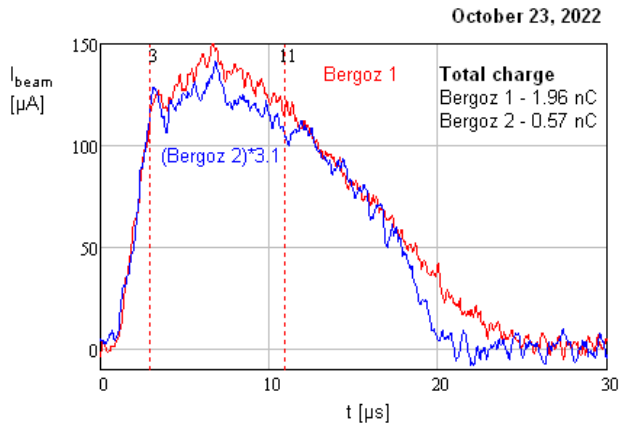

Figure 2: Typical dependencies of ion source beam current on time for ion source operation with $^{132}Xe^{28+}$ ions. Data are taken upstream (red) and downstream (blue) RFQ. The blue line was amplified by factor 3.1 to match curves. Vertical lines mark duration of one Booster revolution.

Figure 2 presents the beam current of $^{132}Xe^{28+}$ ions measured for upstream and downstream of RFQ. As one can see the RFQ accelerates about 30% of the incoming charge. We know that the RFQ accelerates few charge states simultaneously, but presently we can measure charge composition only at the very end of the linac where the first dipoles are installed. Consequently, we cannot accurately measure the beam loss distribution along the linac for the different charges of the ions.

The ion source emittance measurement has similar problem. The emittances were computed from the dependence

† valebedev@jinr.ru

ISBN: 978-3-95450-253-0 ISSN: 2673-5571 doi:10.18429/JACoW-HB2023-THBP57

A NOVEL RF POWER SOURCE FOR THE ESS-BILBAO ION SOURCE

S. Masa*, I. Bustinduy, R. Miracoli, A. Kaftoosian,
P. González, S. Varnasseri, L. Catalina-Medina
Consorcio ESS-Bilbao, Bilbao, Spain

Abstract

This paper presents the improvements in the ESS Bilbao Proton Ion Source by replacing the amplified radio frequency (RF) pulse of a Klystron-based amplification system using a Solid-State Power Amplifier (SSPA). This new amplification system is based on a 1 kW SSPA (2.7 GHz), a Compact-RIO (cRIO) device, a voltage-controlled RF attenuator and auxiliary electronics. The Experimental Physics and Industrial Control System (EPICS) serves as distributed control system (DCS) for controlling and monitoring the data required to achieve a 1.5 ms flat and stable pulse at repetition rate of 10 Hz. The following lines describe the structural and control system changes done in the ion source due to the addition of the SSPA-based amplification system, along with the results of the proton beam extraction tests that demonstrate how this system can serve as a viable substitute for the Klystron-based amplification system.

INTRODUCTION

ESS Bilbao proton source was built as the first step towards an accelerator system able to generate proton beams up to ~32 MeV [1]. In order to handle not only the protons for which it was designed, but also to be adjustable and deal with a variety of positive ions [2], it was designed and built as an Electron Cyclotron Resonance (ECR) ion source, more precisely Microwave Discharge Ion Source (MDIS). Far from the typical design employed in these kind of ion sources that normally use a magnetron as a Radio Frequency (RF) source, ESS Bilbao proton source works with a klystron to feed the plasma chamber with an amplified RF signal. This was done as the K3564 klystron amplifier from CPI, provides a better performance in terms of stability than the magnetron and it is better suited to work in CW (Continuous Wave) and pulsed modes, up to 2 kW. Even if this solution is more expensive than working with the magnetron, the ESS Bilbao proton source klystron has proven to be able to operate properly in the lasts years in a variety of experiments, e.g. [3, 4]. The successive step is to upgrade the ion source amplification system and this was done by building an in-house developed Solid-State Power Amplifier (SSPA) based amplification system. Solid-State technology-based power sources have come into accelerator facilities due to their reliability and lower power supply voltage requirement in comparison with vacuum tubes and there are plenty of research centers using or developing this technology in a variety of accelerator sections [5–9] and even some of them have been designed to work in ion sources [10–12]. This paper describes the ESS Bilbao in-house-developed SSPA-based amplification unit and its effectiveness in the ESS Bilbao ion source in comparison with results obtained by the klystron amplifier employed in this facility during many years.

* smasa@essbilbao.org

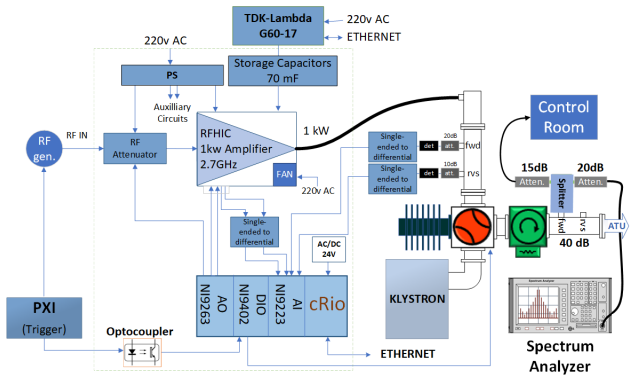

Figure 1: Injector SSPA-based amplification system scheme.

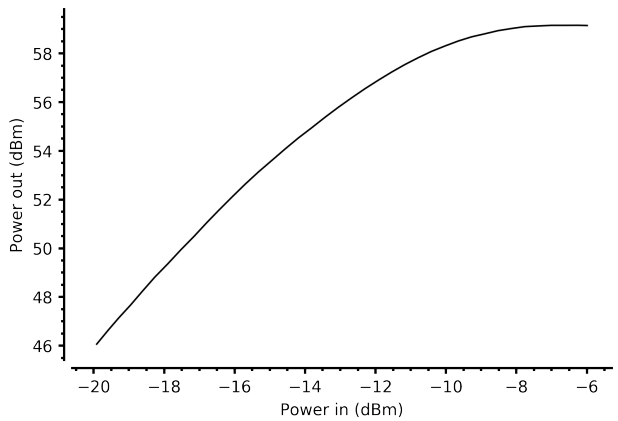

Figure 2: 1 kW SSPA amplifier Pin-Pout measurement (dBm).

HARDWARE SYSTEM

ESS Bilbao in-house developed SSPA-based RF power unit is mainly composed of a commercial Solid-state Power Amplifier [13], a voltage-controlled RF attenuator, a Compact RIO device and auxiliary electronics, shown in Fig. 1

SPA It is an on-shelf amplifier designed to work with pulsed RF signal at 2.7 GHz with 10 percent duty cycle. Based on GaN HEMT Technology provides up to 1 kW output peak power and 68 dB power gain as shown in Fig. 2.

ISBN: 978-3-95450-253-0 ISSN: 2673-5571 doi:10.18429/JACoW-HB2023-THBP59

TOMOGRAPHIC LONGITUDINAL PHASE SPACE RECONSTRUCTION OF BUNCH COMPRESSION AT ISIS

B. Kyle*, H. V. Cavanagh, R. E. Williamson, A. Seville, ISIS, Oxford, UK

Abstract

ISIS is an 800 MeV, high intensity, rapid-cycling synchrotron (RCS) used as a driver for a spallation neutron and muon spectroscopy (μSR) facility. The intensity-limited beam and RCS operation at ISIS poses significant challenges, with non-adiabatic acceleration and space charge forces resulting in distortions to the Hamiltonian longitudinal dynamics. Effective modelling of the machine and benchmarking of models with beam measurements is essential both to improving machine performance, and to the development of the proposed ISIS II facility. The tomographic principle is a well-established tool for the reconstruction of the longitudinal phase space (LPS) of synchrotron beams. Is it operationally desirable for the ISIS accelerator to provide longitudinally compressed proton beams for μSR instrumentation. A new bunch compression scheme has been developed and validated using tomography. A reconstruction of the LPS of the ISIS high-intensity proton beam is presented, along with accompanying benchmarking measurements and beam physics simulations.

INTRODUCTION

Despite the primary scientific output of the ISIS facility making use of spallation neutrons, ISIS also boasts a significant muon exploitation program [1]. Neutron and muon science is enabled by the ISIS accelerators, comprising a 70 MeV injector linac, and an 800 MeV RCS. The accelerators deliver high intensity proton beams, up to 3×10^{13} protons per pulse (ppp), to two target stations at a combined repetition rate of 50 Hz [2]. The energy gain of the beam follows the rising edge of the 50 Hz sinusoidal main dipole field, with acceleration facilitated by six fundamental (1RF) radio-frequency (RF) systems ($h = 2$), and four 2^{nd}-harmonic (2RF) RF systems ($h = 4$) [3]. Each of the RF systems comprise 2 gaps.

Charge-exchange injection facilitates generation of this high-brightness beam, wherein a continuous 70 MeV H^- beam is injected into the RCS along the falling edge of the main magnet sinusoid for a duration of 200-240 μs through a carbon stripping foil to form a proton beam [4]. Over the injection period, the beam phase space is painted actively in the vertical plane with a dedicated magnet, and dispersively in the horizontal plane due to the constant beam energy but decreasing main dipole field [5].

An intermediate graphite target is situated on the beam transfer line to Target Station 1 which is used to produce muon beams for muon spectroscopy (μSR) [1, 6]. Unlike the neutron instruments, which do not have requirements on the longitudinal distribution of the driver beam, the muon experiments are improved by shorter bunch lengths ($\lesssim 60$ ns full width half maximum (FWHM), where an uncompressed bunch length is typically in the range of 60-80 ns depending on the operational state of the machine). This improvement has motivated the development of bunch compression schemes using the synchrotron RF systems to manipulate the longitudinal phase space (LPS) of the proton beam in the synchrotron. This paper presents a possible new bunch compression scheme with simulations and measurements.

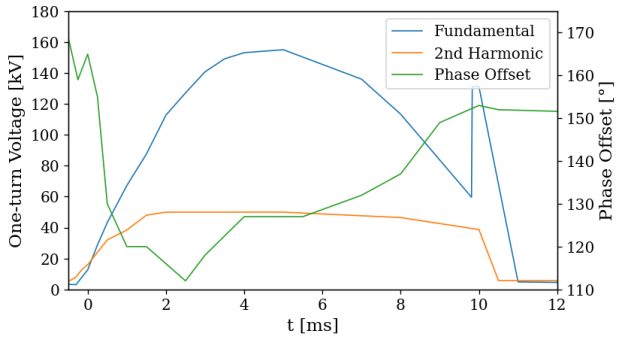

Figure 1: Typical RF voltage and phase offset program used for bunch rotation. The phase offset is in units of degrees of the 2RF.

BUNCH COMPRESSION

Historically, a bunch rotation scheme has been successfully employed for delivery of compressed proton beams on ISIS. LPS rotation comprises two stages. Firstly, the beam is elongated by a steady reduction of the 1RF peak voltage from the uncompressed operational values. This is followed by a rapid increase in the 1RF voltage just prior to extraction (Fig. 1), causing the bunch LPS to rotate at the synchrotron frequency resulting in bunch compression (Fig. 2). This scheme requires careful timing of the RF voltage profile, to ensure that the synchrotron extract kicker magnets fire at the point of minimum bunch length.

Extraction timing occurs within a 350 μs window, and the exact extraction point is established on a pulse-by-pulse basis through synchronisation between neutron instrument choppers and the synchrotron RF. As such, a degree of pulse-to-pulse fluctuation in the extracted bunch length is to be expected. Minimisation of this jitter would aid in maintaining consistent data resolution in μSR measurements.

A new compression program has been investigated which employs a gradual ramp in the phase offset between the 1RF and 2RF systems, Θ_{12}, whilst increasing the ratio $\delta = \hat{V}_{2\text{RF}}/\hat{V}_{1\text{RF}}$, where $\hat{V}$ are the peak one-turn voltages of the ISIS synchrotron RF harmonics (Fig. 3). The ramp in Θ_{12} is linear and commences at 7 ms through the 10 ms ma-

* billy.kyle@stfc.ac.uk

ISBN: 978-3-95450-253-0 ISSN: 2673-5571 doi:10.18429/JACoW-HB2023-FRA1I1

STATUS OF THE IOTA PROTON INJECTOR*

D. Edstrom Jr.†, A. Romanov‡, D. Broemmelsiek, K. Carlson, J.-P. Carneiro, H. Piekarz, A. Shemyakin, A. Valishev, Fermi National Accelerator Laboratory, Batavia, IL, United States

Abstract

The IOTA Proton Injector (IPI), currently under installation at the Fermilab Accelerator Science and Technology facility (FAST), is a machine capable of delivering 20 mA pulses of protons at 2.5 MeV to the Integrable Optics Test Accelerator (IOTA) ring. First beam in the IPI beamline is anticipated in the first half of 2024, when it will operate alongside the existing electron injector beamline to facilitate further beam physics research and continued development of novel accelerator technologies at the IOTA ring. This report details the expected operational profile, known challenges, and the current state of installation.

INTRODUCTION

The proton injector for the Integrable Optics Test Accelerator (IOTA, [1]) is an important capability for the research program at FAST/IOTA [2]. IOTA is a research storage ring constructed and operated by Fermilab to study advanced concepts in accelerator physics. At present, the studies at IOTA are performed with electron beams of up to 150 MeV energy that has negligible space charge effects. The commissioning of 2.5 MeV IOTA proton injector with a beam current of 20 mA will allow experiments with intense beams with strong space charge tune shifts that constitute 10 – 15 % of the total betatron phase advance in the ring. The rich menu of intense-beam research experiments planned at IOTA can be served with either electron or proton beams. The main research thrusts and the corresponding type of beams are:

- Demonstration of integrable optics with special nonlinear magnets (e, p)
- Demonstration of integrable optics with octupoles (e, p)
- Demonstration of integrable optics with non linear electron lenses (e, p)
  - Thin radial kick of McMillan type
  - Axially symmetric kick in constant beta function
- Space-charge compensation with electron lenses (p)
- Space-charge compensation with electron columns (p)
- Optical stochastic cooling (e)
- Electron cooling (p)
  - Electron cooling of protons
  - Diagnostics through recombination
  - Electron cooling and nonlinear integrable optics

PROTON SOURCE

Protons are to be generated with the kinetic energy of 50 keV using a Duoplasmatron ion source (IS) configured for proton production as described in Fig. 1. This source was previously used as a part of the High Intensity Neutrino Source (HINS) experiment [3], and was subsequently adopted by the FAST facility as it fits the desired beam parameters for proton production in the IPI beamline, as shown in Fig. 2. The IS was resurrected briefly in site in the HINS enclosure at the Meson Detector Building (MDB) before being fully disassembled and cleaned. In the process of disassembly, it was noted that the extraction aperture of 1.25 mm in use with HINS was unusually large for a duoplasmatron source, and has been replaced with a 0.7 mm aperture. It has since been reassembled at the FAST facility.

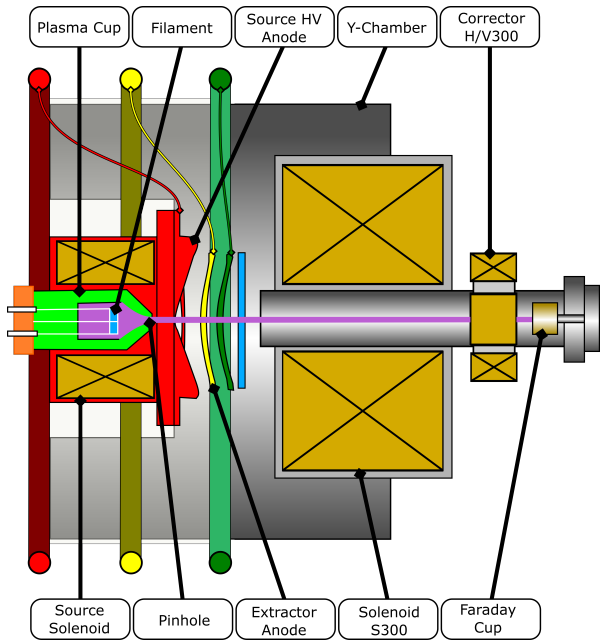

Figure 1: A schematic view of the IS in a test configuration. For extraction of 50 keV protons, the source high voltage anode is charged to a static +50 kV, the extractor anode is set to 40 kV, and the green anode is at ground potential. The S300 solenoid is the first element of the LEBT.

Filaments are prepared on-site using a mixture of Barium, Calcium, and Strontium Carbonates along with Isoamyl Acetate to assist in binding the mixture to the filament. The mixture is dissolved in Acetone to form a thin solution and the cleaned Nickel filament is dipped to deposit a modest coating of the carbonate mixture. It is then activated in a filament activation station referred to simply as *the Jar*, as shown in Fig. 3, by slowly increasing the filament current to the nominal 21 A, as seen in Fig. 4. This burns away the nitrocellulose binder and ultimately converts the carbonate mixture into oxides [4], lowering the work function and facilitating electron transmission on the filament surface. This

* This work has been authored by Fermi Research Alliance, LLC under Contract No. DE-AC02-07CH11359 with the U.S. Department of Energy, Office of Science, Office of High Energy Physics.
† edstrom@fnal.gov
‡ aromanov@fnal.gov

ISBN: 978-3-95450-253-0 ISSN: 2673-5571 doi:10.18429/JACoW-HB2023-FRA1I2

DESIGN AND BEAM COMMISSIONING OF DUAL HARMONIC RF SYSTEM IN CSNS RCS

Hanyang Liu, Shouyan Xu, Liangsheng Huang,Yang Liu, Sheng Wang*
Institute of High Energy Physics, Beijing, China
Spallation Neutron Source Science Center, Dongguan, Guangdong, China

Abstract

The CSNS accelerator achieved an average beam power on target of 100 kW in February 2020 and subsequently increased it to 125 kW in March 2022. Building upon this success, CSNS plans to further enhance the average beam power to 200 kW by doubling the particle number of the circulating beam in the RCS, while keeping the injection energy same. The space charge effect is a main limit for the beam intensity increase in high-power particle accelerators. By providing a second harmonic RF cavity with a harmonic number of 4, in combination with the ferrite cavity with a harmonic number of 2, the dual harmonic RF system aims to mitigate emittance increase and beam loss caused by space charge effects, thereby optimizing the longitudinal beam distribution. This paper will concentrate on the beam commissioning for the 140 kW operation subsequent to the installation of the magnetic alloy (MA) cavity. The commissioning process includes the optimization of RF parameters, beam studies, and evaluation of the beam quality and instability.

INTRODUCTION

The dual harmonic rf system is a key method to optimize the longitudinal beam distribution and alleviate the space charge effect, and it is also one of the important topics in accelerator physics design research for the CSNS-II RCS beam power upgrade project [1]. The beam intensity of CSNS-II RCS will be five times that of CSNS, and the increase in accumulated current intensity will bring more serious space charge effects and beam collective instability. This will be a huge challenge for beam dynamics design, optimization, and beam loss control. The dual harmonic rf system has been added to the RCS in order to alleviate space charge effect and improve beam quality. The injection energy of RCS will be increased from 80 MeV to 300 MeV. The power upgrade has been implemented in stages, and the RCS transformation plan will be carried out before the energy upgrade of the linear accelerator. Therefore, it is essential to complete the dual harmonic longitudinal dynamic design at an injection energy of 80 MeV. The installation and commissioning of the second harmonic cavity are also carried out in batches. At the beginning, the average beam power of RCS is 125 kW. By installing one magnetic alloy (MA) cavities (as shown in Fig. 1) to provide a maximum of about 72 kV second harmonic cavity voltage [2], the average power of 140 kW has been achieved. With two additional MA cavities and some effort, the plan can be to provide a maximum of about 100 kV second harmonic cavity voltage and increase the average power to 200 kW. Finally, combined with the upgrade of injection energy, the design power index of CSNS-II RCS 500 kW will be achieved [1].

The MA cavity has a higher accelerating voltage gradient compared to the ferrite cavity and also a wider bandwidth. However, the beam loading effect of MA cavities is very serious and should be considered carefully in high-intensity proton synchrotrons. To reduce the beam loading effects, a feedback system is used in the MA cavity for compensating the induced voltage.

In order to improve the longitudinal distribution of the beam, the dual harmonic rf system is often used to flatten the longitudinal potential function of the beam. Combined with momentum offset injection, the beam can obtain a larger bunching factor after injection [3]. However, due to the momentum offset, there will be a decrease in bunching factor during the first 1/4 synchrotron oscillation period, which will lead to an increase in space charge force and cause an increase in longitudinal emittance growth during the painting process and even cause beam loss during the injection stage [4]. To address this problem, a method called "matched phase scan" has been used to optimize the bunching factor both during and after the injection in order to improve this longitudinal transient effect during painting [5].

This paper will mainly introduce some issues encountered during the beam commissioning process of CSNS RCS, including beam loading effects, optimization of double harmonic rf parameters, and some related simulation results and beam experiments. The main parameter of RCS at 140 kW is shown in Table 1.

Table 1: RCS Main Parameters

Circumference	227.92 m
Harmonic number	2 / 4
Accelerating frequency	1.022- 2.444 MHz
Repetition	25 Hz
Maximum rf voltage	180 / 60 kV
Energy	0.08 – 1.6 GeV
Gap number of cavity	3
Particle number per bunch	1.092×10^{13} ppp (140 kW)

* wangs@ihep.ac.cn

ISBN: 978-3-95450-253-0 ISSN: 2673-5571 doi:10.18429/JACoW-HB2023-FRA1C1

NEW TECHNIQUES METHOD FOR IMPROVING THE PERFORMANCE OF THE ALPI LINAC

L. Bellan†, A. Pisent, E. Fagotti, F. Grespan, M. Montis, M. Giacchini, M. Comunian, O. Carletto, Y. K. Ong, INFN Legnaro National Labs, Legnaro, Italy

Abstract

The superconductive quarter wave cavities hadron linac ALPI is the final acceleration stage at the Legnaro National Laboratories. It can accelerate heavy ions from carbon to uranium up to 10 MeV/u for nuclear and applied physics experiments. It is also planned to use it for re-acceleration of the radioactive ion beams for the SPES (Selective Production of Exotic Species) project. In this article we will present the innovative results obtained with swarm intelligence algorithms, in simulations and measurements. In particular, the increment of the longitudinal acceptance for RIB (Radioactive Ion Beams) acceleration, and beam orbit correction without the beam first order measurements will be discussed.

INTRODUCTION

The CW heavy ion accelerator facility at Legnaro is composed by two main sections: the injectors and the superconductive independent linac ALPI [1]. The final output energies are for the stable ion beams around 10 MeV/u and the output current are generally around 100 nA. The ion species supplied span from carbon ions up to ^{208}Pb ion. The whole heavy ion complex is commonly called TAP (TANDEM ALPI PIAVE). In this paper we will presents the second part of the tests.

THE SUPERCONDUCTIVE LINAC ALPI AND RECENT RESULTS

The linac is composed by 20 cryostats which house four Quarter Wave Cavities each. Each cavity must independently tune with the beam during the runs. The ALPI linac was one of the first prototype in Europe, designed and built between the 80'-90' and for this reason exploited many innovative techniques at that time. At the design stage the superconductive cavities accelerating filed was designed to achieve 3 MV/m with a diameter bore of 20 mm diameter. To maximize the real estate of the machine, the period of ALPI was designed with one triplet for transverse focusing and 2 cryostats (8 cavities). The design of the cavities, the accelerating field improvements, and the lattice design force a very aggressive transverse focusing, which result in a phase advance, of about 120 deg (see Fig. 1). Such phase advance, beside reducing the overall transverse acceptance, it is also sensible to beam misalignment. Another important fact to consider is that the transverse position of the cavities suffers of an error around 1 mm when cooled down, while, when they are at room temperature, the error can reach several mm, closing the further the aperture. This was the situation when we tested the presented results of the algorithm.

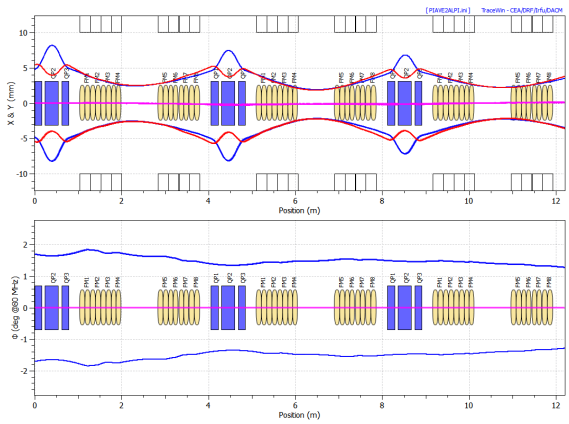

Figure 1: ALPI lattice beam envelopes, with $\sigma_0 = 120$ deg.

In a recent paper [2], we applied the PSO techniques [3] to increase the longitudinal acceptance of the linac. We obtained a double increase of the longitudinal acceptance (see Fig. 2).

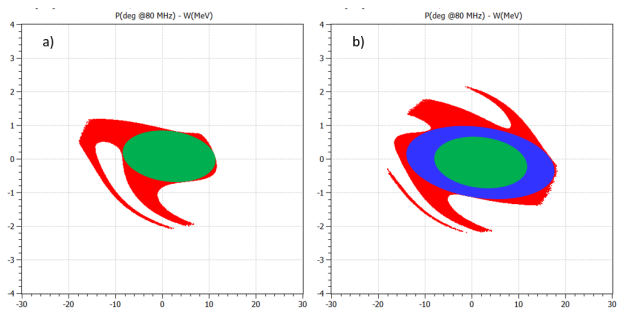

Figure 2: a) green acceptance ellipse calculated over the ALPI alternate gradient acceptance. b) acceptance increase after swarm optimization.

However, this solution required an effective steering procedure, which worsen the situation given by σ_0. Because the steering is very troublesome in ALPI, as explained in Ref. [2], we proposed a different steering which look at the transmission directly. We verified it in simulations and then we applied on the ALPI linac obtaining an increase of transmission from 24% (manual setting) to 35% (automatic setting).

Figure 3 illustrates the layout of the accelerator facility.

† luca.bellan@lnl.infn.it

ISBN: 978-3-95450-253-0 ISSN: 2673-5571 doi:10.18429/JACoW-HB2023-FRC1I1

THE BEAM DESTINATIONS FOR THE COMMISSIONING OF THE ESS HIGH POWER NORMAL CONDUCTING LINAC

Elena Maria Donegani*,1, Saverio Ardovino[1], Vincent Bertrand[2], Ibon Bustinduy[3], Viatcheslav Grishin[1], Tara Hodgetts[4], Emanuele Laface[1], Carlos Neto[1], Anders Olsson[1], Laurence Page[1], Marcos Ruelas[4], Thomas Shea[1]
[1]European Spallation Source (ESS) Lund, Sweden
[2]Pantechnik, Bayeux, France
[3]ESS Bilbao, Zamudio, Spain
[4]RadiaBeam Technologies, Santa Monica, CA, USA

Abstract

At the European Spallation Source (ESS) in Lund (Sweden), the commissioning of the high-power normal conducting linac started in 2018. This paper deals with the beam destinations for the commissioning phases with initially the proton source and LEBT, then the MEBT and lately four DTL sections. The beam destinations were designed to withstand the ESS commissioning beam modes (with proton current up to 62.5 mA, pulse length up to 50 µs and repetition rates up to 14 Hz). The EPICS-based control system allows measurements of the proton current and pulse length in real-time; it controls the motion and the power suppliers, and it also monitors the water cooling systems. Special focus will be on the results of thermo-mechanical simulations in MCNP/ANSYS to ensure safe absorption and dissipation of the volumetric power-deposition. The devices' materials were chosen not only to cope with the high-power proton-beam, but also to be vacuum-compatible, to minimize the activation of the beam destinations themselves and the residual dose nearby. The results of neutronics simulations will be summarized with special focus on the shielding strategy, the operational limits and relocation procedures.

INTRODUCTION

The European Spallation Source (ESS) is going to be a 5 MW pulsed neutron source, relying on a 2 GeV proton linac to produce neutrons via the spallation process [1]. Once fully installed and commissioned, the linac will deliver 2.86 ms long proton pulses with 14 Hz repetition rate. The proton linac comprises firstly the NCL (Normal Conducting Linac) and secondly the SCL (Super Conducting Linac).

First of all, the NCL commissioning started in fall 2018, with protons initially dumped on the Faraday cup (FC) in the Low Energy Beam Transport line (LEBT) [2]. Following the RFQ conditioning and the installation of the Medium Energy Beam Transport (MEBT) [3], the commissioning continued up to the MEBT Faraday cup [4] between fall 2021 and spring 2022. In June 2022, the protons were accelerated for the first time through the first Drift Tube Linac section (DTL1) and dumped in the shielded Faraday cup downstream the DTL1 section [5]. After the installation of three additional DTL sections [6], the protons were accelerated and transported down to the DTL4 section and dumped in the DTL4 Faraday cup in April 2023. Each Faraday cup was designed for specific proton energies and the foreseen beam power density. Table 1 lists the beam destinations that were operational during ESS NCL commissioning phases, as well as the average beam power and the calculated peak temperature.

Table 1: List of beam destinations used for the subsequent phases of the ESS NCL commissioning, at increasing proton energy (E) and average proton beam power (P). The corresponding maximum core temperature (T) was computed via thermo-mechanical simulations.

Destination	E (MeV)	P (W)	T (°C)
LEBT FC	0.075	0.005	800
MEBT FC	3.6	16	960
DTL1 FC	21	170	620
DTL4 FC	[21, 74]	323	1010

GOALS

During the ESS NCL commissioning, four Faraday cups were used as beam destinations, in place of expensive and bulky beam dumps. The goals of the Faraday cups were to fully stop the proton beam, to safely absorb and dissipate the beam power, and to provide real-time measurements of the proton current as well as the pulse length. In addition, the DTL FCs had to be installed in a dedicated shielding for the following three reasons: (I) tunnel accessibility during commissioning, (II) installation work in the SCL in parallel to the commissioning, and (III) dismantling within few weeks after the end of the DTL1 and DTL4 commissioning. All the beam destinations were operated under ultra high vacuum, water-cooled and movable in/out of the beam line by means of a pneumatic actuator.

The beam-intercepting components were designed to withstand the so-called commissioning beam modes: Probe-beam (6 mA, 5 µs, 1 Hz), Fast-tuning (62.5 mA, 5 µs, 14 Hz), and Slow-tuning (62.5 mA, 50 µs, 1 Hz). In addition, the LEBT FC can withstand also the so-called Production-mode (62.5 mA, 2860 µs, 14 Hz).

* elena.donegani@ess.eu

ISBN: 978-3-95450-253-0 ISSN: 2673-5571 doi:10.18429/JACoW-HB2023-FRC1I2

HIGH BEAM CURRENT OPERATION WITH BEAM DIAGNOSTICS AT LIPAc

S. Kwon*, A. De Franco, K. Masuda, K. Hirosawa, T. Akagi, K. Kondo, M. Ohta
National Institutes for Quantum Science and Technology (QST), Aomori, Japan
F. Benedetti[1], F. Cismondi, D. Gex, Y. Carin, Fusion for Energy (F4E), Garching, Germany
J. Marroncle, B. Bolzon, N. Chauvin
Commissariat à l'énergie atomique et aux énergies alternatives (CEA), Saclay, France
D. Jimenez-Rey[2], V. Villamayor, I. Podadera[3], A. RodriguezCentro de Investigaciones Energéticas, Medioambientales y Tecnológicas (CIEMAT), Madrid, Spain
M. Poggi, Istituto Nazionale di Fisica Nucleare (INFN), Legnaro, Italy
J. C. Morales Vega, IFMIF-DONES España, Granada, Spain
L. Maindive, Universidad de Granada (UGR), Granada, Spain
[1]also at CEA, Saclay, France, [2]also at F4E, Garching, Germany
[3]also at IFMIF-DONES España, Granada, Spain

Abstract

The Linear IFMIF Prototype Accelerator (LIPAc) is under commissioning in Rokkasho Fusion Institute in Japan and aims to accelerate 125 mA D+ at 9 MeV in Continuous Wave (CW) mode for validating the IFMIF accelerator design. To ensure a fine characterization and tuning of the machine many beam diagnostics are installed spanning from Injector to the beam dump (BD). The beam operations in 1.0 ms pulsed D+ at 5 MeV was successfully completed with a low power BD (Phase B) in 2019. Despite the challenges posed by the pandemic, the crucial transition to a new LINAC configuration was also finalized to enable operation in 1.0 ms – CW D+ at 5 MeV with the high-power BD (Phase B+). The 1st beam operation of Phase B+ was carried out in 2021. The experiences and challenges encountered during the beam operations we obtained at the last beam operations will be described.

INTRODUCTION

The International Fusion Materials Irradiation Facility (IFMIF) is a fusion neutron source for the material irradiation test of the plasma-facing components in fusion reactors. The data expected from the IFMIF is used to understand the effect of the high energy neutron flux to determine and develop new advanced materials [1]. Through a first decision to start the IFMIF project in 1994, and the conceptual design studies had been carried out by four main members, Russia, the EU, the US and Japan [2]. To pursue a successful engineering design activity, the IFMIF Engineering Design and Engineering Validation Activities (EVEDA) project has been started under the Broader Approach (BA) Agreement between the EU and Japan. One of the activities of the project is the completion of the engineering validation of the Accelerator Facility of IFMIF [3]. The Linear IFMIF Prototype Accelerator (LIPAc) is under commissioning in Rokkasho Fusion Institute of National Institutes of Quantum Science and Technology (QST) in Japan. European institutions such as CEA, CIEMAT, INFN, and SCK-CEN were responsible for the design, manufacture, and testing of the majority of accelerator components: injector, Radio Frequency Quadrupole (RFQ), Low/Medium/High Energy Beam Transport Lines (LEBT/MEBT/HEBT), Superconducting RF (SRF) LINAC, RF systems, Local Control Systems and Beam Diagnostics. QST (former Japan Atomic Energy Agency, JAEA) provides buildings, main auxiliaries systems, the RFQ coupler, MEBT Extension Transport Line (MEL) and Central Control System [4]. Figure 1 shows the final configuration of the LIPAc and each contribution. The LIPAc aims to test the scientific and technical feasibility of the accelerator through a full scale of prototype from the injector to the first cryomodule. Table 1 summarized the goal of the beam characterizations of LIPAc.

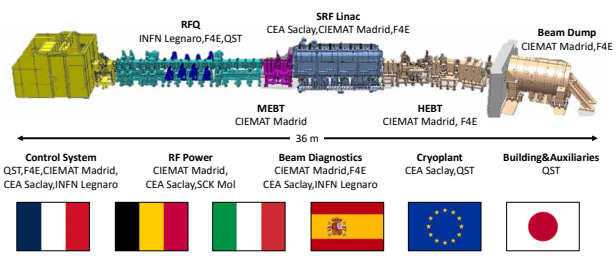

Figure 1: The final configuration of LIPAc.

Table 1: Goal of the LIPAc Beam Operation

Parameter	Values	Units
Duty factor	CW	-
Ion type	D+	-
Beam Current	125	mA
Beam Energy	9	MeV
RF Frequency	175	MHz
Beam Power	1.125	MW
Target of Beam Stop	Cu	-

* kwon.saerom@qst.go.jp

ISBN: 978-3-95450-253-0 ISSN: 2673-5571 doi:10.18429/JACoW-HB2023-FRC1I3

DEVICES FOR HIGH-EFFICIENCY SLOW EXTRACTION AT J-PARC MAIN RING

R. Muto*, T. Kimura, S. Murasugi, K. Numai, K. Okamura, Y. Shirakabe, M. Tomizawa, E. Yanaoka
High Energy Accelerator Research Organization (KEK), Ibaraki, Japan
A. Matsumura, NAT corporation, Ibaraki, Japan

Abstract

J-PARC Main Ring (MR) is a synchrotron that accelerates protons up to 30 GeV and supplies them to the Neutrino Experimental Facility and the Hadron Experimental Facility (HEF). Beam extraction from MR to HEF is performed by slow extraction using third-order resonance. In the slow extraction, electrostatic septa (ESS) are used to scrape off the beam, and it is crucial to reduce the beam loss at the septum electrode of the ESS to supply a high-intensity beam. So far, we have achieved a slow extraction efficiency of 99.5 % by developing an ESS with a thin septum electrode and tuning the orbit bump to reduce the angular spread of the proton beam at the ESS. In addition, a collimator is installed downstream of the ESS to absorb particles scattered by the septum electrode, thereby reducing the activation of the components downstream. In order to achieve further reduction of the beam loss, we are considering installing beam diffusers or bent silicon crystals upstream of the ESS.

INTRODUCTION

At the J-PARC Main Ring, proton beams accelerated up to 30 GeV are extracted towards the Neutrino Experimental Facility or Hadron Experimental Facility (HEF) to promote particle and nuclear physics experiments [1]. Beam extraction to the HEF is performed by slow extraction using the third-order resonance of betatron oscillations. By 2021, we achieved user operation with a beam power of approximately 64 kW with an extraction efficiency of about 99.5 %. In this slow extraction, a device called an electrostatic septum (ESS) [2] is used to extract the beam by scraping off the particles with increased betatron amplitude due to third-order resonance. A high electric field between the septum electrode and the cathode of the ESS achieves beam scraping. Since inserting a septum electrode into the beam is necessary, large beam losses due to particles colliding with the septum electrode are inevitable. Therefore, major issues are reducing beam loss at the septum electrode and localizing peripheral device activation by scattered particles. In this paper, we will briefly explain the slow extraction method at J-PARC Main Ring and then describe the devices and their features.

SLOW EXTRACTION AT J-PARC MAIN RING

Table 1 shows the basic parameters for the slow extraction of the J-PARC Main Ring. The injection energy of the proton beam is 3 GeV, and the ESS is installed in the upstream part of the slow extraction straight section at a transverse position where the septum electrode does not interfere with the injection beam. As the beam emittance decreases with acceleration from 3 GeV to 30 GeV, a orbit bump is created in the slow extraction straight section, bringing the closed orbit of the beam closer to the high electric field region created by the septum electrode and the cathode of the ESS. The electric field is generated between 60 mm and 85 mm in the horizontal position, and the center of the orbit bump is located at 35 mm, here the origin is the center of the circulating beam. Next, by approaching the horizontal betatron tune to 22.333 from below, we will reduce the area of the stable region in the phase space. The particles return to approximately the same position every three turns. However, the amplitude of the particles that protrude into the unstable region gradually increases along the separatrix that separates the stable and unstable regions. Figure 1 shows the movement of particles with various amplitudes in horizontal normalized phase space when the horizontal betatron tune is kept constant.

Table 1: Basic Parameters for the Slow Extraction at J-PARC MR

Parameter	Value
Particle	Proton
Circumference	1567.5 m
Injection energy	3 GeV
Extraction energy	30 GeV
Horizontal betatron tune	22.31 → 22.333
Vertical betatron tune	20.8
Repetition	5.2 s
Spill length	~ 2 s

The high electric field between the septum electrode and the cathode kicks particles that reach the septum electrode of the ESS. In this process, a certain proportion of particles collide with the septum electrode and are scattered at a large angle, resulting in beam loss. Here, step size is defined as the difference between the particle position and that in three turns before. Roughly, the number of beam particles in the ratio of (septum thickness) / (step size at the septum electrode) will collide with the septum electrode. Hence, increasing the step size at the septum electrode and decreasing the septum thickness are important for reducing beam loss. The design value of the step size in J-PARC MR is 20 mm.

Another important point for reducing beam loss is the particles' angular spread at the ESS position. When a par-

* ryotaro.muto@kek.jp

ISBN: 978-3-95450-253-0 ISSN: 2673-5571 doi:10.18429/JACoW-HB2023-FRA2I1

SUMMARY OF THE WORKING GROUP A: BEAM DYNAMICS IN RINGS

H. Bartosik*, G. Rumolo, CERN, Geneva, Switzerland
J.-L. Vay, LBNL, Berkeley, CA, USA
N. Wang, IHEP, Bejing, China

Abstract

The HB-2023 workshop at CERN from October 9 to 13, 2023 is the continuation of the series of workshops, which started in 2002 at FNAL and rotates every two years between America, Europe and Asia. This contribution summarises the main highlights from Working Group A, Beam Dynamics in Rings, in terms of progress and challenges in the achievement of ever higher intensity and brightness hadron beams in accelerator rings around the world.

INTRODUCTION

The HB-2023 workshop at CERN from October 9 to 13, 2023 is the continuation of the series of workshops, which started in 2002 at FNAL and rotates every two years between America, Europe and Asia. This contribution summarises the main highlights from Working Group A, Beam Dynamics in Rings, in terms of progress and challenges in the achievement of ever higher intensity and brightness hadron beams in accelerator rings around the world. The following main themes have been treated during the Working Group A sessions:

- Understanding and mitigating space charge effects;
- Studies for characterizing luminosity;
- Understanding and mitigating beam instabilities;
- The pursuit for more powerful simulation tools.

A short summary of the main highlights from each of these themes will be given in the following, and the main challenges ahead will then be discussed.

UNDERSTANDING AND MITIGATING SPACE CHARGE EFFECTS

Losses and emittance growth due to space charge effects in combination with resonances, lattice driven or space charge driven, remain among the most prominent performance limitations for high brightness and high power circular hadron machines.

Careful optimization of the tune working point for avoiding resonances (e.g. Montague resonance and half integer resonances) allows reaching large space charge tune spreads at injection with losses below the percent level. This was shown for the case of the CSNS rapid cycling synchrotron, where a tune variation along the cycle ("tune pattern") through a modulation of the quadrupole fields was developed to mitigate space charge effects at injection and suppress beam instabilities during the ramp [1]. Like this, loss levels could be maintained at a minimum for the nominal 100 kW beam power (and beyond) when combined with correlated injection painting [2]. However, foil heating remains a big challenge. A new painting scheme using a pulsed injection chicane, combining the injection chicane and the painting bump, was developed for CSNS-II in order to reduce the foil temperature and the edge focusing effects from the injection chicane [2]. This scheme saves one set of bumper magnets, and reduces the optics distortion and resonance excitation, which in turn allows for smaller transverse emittances and higher intensities.

As shown in several contributions at the workshop, the compensation of lattice or injection chicane driven resonances through dedicated corrector magnets is nowadays standard practice in many machines. Identifying the magnetic errors through beam-based measurement of resonance driving terms from turn-by-turn beam position data has proved quite successful, as demonstrated for example in the studies at Fermilab [3]. These beam-based measurement techniques are particularly relevant for existing machines, for which detailed magnetic modelling is not available.

Another method for identifying magnetic errors through beam-based measurements has also been presented, the so-called "Deep Lie-Map Networks" [4]. This method builds an improved accelerator model with magnetic errors such that simulated tracking of single particles through Lie Maps reproduces the measured turn-by-turn beam position data along the machine. A first proof-of-principle experiment was performed at GSI to identify sextupole errors from trajectory data, and further experimental campaigns are planned. During the workshop, it was suggested to extend the method by including also the tunes and chromaticity as objectives for the algorithm.

The compensation of resonances excited by the nonlinear potential of the space charge force itself is particularly challenging, but was successfully demonstrated at the J-PARC main ring [5]. In particular, minimizing the driving term of the $8Q_y = 171$ structure resonance through the optimization of the arc phases advance while maintaining the overall tunes of the machine through adjustments of the straight section optics resulted in reduced beam loss in operation.

In the context of discussing resonance compensation schemes in different machines, A. Oeftiger proposed to formulate the efficiency of resonance compensation in the sense of "how much intensity could be gained by resonance compensation for a given amount of acceptable losses".

An open question raised by V. Lebedev at the workshop concerns the maximum achievable space charge tune shift in a real machine with a highly super-periodic lattice operating above the half-integer. While this question was not answered at the workshop, the maximum tolerable space charge tune

* Hannes.Bartosik@cern.ch

ISBN: 978-3-95450-253-0 ISSN: 2673-5571 doi:10.18429/JACoW-HB2023-FRA2I2

SUMMARY OF WORKING GROUP B

N. J. Evans, ORNL, Oak Ridge, TN, USA
F. Bouly, LPSC, Université Grenoble-Alpes, CNRS/IN2P3, Grenoble, France
H. W. Zhao, Institute of Modern Physics, Chinese Academy of Sciences, Lanzhou, China

Working group B, Beam Dynamics in Linacs, featured 8 invited and 13 contributed talks over 5 sessions covering a broad range of topics relevant to linacs from operational experience to novel theoretical techniques to aid in the design and analysis of accelerators. Highlights from each session are presented below, followed by remarks from the conveners.

SESSION 1

Nicolas Chauvin, **CEA Saclay**, presented R&D activities focused on high-intensity proton and deuteron beams for the high-intensity proton injector IPHI that has been designed and developed with the primary objective of accelerating a continuous beam of 100 mA to 3 MeV [1]. This machine consists of a high-intensity ECR ion source, a low-energy beam line, a 352 MHz RFQ, and a medium-energy transport line equipped with diagnostics. The commissioning of the IPHI facility started several years ago with a proton beam operating at a low duty cycle (0.1 %) and a current of 65 mA. Since then, he showed that significant progress has been made, resulting in an accelerated beam power exceeding 30 kW. In addition, extensive measurements have been conducted to thoroughly characterize the beam accelerated by IPHI and its transport through the beam lines. he detailled end-to-end numerical model in - high space charge regime - of the IPHI accelerator and validated it against experimental data; showing that "semi-empirical" model gave an accurate description of the beam dynamics and the space charge compensation.

Austin Hoover, **ORNL**, presented simulation work showing the effects of previously observed high-dimensional correlations in phase space present at the output of the SNS RFQ on downstream beam behavior at the SNS Beam Test Facility (BTF) [2]. These correlations have been measured at the BTF, and can be reproduced in PARMTEQ simulations. The downstream evolution of the bunch appears largely independent of the presence of these correlations, as beams with the correlations artificially removed quickly converge to resemble the correlated bunches: in both an RMS sense and more general structural appearance. This work has implications for future studies examining halo formation in high-power linacs. Part of these developments are also linked to work on effect of three-dimensional quadrupole magnet model On beam Dynamics presented by **Trent E. Thompson**, **ORNL** [3].

In this session **Yuri Batygin** also discussed the feature of the **LANSCE** accelerator facility with multi-beam operation, simultaneously delivering beams to five experimental areas [4]. He showed that multi-beam operation requires compromises in beam tuning to meet beam requirements and losses throughout the accelerator. Upgrade of the facility (new 100 MeV front end), with expected significant improvement of beam quality, was also presented.

SESSION 2

Shuhui Liu, **Institute of Modern Physics, CAS** presented the design of the Chinese Accelerator Driven System (CiADS), with particular emphasis on features meant to improve availability of the machine [5]. The LEBT is designed to clean the proton beam of contaminating H_2^+ and H_3^+ prior to injection to the RFQ, and the superconducting linac begins immediately after the RFQ and MEBT at 2.1 MeV. Notably, fault recovery by online re-tuning of cavities and magnets in the vicinity of a cavity failure is built into the design, which should help the CiADS meet the strict availability requirements set on ADS. First beam at 500 MeV is expected in 2027.

Andrei Shishlo, **ORNL** gave an update on progress made in understanding SNS linac beam dynamics. Dr. Shishlo drew on a talk given by A. Aleksandrov at HB in 2010 to show how much progress has been made in understanding centroid motion, RMS size and beam loss/transmission transversely and longitudinally. Despite progress in nearly all areas, mostly using envelope-only tracking in OpenXAL, empirical tuning still drives operation. Studies with the PIC code pyORBIT show no contradiction with classical models used in accelerator design, but do not have the resolution to identify the low-loss operating point [6].

Sasan Ahmadiannamin, **STFC/RAL/ISIS**, also presented studies focused on beam physics simulation conducted on the current ISIS linac, aiming to gain a deeper understanding and analysis of various phenomena observed during routine operations and accelerator physics experimentation [7]. While **Juan E. Muller** presented beam dynamics studies and codes benchmarking activities carried out at **ESS** [8]. The aim was to Evaluate PyORBIT as a unified simulation tool for beam dynamics modeling.

SESSION 3

Jean-Michel Lagniel, **GANIL**, discussed about synchronous phases (ϕ_s) and transit time factors (T) are the key parameters for linac designs and operations [9]. He mentionned that while the couple (ϕ_s, T) is still our way of thinking the longitudinal beam dynamics, it is important to have in mind that the original "Panofsky definition" of these parameters is no longer valid in the case of high accelerating gradients in multi-gap cavities. He proposed new methods to tune cavities with respect to their buncher phase. He also presented a new definition of the synchronous phase in order

ISBN: 978-3-95450-253-0 ISSN: 2673-5571 doi:10.18429/JACoW-HB2023-FRA2I3

SUMMARY OF THE WORKING GROUP C ON ACCELERATOR SYSTEMS

S. Machida, Rutherford Appleton Laboratory, Didcot, Oxfordshire, U.K.
H. Huang, Brookhaven National Laboratory, Upton, NY, USA
P. K. Saha, Japan Atomic Energy Agency, Tokai, Ibaraki, Japan

Abstract

This is the summary of all overall presentations and discussions of the working group C on accelerator systems at the 68th ICFA Advanced Beam Dynamics Workshop on High-Intensity and High-Brightness Hadron Beams, named HB2023 held at CERN during October 9-13, 2023.

INTRODUCTION

In this working group (WG), we had a total of 18 oral presentations, equally divided into half and were held in 4 parallel sessions. There were also 5 posters presented under this WG. Among 18 oral presentations, we considered a complete geographical balance by selecting 6 talks each from Asia, America and EMEA (Europe, Middle East, and Africa). The main motivation of this WG was to get full pictures and details of high-intensity accelerators worldwide to date and future developments and upgrades with new techniques and modifications by covering the following 6 categories: 1) Injection and Extraction, 2) RF systems, 3) Impedance and Instabilities, 4) New techniques and Novel ideas, 5) High-power targets and 6) Upgrades and Future Projects. We arranged joint sessions for 2) RF systems and 3) Impedance and Instabilities with WGA (Beam Dynamics in Rings) and WGE (Beam Instrumentation and Intercepting Devices). In this report, we present a summary of the key points and highlights of each presentation and some general remarks on the working group perspective.

INJECTION AND EXTRACTION

Vincent Schoefer: Mitigation of space charge effects in RHIC and its injectors

The RHIC heavy ion and spin physics program requirements provide an array of intensity and space charge related challenges to performance optimization. For polarized proton beam at the injection of AGS Booster and AGS, the space charge driven bottlenecks are mitigated by bunch lengthening with dual RF harmonics and stopband correction. The low energy Beam Energy Scan-II program in RHIC uses the Au beam below the nominal injection energy due to a combination of effects from space charge, IBS. The effects are mitigated by moving working point and optimizing the electron cooling beam current. In the future, more comprehensive simulations could be performed to identify specific drivers of intensity dependent emittance growth and beam loss.

Nicholas Evans: Self-consistent injection painting for space charge mitigation

Danilov distribution can be created by uniformly filling one transverse mode of a coupled ring. It offers an opportunity to create a beam with several properties of interest for high brightness beams. Such a distribution could be constructed using a sufficiently flexible charge exchange injection system, such as at the Spallation Neutron Source (SNS). Extensive simulations have been done to compare with the eigen painting experiment results. They have achieved the initial goal of developing a procedure for eigenpainting into a ring and are currently preparing a detailed analysis of the resulting experiments. They have identified several opportunities for improvement at SNS.

Chiara Bracco: Shaping high brightness and fixed target beams with the CERN PSB charge exchange injection

This paper first gave a brief history of CERN PS Booster (PSB) and the upgrade to 160MeV H^- charge exchange injection. With higher energy and H^- injection, the space charge effect has been greatly mitigated. The PSB commissioning started in December 2020. The paper described the steering and injection setup, injection painting setup and optimization, and stripping foil performance. The results achieved up to now meet the upgrade goals. Nonetheless, relentless endeavours persist in pushing the boundaries to assess the ultimate levels of the achievable intensity and brightness.

RF SYSTEMS

Fumihiko Tamura: RF systems of J-PARC Proton Synchrotrons for high-intensity longitudinal beam optimization and handling

The application of magnetic alloy (MA) cores to the accelerating RF cavities in high intensity proton synchrotrons for the J-PARC synchrotrons, the RCS and MR are summarized. The MA loaded cavities can generate high accelerating voltages. The wideband frequency response of the MA cavity enables the frequency sweep to follow the velocity change of protons without the tuning loop. The dual harmonic operation is indispensable for the longitudinal bunch shaping to alleviate the space charge effects in the RCS. On the other hand, since the wake voltage consists of several harmonics, which can cause coupled-bunch instabilities, the beam loading compensation must be multi-harmonic. The operation of tubes in the final stage amplifier is not trivial when accelerating very high intensity beams;

ISBN: 978-3-95450-253-0 ISSN: 2673-5571 doi:10.18429/JACoW-HB2023-FRA2I4

SUMMARY OF THE COMMISSIONING AND OPERATIONS AND PERFORMANCE WORKING GROUP FOR HB2023 WORKSHOP

N. Milas, European Spallation Source ERIC, Lund, Sweden
M. Bai, SLAC, Palo Alto, USA
S. Wang, IHEP, Beijing, People's Republic of China

Abstract

As hadron machines enter the multi-megawatt era issues such as machine activation caused by beam loss, machine protection and machine availability become more critical concerns. The operational experience of the high power, high intensity facilities in these areas is compared. In addition, upgrade plans and commissioning results are discussed and operational optimizations and routines and presented.

INTRODUCTION

In this working group, the focus was on the commissioning and operational advancements within high intensity hadron facilities. Commissioning developments included the initial results from global facilities like ESS, GANIL, Spiral 2, and LIPAc. On the operational front, a prevalent theme was high power operation, exemplified by the multi-megawatt beam operation at facilities such as SNS, FRIB, and J-PARC, along with their upcoming upgrade plans. Particularly significant was the progress at HIPA in PSI, which has seen a remarkable 24-fold increase in its original design power, alongside components reaching the impressive milestone of 60 years of operation. The presentation encompassed an overview of maintenance strategies and a roadmap for ensuring continuous, reliable operations.

Additionally, high power facilities main challenges are related to machine protection, residual activation resulting from uncontrolled beam loss, and machine reliability. Insights from major facilities such as ISIS, CSNS, IMP, and CERN AD were presented. Details of each of the session contributions are presented in the individual papers. In this summary, we concentrate rather on the common themes.

FACILITY COMMISSIONING AND STATUS

The primary objective in any commissioning stage is the integration and verification of all essential sub-systems with the beam, demonstrating the capability to transport and accelerate a nominal beam. In the case of the SPIRAL2 linac, successful commissioning has been achieved, with H^+, $^4He^{2+}$, D^+, and $^{18}O^{6+}$ ions accelerated up to nominal parameters. Additionally, $^{18}O^{7+}$ and $^{40}Ar^{14+}$ beams have been accelerated up to 7 MeV/A. Noteworthy observations during the commissioning phase include the necessity for improved matching to the linac, tuning procedures for the 3 Medium Energy Beam Transport (MEBT) rebunchers, and 26 linac Superconducting (SC) cavities.

During the ESS NCL commissioning period, a proton pulse of 50 µs and 65.2 mA was successfully transported to the end of the DTL4 tank. Various strategies for cavity tuning were tested during this period. The Linear IFMIF Prototype Accelerator, LIPAc, accomplished the acceleration and transport of a nominal beam of 5 MeV−125 mA in 1 ms/1 Hz pulsed mode in 2019. Resuming beam operation since July 2023, the focus has shifted towards the commissioning of the full configuration, emphasizing the RFQ behavior with high duty cycle and longer pulses.

In the context of the SARAF project, significant progress has been made, including the updating of the injector control system and the installation and integration of the MEBT line into the infrastructure. Recent testing and commissioning of the injector and MEBT with 5 mA continuous wave (CW) protons and 5 mA pulsed Deuterons were completed in 2022 and 2023. These tests involved multiple emittance measurements and exercises in cavity tuning.

CAFe2, an evolution of its predecessor CAFe, initially designed as a proton demonstrator linac for Accelerator-Driven Systems (ADS), has undergone substantial upgrades. Since 2021, CAFe2 has logged over 2400 hours of operation, delivering heavy beams for Superheavy Element (SHE) experiments.

The IOTA ring is now being prepared to receive its first protons and the injector, capable of delivering 20 mA pulse of 2.5 MeV is under installation. This proton source will operate concurrently with its electron counterpart and is integral to the fundamental accelerator research program conducted at the facility.

The presentations highlighted the ongoing commissioning efforts across various facilities. A common theme emphasized the critical importance of machine characterization during these early stages and throughout the commissioning process. This includes, but is not limited to, having a profound understanding of the machine dynamics, recognizing the limitations of diagnostics, assessing the fidelity of the machine model concerning reality, and understanding of longitudinal tuning, particularly in the context of linacs and low-energy machines.

FACILITY UPGRADE PLANS

In the era of multi-megawatt linacs and synchronous operation, existing facilities are on the way of expanding their capabilities and achieving higher performance levels. Facilities such as SNS, FRIB, JPARC, and HIPA are in the process of implementing upgrade plans, with a primary focus on power ramp-up while ensuring effective loss control

ISBN: 978-3-95450-253-0 ISSN: 2673-5571 doi:10.18429/JACoW-HB2023-FRA2I5

SUMMARY OF WORKING GROUP E: INSTRUMENTATION AND INTERCEPTING DEVICES

P. Forck, GSI, Darmstadt, Germany
P. Hurh, Fermilab, Batavia, IL, USA
K. Satou, J-PARC/KEK, Tokai, Japan

Abstract

The contribution summarizes the talks and discussion of Working Group E related to Instrumentation and Intercepting Devices. The discussion topics are summarized in addition.

INTRODUCTION

The HB conference brings together experts from beam dynamics, operation, and instrumentation, providing an optimal platform for discussing topics relevant to high-brightness beams. Modeling of accelerator performance is the basis for any facility. Beam instrumentation should fulfill the appropriate requirements for operation and dedicated machine studies; however, some device limitations might exist, which must be considered for a correct data interpretation, calling for an experience exchange between experts with different application perspectives. Related to the high beam brightness, non-invasive instrumentation is required to monitor undisturbed beam parameters; those instruments have been developed in the last few years as an alternative to traditional intercepting devices. Generally, intercepting devices are used not only for diagnostics but frequently for collimation, injection devices, and, naturally, as targets. Material modifications and handling are essential issues to be discussed at the HB conference. Near targets and further loss locations, the thermal load, radiation level, and activation can be high, leading to material modifications.

The talks within Working Group E (WGE) address those topics and are briefly summarized; for more details, the reader is referred to the individual conference publications.

SESSION 1: BEAM INSTRUMENTATION IN A HIGH RADIATION ENVIRONMENT

The first session of WGE was comprised of four talks focused on beam instrumentation in high-power accelerator target facilities, both currently operating and future facilities. The talks represented the unique intersection of high-power targetry and high-power beam instrumentation, where extremely high radiation background, radiation damage to materials, and thermal energy deposition combine to challenge both the function and the lifetime of instrumentation. The first and third talks highlighted ongoing beam and target health monitoring instrumentation at high-power neutrino target facilities (NuMI at Fermilab and T2K at J-PARC). The second talk presented an upgrade to a passive cavity beam current monitor that has successfully operated under heavy heat load and radiation since 2015 at PSI. The final presentation showed plans for the flowing liquid lithium target diagnostics for the future 5 MW IFMIF-DONES facility. The session prompted several discussions both in the question periods and during the break, where participants discussed common issues, compared techniques, and potential future collaboration.

"Radiation hardened Beam Instrumentations for multi-Mega-Watt Beam Facilities" by Katsuya Yonehara, Fermilab

This talk included a brief summary of the 2022 mini-workshop (virtual) held as a subgroup of the Accelerator Frontier Technology R&D group from Snowmass'21, "Rad Hard Beam Instrumentation Workshop", and an overview of the instrumentation tools used to monitor beam and target health at the NuMI beamline at Fermilab. Highlights include a unique "Target Position Thermometer" (TPT), which gives a measurement of beam profile and position on target at high intensity (up to 1 MW in operation). Drawbacks of the TPT include the time to reach thermal equilibrium (several minutes) and the necessity to use complicated analysis tools to calibrate and extract good data. Another highlight is the results of using Machine Learning to interpret noisy muon monitor data and extract meaningful beamline parameters, such as horn current and beam intensity with accuracy below ±0.1%.

"Improvement Design of a Beam Current Monitor based on a Passive Cavity under Heavy Heat Load and Radiation" by Jilei Sun, PSI

This talk focused on the improvements made to the design of a radiation-hard passive cavity beam current monitor, which has been in use at PSI since 2015. The upgrades to the monitor, termed "MHC5", include changing the resonator cavity material from aluminum to graphite to reduce resonance shifts from thermal expansion. The design is self-compensating, using an aluminum shim that expands to compensate for temperature increase. Other upgrades included four beam position pick-ups and several remote handling features to ease replacement and reduce the dose to a worker. Lab tests with the new design will take place early in 2024.

"Beam Diagnosis and Soundness Check System for Neutrino Production Targets" by Megan Friend, KEK

This talk presented an overview of the beam and target health instrumentation used at both Fermilab's NuMI neutrino beamline (see the first talk above) and J-PARC's T2K neutrino beamline. Unique instruments at T2K include an Optical Transition Monitor just upstream of the target and a new prototype Beam Induced Fluorescence (BIF) monitor. The BIF description generated quite a few discussion points to identify possible additional applications at other